

Proteomic analysis of leukaemogenic protein tyrosine
kinase action

A thesis submitted to The University of Manchester for the degree of
Doctor of Philosophy
in the Faculty of Medical and Human Sciences

2011

François Griaud

School of Medicine

LIST OF CONTENTS

LIST OF CONTENTS.....	2
LIST OF FIGURES.....	6
LIST OF TABLES.....	9
LIST OF APPENDICES.....	9
ABSTRACT.....	10
DECLARATION.....	11
COPYRIGHT STATEMENT.....	11
LIST OF ABBREVIATIONS.....	12
AMINO ACID CODE AND ISOTOPIC MASSES.....	20
ACKNOWLEDGEMENTS.....	21
DEDICATION.....	22
CHAPTER 1. INTRODUCTION.....	23
1.1. GENERAL INTRODUCTION.....	23
1.2. HAEMOPOIESIS.....	24
1.3. LEUKAEMOGENIC PROTEIN TYROSINE KINASES AND RELATED DISEASES.....	27
1.3.1. <i>BCR/ABL and chronic myeloid leukaemia (CML)</i>	29
1.3.2. <i>JAK2 mutants and Ph-negative myeloproliferative diseases (MPDs)</i>	32
1.3.3. <i>FLT3 and acute myeloid/lymphoid leukaemia (AML/ALL)</i>	33
1.3.4. <i>KIT mutants and acute myeloid leukaemia (AML)</i>	33
1.3.5. <i>TEL/PDGFRβ and chronic myelomonocytic leukaemia (CMML)</i>	34
1.3.6. <i>NPM/ALK and anaplastic large cell lymphoma (ALCL)</i>	34
1.3.7. <i>Cell model for the study of leukaemogenic protein tyrosine kinases (PTKs)</i>	35
1.3.8. <i>Conclusion</i>	35
1.4. EXCESSIVE PRODUCTION OF REACTIVE OXYGEN SPECIES (ROS) AND ITS CONSEQUENCES ON CELL REGULATION AND DNA INTEGRITY.....	36
1.4.1. <i>Production and function of ROS in haemopoietic cells</i>	36
1.4.2. <i>ROS are a source of DNA damage</i>	37
1.4.3. <i>Antioxidant mechanisms in haemopoietic cells</i>	38
1.4.4. <i>Oxidative stress by leukaemogenic protein tyrosine kinases (PTKs)</i>	41
1.4.5. <i>Conclusion</i>	43
1.5. DNA DOUBLE STRAND BREAK SENSING/REPAIR SIGNALLING.....	45
1.5.1. <i>DNA double strand breaks</i>	45
1.5.2. <i>Response to DNA double strand breaks</i>	46
1.5.3. <i>DNA double strand break repair processes</i>	55
1.5.4. <i>Misregulation of the DNA damage response signalling and stimulation of unfaithful DNA double strand break repair processes by leukaemogenic PTKs</i>	58
1.6. APPROACHES AND TECHNOLOGIES IN PROTEOMICS.....	64

1.6.1.	<i>Approaches to the proteome definition</i>	65
1.6.2.	<i>Principle of mass spectrometry</i>	67
1.6.3.	<i>Sources in mass spectrometry</i>	68
1.6.4.	<i>Analysers in mass spectrometry</i>	70
1.6.4.a.	<i>Quadrupole analyser</i>	70
1.6.4.b.	<i>Ion trap analyser</i>	72
1.6.4.c.	<i>Time-of-flight (TOF) analyser</i>	75
1.6.4.d.	<i>Fourier transform ion cyclotron resonance (FTICR) analyser</i>	76
1.6.4.e.	<i>Orbitrap analyser</i>	79
1.6.5.	<i>Detectors in mass spectrometry</i>	80
1.6.6.	<i>Tandem mass spectrometry</i>	81
1.6.7.	<i>Sequence databases and proteomic software</i>	84
1.7.	STRATEGIES FOR PHOSPHOPROTEOMICS	86
1.7.1.	<i>Function, control and identification of protein phosphorylation</i>	86
1.7.2.	<i>Phosphoprotein and phosphopeptide immunoprecipitation</i>	88
1.7.3.	<i>Ion metal affinity chromatography (IMAC)</i>	89
1.7.4.	<i>TiO₂ and ZrO₂ affinity chromatography</i>	89
1.7.5.	<i>Sequential elution from IMAC (SIMAC)</i>	90
1.7.6.	<i>Strong cation exchange chromatography (SCX)</i>	90
1.7.7.	<i>Phosphosite tagging by chemical derivatization</i>	91
1.7.8.	<i>Experimental approaches for dissecting functional roles of protein phosphorylation</i>	91
1.8.	STRATEGIES FOR QUANTITATIVE PROTEOMICS	92
1.8.1.	<i>Strategies for label free quantification</i>	93
1.8.2.	<i>Isotope-coded affinity tags (ICAT)</i>	93
1.8.3.	<i>Stable isotope labelling by amino acids in cell culture (SILAC)</i>	94
1.8.4.	<i>Isobaric tags for relative and absolute quantification (iTRAQ™)</i>	95
1.8.5.	<i>Absolute quantification in peptide mass spectrometry (AQUA™)</i>	98
1.9.	AIMS AND OBJECTIVES	100
	CHAPTER 2. MATERIALS AND METHODS	101
2.1.	CELL CULTURE	101
2.1.1.	<i>Ba/F3 cell culture</i>	101
2.1.2.	<i>Ba/F3 cell stable gene transfection</i>	101
2.1.3.	<i>Ba/F3 cell transient gene transfection</i>	102
2.1.4.	<i>Preparation of Lin⁻ cells and mast cells (CD45 WT/null)</i>	103
2.1.5.	<i>Human primary cell culture</i>	104
2.1.6.	<i>K562 cell culture</i>	104
2.1.7.	<i>Chemicals and inhibitors</i>	104
2.1.8.	<i>γH2AX assay</i>	105
2.1.9.	<i>Apoptosis assay</i>	106
2.1.10.	<i>Flow cytometry analysis of Thoc5/Fmip tyrosine phosphorylation</i>	106
2.1.11.	<i>Immunofluorescence of Thoc5/Fmip tyrosine phosphorylation</i>	107
2.2.	SAMPLE PREPARATION FOR PROTEIN AND PROTEOMIC ANALYSIS	107
2.2.1.	<i>Whole cell lysis</i>	107
2.2.2.	<i>Nuclear preparation</i>	108

2.2.3.	<i>Protein assay</i>	108
2.2.4.	<i>Western blot analysis</i>	109
2.2.5.	<i>Study of the etoposide-induced genotoxic stress with iTRAQ™ peptide labelling</i> ...	110
2.2.6.	<i>Phosphopeptide enrichment with TiO₂ affinity chromatography</i>	111
2.2.7.	<i>Phosphopeptide fractionation with high-pH reversed phase (RP) chromatography</i> ..	111
2.3.	MASS SPECTROMETRY	112
2.3.1.	<i>Study of the etoposide-induced genotoxic stress</i>	112
2.3.2.	<i>Data analysis</i>	113
2.3.3.	<i>Validation with selected reaction monitoring (SRM)</i>	115
2.4.	STATISTICAL METHODS.....	116
2.4.1.	<i>Parametric tests</i>	116
2.4.2.	<i>Non-parametric tests</i>	117
2.4.3.	<i>Standard error of the mean</i>	118

CHAPTER 3. SITE-SPECIFIC QUANTITATIVE PHOSPHOPROTEOMIC ANALYSIS OF BCR/ABL PTK CROSSTALK ON ETOPOSIDE-INDUCED DNA DAMAGE RESPONSE IDENTIFIES A SYNERGISTIC PHOSPHORYLATION CHANGE ON DEVELOPMENTAL PROTEIN HEMOGEN.....119

3.1.	INTRODUCTION	119
3.2.	RESULTS	120
3.2.1.	<i>Induction of DNA damage and DNA repair with etoposide</i>	120
3.2.2.	<i>Phosphoproteomic analysis of etoposide-induced events in the presence and absence of BCR/ABL PTK</i>	127
3.2.3.	<i>γH2AX, ATM and 53BP1 respond to etoposide</i>	133
3.2.4.	<i>BCR/ABL PTK signalling acts on proteins within multiple pathways</i>	137
3.2.5.	<i>Phosphosite-specific overlap of etoposide and BCR/ABL PTK signalling</i>	141
3.2.6.	<i>Validation of Hemogen phosphorylation on serine 380 with AQUA™</i>	158
3.2.7.	<i>Pathway analysis pinpoints the B-WICH and NF-κB complexes as potential mediators of BCR/ABL PTK-mediated genomic instability</i>	166
3.3.	DISCUSSION.....	171

CHAPTER 4. A SIGNALLING PATHWAY FROM RECEPTOR ACTIVATION AND OXIDATIVE STRESS TO THO COMPLEX PHOSPHORYLATION POTENTIATED BY LEUKAEMOGENIC PROTEIN TYROSINE KINASES AND STEM CELL HOMING CHEMOKINES.....182

4.1.	INTRODUCTION	182
4.2.	RESULTS	185
4.2.1.	<i>Structure/function analysis on NPM/ALK reveals the key residues for activation of Thoc5/Fmip tyrosine phosphorylation</i>	185
4.2.2.	<i>Thoc5/Fmip phosphorylation on tyrosine 225 is increased by oxidative stress</i> ...	187
4.2.3.	<i>Nucleocytoplasmic distribution of Thoc5/Fmip tyrosine phosphorylation</i>	190
4.2.4.	<i>Thoc5/Fmip tyrosine phosphorylation relies on proto-oncogene Src</i>	194
4.2.5.	<i>CD45/Src signalling pathway is upstream of Thoc5/Fmip tyrosine phosphorylation</i>	200
4.2.6.	<i>THOC5/FMIP tyrosine phosphorylation is elevated in primary CML stem cells</i>	203

4.2.7. <i>Thoc5/Fmip phosphorylation on tyrosine 225 in mediation of apoptosis in response to oxidative stress</i>	207
4.2.8. <i>Thoc5/Fmip tyrosine phosphorylation does not mediate protein levels of Hsp40 and Hsp70 in response to etoposide and H₂O₂</i>	209
4.3. DISCUSSION.....	213
CHAPTER 5. GENERAL DISCUSSION, FUTURE WORK AND CONCLUSION.....	220
5.1. GENERAL DISCUSSION	220
5.2. FUTURE WORK	224
5.3. CONCLUSION.....	226
CHAPTER 6. REFERENCES.....	227
CHAPTER 7. APPENDICES	262
7.1. γ H2AX ASSAY WITH FLOW CYTOMETRY	262
7.2. APOPTOSIS ASSAY WITH FLOW CYTOMETRY	263
7.3. COMPARISON BETWEEN QSTAR® XL AND QSTAR® ELITE	265
7.4. PHOSPHOENTITIES POTENTIALLY REGULATED BY ETOPOSIDE AND/OR BCR/ABL PTK	266
7.5. PHOSPHOENTITIES OF THO COMPLEX MEMBERS IN THE PRESENCE OF BCR/ABL PTK AND ETOPOSIDE	274
7.6. CONTROLS FOR ABSOLUTE QUANTIFICATION (AQUA™) OF HEMOGEN PHOSPHORYLATION ON SERINE 380	275

Word count: 67,399

LIST OF FIGURES

Figure 1.1: Haemopoiesis.....	26
Figure 1.2: p210 BCR/ABL leukaemogenic protein tyrosine kinase	30
Figure 1.3: Leukaemogenic PTKs impair ROS functions.	44
Figure 1.4: DNA double strand break (DSB) signalling pathways (1).....	50
Figure 1.5: DNA double strand break (DSB) signalling pathways (2).....	51
Figure 1.6: DNA double strand break (DSB) signalling pathways (3).....	52
Figure 1.7: DNA double strand break (DSB) signalling pathways (4).....	53
Figure 1.8: DNA double strand break (DSB) signalling pathways (5).....	55
Figure 1.9: DNA double strand break repair processes in mammals.....	57
Figure 1.10: THO complex is a potential target for leukaemogenic PTKs to promote chromosomal instability and disease progression	60
Figure 1.11: Sample preparation differences between “Bottom-Up”, “Middle-down” and “Top-down” proteomics	66
Figure 1.12: Principles of mass spectrometry (MS)	67
Figure 1.13: A depiction of the electrospray ionisation (ESI) source	69
Figure 1.14: Principle of a quadrupole analyzer.....	71
Figure 1.15: Mathieu stability diagram.....	71
Figure 1.16: Structure of a three dimensional ion trap analyser.....	73
Figure 1.17: Peptide fragmentation in the ion trap analyser.....	74
Figure 1.18: Principle of the time-of-flight (TOF) analyser	76
Figure 1.19: Principle of the Fourier transform ion cyclotron resonance (FTICR) mass analyser.....	78
Figure 1.20: Structure of the orbitrap analyser	80
Figure 1.21: Peptide fragmentation in ion series	82
Figure 1.22: QTRAP™ acquisition modes	83
Figure 1.23: Flowchart of protein identification in proteomics	85
Figure 1.24: Design of the iTRAQ™ reagents.	96
Figure 1.25: Workflow for relative quantification of phosphopeptides with iTRAQ™ peptide labelling.....	97
Figure 1.26: Principle of the absolute quantification (AQUA™) method	99
Figure 3.1: Etoposide-induced DNA double strand breaks in Ba/F3 cells in the presence or absence of BCR/ABL PTK.	121
Figure 3.2: Etoposide-induced apoptosis in Ba/F3 cells in the presence or absence of BCR/ABL PTK (1).....	123
Figure 3.3: Etoposide-induced apoptosis in Ba/F3 cells in the presence or absence of BCR/ABL PTK (2)	124
Figure 3.4: DNA double strand break repair in Ba/F3 cells in the presence or absence of BCR/ABL PTK.....	126
Figure 3.5: Schematic workflow of the phosphosite-specific proteomic analysis of etoposide-induced nuclear effects in Ba/F3 cells in the presence and absence of BCR/ABL PTK.....	128
Figure 3.6: Distribution of biological controls.....	129

Figure 3.7: Clustering of phosphoentities.....	131
Figure 3.8: Comparison of phosphoentities and proteins consistently regulated by BCR/ABL PTK and/or etoposide in 2 biological replicates	132
Figure 3.9: Potential regulation of γ H2AX, ATM and Etoposide-induced protein 24 (Ei24) phosphoentities after etoposide exposure.....	134
Figure 3.10: Dynamics of 53BP1 phosphoresidues after etoposide exposure	135
Figure 3.11: Phosphoentities of BRCA1, Rad50, Rad51ap1 and Xrcc1 following etoposide exposure	136
Figure 3.12: Regulation of Abi1, Abl1 and BCR phosphoentities by BCR/ABL PTK expression.....	138
Figure 3.13: Regulation of Jun, Myc and Ncf2 phosphoentities by BCR/ABL PTK expression.....	139
Figure 3.14: Regulation of Kdm2a, Lig1, Top2a and Whsc1 phosphoentities by BCR/ABL PTK expression.....	140
Figure 3.15: Histone H1 phosphoentities are regulated by BCR/ABL PTK and etoposide (1)	142
Figure 3.16: Histone H1 phosphoentities are regulated by BCR/ABL PTK and etoposide (2)	143
Figure 3.17: Histone H1 phosphoentities are regulated by BCR/ABL PTK and etoposide (3)	144
Figure 3.18: Histone H1 phosphoentities are regulated by BCR/ABL PTK and etoposide (4)	145
Figure 3.19: Regulation of Clk3, Gnl3, Stk10, Incenp and Anln phosphoentities by BCR/ABL PTK and etoposide.....	146
Figure 3.20: Regulation of Anln and Zfp828 phosphoentities by BCR/ABL PTK and etoposide	147
Figure 3.21: Regulation of Bcl7c, DNA ligase 1 and Hmga1 phosphoentities by BCR/ABL PTK and etoposide.....	149
Figure 3.22: Regulation of Cbx3, Gatad2a, Hnrnpc and Safb2 by BCR/ABL PTK and etoposide	150
Figure 3.23: Different regulations of Mybbp1a phosphoentities by BCR/ABL PTK and etoposide (1).....	152
Figure 3.24: Different regulations of Mybbp1a phosphoentities by BCR/ABL PTK and etoposide (2).....	153
Figure 3.25: MDC1 dephosphorylation on serine 929 upon etoposide exposure	154
Figure 3.26: Different dynamics of MDC1 phosphoentities upon etoposide exposure and BCR/ABL PTK expression.....	155
Figure 3.27: Dynamics of Hemogen phosphorylation on serine 380 upon etoposide exposure and BCR/ABL PTK expression.....	156
Figure 3.28: Hemogen protein expression after etoposide exposure.....	157
Figure 3.29: Phosphosite mapping of Hemogen serine 380	158
Figure 3.30: Elution profile of peptides on an off-line high pH reversed phase.....	160
Figure 3.31: Hemogen pS380 in MSCV control Ba/F3 cells	161
Figure 3.32: Hemogen pS380 in MSCV Ba/F3 cells treated with etoposide.....	162
Figure 3.33: Hemogen pS380 with BCR/ABL PTK expression	163

Figure 3.34: Hemogen pS380 with BCR/ABL PTK expression and etoposide exposure	164
Figure 3.35: Absolute quantification of murine Hemogen pS380 upon etoposide exposure and in the presence of BCR/ABL PTK.....	165
Figure 3.36: Study of NF- κ B levels in nuclear samples following etoposide exposure in the presence of BCR/ABL PTK.....	166
Figure 3.37: Annotated Ingenuity pathway analysis for a subset of proteins consistently modulated by BCR/ABL PTK and etoposide	168
Figure 3.38: Dynamics of DDX21 and Baz1b/WSTF phosphoentities upon etoposide exposure and BCR/ABL PTK expression.....	169
Figure 3.39: H2AX phosphorylation on tyrosine 142.....	170
Figure 3.40: BCR/ABL PTK may regulate several phosphoproteins involved in the survival/death switch and genomic stability	180
Figure 4.1: Site directed mutagenesis of NPM/ALK PTK identified tyrosine 567 upstream of Thoc5/Fmip phosphorylation on tyrosine 225	186
Figure 4.2: Thoc5/Fmip phosphorylation on tyrosine 225 in response to etoposide, H ₂ O ₂ and 4-HNE oxidative stress.....	188
Figure 4.4: Effect of N-acetylcysteine on Thoc5/Fmip phosphorylation pY225	189
Figure 4.3: Etoposide-mediated Thoc5/Fmip phosphorylation on tyrosine 225 in the presence or not of BCR/ABL PTK.....	189
Figure 4.5: Nucleocytoplasmic distribution of Thoc5/Fmip and Thoc5/Fmip Y225F.....	191
Figure 4.6: Prediction of a nuclear export signal in Thoc5/Fmip sequence between leucine 622 and valine 631	193
Figure 4.7: Nucleocytoplasmic distribution study of Thoc5/Fmip phosphorylation at tyrosine 225 with and without Crm1/Exportin1-mediated nuclear export inhibition by leptomycin B	194
Figure 4.8: Kinase inhibition study on Thoc5/Fmip pY225.....	195
Figure 4.9: Combination of MEK1/2 inhibitor and etoposide in Ba/F3 cells.....	196
Figure 4.10: Combination of ATM or ABL inhibitors with etoposide in Ba/F3 cells.....	197
Figure 4.11: SFK and MEK1/2 inhibition impact on Thoc5/Fmip phosphorylation on tyrosine 225 after etoposide, H ₂ O ₂ and 4-HNE treatments.....	198
Figure 4.12: SFK inhibition impact on Thoc5/Fmip phosphorylation on tyrosine 225	199
Figure 4.13: Expression of vSrc and Src WT in MSCV Ba/F3 cells.....	200
Figure 4.14: Thoc5/Fmip phosphorylation on tyrosine 225 following SDF-1 treatment.....	201
Figure 4.15: Thoc5/Fmip phosphorylation on tyrosine 225 in CD45 WT and Null cells	202
Figure 4.16: Thoc5/Fmip phosphorylation on tyrosine 225 in K562 CML cell line.....	205
Figure 4.17: Thoc5/Fmip phosphorylation on tyrosine 225 in primary CML and non-CML CD34+ cells.....	206
Figure 4.18: Etoposide and H ₂ O ₂ -mediated apoptosis in Thoc5/Fmip WT and Y225F-expressing Ba/F3 cells.....	209
Figure 4.19: Comparison of Hsp40 and Hsp70 expression levels between control, Thoc5/Fmip WT and Y225F-expressing Ba/F3 cells.....	210
Figure 4.20: Hsp40 and Hsp70 expression levels with expression of Thoc5/Fmip WT and Y225F	212
Figure 4.21: Thoc5/Fmip phosphorylation on tyrosine 225 and its potential biological functions	219

LIST OF TABLES

Table I: Leukaemias and their association with protein tyrosine kinases.....	28
Table II: Parameters used for selected reaction monitoring for the native and the AQUA™ Hemogen peptides.....	116

LIST OF APPENDICES

Appendix 7.1: Representative histogram overlay of anti- γ H2AX-FITC fluorescence for control cells and cells exposed to etoposide.....	262
Appendix 7.2: Representative bivariate dot plots for etoposide-induced apoptosis in Ba/F3 cells in the presence or absence of BCR/ABL PTK	263
Appendix 7.3: Representative bivariate dot plots for etoposide-induced apoptosis in Thoc5/Fmip WT and Y225F-expressing Ba/F3 cells	264
Appendix 7.4: Number of proteins and phosphoentities identified by QSTAR® XL and QSTAR® Elite	265
Appendix 7.5: Phosphosite-specific action of BCR/ABL PTK only (1/2).....	266
Appendix 7.6: Phosphosite-specific action of BCR/ABL PTK only (2/2).....	267
Appendix 7.7: Phosphosite-specific crosstalk between BCR/ABL PTK and etoposide action (1/3).....	268
Appendix 7.8: Phosphosite-specific crosstalk between BCR/ABL PTK and etoposide action (2/3).....	269
Appendix 7.9: Phosphosite-specific crosstalk between BCR/ABL PTK and etoposide action (3/3).....	270
Appendix 7.10: Phosphosite-specific action of etoposide only (1/3)	271
Appendix 7.11: Phosphosite-specific action of etoposide only (2/3)	272
Appendix 7.12: Phosphosite-specific action of etoposide only (3/3)	273
Appendix 7.13: Identification of Thoc2 and Thoc5/Fmip phosphoentities.....	274
Appendix 7.14: Background determination for the transitions of the native and AQUA™ Hemogen peptide in nuclear material	275

ABSTRACT

François Griaud

The University of Manchester

24/10/11

PhD thesis title: Proteomic analysis of leukaemogenic protein tyrosine kinase action

Introduction: Chronic myeloid leukaemia is a blood cancer which progresses from a chronic phase to an acute blast crisis if untreated. Disease progression and treatment resistance may be precipitated by the mutator action of BCR/ABL protein tyrosine kinase (PTK), but only few protein phosphosites involved in the DNA damage response have been investigated with respect to BCR/ABL action.

Aim: The aim of this PhD project was to demonstrate that BCR/ABL PTK expression can affect the response to genotoxic stress signalling at the protein phosphorylation level.

Methodology: Etoposide-induced DNA damage response has been studied in control and BCR/ABL PTK-expressing Ba/F3 cells using apoptosis and γ H2AX assays. Quantitative phosphoproteomics was performed with iTRAQTM peptide labelling to discover putative modulated phosphorylation sites. Absolute quantification (AQUATM) performed with selected reaction monitoring was used to validate discovery phosphoproteomics. The effect of genotoxic stress on the THO complex protein Thoc5/Fmip was studied using western blots.

Results: The expression of BCR/ABL PTK induced γ H2AX phosphorylation after etoposide exposure. This was associated with the modulation of H2AX tyrosine 142 phosphorylation, MDC1 (serines 595 and 1053) and Hemogen serine 380 phosphorylation among proteins regulated by both BCR/ABL PTK and etoposide. We identified that leukaemogenic PTKs mediate Thoc5/Fmip phosphorylation on tyrosine 225 *via* Src proto-oncogene and oxidative stress, while ATM and MEK1/2 may control its phosphorylation. Human CD34⁺ CD38⁻ leukaemic stem cells showed pronounced level of THOC5/FMIP tyrosine phosphorylation. Expression of phosphomutant Thoc5/Fmip Y225F might reduce apoptosis mediated by etoposide and H₂O₂.

Conclusion: BCR/ABL PTK can sustain, create, block and change the intensity of protein phosphorylation related to genotoxic stress. Modulation of H2AX, MDC1, Hemogen and Thoc5/Fmip post-translational modifications by BCR/ABL PTK might promote unfaithful DNA repair, genomic instability, anti-apoptotic signalling or abnormal cell differentiation, resulting in leukaemia progression.

DECLARATION

No portion of the work referred to in the thesis has been submitted in support of an application for another degree or qualification of this or any other university or other institute of learning.

The thesis contains data obtained and used with permission from Dr. Andrew Pierce of The University of Manchester (Figures 4.1 and 4.5-B) as well as from Prof. Tessa Holyoake and Dr. Mary Scott of the Paul O'Gorman Leukaemia Research Centre at the University of Glasgow (Figures 4.16 and 4.17).

COPYRIGHT STATEMENT

- i. The author of this thesis (including any appendices and/or schedules to this thesis) owns certain copyright or related rights in it (the "Copyright") and s/he has given The University of Manchester certain rights to use such Copyright, including for administrative purposes.
- ii. Copies of this thesis, either in full or in extracts and whether in hard or electronic copy, may be made **only** in accordance with the Copyright, Designs and Patents Act 1988 (as amended) and regulations issued under it or, where appropriate, in accordance with licensing agreements which the University has from time to time. This page must form part of any such copies made.
- iii. The ownership of certain Copyright, patents, designs, trade marks and other intellectual property (the "Intellectual Property") and any reproductions of copyright works in the thesis, for example graphs and tables ("Reproductions"), which may be described in this thesis, may not be owned by the author and may be owned by third parties. Such Intellectual Property and Reproductions cannot and must not be made available for use without the prior written permission of the owner(s) of the relevant Intellectual Property and/or Reproductions.
- iv. Further information on the conditions under which disclosure, publication and commercialisation of this thesis, the Copyright and any Intellectual Property and/or Reproductions described in it may take place is available in the University IP Policy (see <http://www.campus.manchester.ac.uk/medialibrary/policies/intellectual-property.pdf>), in any relevant Thesis restriction declarations deposited in the University Library, The University Library's regulations (see <http://www.manchester.ac.uk/library/aboutus/regulations>) and in The University's policy on presentation of Theses.

LIST OF ABBREVIATIONS

γ H2AX: histone H2AX phosphorylated on serine 139
 μ g: microgram
 μ L: microliter
 μ M : micromolar
 μ m: micrometer
2D: two-dimensional
3D: three-dimensional
4-HNE: 4-hydroxynonenal
53BP1: tumour suppressor p53-binding protein 1
7-AAD: 7-aminoactinomycin D
ABL: Abelson protein tyrosine kinase 1
ABLi: inhibitor of Abelson protein tyrosine kinase 1
AC: alternating current
AGM: aorta-gonad-mesonephros
AID: activation-induced cytidine deaminase
AKT: protein kinase B
ALCL: anaplastic large cell lymphoma
ALK: anaplastic lymphoma kinase
ALL: acute lymphoid leukaemia
AML: acute myeloid leukaemia
ANN : artificial neural network
AP-1 : transcription factor activator protein 1
APC: allophycocyanin
APS: ammonium peroxodisulfate
AQUA™: absolute quantification
ATCC: American type culture collection
ATM : ataxia telangiectasia mutated serine/threonine protein kinase
ATMi: inhibitor of ataxia telangiectasia mutated serine/threonine protein kinase
ATP: adenosine-5'-triphosphate
ATR: ataxia telangiectasia and Rad3-related protein
ATRIP: ATM and Rad3-related-interacting protein
Ba/F3: pro-B cell line derived from BALB/c mouse
BALB/c: type of albino mouse strain
BAX: Bcl-2-like protein 4
Baz1b : bromodomain adjacent to zinc finger domain protein 1B
Bcl7c: B-cell CLL/lymphoma 7 protein family member C
BCR/ABL: breakpoint cluster region/Abelson
BCR: breakpoint cluster region
BER: base excision repair
BID: BH3-interacting domain death agonist

BLM: Bloom syndrome protein
BRCA1: breast cancer type 1 susceptibility protein
BSA: bovine serum albumin
B-WICH complex: WSTF-ISWI (imitation switch protein) chromatin remodelling complex associated with other nuclear proteins
C: coulombs
C/EBP α : CCAAT/enhancer-binding protein alpha
C₁₈: alkyl chain composed of 18 atoms of carbon
C57BL/6: type of black mouse strain
CAF-1: chromatin-assembly factor 1
Cbx3: chromobox protein homolog 3
CD: cluster of differentiation
CD45 : receptor-type tyrosine-protein phosphatase C
CDK: cyclin-dependent kinase
cDNA: complementary deoxyribonucleic acid
CE: collision energy
CFU(-S): colony-forming unit-spleen
CHK: checkpoint kinase
CHK1: checkpoint kinase 1
cIAP: cellular apoptosis inhibitor IAP
CID: collision-induced dissociation
CLL: chronic lymphoid leukaemia
CLP: common lymphoid progenitor
cm: centimeter
CML: chronic myeloid leukaemia
CMML: chronic myelomonocytic leukaemia
CMP: common myeloid progenitor
CNL: chronic neutrophilic leukaemia
CPC: chromosomal passenger complex
cps: counts per second
CRKL: oncogene Crk-like protein
CtIP: DNA endonuclease c-terminal-binding protein (CtBP)-interacting protein
CXCL12: C-X-C motif chemokine 12
CXCR4: C-X-C chemokine receptor type 4
D Domain: docking domain
Da: Dalton
DAPI: 4',6-diamidino-2-phenylindole
DDX21: nucleolar RNA helicase DEAD box protein 21
DEAD box: amino acid sequence motif composed of aspartic acid (D), glutamic acid (E), alanine (A) and aspartic acid (D)
DHB: 2,5-dihydroxybenzoic acid
DMEM: Dulbecco's modified eagle medium

DNA: deoxyribonucleic acid
DNA-PKcs: DNA protein kinase catalytic subunit
DSB: double strand break
DSBR: double strand break repair
DSBs: double strand breaks
ECL: enhanced chemiluminescence
EDTA: ethylenediaminetetraacetic acid,
EGFR: epidermal growth factor receptor
Ei24: etoposide-induced protein 24
ELKS: regulatory subunit of the IKK (inhibitor of nuclear factor kappa-B kinase) complex
EMBL: European molecular biology laboratory
EMSA: electrophoretic mobility shift assay
ERG: Ets-related gene
ERK: extracellular signal-regulated kinase
ESI: electrospray ionisation
ET: essential thrombocythaemia
Ets: transcription factor E26-AMV virus oncogene cellular homolog
EYA1/3: eyes absent homolog 1/3
FA: Fanconi anaemia
FACS: fluorescence activated cell sorting
FANCD2: Fanconi anaemia group D2 protein
FCS: fetal calf serum
FDCP-mix: factor-dependent cell Paterson-mix progenitor cell line
FDR: false discovery rate
FITC: fluorescein isothiocyanate
FLT3/ITD: Fms-related tyrosine kinase 3 with internal tandem duplication
FLT3: Fms-like tyrosine kinase 3
FMIP: Fms-interacting protein
fmol: femtomole
Fms: protein tyrosine kinase product of the oncogene of the McDonough strain of feline sarcoma virus
FTICR: Fourier transform ion cyclotron resonance
FTK : fusion tyrosine kinase
g: gram
GAPDH: glyceraldehyde-3-phosphate dehydrogenase
Gatad2a: GATA zinc finger domain-containing protein 2A
G-CSF: granulocyte colony-stimulating factor
GM-CSF: granulocyte macrophage colony-stimulating factor
GEF: guanine nucleotide exchange factor
GFP: green fluorescent protein
GPAM: amphotropic retroviral env glycoprotein GP+envAm12
h: hours

HBSS: Hank's buffered salt solution
HDAC: histone deacetylase
HEL/CEL: hypereosinophilic syndrome/chronic eosinophilic leukaemia
HEPES: 4-(2-hydroxyethyl)-1-piperazineethanesulfonic acid
HMM: hidden Markov model
hnRNPE2: heterogeneous nuclear ribonucleoprotein E2
HP1 α : heterochromatin protein 1 alpha
Hpr1: hyperrecombination protein 1 (Thoc1)
HR: homologous recombination
HRP: horseradish peroxidase
HRR : homologous recombination repair
HSF: heat shock factor
Hsp: heat shock protein
Hz: Hertz
IAP1: inhibitor of apoptosis 1
ICAT: isotope-coded affinity tags
IDA: information-dependent acquisition
IEX: ion exchange chromatography
IKK : inhibitor of nuclear factor kappa-B kinase
IL-3: interleukin-3
IMAC: ion metal affinity chromatography
IMF: idiopathic myelofibrosis
IP: immunoprecipitation
IRES: internal ribosome entry site
iTRAQTM: isobaric tags for relative and absolute quantification
I κ B : inhibitor of nuclear factor kappa-B (NF- κ B)
JAK/STAT: Janus kinase/signal transducer and activator of transcription
JAK2: Janus kinase 2
JAK2V617F: point mutation at position 617 from valine to phenylalanine on Janus kinase 2
JNK: Jun N-terminal kinase
K562: human erythromyeloblastoid leukemia cell line
kDa: kiloDalton
KEGG: Kyoto encyclopedia of genes and genomes
KLS: c-KIT Lineage (Lin) Sca
L: liter
LASER: light amplification by stimulated emission of radiation
LC/MS: liquid chromatography coupled to mass spectrometry
LC: liquid chromatography
Lck: lymphocyte cell-specific protein-tyrosine kinase
LC-SRM: liquid chromatography coupled to selected reaction monitoring
LIF: leukaemia inhibitory factor
Lin-: lineage negative cells
LIT: linear ion trap

Lok : lymphocyte-oriented kinase
m/z: mass-to-charge ratio
M: molar
MALDI: matrix-assisted LASER desorption ionisation
MAPK: mitogen-activated protein kinases
mAU: milliabsorbance unit
M-CSF: macrophage colony-stimulating factor
MDC1: mediator of DNA damage checkpoint protein 1
MEFs: mouse embryonic fibroblasts
MEK1/2: dual specificity mitogen-activated protein kinase kinase 1 (MAPK/ERK kinase 1)
MEK1/2i: inhibitor of MEK1/2
mg: milligram
mIL-3: murine interleukin 3
min: minutes
MIP- α : macrophage inflammatory protein 1 alpha
mL: milliliter
MLL: mixed lineage leukaemia
mM: millimolar
mmol: millimole
MMTS: methyl methanethiosulfonate
mmu: millimass unit
MPD: myeloproliferative disorders
MRE11: meiotic recombination 11 homolog 1
MRM: multiple reaction monitoring
MRN: MRE11-RAD50-NBS1 complex
mRNA: messenger ribonucleic acid
mRNP: messenger ribonucleoprotein particle
MS: mass spectrometry
MSCV: murine stem cell virus
MSDB: mass spectrometry database
MudPIT: multi-dimensional protein identification technology
Myc: proto-oncogene Myc
NAC : N-acetylcysteine
NADPH: nicotinamide adenine dinucleotide phosphate
NaOH: sodium hydroxide
NBCS: new born calf serum
NBS1: Nijmegen breakage syndrome protein 1
NDR: negative differentiation regulator
NEMO: nuclear factor-kappa-B essential modulator
NER: nucleotide excision repair
NES: nuclear export signal
NFIL3: nuclear factor interleukin-3-regulated protein

NFS60: murine myeloblastic cell line established from murine leukemic cells
NF- κ B: nuclear factor-kappa-B
ng: nanogram
NHEJ: non-homologous end joining
NHS: N-hydroxysuccinimide
NIH/3T3 : National Institutes of Health/3-day transfer, inoculum 3×10^5 cells
NK: natural killer
nL: nanoliter
NLS: nuclear localization signal
nmol: nanomole
NOX: NADPH oxidase
NOXA: latin word for injury; protein which leads to caspase activation and apoptosis
NPM/ALK: nucleophosmin-anaplastic lymphoma kinase
O-domain: oligomerisation domain
ORF: open reading-frame
P: p-value of a statistical test
PAGE: polyacrylamide gel electrophoresis
Parp-1: poly [ADP-ribose] polymerase 1
pBI: plasmid with bidirectional promoter
PBS: phosphate buffer saline
pcDNA: plasmid with complementary deoxyribonucleic acid
pCRKL: phosphorylated oncogene Crk-like protein
PDGF-BB: dimeric platelet derived growth factor composed of B chains
PDGFR α/β : platelet derived growth factor receptor alpha/beta
PE: phycoerythrin
PerCP: peridinin-chlorophyll-protein
Ph: Philadelphia chromosome
pH: potential Hydrogen
PI3K: phosphatidylinositol 3-kinases
PI3Ki: inhibitor of phosphatidylinositol 3-kinases
PIKKs: phosphatidyl inositol 3-kinase-like serine/threonine protein kinases
PIP3: phosphatidylinositol (3,4,5)-triphosphate
PKA: protein kinase A
PKB: protein kinase B
PKcs: protein kinase catalytic subunit
PKC- α : protein kinase C alpha
pmol: picomole
PP2A: protein phosphatase 2A
PP4: protein phosphatase 4
ppm: parts per million
PST: proline-serine-threonine rich domain
PTB: phosphotyrosine domain

PTEN: phosphatase and tension homolog deleted on chromosome 10
PTK: protein tyrosine kinase
PTM: post-translational modification
PTPRC: protein tyrosine phosphatase receptor type C
PUMA: p53 up-regulated modulator of apoptosis
PV: polycythaemia vera
QqQ: quadrupole(quadrupole)quadrupole
QqTOF: quadrupole time-of-flight hybrid mass spectrometer
QTRAP: quadrupole/linear ion trap hybrid mass spectrometer
R: resolution
Rad: radiation
RCF: relative centrifugal force
RF: radiofrequency
RFC: replication factor C
RIPA : radio immunoprecipitation assay
RNA: ribonucleic acid
RNF8: E3 ubiquitin-protein ligase RING finger protein 8
ROS: reactive oxygen species
RP: reversed phase chromatography
RPA: replication protein A
RPMI: Roswell park memorial institute
RT-PCR: reverse transcriptase – polymerase chain reaction
s: seconds
SCALPL: stem cell and leukaemia proteomics laboratory
SCF: stimulating colony factor
SCX: strong cation exchange chromatography
SDF-1: stromal cell-derived factor 1
SDS: sodium dodecyl sulfate
SDS-PAGE: sodium dodecyl sulfate – polyacrylamide gel electrophoresis
SEM: standard error of the mean
SFKi: inhibitor of Src family kinases
SFKs: Src family kinases
SH: Src homology domain
Shc1: Src homology 2 domain-containing-transforming protein 1
SILAC: stable isotope labelling by amino acids in cell culture
SIMAC: sequential elution from IMAC
siRNA: small interfering ribonucleic acid
SOD: superoxide dismutase
Src: proto-oncogene identified in Rous sarcoma virus
SRM: selected reaction monitoring
SSA: single-strand annealing
SSB: single strand break

SSBR: single strand break repair
STAT: signal transducer and activator of transcription
Stk10: serine threonine kinase 10
SWI/SNF: switch/sucrose nonfermentable
TAC: tetrameric antibody complexes
TCEP: tris(2-carboxyethyl)phosphine
TCR: T-cell receptor
TEAB: triethylammonium bicarbonate
TEL/PDGFR β : transcription factor TEL/ platelet derived growth factor receptor beta
TEMED: N,N,N',N'-tetramethylethylenediamine
TER119: monoclonal antibody recognizing an antigen on murine erythroid cells
TFA: trifluoroacetic acid
Th: Thomson
THO: suppressors of the transcriptional defects of Hpr1 Δ (mutation of hyperrecombination protein 1) by overexpression
Thoc1: THO complex member 1 (Hpr1)
Thoc5/Fmip: THO complex subunit 5/ Fms-interacting protein
TiO₂: titanium dioxide
TOF: time-of-flight
TOPBP1: DNA topoisomerase 2-binding protein 1
TPA: 12-O-tetradecanoylphorbol-13-acetate
TPO-R: thymopoietin receptor
TREX: transcription/export complex
UK: United Kingdom
UPLC: ultra performance liquid chromatography
UV: ultraviolet
V(D)J: variable (diversity) joining
v/v: volume/volume
V: volts
vSrc: viral non-receptor tyrosine kinase from Rous sarcoma virus
w/v: weight/volume
Whsc1: Wolf-Hirschhorn syndrome candidate 1
WICH: WSTF-ISWI (imitation switch protein) chromatin remodelling complex
WINAC: WSTF including nucleosome assembly complex
WIP1: wild-type (wt) p53-induced protein phosphatase 1
WRN: Werner syndrome ATP-dependent helicase
WSTF: Werner syndrome transcription factor
WT: wild-type
XIC: extracted ion chromatogram
Y225F: mutation at position 225 from tyrosine to phenylalanine on Thoc5/Fmip protein
ZrO₂: zirconium dioxide

AMINO ACID CODE AND ISOTOPIC MASSES

Amino acid	Three letter code	One letter symbol	Composition	Monoisotopic mass (Da)
Alanine	Ala	A	C ₃ H ₅ NO	71.03711
Arginine	Arg	R	C ₆ H ₁₂ N ₄ O	156.10111
Asparagine	Asn	N	C ₄ H ₆ N ₂ O ₂	114.04293
Aspartic acid	Asp	D	C ₄ H ₅ NO ₃	115.02694
Cysteine	Cys	C	C ₃ H ₅ NOS	103.00919
Glutamic acid	Glu	E	C ₅ H ₇ NO ₃	129.04259
Glutamine	Gln	Q	C ₅ H ₈ N ₂ O ₂	128.05858
Glycine	Gly	G	C ₂ H ₃ NO	57.02146
Histidine	His	H	C ₆ H ₇ N ₃ O	137.05891
Isoleucine	Ile	I	C ₆ H ₁₁ NO	113.08406
Leucine	Leu	L	C ₆ H ₁₁ NO	113.08406
Lysine	Lys	K	C ₆ H ₁₂ N ₂ O	128.09496
Methionine	Met	M	C ₅ H ₉ NOS	131.04049
Phenylalanine	Phe	F	C ₉ H ₉ NO	147.06841
Proline	Pro	P	C ₅ H ₇ NO	97.05276
Serine	Ser	S	C ₃ H ₅ NO ₂	87.03203
Threonine	Thr	T	C ₄ H ₇ NO ₂	101.04768
Tryptophan	Trp	W	C ₁₁ H ₁₀ N ₂ O	186.07931
Tyrosine	Tyr	Y	C ₉ H ₉ NO ₂	163.06333
Valine	Val	V	C ₅ H ₉ NO	99.06841

The isotopic masses are included for amino acids within the amide bond. The mass of a peptide or a free amino acid can be obtained by adding the masses of both hydrogen (1.00782) and hydroxyl (17.00274) for the N-terminal and C-terminal sides, respectively [C: carbon, H: hydrogen, O: oxygen, N: nitrogen, S: sulfur].

ACKNOWLEDGEMENTS

I would like to deeply thank my supervisor, Prof. Anthony Whetton who offered me the opportunity to pursue a PhD in the Stem Cell and Leukaemia Proteomics Laboratory (SCALPL). I am glad that this project encompassed my original research proposal and I am also grateful that I could explore subjects beyond it. Also, I would like to thank Drs. Elaine Spooncer and Georges Lacaud, who in their role of co-supervisor and advisor, respectively, provided helpful advice and support throughout the PhD.

This project would not have been possible without the training, knowledge, judgement and technical support offered by Drs. Andrew Pierce “Andy”, Andrew Williamson “Wilf” and Ewa Jaworska. A big thank you to them! I also would like to thank Prof. Tessa Holyoake and Dr. Mary Scott from the Paul O’Gorman Leukaemia Research Centre at the University of Glasgow, for their great contribution to this thesis. Thank you also to Drs. John Griffiths and Richard Unwin for starting my training in mass spectrometry. I would like to thank Drs. Samuel Taylor, Emma Carrick, Michael Walker and Cong Zhou “Joe” for discussing different data analysis methods. Also, thank you Emma, Michael and John for giving me feedback and tips on data presentation and mass spectrometry. Thank you to Dave Potier for helping me with his QTRAP! I also would like to thank current and former members of the SCALPL group for the nice atmosphere they have created throughout these 3 years. Thank you to Drs. Stefan Meyer, Daniel White “Dan”, Claire Bristow, Liqun Zhang, Mark Aspinall-O’Dea, Sara Cadeco and Joanne Muter “Jo” for the nice daily chats. More particularly, I would like to thank Drs. Maria Belen Gonzalez Sanchez and Manuela Piazzini for the laughs, lively chats about European History and the support they generously offered at the beginning of the PhD.

Importantly, I would like to deeply thank the British Council and the Entente Cordiale Scholarship scheme for providing additional funding for the last year of this PhD, more particularly Mrs. Sarah Bagshaw, project manager, and Sara Gill, co-coordinator at the British Embassy, Paris. Also, I am very grateful to the British Society for Proteome Research (BSPR) for awarding me a Michael J. Dunn Fellowship to attend the BSPR meeting 2010 in Cambridge.

Finally, I would like to thank my friends and my family, especially my grand-parents Gabriel and Gisèle Griaud, for their questions, benevolence and for giving me inspiration in my life.

DEDICATION

To Emilie, Mum and Dad for their love and infinite support

Chapter 1.

Introduction

1.1. General introduction

Leukaemias and related disorders are blood cell cancers. In some instances there is strong evidence that these specific diseases are associated with and possibly caused by the abnormal expression of specific dysregulated protein tyrosine kinases. Such enzymes are able to catalyze the addition of a phosphate group onto tyrosine residues of key proteins, hence deregulating normal biological processes such as proliferation, differentiation and survival (Delhommeau, *et al* 2006). Protein tyrosine kinase inhibitors have been developed to treat patients but resistance may occur, especially in advanced phase of these diseases (Goldman and Melo 2008). Protein tyrosine kinase action can also promote genomic instability potentially caused by reactive oxygen species (ROS) enhanced production along with DNA damage misrepair and promotion of cell survival, allowing the acquisition of further phenotypes causing disease progression (Cramer, *et al* 2008, Nowicki, *et al* 2004, Skorski 2002).

The hypothesis tested in this project is that DNA damage sensing/repair as well as genotoxic stress signalling pathways may be altered in protein tyrosine kinase expressing leukaemic cells. The aim is to determine which proteins and events may create, sustain or alter genotoxic stress signalling to increase mutation frequency, leukaemia cell survival and proliferation. To answer this question, quantitative discovery phosphoproteomics as well as targeted analysis of protein phosphorylation have been applied to identify and compare events triggered by genotoxic stress between cells expressing or not a leukaemogenic protein tyrosine kinase.

By providing in-depth knowledge of disease progression mechanisms, proteomics may help to focus on key proteins for cancer therapy either with small kinase inhibitors, protein-protein interaction inhibitors, recombinant antibodies or interfering RNA technologies.

1.2. Haemopoiesis

In higher eukaryotic organisms like the human, blood is composed of a variety of specialized cells which exhibit specific functions. All these mature cells are unequivocally derived from haemopoietic stem cells, which function to maintain normal blood cell production called haemopoiesis (Weissman 2000). Haemopoiesis is the continuously regulated production of blood cells. Haemopoietic stem cells were first described by Till and McCulloch in 1961 (Till and McCulloch 1961). Injection of syngeneic bone marrow into potentially irradiated mice led to recovery of normal blood cell production. Some marrow cells formed macroscopic colonies, containing differentiated cell populations, called colony-forming units-spleen (CFU-S). These colonies, when resuspended, could give rise to further CFU-S after secondary transplant. Thus, the first property of haemopoietic stem cells, i.e. multipotency, is the ability to produce a wide range of haemopoietic cells. The second main characteristic of haemopoietic stem cells, the capacity of self-renewal, allows haemopoietic stem cells to maintain their own numbers.

Haemopoietic cell development can broadly be divided into four compartments including stem, progenitor, precursor and mature cells (Figure 1.1) in which two main compartments, called lymphoid and myeloid, can be described. The lymphoid lineage gives rise to lymphocyte B and T types which respectively are responsible for antibody production and cytotoxic immune response. Natural Killer cells (NK), mainly involved in regulating the immune response, also derive from this lineage. Conversely, the myeloid lineage contains five types of mature cells. Thrombocytes or platelets are required for blood clotting. Erythrocytes carry oxygen from lungs to organs. Granulocytes, sub-divided into neutrophils, basophils and eosinophils, are mainly important for fighting bacteria infection,

in inflammatory responses or in parasite and allergy responses respectively. Mast cells play a role both in allergy and defense against pathogens. Finally, monocytes help to fight infection by quickly differentiating into macrophages which can phagocytose pathogenic intruders. Growth, proliferation and differentiation are promoted by adequate expression of growth factors and/or cytokines by surrounding cells composing the stromal environment of the bone marrow (Whetton and Graham 1999). When cells mature, they usually reduce their size and their nucleo-cytoplasmic ratio. The nucleolus disappears and chromatin condenses. For granulocytes, nuclei are polymorphic, granules appear in the cytoplasm and specific membrane proteins are expressed.

Haemopoiesis takes place in different organs during the individual's life. The yolk sac has been shown to be the first site of primitive haemopoiesis during embryonic life, followed by liver and spleen which receive the first population of definitive stem cells coming from the aorta-gonad-mesonephros (AGM) embryonic mesoderm region (Whetton and Graham 1999). The haemopoietic lineage emerges from the haemangioblast after a haemogenic endothelium stage (Lancrin, *et al* 2009). After birth, haemopoiesis is maintained in bone marrow and develops also in vertebrae, ribs, sternum, skull, sacrum and pelvis at the adult age. When mature, cells can leave the bone marrow to access the appropriate tissue *via* the blood circulatory system.

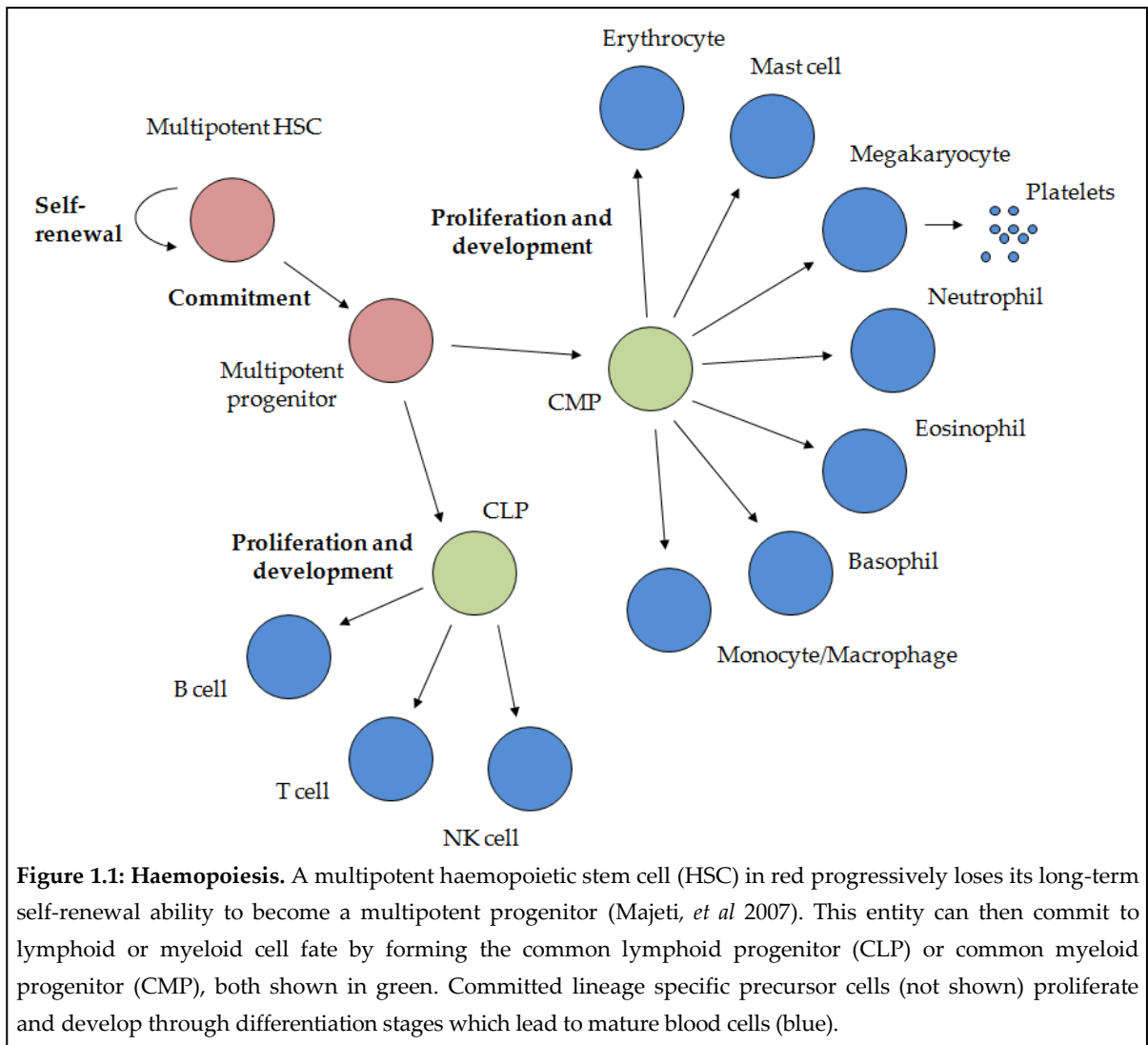


Figure 1.1: Haemopoiesis. A multipotent haemopoietic stem cell (HSC) in red progressively loses its long-term self-renewal ability to become a multipotent progenitor (Majeti, *et al* 2007). This entity can then commit to lymphoid or myeloid cell fate by forming the common lymphoid progenitor (CLP) or common myeloid progenitor (CMP), both shown in green. Committed lineage specific precursor cells (not shown) proliferate and develop through differentiation stages which lead to mature blood cells (blue).

1.3. Leukaemogenic protein tyrosine kinases and related diseases

Approximately 30,000 new cases of leukaemia, lymphoma, multiple myeloma and related blood disorders are diagnosed each year in the United Kingdom, corresponding to 8% of all cancers (Cancer Research UK 2011, Haematological Malignancy Research Network 2011). Blood cancer is the most common cause of cancer death in people aged 1-24 (Cancer Research UK 2011). Overall, around 7700 people were diagnosed with leukaemia in 2008 representing approximately 2.5% of all cancers, while around 3300 people were diagnosed with myeloproliferative disorders (MPDs) (Cancer Research UK 2011, Haematological Malignancy Research Network 2011). Leukaemia and MPDs result in an increase in the blood cell count but are classified separately according to the cell lineage affected and their different molecular signatures (Smith, *et al* 2003, Tefferi and Gilliland 2007). Thus there are different types of leukaemias, for example chronic myeloid leukaemia (CML), chronic lymphoid leukaemia (CLL), acute myeloid leukaemia (AML) and acute lymphoid leukaemia (ALL). MPDs include polycythaemia vera (PV), essential thrombocythaemia (ET), idiopathic myelofibrosis (IMF), chronic neutrophilic leukaemia (CNL) and hypereosinophilic syndrome/chronic eosinophilic leukaemia (HES/CEL) among other premalignancies. Chronic myelomonocytic leukaemia (CMML) is classified separately in “mixed myelodysplastic syndromes and myeloproliferative disorders”.

Leukaemogenic protein tyrosine kinases have been identified and studied as potential causes of several different blood cancers and MPDs (Delhommeau, *et al* 2006, Smith, *et al* 2003, Tefferi and Gilliland 2007, Turner and Alexander 2006). A subset of these fusion or mutated protein kinases will be presented in the following sections as well as in Table I.

Table I: Leukaemias and their association with protein tyrosine kinases

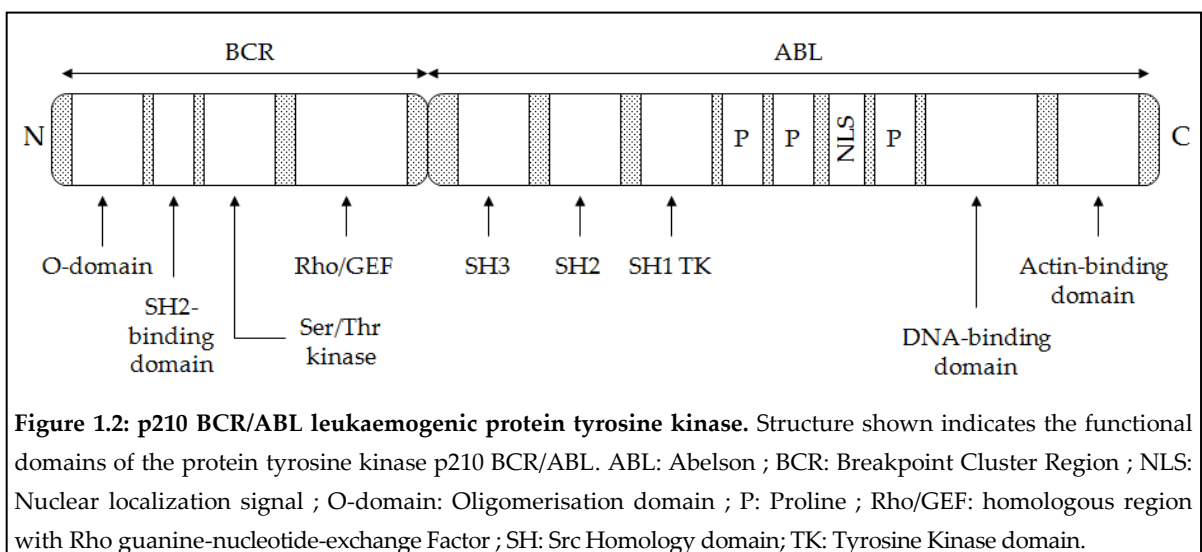
Disease	Protein tyrosine kinase	Chromosomal rearrangement / mutation	References
CML	BCR/ABL	t(9;22)(q34;q11)	(Rowley 1973)
AML	FLT3	ITD at 13q12 and "activation loop" mutations	(Gilliland and Griffin 2002)
	KIT	Point mutation (D816V)	(Beghini, <i>et al</i> 2000, Furitsu, <i>et al</i> 1993, Kitayama, <i>et al</i> 1995)
CMML	TEL/PDGFR β	t(5;12)(q33;p13)	(Keene, <i>et al</i> 1987, Lerza, <i>et al</i> 1992)
Mastocytosis	KIT	Point mutation (D816V)	(Longley, <i>et al</i> 1999, Nagata, <i>et al</i> 1995)
CEL	FIP1/PDGFR α	del(4)(q12;q12)	(Gotlib, <i>et al</i> 2004)
ALL	BCR/ABL	t(9;22)(q34;q11)	(Basecke, <i>et al</i> 2002, Castor, <i>et al</i> 2005)
	FLT3	ITD at 13q12 and "activation loop" mutations	(Gilliland and Griffin 2002)
MDS	FLT3	ITD at 13q12 and "activation loop" mutations	(Gilliland and Griffin 2002)
MPD	JAK2	Point mutation (V617F, K539L)	(James, <i>et al</i> 2005, Levine, <i>et al</i> 2005, Tefferi and Gilliland 2007)
	MPL	Point mutation (W515L)	(Pikman, <i>et al</i> 2006)
ALCL	NPM/ALK	t(2;5)(p23;q35)	(Morris, <i>et al</i> 1994)

Key: t=translocation, d=deletion, ITD=internal tandem duplication, CML=chronic myeloid leukaemia, AML=acute myeloid leukaemia, ALL=acute lymphoid leukaemia, CMML=chronic myelomonocytic leukaemia, CEL=chronic eosinophilic leukaemia, MDS=myelodysplastic syndrome, MPD=myeloproliferative disease, ALCL=anaplastic large cell lymphoma

1.3.1. BCR/ABL and chronic myeloid leukaemia (CML)

Chronic myeloid leukaemia (CML) is an acquired clonal malignancy and is a haemopoietic stem cell disease (Fialkow, *et al* 1967, Fialkow, *et al* 1977). Diagnosed by abnormal white blood and immature cell counts, this myeloid disease progresses slowly with few specific symptoms during the chronic phase, lasting about four to six years, then it evolves to accelerated and blast phases, which last three to nine months. Blast crisis is related to the differentiation arrest and expansion of blast cells, of myeloid (60%), B lymphoid (30%) or biphenotypic myeloid/lymphoid (10%) lineage (Calabretta and Perrotti 2004, Klemm, *et al* 2009). Early research deemed that 90% of CML patients display a somatic chromosomal translocation t(9;22) (q34;q11), hence resulting in the shortened chromosome 22 called Philadelphia (Ph) chromosome, first described in 1960 (Basecke, *et al* 2002, Nowell and Hungerford 1960). This event leads to the fusion of two genes carried by these two chromosomes thereby expressing a fusion tyrosine kinase called breakpoint cluster region/Abelson (BCR/ABL) (Figure 1.2). However, the chromosomal translocation should not be considered as a strict indicator of clinical symptoms but rather as a predisposing factor for the disease (Basecke, *et al* 2002). Nonetheless, BCR/ABL PTK is the hallmark of CML, while this oncoprotein is found in 5% and 25% of childhood and adult B-ALL, respectively (Basecke, *et al* 2002) and it is estimated to be the molecular entity of approximately 15% of all myeloproliferative diseases (Delhommeau, *et al* 2006). The expression of different protein tyrosine kinase isoforms results from different breakpoint possibilities on BCR gene. Most of the cases in CML are caused by the expression of a 210 kilodalton (kDa) PTK (p210) whereas a 190 kDa PTK (p190) is required for *de novo* AML (Benneriah, *et al* 1986, Daley, *et al* 1990, Delhommeau, *et al* 2006) as well as adult (50% of isoforms) and children (80% of isoforms) Ph+ B-ALL cases, respectively (Druker, *et al* 2001, Hu, *et al* 2004, Sawyers 1999). A third PTK isoform (p230) can also lead to a less aggressive CML (Basecke, *et al* 2002). All isoforms can promote myeloid or lymphoid leukaemias (Klco, *et al* 2008, Li, *et al* 1999), although difference may exist between isoforms as p190 BCR/ABL may originate in committed B-cell progenitors and p210 BCR/ABL in multipotent haemopoietic stem cells (Castor, *et al* 2005). Tetramerisation is a property of

BCR/ABL PTK due to a coiled coil motif found in the BCR sequence (Warmuth et al., 1999). Also, the BCR gene encodes a serine/threonine kinase (Figure 1.2). This seems to be inhibited by ABL kinase activity on BCR tyrosine 328 and 360 (Arlinghaus 2002, Maru and Witte 1991). The BCR/ABL fusion gene leads to the activation of the ABL tyrosine kinase which affects many protein post-translational modifications for the oncogenic transformation. BCR/ABL has been shown to affect proteins in multiple signalling pathways like RAS, MAPK, PI3K/AKT, NF- κ B, CRKL, JAK/STAT, Src for the promotion of cell survival and proliferation but also proteins involved in DNA repair mechanisms such as homologous recombination (HR) or non-homologous end joining (NHEJ) (Delhommeau, et al 2006, Jagani, et al 2008, Slupianek, et al 2006, Slupianek, et al 2001, Smith, et al 2003, Warmuth, et al 1999). It has been suggested that genomic instability mediated by BCR/ABL PTK promotes disease progression to blast crisis (Skorski 2002). Thus other events or oncogene pathways may be acquired and potentially required during disease progression such as mutations in p53, p16^{INK4a} and Rb genes, translocations like t(8;21)(q22;q22) (AML1-ETO) and t(3;21)(q26;q22) (AML1-EV11) as well as other abnormalities (Calabretta and Perrotti 2004, Delhommeau, et al 2006, Dierov, et al 2009). The differentiation blockade characterising the blast crisis is thought to be caused by the inhibitory action of induced hnRNP E2 on the translation of CEBPA mRNA in the presence of BCR/ABL PTK, and the consequent downregulation of C/EBP α protein involved in granulocytic differentiation (Perrotti, et al 2002).



A BCR/ABL kinase inhibitor, called imatinib mesylate (imatinib), is used to maintain patients in chronic phase for prolonged periods. Imatinib stabilizes a BCR/ABL inactive conformation by competitively inhibiting the ATP-binding site of the tyrosine kinase domain. Sixty to seventy percents of patients demonstrated cytogenetic remission after 5 years of imatinib treatment (Slupianek, *et al* 2011a). However, resistance mechanisms such as point mutations in the different protein domains, including the ATP binding site, which block the inhibitor binding can affect therapy efficiency, the most frequent being the gatekeeper T315I mutant (Branford and Hughes 2011, Nardi, *et al* 2004). Gene amplification and alternative splicing may also promote imatinib resistance (Gruber, *et al* 2006). However, other proteins have also been linked to imatinib and nilotinib (a second generation tyrosine kinase inhibitor) resistance in CML cells like Hsp70 and the Src family kinases Lyn and Hck, the latter being also required for myeloid cell transformation and the induction of B-ALL by BCR/ABL PTK (Donato, *et al* 2003, Gioia, *et al* 2011, Hu, *et al* 2004, Klejman, *et al* 2002, Pene-Dumitrescu and Smithgall 2010, Pocaly, *et al* 2007, Rubbi, *et al* 2011). Treatment with second generation inhibitors dasatinib and nilotinib, which can inhibit Src family kinases but not the T315I mutant, enable 40 to 50 % of patients having previously not responded to imatinib to achieve cytogenetic remission but 20% of patients still remain resistant (Deguchi, *et al* 2008, Slupianek, *et al* 2011a, Talpaz, *et al* 2006). Importantly, the CML patients whose disease is managed long term by BCR/ABL PTK inhibitors can still harbor the BCR/ABL transcript in the CD34+ CD38- primitive cell compartment, despite complete cytogenetic response (Bhatia, *et al* 2003, Corbin, *et al* 2011). This cancer stem cell population is believed to be the source of relapse and understanding further the functions of BCR/ABL PTK may enable the development of new strategies to extinguish this resistant cell population in patients.

1.3.2. JAK2 mutants and Ph-negative myeloproliferative diseases (MPDs)

The Janus Kinase 2 (JAK2) binds to the cytoplasmic domain of many cytokine receptors (e.g. G-CSF, Epo, TPO-R). JAK2 is activated by transphosphorylation, and in turn can activate PI3K, STAT5 and RAS-MAPK signalling pathways in response to various cytokines (Delhommeau, *et al* 2006, James, *et al* 2005, Levine, *et al* 2005). Remarkably, JAK2 has been shown to modulate BCR/ABL protein stability and signalling by phosphorylation on tyrosine 177 (Samanta, *et al* 2011). Polycythaemia vera (PV), essential thrombocythaemia (ET) and idiopathic myelofibrosis (IMF) are diseases which do not exhibit the Philadelphia chromosome (Ph), but instead have been related to the constitutive activation of mutated JAK2 V617F in 90% (PV), 70% (ET) and 50% (IMF) of the cases respectively (Delhommeau, *et al* 2006, James, *et al* 2005, Levine, *et al* 2005). JAK2 V617F may account for 30-35 % of all MPDs (Delhommeau, *et al* 2006). PV is characterized by high red blood and platelet cell counts, leading to blood thickness and higher risks of stroke or heart attack. High platelet cell count can also be a hallmark of ET which is due to abnormal megakaryocytes in bone marrow. In IMF, megakaryocytes abnormally stimulate fibroblasts to secrete high amounts of fibrin, thickening bone marrow and progressively reducing haemopoiesis. The JAK2 mutation is acquired by a somatic mutation and other predisposing factors may be required to promote MPDs. Other mutations in JAK2 exon 12 such as K539L have also been related to MPDs (Scott, *et al* 2007, Tefferi and Gilliland 2007). Interestingly, JAK2 is also found in translocation with TEL t(9;12)(p24;p13), BCR t(9;22)(p24;q11.2) and PCM1 t(8;9)(p22;p24) in AML and unclassified MPDs (Tefferi and Gilliland 2007). JAK2 has been found to induce genomic instability by the induction of DNA damage and the modulation of DNA repair mechanisms such as homologous recombination (Cross, *et al* 2008), suggesting it may modulate common pathways with BCR/ABL PTK. A somatic point mutation in the thrombopoietin receptor (MPL) has also been detected (W515L) and related to 1% and 5% of ET and IMF, respectively (Pikman, *et al* 2006, Tefferi and Gilliland 2007).

1.3.3. FLT3 and acute myeloid/lymphoid leukaemia (AML/ALL)

Fms like tyrosine kinase 3 (FLT3) is overexpressed in AML, ALL and CML in blast crisis (Gilliland and Griffin 2002). AML is mainly characterized by elevated immature myeloid cell concentrations in bone marrow and consequently a reduction of differentiated neutrophils in blood. FLT3 receptor tyrosine kinase is normally expressed in haemopoietic stem and progenitor cells, while its constitutive activation is triggered by internal tandem duplication (ITD) of the juxtamembrane domain or point mutations on aspartic acid 835 (Gilliland and Griffin 2002, Sallmyr, *et al* 2008a). Activated FLT3 is found in approximately one third of AML patients. FLT3 signalling activates many pathways such as RAS-MAPK, PI3K and Src following normal stimulation by its ligand (Gilliland and Griffin 2002).

1.3.4. KIT mutants and acute myeloid leukaemia (AML)

C-KIT is a stem cell transmembrane receptor tyrosine kinase which triggers signalling from its ligand stem cell factor (SCF), secreted by stromal cells. In AML and in some cases of blast crisis in CML, c-KIT receptor autophosphorylation is activated without the stimulation of SCF, hence promoting constitutively cell proliferation. Moreover, autocrine activation of SCF has been proposed in AML cells (Kanakura, *et al* 1993). An activating point mutation has been shown in the cytoplasmic domain of c-KIT at codon 52, encoding for asparagine instead of aspartic acid (Boissan, *et al* 2000, Nakata, *et al* 1995). This mutation was found in patients suffering from IMF and CML. This mutation, close to the binding site of SCF, could change the c-KIT structure to the activated state. Also, another c-KIT mutation at position 816 leads to a substitution of aspartic acid to valine and is related to mastocytosis and mast cell leukaemia (Beghini, *et al* 2000, Furitsu, *et al* 1993, Kitayama, *et al* 1995). Interestingly, SCF stimulates mast cell motility (Meininger, *et al* 1992).

1.3.5. TEL/PDGFR β and chronic myelomonocytic leukaemia (CMML)

Chronic myelomonocytic leukaemia (CMML) shares common features between myelodysplastic syndromes and myeloproliferative disorders. It is characterized by an abnormal increase of monocytic blood cells in the blood and bone marrow. It has been associated with the chromosomal translocation t(5;12)(q33;p13) in 1 to 4% of cases which fuses two genes encoding respectively Ets Variant Gene 6 (ETV6, Tel oncogene) and the transmembrane/intracellular kinase domain of the PDGF receptor β (Golub, *et al* 1994). These patients may respond favourably with the use of imatinib. This chimeric cytosolic protein is not regulated by the binding of its ligand, PDGF-BB, but instead is constitutively activated and locates in the cytosol in oligomers (Jousset, *et al* 1997).

1.3.6. NPM/ALK and anaplastic large cell lymphoma (ALCL)

Nucleophosmin-anaplastic lymphoma kinase (NPM/ALK) t(2;5)(p23;q35) translocation is associated with anaplastic large cell lymphoma (ALCL). ALCL is a type of non-Hodgkin lymphoma, which affects T lymphocytes and null cells (expressing neither T nor B cell receptors) in the lymphatic tissue. NPM, a RNA binding protein involved in the regulation of p53 activity, centrosome duplication and DNA repair (Palmer, *et al* 2009, Turner and Alexander 2006), is fused with the cytoplasmic catalytic domain of ALK PTK. In fact, data suggest that t(2;5) is found in nonmalignant tissue and it could be expressed ubiquitously either for a survival advantage or an increase in genetic instability or both (Basecke, *et al* 2002). ALK PTK is important for embryonic development, more particularly for neuronal development. Notably, NPM/ALK PTK signalling includes Shc1 (Src homology 2 domain-containing-transforming protein 1), PI3K, MAPK as well as JAK/STAT pathways and results in the regulation of transcription factors such as FoxO3a and NF- κ B (Palmer, *et al* 2009). Many translocations of the ALK PTK have also been shown to play roles in non-small cell lung cancers, diffuse large B-cell lymphomas and squamous cell carcinoma (Palmer, *et al* 2009). ALK PTK can also be activated by point mutations in neuroblastoma

(Chen, *et al* 2008c, George, *et al* 2008, Janoueix-Lerosey, *et al* 2008, Mosse, *et al* 2008, Palmer, *et al* 2009).

1.3.7. Cell model for the study of leukaemogenic protein tyrosine kinases (PTKs)

The oncogenic potential of each leukaemogenic PTK described above was assessed by the ability to transform growth factor-dependent cells, such as Ba/F3 or FDCP-mix cell lines, to growth factor independence (Carroll, *et al* 1996, Daley and Baltimore 1988, Daley, *et al* 1987, Dosil, *et al* 1993, James, *et al* 2005, Kitayama, *et al* 1995, Levine, *et al* 2005, Pikman, *et al* 2006). Ba/F3 cells are murine interleukin-3 dependent pro-B cells isolated from BALB/c mouse bone marrow (Palacios and Steinmetz 1985). This cell line has been used to compare systematically the common and different signalling of leukaemogenic PTKs (Pierce, *et al* 2008b).

1.3.8. Conclusion

Several PTKs are associated with leukaemias. A multitude of translocations and mutations can arise in leukaemias from deficiencies in mechanisms of DNA repair, but the characteristics of only few of them are used to orientate the choice of therapy (Nickoloff, *et al* 2008, Zhang and Rowley 2006). The hypothesis that PTK action may have a role in disease progression and kinase inhibitor resistance by modulating DNA repair pathways has long been investigated with PTKs such as BCR/ABL PTK (Skorski 2002, Slupianek, *et al* 2002). CML progression as well as BCR/ABL PTK-mediated response to DNA damage is characterized by further chromosomal aberrations (Cramer, *et al* 2008, Dierov, *et al* 2009). This genomic instability is thought to result from the combination of three factors, i.e. DNA damage increase by reactive oxygen species (ROS) production (Cramer, *et al* 2008, Nowicki, *et al* 2004) as well as defect(s) in DNA repair and anti-apoptosis mechanisms (Burke and Carroll 2010, Skorski 2002).

1.4. Excessive production of reactive oxygen species (ROS) and its consequences on cell regulation and DNA integrity

1.4.1. Production and function of ROS in haemopoietic cells

A panel of transient molecules can result from the metabolism of oxygen. These compounds called reactive oxygen species (ROS) include superoxide anion (O_2^-), hydrogen peroxide (H_2O_2) and hydroxyl radical ($\cdot\text{OH}$). They are produced by cyclooxygenases, 5-lipoxygenases, xanthine oxidase and membrane-bound NADPH oxidases (NOX) after the stimulation of cytokine receptors or by the mitochondrial electron transport chain if the glycolytic pathway is saturated as a result of high ATP concentrations (Droge 2002). They play a major role in the “oxidative burst” of the phagocytic inflammatory response to fight pathogens but only a secondary role in apoptosis. Mice lacking NOX display susceptibility to infection (Droge 2002), but the functions of the different NOX family members expressed in haemopoietic progenitor cells are still poorly understood (Hole, *et al* 2011).

ROS are also involved in the regulation of multiple signalling pathways through protein modifications mediated by thiol/disulfide redox such as cysteine oxidation present in protein kinase domain like ataxia telangiectasia mutated (ATM), Src, the tumour suppressor p53 or in transcription factors like NF- κ B and AP-1 for efficient DNA binding (Ghaffari 2008). ROS could also mediate the degradation of I κ B, the inhibitor of NF- κ B, by the proteasome (Droge 2002). By contrast, oxidative stress can inhibit protein tyrosine phosphatases, such as PTEN, CDC25 or CD45 (Droge 2002, Ghaffari 2008, Migliaccio, *et al* 1999, Rider, *et al* 2003). Therefore multiple cell signalling can be affected by ROS, especially by hydrogen peroxide which fulfills the role of a second messenger (Droge 2002, Forman, *et al* 2010) when it activates PKC- α , JAK/STAT, PI3K/AKT and MAPK signalling pathways and modulate cell cycle progression following cytokine receptor activation (Iiyama, *et al* 2006). ROS are also responsible for the loss of the self-renewal property of haemopoietic

stem cells as they prime haemopoietic progenitor cells for differentiation (Ito, *et al* 2004, Owusu-Ansah and Banerjee 2009) and may affect the stem cell niche structure (Ghaffari 2008).

1.4.2. ROS are a source of DNA damage

ROS can react with different components of the cell, such as lipid, protein and DNA, and can induce genotoxic stress as well as apoptosis (Wiseman and Halliwell 1996). Although H_2O_2 and $^-\text{O}_2$ do not interact with bases, they can produce hydroxyl radical $\cdot\text{OH}$ with a Fenton reaction (Cooke, *et al* 2003). The hydroxyl radical is the most unstable ROS and its reaction with DNA bases can result in a variety of oxidated products from radical adducts such as the mutagenic 8-oxoguanine (Cooke, *et al* 2003). ROS reaction with DNA can result in multiple damage such as nucleotide oxidation, methylation, depurination and deamination (Wiseman and Halliwell 1996). Modified nucleotides could also be incorporated in DNA (Koptyra, *et al* 2006). These modifications can alter DNA conformation during replication or transcription, increase microsatellite instability and loss of heterozygosity. These modifications can also affect the binding of transcription factors to promoters leading to misregulated gene expression (Cooke, *et al* 2003). Hydroxyl radical $\cdot\text{OH}$ can also react with 2'-deoxyribose and sugar modification can lead to DNA strand breaks and spontaneous DNA double strand breaks (Cooke, *et al* 2003, Karanjawala, *et al* 2002). Lipid peroxidation can also induce DNA damage and affect lipid-mediated signalling while protein modifications can affect efficiency and fidelity of polymerases, topoisomerases and other chromatin remodelling factors during DNA replication and DNA repair processes, thus leading to DNA damage (Wiseman and Halliwell 1996). Finally, DNA protein cross-linking can also occur (Cooke, *et al* 2003).

Thus ROS can induce a variety of DNA damage which will be dealt by different DNA repair mechanisms such as base excision repair (BER), nucleotide excision repair (NER), DNA single and double strand break repair (SSBR/DSBR).

1.4.3. Antioxidant mechanisms in haemopoietic cells

Although ROS production is required for haemopoiesis, immunity and cell signalling, mechanisms have been developed to prevent DNA damage as well as misregulation of proliferation and differentiation. To do so, cells use a panel of antioxidant molecules and enzymes to reduce oxidative stress. Proteins, amino acids and other substances like glutathione can reduce cellular oxidative stress. Alternatively enzymes like superoxide dismutase (SOD), catalase and glutathione peroxidase work in cascade to help detoxify cells from ROS (Droge 2002). SOD family members are expressed close to the site of ROS production to enhance ROS detoxification (Hole, *et al* 2011). It has been shown that normal haemopoiesis relies on SOD antioxidant enzymes and the antioxidant response element is regulated by transcription factors Nrf1/2 (Ghaffari 2008). Targeted disruption of the SOD2 gene leads to embryonic or neonatal lethality in mice cells, suggesting this gene is important for development (Friedman, *et al* 2001). To determine the impact of SOD2 deficiency in the production of blood cells, Friedman and colleagues used SOD2 *-/-* cells obtained from fetal liver and transplanted them in lethally irradiated congenic mice. Although SOD2 *-/-* cells did reconstitute myeloid and lymphoid compartments, SOD2 *-/-* engrafted mice suffered from sideroblastic anaemia caused by erythroid cell development failure and protein oxidation in red blood cells.

The expression of peroxiredoxin-1, heme oxygenase-1 and cystine transporter xc- is induced by oxidative stress (Droge 2002, Rhee, *et al* 2005). Importantly, mice lacking functional peroxiredoxin-1 gene develop haemolytic anaemia as well as various malignant cancers in association with increased ROS production in erythrocytes and oxidative DNA damage (Neumann, *et al* 2003). Loss of peroxiredoxin-2 also leads to haemolytic anaemia, although it is compensated by erythropoietin expression (Lee, *et al* 2003). Peroxiredoxins reduce the intracellular level of hydrogen peroxide and thus block the activation of NF- κ B (Kang, *et al* 1998). N-acetylcysteine (NAC), a glutathione precursor, also blocks NF- κ B activation (Droge 2002, Magne, *et al* 2006). Moreover, the activation of AP-1 and NF- κ B

could control the expression of oxidoreductase gene Trx and SOD (Droge 2002, Kamata, *et al* 2005, Maehara, *et al* 2000).

The control of oxidative stress by these antioxidant enzymes is particularly important to maintain stem cell quiescence. Stem cell renewal and cell cycle progression are regulated by ATM which represses the level of ROS in coordination with tumour suppressor protein p53 and the Forkhead Box O (FoxO) transcription factor FoxO3 (Ghaffari 2008, Ito, *et al* 2004). ATM deficiency leads to an increase in ROS accumulation in haemopoietic stem cells, bone marrow failure as well as genomic instability and predisposes to neuronal degeneration, immunodeficiency and lymphomas (Barlow, *et al* 1996, Savitsky, *et al* 1995, Shiloh and Rotman 1996). Ito and colleagues demonstrated that ATM null haemopoietic stem cells lack long-term haemopoiesis reconstitution capacity in lethally irradiated mice, while this stem cell function deficiency is primarily linked to increased levels of ROS (Ito, *et al* 2004). Administration of the antioxidant NAC before and after bone marrow transplantation of ATM null c-KIT⁺ Lin⁻ Sca⁺ (KLS⁺) haemopoietic stem cells rescued their repopulating capacity in recipient mice. This response was associated with the inactivation of the tumour suppressor p16^{INK4a}-Rb pathway, while its activation was the cause of stem cell function deficiency found in these ATM null mice (Ito, *et al* 2004). Interestingly, p16^{INK4a} is a target of p38 MAPK, a kinase also playing a crucial role in the loss of self-renewal in haemopoietic stem cells (Bulavin and Fornace 2004, Bulavin, *et al* 2004, Ito, *et al* 2006). Using ATM null mice, the same group reported that p38 MAPK is activated by increasing levels of ROS associated with the loss of quiescence in ATM ^{-/-} haemopoietic stem cells. The inhibition of p38 MAPK restored repopulating capacity as well as quiescence of these cells so that it prevented bone marrow failure. Similarly, the mutation of the cytoplasmic signal transducer p66Shc can result in oxidative stress resistance and increases mammalian lifespan (Droge 2002, Ghaffari 2008, Migliaccio, *et al* 1999, Rider, *et al* 2003).

Interestingly, ATM expression has been found to be downregulated in FoxO3a null cells (Yalcin, *et al* 2008), while the functional interaction between ATM and FoxO3a has been

demonstrated (Tsai, *et al* 2008). This could suggest that the p16^{INK4a}-Rb pathway could be activated in the absence of FoxO3a to lead to self-renewal deficiency. Conversely, the tumour suppressor p53, a target of ATM in response to DNA damage, is activated in FoxO3 null cells, in which it may regulate apoptosis and cell cycle arrest (Cann and Hicks 2007, Yalcin, *et al* 2008). FoxO3 appears to play a fundamental role in the regulation of haemopoiesis, which cannot be fully complemented by other members of the FoxO family of transcription factors (Tothova, *et al* 2007, Yalcin, *et al* 2008). Importantly, deletion of FoxO3 results in loss of quiescence, increased levels of ROS, apoptosis and bone marrow failure in mice (Yalcin, *et al* 2008). During erythroid differentiation, FoxO3 protein expression increases, whereas the loss of FoxO3 results in ROS accumulation, oxidative damage, reduced life-span and poor cell maturation of erythrocytes (Marinkovic, *et al* 2007). However, these effects could be reverted with antioxidant treatment (Marinkovic, *et al* 2007). ATM, p53 and FoxO3 compose a network which protects stem cells and their clonal progeny from genomic instability by inducing the expression of the antioxidant enzymes SOD1, SOD2, catalase and glutathione peroxidase along with cell cycle control (Marinkovic, *et al* 2007, Yalcin, *et al* 2008).

As mentioned earlier ROS is required to prime stem cells for differentiation (Ito, *et al* 2004, Owusu-Ansah and Banerjee 2009). This is initiated by PI3K/AKT-mediated FoxO3 inactivation, whereas a feedback control induced by JNK later activates FoxO3 to reduce ROS and complete cell maturation (Ghaffari 2008, van der Horst and Burgering 2007). In contrast to FoxO deficient cells which show increased levels of ROS, apoptosis and loss of quiescence (Tothova, *et al* 2007), AKT deficiency shows an increase in quiescence associated with a decrease in ROS levels, while AKT activity itself blocks stem cell quiescence and leads to bone marrow failure (Juntilla, *et al* 2010, Kharas, *et al* 2010).

Finally, haemopoietic stem cells have adapted their metabolism to their hypoxic micro-environment by using preferentially glycolysis rather than mitochondrial oxidative phosphorylation to reduce damage caused by oxidative stress (Simsek, *et al* 2010, Unwin, *et al* 2006b).

1.4.4. Oxidative stress by leukaemogenic protein tyrosine kinases (PTKs)

As shown previously, it is important for haemopoietic cells to tightly control ROS homeostasis in order to reduce DNA damage and degeneration of specific biological functions. However, it has been shown that cells expressing fusion PTKs contain more ROS than control cells (Cramer, *et al* 2008, Nowicki, *et al* 2004, Skorski 2002). It is also the case with JAK2V617F expressing cells (Walz, *et al* 2006, Wernig, *et al* 2008). It has been demonstrated that BCR/ABL PTK increases ROS levels by the constitutive stimulation of the GTP-binding protein RAS which leads to the MAPK cascade activation (Sattler, *et al* 2000). RAS-mediated increase in ROS production has been shown to depend on NADPH oxidase stimulation and to result in growth factor independent proliferation of human haemopoietic progenitor CD34+ cells (Hole, *et al* 2010). Also, BCR/ABL PTK may enhance activation of NOX-4 NADPH oxidase and mitochondrial electron transport chain resulting in increase in ROS production and PI3K/AKT activation (Kim, *et al* 2005, Naughton, *et al* 2009, Sallmyr, *et al* 2008b), although ROS can also be downstream of PI3K signalling (Kim, *et al* 2005, Turner and Alexander 2006). Increase in ROS may affect proliferative, apoptosis and cell cycle responses, while NOX also regulates migration and cell growth in the presence of oncogenic tyrosine kinases (Reddy, *et al* 2011)

This increase in ROS concentrations can generate DNA damage such as 8-oxoguanine formation as well as mutations in the kinase domain of BCR/ABL PTK, resulting in imatinib resistance (Koptyra, *et al* 2006). Mutations could be the results of defective base excision repair (BER) and homologous recombination (HR) repair mechanisms (Koptyra, *et al* 2006). However, BCR/ABL PTK may in part protect cells from excessive oxidative stress by NF- κ B and STAT5 activation (Gesbert and Griffin 2000, Reuther, *et al* 1998, Sillaber, *et al* 2000, Stein and Baldwin 2011). Similarly, oxidative stress may promote AML progression and poor prognosis as FLT3/ITD PTK has been shown to phosphorylate STAT5 which binds Rac1 to activate NOX leading to ROS production, while STAT5 knock down reduces ROS expression (Sallmyr, *et al* 2008a, Sallmyr, *et al* 2008b). Although it has not been described yet, oxidative stress in CMML is expected to be increased due to the

high percentage of RAS mutations found in this disease (Hirschginsberg, *et al* 1990, Tefferi and Gilliland 2007). Interestingly, p38 MAPK activity enables cells to avoid transformation by RAS (Dolado, *et al* 2007). However, p38 MAPK activation by ROS is reduced in cancer cell lines and its downstream target p16^{INK4a} is down-regulated in AML which means the normal stress response is altered in cancer cells (de Jonge, *et al* 2009, Hole, *et al* 2011). Interestingly, the increase in ROS observed in the absence of FoxO3 enables the development of myeloproliferative syndrome by the amplification of cytokine signalling through the AKT pathway (Yalcin, *et al* 2010). In ALCL, NPM/ALK PTK enhances the production of ROS by the lipoxygenase enzyme family as well as cell survival by AKT-mediated inhibition of FoxO3a (Gu, *et al* 2004, Thornber, *et al* 2009). FLT3/ITD PTK has also been shown to inactivate FoxO3-mediated apoptosis (Scheijen, *et al* 2004). Thus, FoxO transcription factors appear to be particularly important targets for the regulation of cell survival downstream of PI3K/AKT, ROS and leukaemogenic PTKs. AKT activation and resulting FoxO3 proteasomal degradation in the presence of BCR/ABL PTK inhibits the transcription of pro-apoptotic and cell cycle genes but also blocks erythroid differentiation through Id1 upregulation (Birkenkamp, *et al* 2007, Ghaffari, *et al* 2003, Jagani, *et al* 2008). However, this degradation may happen only in c-KIT⁺ Lin⁻ Sca⁻ (KLS⁻) cells, which do not initiate leukaemia upon bone marrow transplantation (Naka, *et al* 2010). Naka and colleagues demonstrated that FoxO3 is activated in more primitive leukaemia-initiating cells c-KIT⁺ Lin⁻ Sca⁺ (KLS⁺), in correlation with reduced AKT phosphorylation. In this study, the activation of FoxO3a was required to generate leukaemia-initiating cells after serial bone marrow transplantation. FoxO3a, downstream of TGF- β signalling, promoted self-renewal capacity and imatinib resistance of leukaemia-initiating cells (Jagani, *et al* 2008, Naka, *et al* 2010).

Finally, FoxO binds to β -catenin upon oxidative stress and this association appears to regulate resistance to oxidative stress (Essers, *et al* 2005), while β -catenin activation enhances leukaemic stem cell self-renewal capacity in CML blast crisis (Jamieson, *et al* 2004).

1.4.5. Conclusion

In conclusion, leukaemogenic PTKs can modulate the production, the signalling and the effectors of both the oxidative stress response and stem cell quiescence (Figure 1.3). In turn, leukaemogenic PTKs have elaborated anti-apoptotic defence mechanisms against ROS genotoxicity thus increasing the probability to generate mutations from DNA damage in haemopoietic cells. As the genomic instability promoted by leukaemogenic PTKs may be involved in disease progression and imatinib resistance, the response elicited by DNA double strand breaks and its potential misregulations will be presented in the following section.

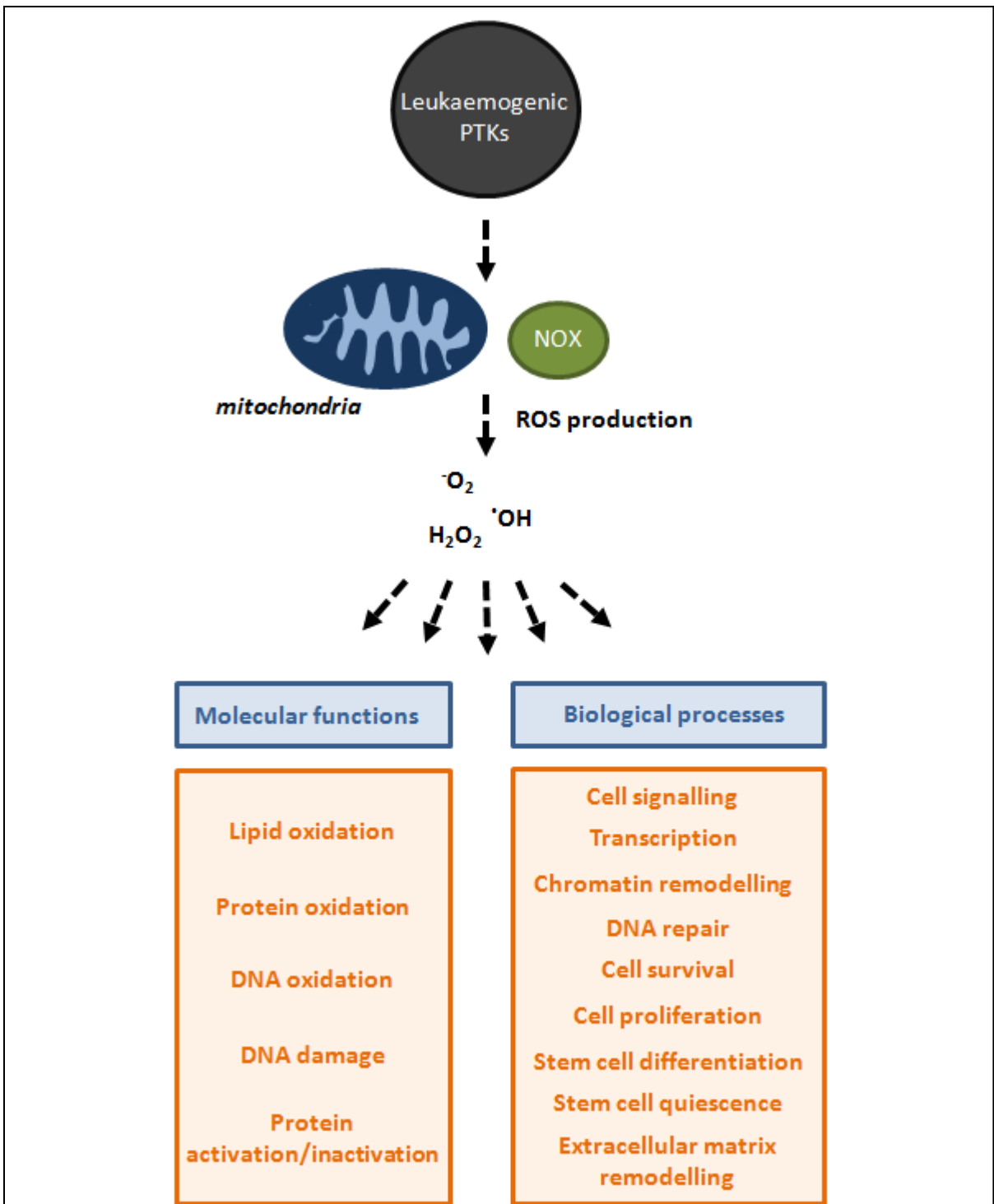


Figure 1.3: Leukaemogenic PTKs impair ROS functions. Leukaemogenic PTKs have been shown to promote reactive oxygen species (ROS) production by mitochondrial electron transport chain and NADPH oxidase (NOX) family members. ROS play a regulatory role in cellular signalling as second messengers by modulating the thiol/disulfide redox of cysteines in protein kinases or phosphatases. ROS can oxidize biomolecules such as lipid, DNA and protein thus affecting the functions of these entities and causing DNA damage. ROS and the control of oxidative stress homeostasis play fundamental roles in cell signalling, survival, proliferation and haemopoietic stem cell differentiation. Leukaemogenic PTKs alter the response to ROS by modulating proteins involved in oxidative stress response, stem cell quiescence and DNA repair among other biological processes.

1.5. DNA double strand break sensing/repair signalling

1.5.1. DNA double strand breaks

DNA double strand breaks (DSBs) are one of the most dangerous genotoxic events occurring in cells (Riches, *et al* 2008). They correspond to the breakage of both DNA strands in the same locus. Cells respond to them through several signalling cascades involving multiple protein post-translational modifications such as phosphorylation, methylation, ubiquitination or acetylation (Cohn and D'Andrea 2008, Lee, *et al* 2010b, Matsuoka, *et al* 2007, van Attikum and Gasser 2009). These cascades precipitate cell cycle arrest either to allow time for cells to repair the damage or to prevent excessive damage and unsuccessful repair to replicate before cell death. DNA DSBs can be repaired by homologous recombination (HR), non-homologous end joining (NHEJ) or single-strand annealing (SSA). Some of the DNA damage responses may be modulated to increase genomic instability (Cann and Hicks 2007), in the form of misrepairs, like mutations, deletions or even chromosomal translocations. Despite its toxicity, it has also been shown that DNA DSBs also have a functional role in differentiation when it occurs in V(D)J lymphocyte recombination or class switch recombination (Downs 2007).

To induce DNA DSBs ionizing radiation, drugs or ROS can be used. Etoposide, a topoisomerase 2 inhibitor, causes mainly DNA DSBs (Smart, *et al* 2008), although it may also generate single strand breaks and replication lesion DNA damage at low concentrations (Helleday, *et al* 2008, Montecucco and Biamonti 2007). Topoisomerase 2 cleaves and religates DNA strands to change DNA helical topology (Burden and Osheroff 1998). Etoposide reduces the DNA strand religation rate and increases the amount of covalent topoisomerase 2-DNA cleavage complexes. Permanent DNA DSBs are generated when replication and/or transcription machineries collide with these complexes (Burden and Osheroff 1998, Sung, *et al* 2006, Wang 2002). DNA cleavage as well as chromosomal aberrations induced by etoposide may be associated with therapy-related AML and

etoposide is usually found in treated patient serum at concentration ranging from 25 to 75 μM (Ratain and Rowley 1992, Sung, *et al* 2006).

1.5.2. Response to DNA double strand breaks

The DNA damage response is regulated by PIKKs (Phosphatidylinositol 3-kinase-like serine/threonine protein kinases). ATM and ATR (ATM and RAD3-related protein), among other proteins, belong to this family. Different DNA end structures activate these two kinases, as detailed below, and regulatory mechanisms of DNA end processing depending on cell cycle may lead to a switch between these two kinase partners and their respective downstream signalling (Cimprich and Cortez 2008, Shiotani and Zou 2009). ATM is activated rapidly irrespective of the cell cycle while ATR activation is slower and more efficient in S and G2 phases (Cimprich and Cortez 2008).

Free DNA ends seem to be first detected by the meiotic recombination protein-11 (Mre11)-Rad50-Nijmegen breakage syndrome protein-1 (Nbs1) or MRN complex (Figure 1.4), which is a heterohexameric complex. Both Mre11 and Rad50 bind to DNA (Jungmichel and Stucki 2010, Williams, *et al* 2007). One of the functions of the MRN complex is to maintain telomeres and the replication fork (Riches, *et al* 2008). Once the MRN complex has detected a DNA DSB, it interacts with the inactive dimeric ATM form, inhibited by the protein phosphatase 2 (PP2A). This interaction between the ATM catalytic domain and Nbs1 results in the autophosphorylation of ATM on human serine 1981 (murine serine 1987), the ATM dissociation from PP2A and ATM monomerisation (Riches, *et al* 2008) (Figure 1.4). This ATM activation can be observed very rapidly (30 sec-5 min) with a maximal activation after 15 min depending on experimental conditions, then this activated state decreases after 4 to 8 hours (Bakkenist and Kastan 2003, Horejsi, *et al* 2004). Another signalling pathway can result in the activation of ATR, usually activated by DNA single strand breaks. Thus, this pathway involves the end-resection of DNA DSBs and the recognition of a DNA single strand intermediate structure by replication protein A (RPA), Rad9-Rad1-Hus1 (9-1-1), topoisomerase binding protein 1 (TOPBP1), Rad17-

replication factor C (RAD17-RFC) and ATR interacting protein (ATRIP). End-resection of DNA DSBs by nucleases such as the MRN complex, CtIP or Exo1 progressively triggers the activation of ATR (Lamarche, *et al* 2010, Shiotani and Zou 2009) at the expense of ATM, although no post-translational modifications have as yet been correlated to this activation (Cimprich and Cortez 2008) (Figure 1.4).

Activated ATM phosphorylates mediator of DNA damage checkpoint protein 1 (MDC1), breast cancer type 1 susceptibility protein (BRCA1), tumour suppressor p53-binding protein 1 (53BP1) and the rare histone variant H2AX on serine 139 (Cann and Hicks 2007). This H2AX phosphorylated form, called γ H2AX, is detected a few minutes after DNA damage (Rogakou, *et al* 1998), recruits further MRN complexes and amplifies the DNA DSB sensing and signalling (Cimprich and Cortez 2008) (Figure 1.5). However, MDC1, BRCA1 and 53BP1 recruitment at site of DNA damage may not require γ H2AX (Cann and Hicks 2007). ATR and DNA PKcs are also involved in the γ H2AX activation (Riches, *et al* 2008, Rogakou, *et al* 1998), while γ H2AX dephosphorylation may be catalysed by PP2A, PP4, or WIP1 phosphatases, possibly in response to different DNA damage (Macurek, *et al* 2010, Nakada, *et al* 2008). It is now clear that the dynamics of H2AX post-translational modifications is crucial for cell fate. Tyrosine 142 has been recently found to be dephosphorylated upon DNA damage (Cook, *et al* 2009, Xiao, *et al* 2009) and this event, once coupled to serine 139 phosphorylation, is required for MDC1 binding to H2AX leading to cell survival and DNA repair (Figure 1.5). If both H2AX serine 139 and tyrosine 142 remain phosphorylated, the c-Jun N-terminal kinase 1 (JNK1), but not MDC1, is recruited to H2AX and cells undergo apoptosis (Cook, *et al* 2009). JNK1 is a stress response kinase which has been shown to phosphorylate H2AX on serine 139 and promote DNA fragmentation mediated by the aspartic-acid-specific cystein protease 3 (caspase 3) and caspase-activated DNase (CAD) (Lu, *et al* 2006). Interestingly, MDC1 is degraded by caspase 3 during apoptosis (Solier and Pommier 2011). Therefore, MDC1 recruitment is primordial for cells to survive and repair DNA damage. MDC1 is required for 53BP1 and BRCA1 accumulation and retention at DNA DSBs, through the activity of E3 ubiquitin ligase RNF8 (Figure 1.5). Importantly, MDC1, 53BP1 and BRCA1 interactions and

functions are regulated through the phosphorylation of specific residues (Jungmichel and Stucki 2010, Riches, *et al* 2008). MDC1 sustains MRN complex retention through phosphorylation of MDC1 SDT domain by casein kinase 2, although its initial recruitment is independent of MDC1. Importantly, several domains of MDC1 are involved in DNA damage checkpoint response (Jungmichel and Stucki 2010). Other histone phosphorylation may be involved in the death/survival switch (Solier and Pommier 2009). The switch in cell fate is depending on the balance of tyrosine 142 phosphorylation coordinated by the activities of EYA1/3 phosphatase and WSTF/Baz1b kinase (Stucki 2009), the latter protein being a versatile member of multiple chromatin remodelling complexes like WINAC, WICH and B-WICH, involved in transcription, DNA replication and DNA repair (Barnett and Krebs 2011) (Figure 1.5).

Another pathway can also result in cell survival. Once activated, ATM can bind to NEMO and NEMO ubiquitination results in their translocation to the cytoplasm (Habraken and Piette 2006). There, they associate with IKK(α/β) and ELKS and phosphorylates I κ B which will then be degraded by the proteasome. This event activates NF- κ B which translocates into the nucleus to regulate the expression of anti-apoptotic genes like Bcl-2 and c-IAP1/2 (Figure 1.6). It has been shown that c-IAP1 can inhibit pro-caspase3 (Deveraux, *et al* 1998, Deveraux, *et al* 1997), which has been shown in turn to inactivate MDC1 (see above). Intriguingly, NF- κ B activity is negatively regulated by WIP1 phosphatase, similarly as H2AX serine 139 (Chew, *et al* 2009).

Once ATM and ATR are activated, they both phosphorylate the tumour suppressor p53 through transducer checkpoint kinases 2 or 1 (CHK2 or CHK1), respectively. Its activation results in pro-apoptotic signalling and pro-apoptotic gene expression such as PUMA, BID, BAX and NOXA (Figure 1.6). These effectors are released into the cytoplasm to bind to the anti-apoptotic Bcl-2 family member Bcl-xL, thereby promoting the release of cytochrome C from mitochondria. Diablo is activated by BAX and inactivates cIAP, resulting in a tight regulation of survival/apoptosis factors (Wu, *et al* 2000). Cytochrome C triggers Apaf1/caspase 9 cascade resulting in apoptosis activation leading to chromatin

condensation, DNA fragmentation and cell shrinkage (Cann and Hicks 2007). Cell cycle regulation is also activated by ATM and ATR as CHK1, CHK2 and p53 activation results in G1/S or intra-S-phase checkpoints by targeting Cdk2, as well as the inhibition of the G2/M phase transition when Cdk1 is involved (Cann and Hicks 2007) (Figure 1.7). Importantly, MDC1 is also involved in cell cycle regulation (Jungmichel and Stucki 2010).

ATM-mediated DNA damage response has long been investigated and inhibitors of ATM kinase activity are currently in development to enhance cell sensitivity to drug therapy (Rainey, *et al* 2008), decreasing DNA repair in malignant cells (Figure 1.8).

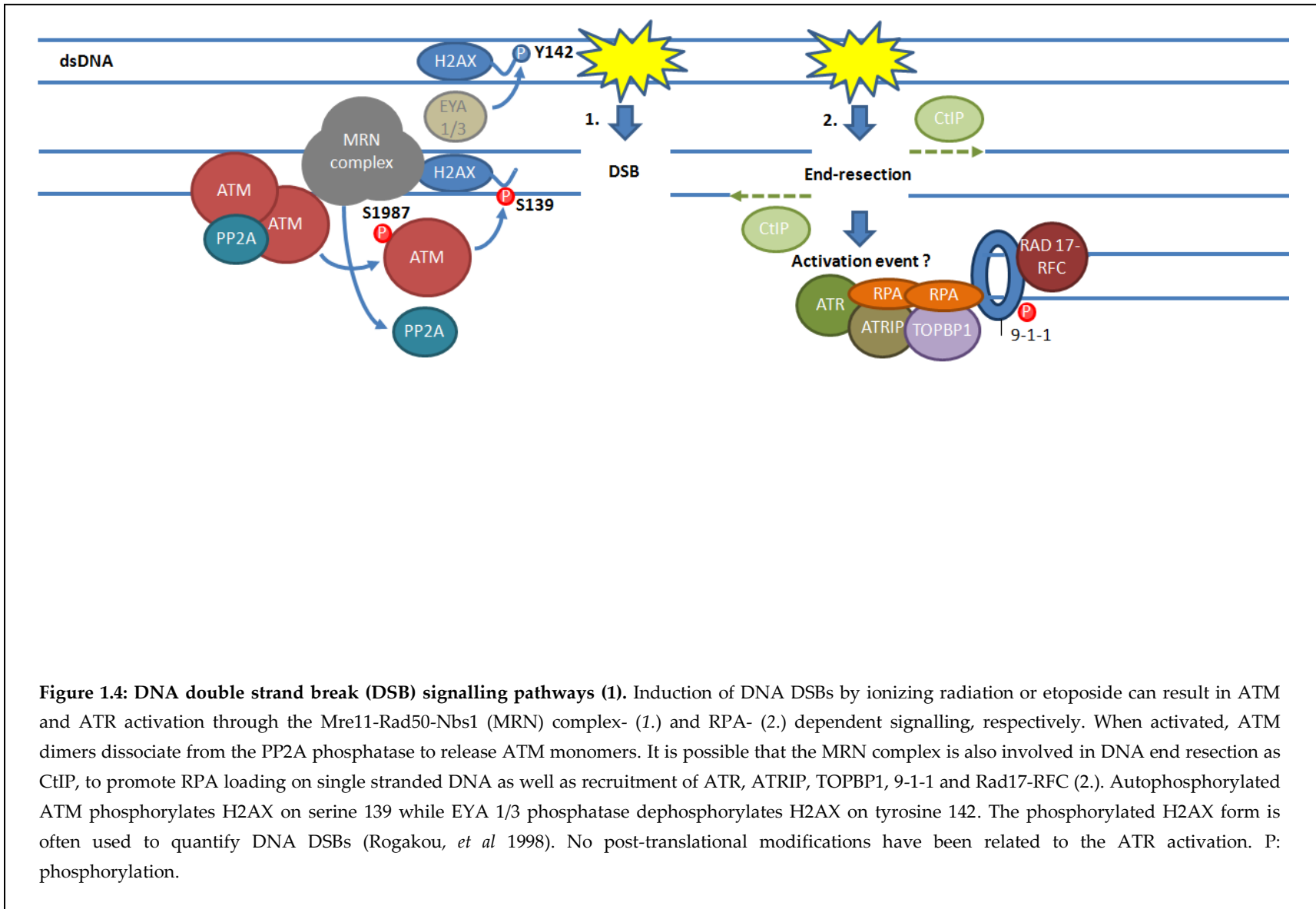


Figure 1.4: DNA double strand break (DSB) signalling pathways (1). Induction of DNA DSBs by ionizing radiation or etoposide can result in ATM and ATR activation through the Mre11-Rad50-Nbs1 (MRN) complex- (1.) and RPA- (2.) dependent signalling, respectively. When activated, ATM dimers dissociate from the PP2A phosphatase to release ATM monomers. It is possible that the MRN complex is also involved in DNA end resection as CtIP, to promote RPA loading on single stranded DNA as well as recruitment of ATR, ATRIP, TOPBP1, 9-1-1 and Rad17-RFC (2.). Autophosphorylated ATM phosphorylates H2AX on serine 139 while EYA 1/3 phosphatase dephosphorylates H2AX on tyrosine 142. The phosphorylated H2AX form is often used to quantify DNA DSBs (Rogakou, *et al* 1998). No post-translational modifications have been related to the ATR activation. P: phosphorylation.

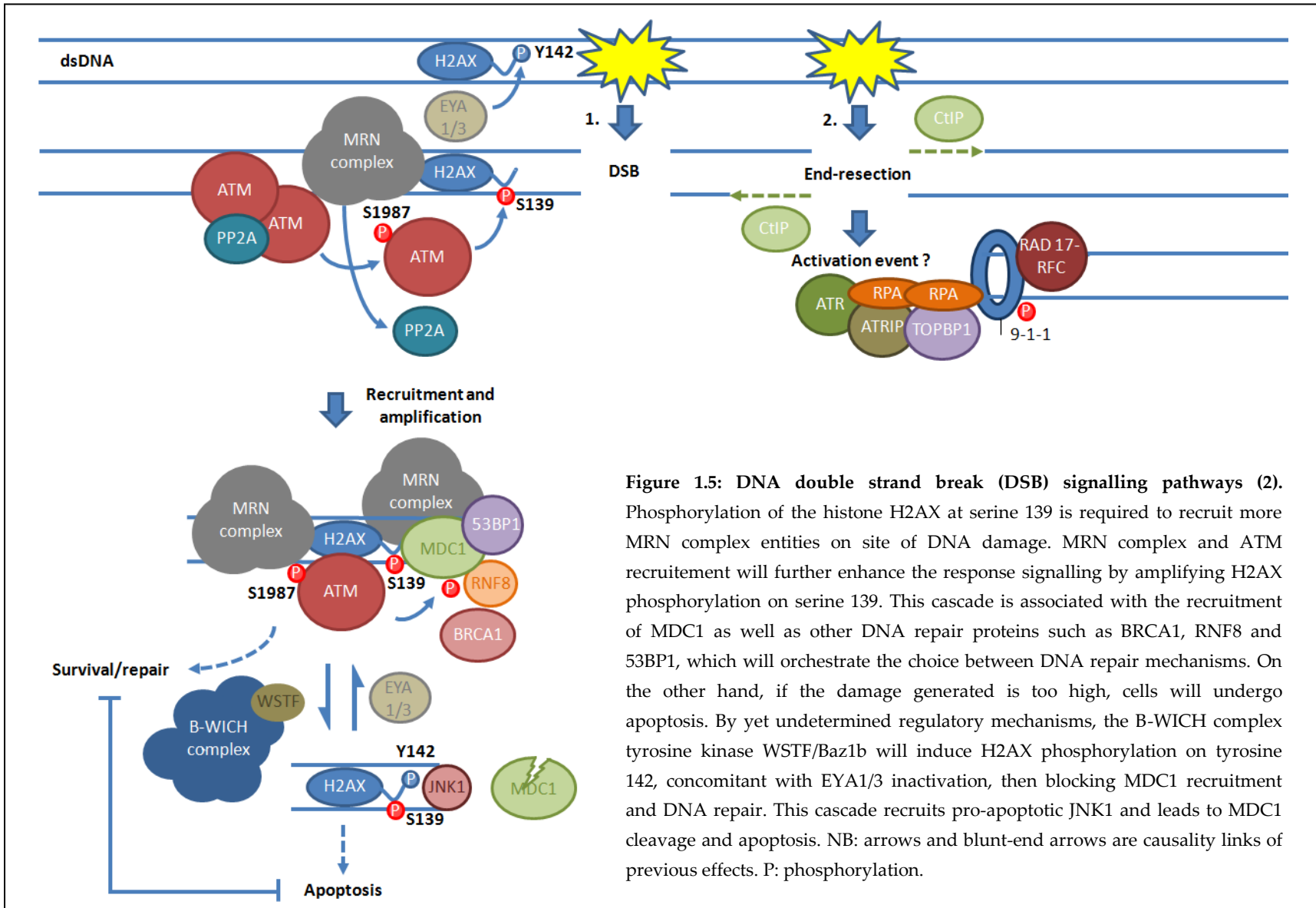


Figure 1.5: DNA double strand break (DSB) signalling pathways (2). Phosphorylation of the histone H2AX at serine 139 is required to recruit more MRN complex entities on site of DNA damage. MRN complex and ATM recruitment will further enhance the response signalling by amplifying H2AX phosphorylation on serine 139. This cascade is associated with the recruitment of MDC1 as well as other DNA repair proteins such as BRCA1, RNF8 and 53BP1, which will orchestrate the choice between DNA repair mechanisms. On the other hand, if the damage generated is too high, cells will undergo apoptosis. By yet undetermined regulatory mechanisms, the B-WICH complex tyrosine kinase WSTF/Baz1b will induce H2AX phosphorylation on tyrosine 142, concomitant with EYA1/3 inactivation, then blocking MDC1 recruitment and DNA repair. This cascade recruits pro-apoptotic JNK1 and leads to MDC1 cleavage and apoptosis. NB: arrows and blunt-end arrows are causality links of previous effects. P: phosphorylation.

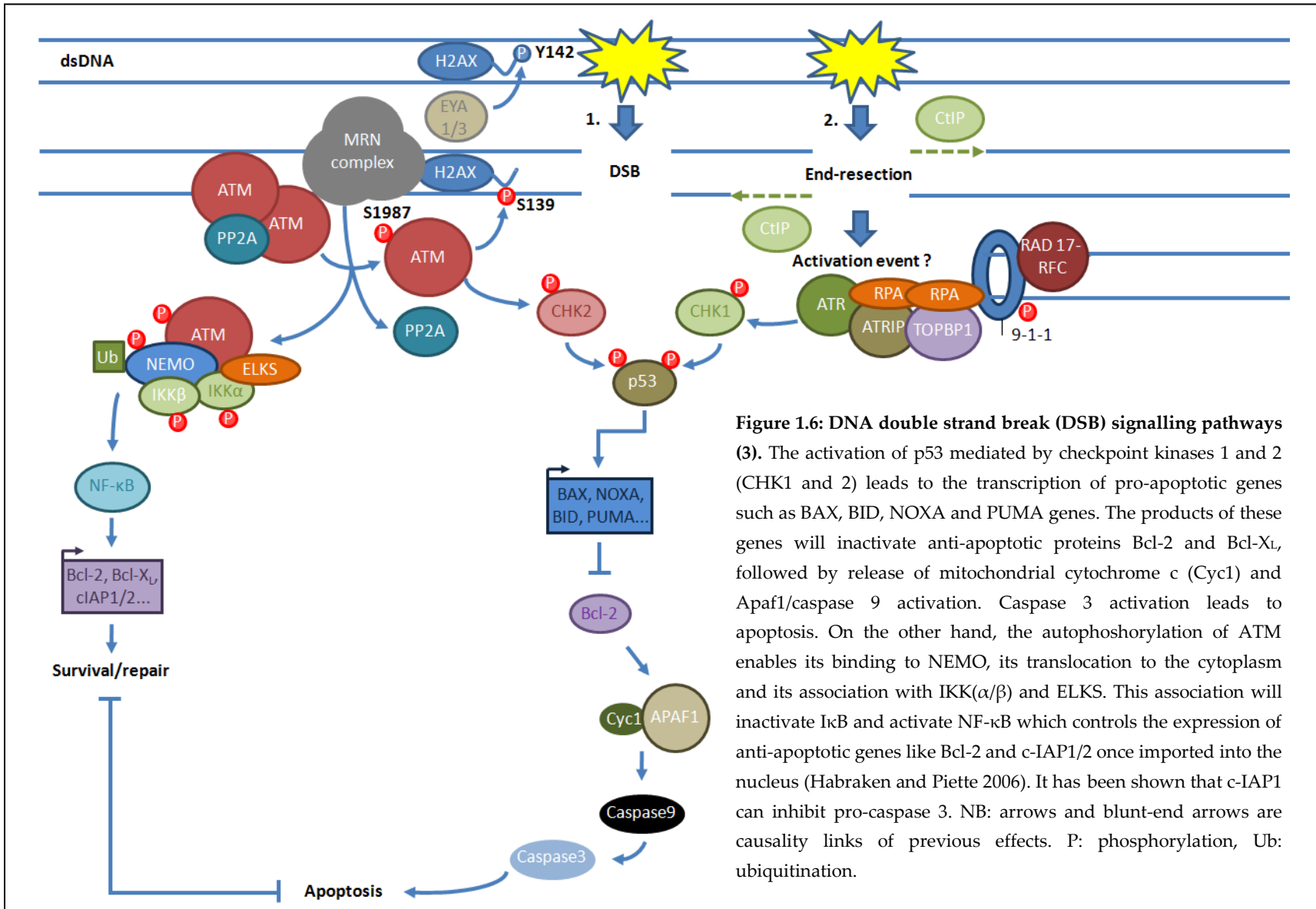
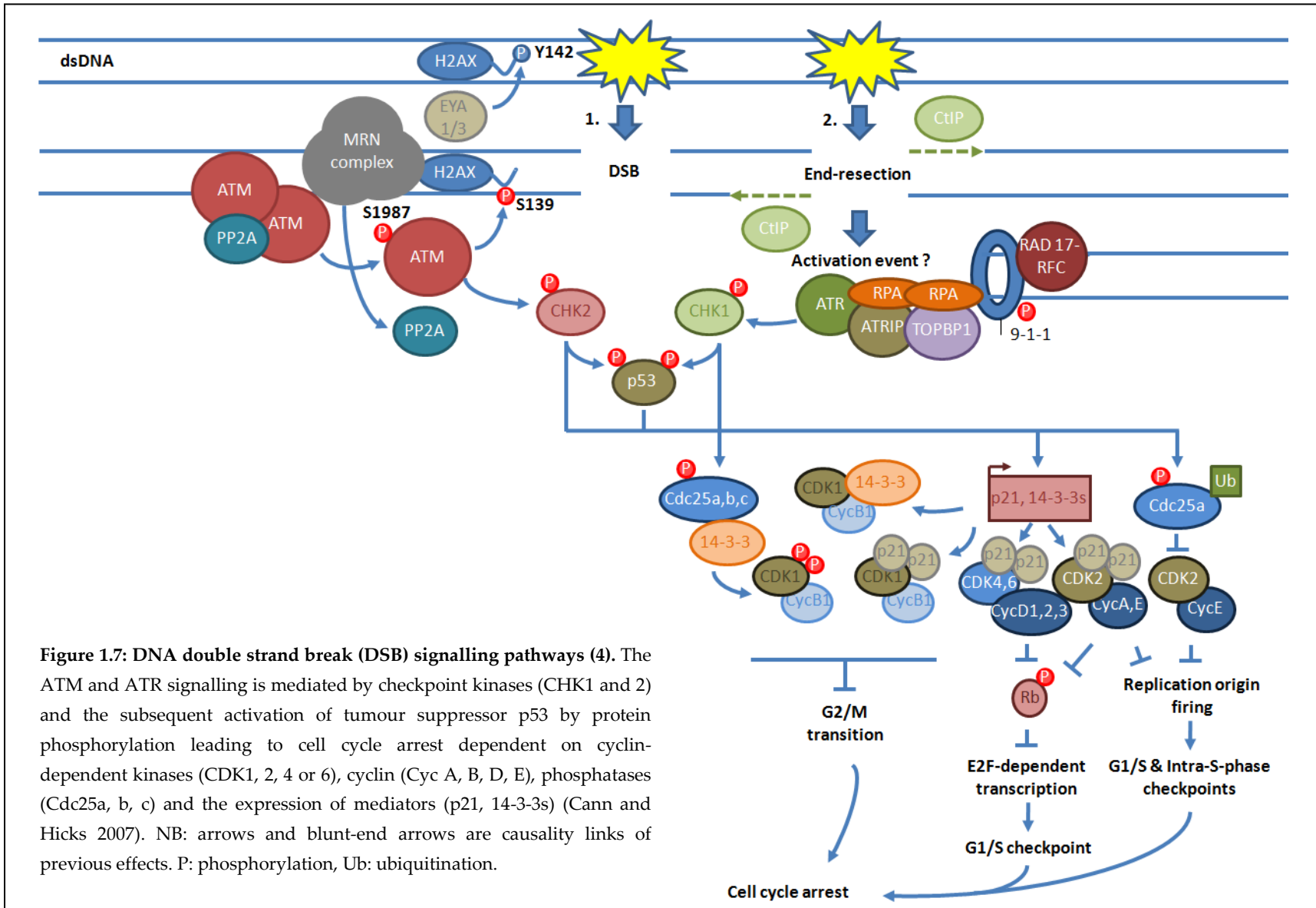


Figure 1.6: DNA double strand break (DSB) signalling pathways (3). The activation of p53 mediated by checkpoint kinases 1 and 2 (CHK1 and 2) leads to the transcription of pro-apoptotic genes such as BAX, BID, NOXA and PUMA genes. The products of these genes will inactivate anti-apoptotic proteins Bcl-2 and Bcl-X_L, followed by release of mitochondrial cytochrome c (Cyc1) and Apaf1/caspase 9 activation. Caspase 3 activation leads to apoptosis. On the other hand, the autophosphorylation of ATM enables its binding to NEMO, its translocation to the cytoplasm and its association with IKK(α/β) and ELKS. This association will inactivate IκB and activate NF-κB which controls the expression of anti-apoptotic genes like Bcl-2 and c-IAP1/2 once imported into the nucleus (Habracken and Piette 2006). It has been shown that c-IAP1 can inhibit pro-caspase 3. NB: arrows and blunt-end arrows are causality links of previous effects. P: phosphorylation, Ub: ubiquitination.



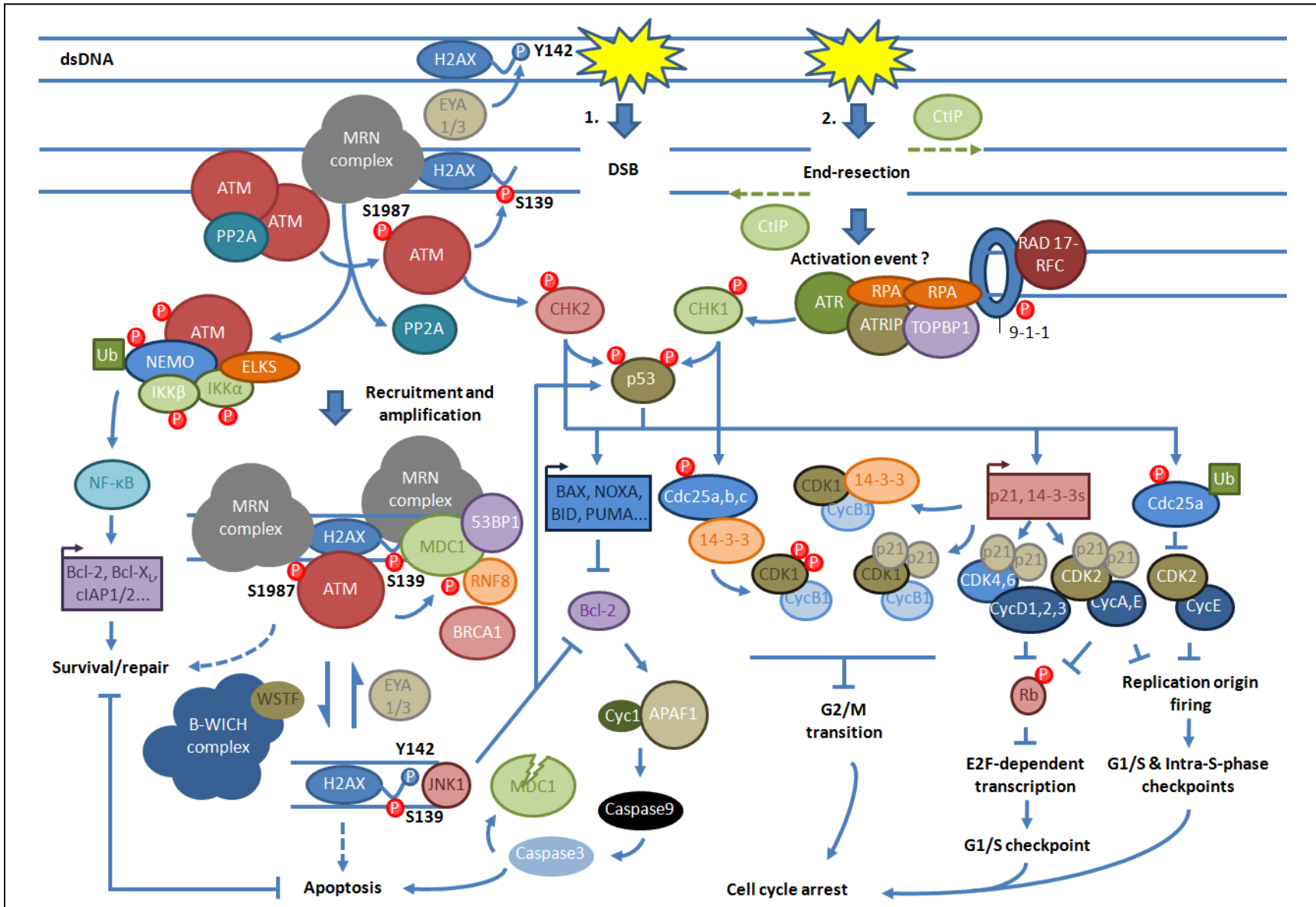


Figure 1.8: DNA double strand break (DSB) signalling pathways (5) (Figure on previous page). DNA damage signalling induces two opposite responses concomitant with cell cycle arrest leading to apoptosis or cell survival and DNA repair. Cell fate decision is based on molecular mechanisms involving either pro-apoptotic factors *via* histone H2AX post-translational modifications and caspase activation or anti-apoptotic signals mediated by NF- κ B transcription factor as well as a different histone H2AX “code”. These pathways are tightly interconnected from the start to the end of the DNA DSB signalling as ATM can promote both p53 and NF- κ B activation, cIAP can suppress caspase 3 action and BAX-mediated Diablo activation can inactivate cIAP (not shown). Fine-tuning of these pathways is also orchestrated by the B-WICH complex tyrosine kinase WSTF/Baz1b which can promote p53 activation and Bcl-2 inactivation from the recruitment of JNK1 pro-apoptotic factor.

1.5.3. DNA double strand break repair processes

Repair pathways of DNA double strand breaks (DSBs) can involve homologous recombination (HR), non-homologous end joining (NHEJ) and single-strand annealing (SSA) (Figure 1.9) (Pastink, *et al* 2001). HR is the most accurate DNA double strand break repair process when it uses the sister chromatid as template while it can result in loss of heterozygosity from the use of homologous chromosomes *via* allelic recombination or similar sequences/repeats *via* homeologous recombination (Mezard and Nicolas 1994, Moynahan and Jasin 1997, Skorski 2002). Moreover, HR can result in aneuploidy and chromosomal rearrangements if it is misregulated by Rad51, its key component (Richardson, *et al* 2004). NHEJ is an error-prone repair pathway as it does not need sequence homology for the processing and ligation of DNA ends. A classical and an alternative (or back-up) NHEJ pathways have been described (Nickoloff, *et al* 2008, Sallmyr, *et al* 2008b). By contrast, SSA repair, a pathway shared between NHEJ and HR, needs the annealing of sequence repeats in the genome and eventually leads to non-homologous end deletion which may be a source of significant losses of genetic material on one of the homologous chromosomes (Elliott, *et al* 2005, Valerie and Povirk 2003) (Figure 1.9).

The cellular choice of the repair mechanism is not yet well understood. It has been suggested that the presence of sister chromatids in late S and G2 phases would favor HR, whereas NHEJ would be the major pathway in G1 and early S phases (Helleday, *et al* 2008).

Moreover, recruitment of specific DNA repair proteins would lead cells to a choice between the different repair processes. For example, CtIP nuclease is involved in DNA end resection with the MRN complex during early steps of HR (Figure 1.9). CtIP expression and phosphorylation levels increase considerably during cell cycle phases S and G2 and such regulation may favour DNA repair by HR, while the expression of Ku proteins has been shown to inhibit HR and promote NHEJ (Lamarque, *et al* 2010). Similarly, BRCA1 and 53BP1 appear to be recruited to MDC1 exclusively for HR or canonical NHEJ respectively while 53BP1 can also inhibit BRCA1 function in HR (Bothmer, *et al* 2010, Bouwman, *et al* 2010, Bunting, *et al* 2010, Difilippantonio, *et al* 2008, Dimitrova, *et al* 2008, Jungmichel and Stucki 2010, Kass, *et al* 2010, Lowndes 2010, Moynahan, *et al* 1999, Nakamura, *et al* 2006, Riches, *et al* 2008, Xie, *et al* 2007). However different MDC1 domains are required for BRCA1 recruitment and MDC1-mediated HR which would suggest that independent pathways exist in HR (Xie, *et al* 2007). MDC1 would be involved preferentially in HR and sister chromatid recombination following its interaction with H2AX while 53BP1 favours NHEJ independently of H2AX post-translational modifications (Xie, *et al* 2007). Interestingly, the association of BRCA1 with CtIP and the MRN complex specifically in S and G2 phases may be a molecular switch towards HR (Chen, *et al* 2008b, Limbo, *et al* 2007, Takeda, *et al* 2007, Yun and Hiom 2009). However, CtIP may also have a role in NHEJ during G1 phase along with the MRN complex when it is phosphorylated on threonine 847, but not on the serine 327 residue as required for HR (Quennet, *et al* 2011). There are data that suggest that ATM could be important for HR (Bunting, *et al* 2010). By contrast, MDC1 and the MRN complex seem to be involved in both HR and NHEJ (Figure 1.9). Indeed, Mre11 nuclease activity leads end-resection to prime the loading of RPA in HR, but also in NHEJ where it acts before the ligation of DNA ends by XRCC4 and Ligase 4 (Jungmichel and Stucki 2010, Lamarque, *et al* 2010).

Along the recruitment of DNA repair proteins, it has also been suggested that histone post-translational modifications, such as phosphorylation and methylation, would also be involved in the repair pathway choice (Fnu, *et al* 2011, Riches, *et al* 2008, Xie, *et al* 2007).

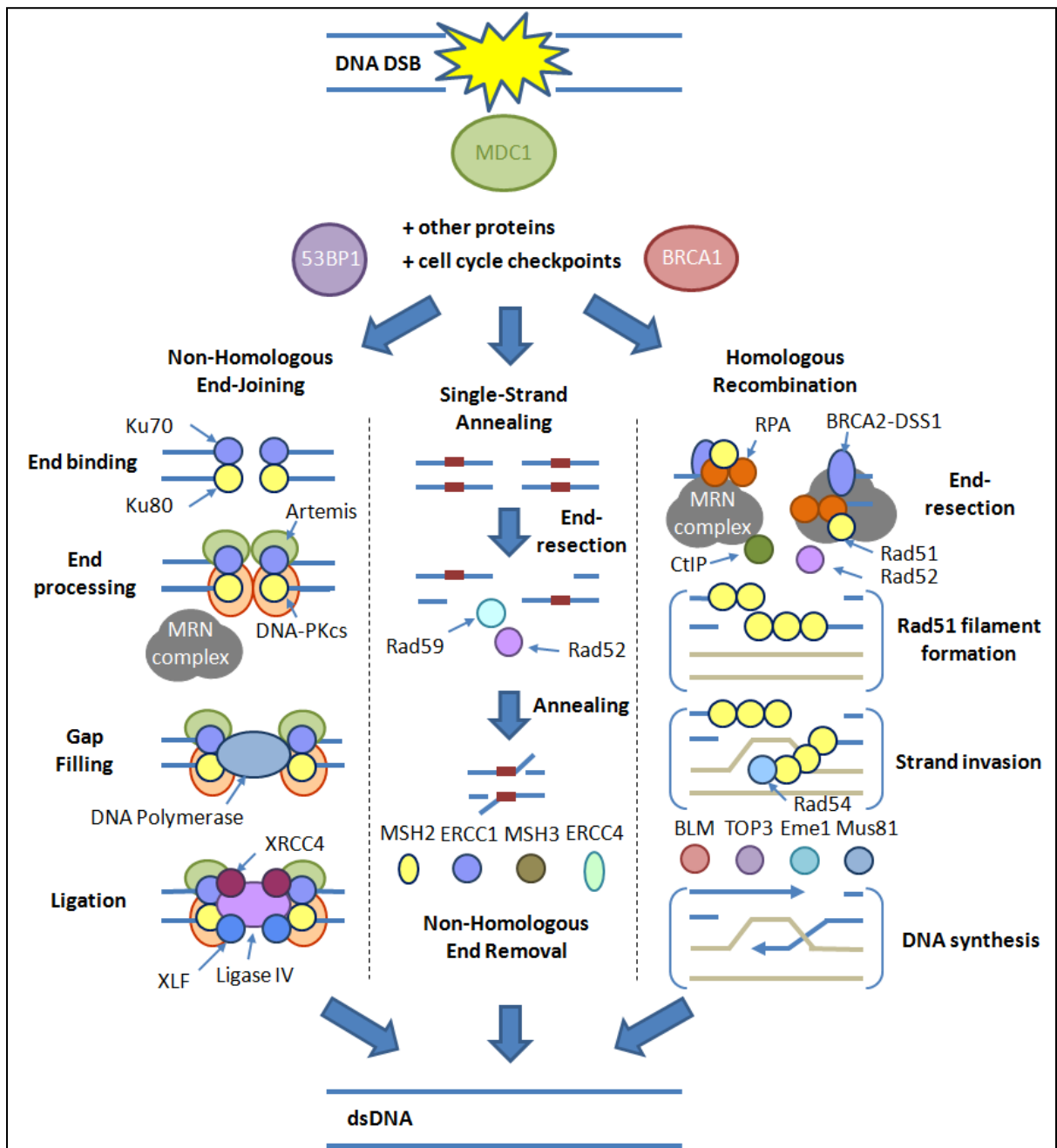


Figure 1.9: DNA double strand break repair processes in mammals (Adapted from KEGG pathways). Non-homologous end joining (NHEJ), single-strand annealing (SSA) and homologous recombination (HR) DNA repair pathways are shown for mammals. The choice of the pathway depends on the recruitment of multiple proteins at the site of DNA damage as well as cell cycle phase. Phosphoprotein 53BP1 can inhibit BRCA1 and reduce the frequency of HR, so do the Ku proteins Ku70 and Ku80 required for NHEJ. Phosphorylation of MDC1 and the activation of Mre11-Rad50-Nbs1 (MRN) complex are involved in HR and NHEJ. In NHEJ, DNA protein kinase catalytic subunit (DNA-PKcs), Artemis and a DNA polymerase are required for DNA end processing and gap filling in association with DNA ligase IV, X-ray repair cross-complementing protein 4 (XRCC4) and NHEJ factor 1 (NHEJ1/XLF) for DNA ligation. The alternative/back up NHEJ involves extensive resection, alignment of microhomologies by Poly[ADP-ribose] polymerase 1 (PARP-1), XRCC1 and DNA ligase III (not shown). *To be continued on next page.*

Figure 1.9 DNA double strand break repair processes in mammals (Adapted from KEGG pathways) (continued from previous page). SSA and HR are primed by end-resection, probably by the MRN complex or CtIP, and loading of replication protein A (RPA) on single DNA strands. In SSA, annealing of complementary single-stranded DNA is promoted by DNA repair and recombination proteins Rad52 and Rad59. Then non-homologous end removal is performed by DNA mismatch repair protein MSH2 and MSH3 as well as DNA excision repair ERCC1 and 4. In HR, RPA loading is concomitant with Breast cancer type 2 susceptibility protein (BRCA2) action in association with 26S proteasome complex subunit (DSS1), and the recruitment of DNA repair and recombination proteins Rad51 and Rad52. Rad51 monomers create a Rad51 filament, which enables homologous strand invasion with recruitment of Rad54. Then, the helicase Bloom syndrome protein (BLM), DNA topoisomerase 3 (TOP3), the crossover junction endonucleases Eme1 and Mus81 are required for DNA repair after a Holliday junction intermediate and DNA synthesis.

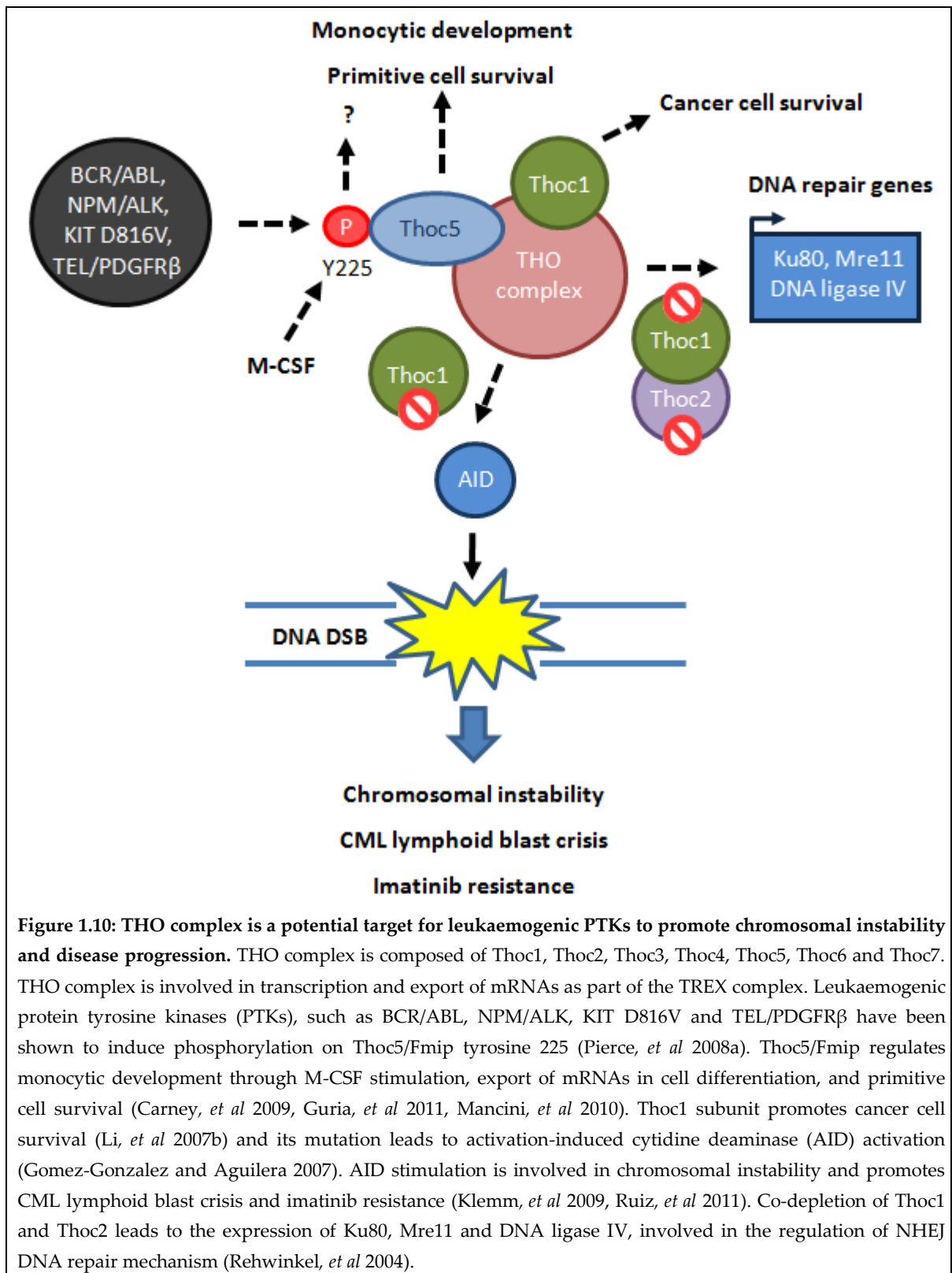
1.5.4. Misregulation of the DNA damage response signalling and stimulation of unfaithful DNA double strand break repair processes by leukaemogenic PTKs

As described above, leukaemogenic PTKs can deregulate DNA damage repair processes as well as inducing more DNA damage through ROS production and promoting cell survival (Cramer, *et al* 2008, Nowicki, *et al* 2004, Skorski 2002). The modulation of DNA damage repair mechanisms has been strongly established and appears to be observed in almost every process. BCR/ABL enhances efficiency of unfaithful NHEJ (Poplawski and Blasiak 2010, Salles, *et al* 2011, Sallmyr, *et al* 2008b, Sallmyr, *et al* 2008c, Slupianek, *et al* 2006, Slupianek, *et al* 2011b) and stimulates HR (Nowicki, *et al* 2004, Slupianek, *et al* 2002, Slupianek, *et al* 2011b, Slupianek, *et al* 2001) as well as SSA (Cramer, *et al* 2008, Fernandes, *et al* 2009, Salles, *et al* 2011, Slupianek, *et al* 2011b).

BCR/ABL PTK affects canonical NHEJ by increasing the rate of degradation of DNA-PKcs (Delhommeau, *et al* 2006, Deutsch, *et al* 2001), but stimulates the error-prone alternative NHEJ pathway, a DNA-PKcs-independent process (Salles, *et al* 2011, Sallmyr, *et al* 2008c, Skorski 2002). Remarkably DNA-PKcs has been shown to inhibit WRN helicase which is upregulated in the presence of BCR/ABL and other leukaemogenic PTKs and which may play a significant role in alternative NHEJ, by increasing the size of deletions following DNA DSB repair (Sallmyr, *et al* 2008c, Slupianek, *et al* 2011b). It has been proposed that BCR/ABL may also form a complex with WRN and modulate its nuclease activity by

tyrosine phosphorylation. WRN protects BCR/ABL PTK-expressing cells from apoptosis induced by genotoxic stresses, and consequently may promote genomic instability in CML chronic phase responsible for disease progression. Recently, it has been shown that Parp-1 and DNA ligase III are overexpressed by BCR/ABL PTK to enhance alternative NHEJ (Sallmyr, *et al* 2008c). It has been proposed that WRN and DNA ligase III switch DNA repair to alternative NHEJ pathway to overcome the decrease in DNA PKcs, Artemis and DNA ligase IV (Poplawski and Blasiak 2010, Sallmyr, *et al* 2008b, Sallmyr, *et al* 2008c) although the downregulation of these proteins has not always been described (Slupianek, *et al* 2011b). Similarly, NHEJ alternative pathway is promoted in the presence of FLT3/ITD PTK positive AML (Sallmyr, *et al* 2008a). Other helicases such as BLM may be upregulated upon BCR/ABL PTK expression and may modulate the response to DNA damage (Slupianek, *et al* 2005). NHEJ is also stimulated by CtIP overexpression, observed in the presence of BCR/ABL PTK (Salles, *et al* 2011). Imatinib resistance and CML disease progression to B lymphoid blast crisis has been recently linked to overexpression of the B cell mutator activation-induced cytidine deaminase (AID), generating DNA single and double strand breaks, hypermutation and genomic instability (Feldhahn, *et al* 2007, Gruber, *et al* 2010, Klemm, *et al* 2009). AID processes cytidine to uridine and generates mutations and DNA DSBs following BER and mismatch repair mechanisms during immunoglobulin class switch recombination (Ruiz, *et al* 2011). AID-mediated DNA DSBs may be repaired through NHEJ and promote chromosomal translocations, especially in THO complex mutants (Ruiz, *et al* 2011), while AID activity is directly stimulated in THO mutants (Gomez-Gonzalez and Aguilera 2007). THO and the transcription/export (TREX) complex are involved in transcription, mRNP biogenesis and mRNA export as well as genomic stability maintenance (Gonzalez-Barrera, *et al* 2002, Jimeno, *et al* 2002). Moreover, THO complex subunit Thoc1 is required for cancer cell survival (Li, *et al* 2007b), while its co-depletion with Thoc2 increases expression of DNA repair genes involved in NHEJ such as Ku80 and DNA ligase IV as well as the MRN complex protein Mre11 (Rehwinkel, *et al* 2004). Thoc5/Fmip subunit is required for primitive cell survival (Mancini, *et al* 2010) and is a target of DNA damage and leukaemogenic PTKs (Matsuoka, *et al* 2007, Pierce, *et al* 2008a). It also regulates transcription factor expression (Carney, *et al* 2009, Mancini, *et al*

2007). Thus the modulation of the THO complex by leukaemogenic PTKs may play a role in disease progression and genomic instability (Figure 1.10).



BCR/ABL oncogene expression has been shown to increase the rate of HR by multiple mechanisms (Delhommeau, *et al* 2006, Skorski 2002). Indeed, BCR/ABL PTK increases Rad51 protein expression through STAT5-mediated transcription (Slupianek, *et al* 2002, Slupianek, *et al* 2001), Rad51 phosphorylation on tyrosine 315 (Slupianek, *et al* 2001) and Rad51 reduced proteolysis by inactivation of caspase 3 (Amarante-Mendes, *et al* 1998, Dubrez, *et al* 1998, Slupianek, *et al* 2001). WRN has also been shown to stimulate HR in the presence of BCR/ABL PTK, as this helicase interacts with Rad51 (Slupianek, *et al* 2011b). Overexpression and phosphorylation of Rad51 in the presence of BCR/ABL PTK could generate genomic instability as well as resistance to DNA alkylating agents mitomycin C and cisplatin by altering the fidelity of HR, the balance between different DNA repair mechanisms and or the cell cycle checkpoints (Richardson, *et al* 2004, Slupianek, *et al* 2001). BCR/ABL interacts with and phosphorylates Rad51 paralog Rad51B (Slupianek, *et al* 2009) and Rad51 on tyrosine 315 to mediate unfaithful homeologous recombination (Slupianek, *et al* 2011a), which cannot be inhibited by mismatch repair, also misregulated in CML and by multiple leukaemogenic PTKs (Pierce, *et al* unpublished observations, Stoklosa, *et al* 2008). Rad51 is also upregulated by FLT3/ITD PTK in AML (Sallmyr, *et al* 2008a). Moreover, CtIP nuclease has been shown to be overexpressed by BCR/ABL PTK and may imbalance HR in combination with BRCA1 downregulation (Deutsch, *et al* 2003, Salles, *et al* 2011). It has been proposed that BCR/ABL PTK misregulation of HR may be the source of imatinib resistance (Koptyra, *et al* 2006).

It has also been demonstrated that BCR/ABL PTK can enhance SSA, possibly by WRN and CtIP overexpression (Cramer, *et al* 2008, Fernandes, *et al* 2009, Salles, *et al* 2011, Slupianek, *et al* 2011b), a process yet inhibited by Rad51 (Stark, *et al* 2004). Moreover BCR/ABL PTK may also direct mutagenic processes by promoting the expression of DNA polymerase β , which is the most inaccurate polymerase in mammalian cells (Skorski 2002, Turner and Alexander 2006).

Misregulation of the DNA damage response signalling by leukaemogenic PTKs has also been described upstream of the repair mechanism choice, the control of cell cycle

checkpoints and the recruitment of survival factors. In leukaemic cells, BCR/ABL PTK binds to ATM and ATR, preventing ATR from phosphorylating CHK1 after possible translocation to the nucleus, thus inhibiting normal DNA damage signalling (Dierov, *et al* 2004). Also, BCR/ABL oncogene expression has been shown to delay the S and G2/M cell cycle phases to potentially mediate DNA repair/misrepair (Nieborowska-Skorska, *et al* 2006, Skorski 2002, Slupianek, *et al* 2002). H2AX phosphorylation and H2AX foci formation at sites of DNA DSBs has been shown to be higher upon expression of leukaemogenic PTKs (Cramer, *et al* 2008). Interestingly haploinsufficiency of H2AX can result in loss of H2AX gene expression and can promote CML blast crisis in the presence of BCR/ABL PTK, suggesting that regulation of H2AX post-translational modifications may participate in genomic instability and the disease progression, along with other genes (Nagamachi, *et al* 2009). More recently, BCR/ABL PTK has been shown to affect the Fanconi anaemia (FA) DNA repair pathway, by reducing FANCD2 foci formation (Valeri, *et al* 2010) and increasing FANCD2 mono-ubiquitination in response to oxidative stress (Koptyra, *et al* 2011). To date however, no global analysis of BCR/ABL PTK effects on DNA repair has been pursued.

Some systematic knowledge has been gained on the effects of leukaemogenic PTKs on the protein Nbs1. The modulation of the MRN complex subunit Nbs1 may be responsible for BCR/ABL PTK-mediated chemotherapy resistance. Nbs1 expression and ATM-dependent Nbs1 phosphorylation on serine 343 are enhanced after DNA damage in cells expressing a variety of leukaemogenic PTKs (Rink, *et al* 2007). The phosphorylated Nbs1 form promotes cell cycle checkpoint regulation by prolonging the intra-S-phase checkpoint, and may potentiate HR along with survival, but did not affect NHEJ. Targeting Nbs1 phosphorylation in combination with imatinib improved the efficiency of imatinib to inhibit BCR/ABL PTK. Localization of Nbs1 to γ H2AX foci, *via* MDC1 phosphorylation, may also affect the intra-S-phase checkpoint. Other MDC1 phosphorylation events may be involved in regulating G2/M phase transition (Wu, *et al* 2008). Remarkably, several MDC1 and 53BP1 phosphorylations have been identified with several leukaemogenic PTKs (Pierce, *et al* unpublished observations) while downregulation of MDC1 and 53BP1 upon

BCR/ABL PTK expression has been described but may be cell line dependent (Salles, *et al* 2011). Intriguingly, the expression of Mre11 and Nbs1 increases with BCR/ABL PTK as well as IL-3 and higher levels of these proteins correlated with CML disease progression to blast crisis (Rink, *et al* 2007).

To block apoptosis normally triggered by excessive DNA damage, BCR/ABL PTK enhances the expression of the Bcl-2 family member Bcl-xL through STAT5 activation (Gesbert and Griffin 2000). BCR/ABL PTK resists apoptosis induced by etoposide, mitomycin C and cisplatin (McGahon, *et al* 1994, Rink, *et al* 2007), and reduces apoptosis signalling by blockage of mitochondrial cytochrome C release and modulation of caspase3 activation (Amarante-Mendes, *et al* 1998, Dubrez, *et al* 1998).

In conclusion, leukaemogenic PTKs may be potentially involved in regulating key nodes of DNA repair signalling pathways and orientate DNA repair choice. The aforementioned studies mainly concentrated on the modulation of proteins, and a limited set of phosphosites (Rink, *et al* 2007, Slupianek, *et al* 2001). Systems-level studies have been recently carried out to decipher dynamics of phosphosites and proteins following DNA damage induced by ionizing radiation or etoposide (Bennetzen, *et al* 2010, Boisvert, *et al* 2010, Matsuoka, *et al* 2007), while others have concentrated on mapping phosphosites and identifying proteins modulated by active and inactive BCR/ABL as well as other leukaemogenic PTKs (Choudhary, *et al* 2009, Pan, *et al* 2009, Rubbi, *et al* 2011), potentially involved in the DNA damage response and other stress signalling. Nevertheless, no such studies have focused on the overlap of the DNA damage response and BCR/ABL PTK signalling on phosphosites *per se* using a global approach.

A whole picture of the conservation of protein phosphosites regulated upon genotoxic stress in the presence of a leukaemogenic PTK is needed to identify modulations promoted by oncogenic PTKs relevant to stress and thereby to conceive adequate targeted approaches to potentially block further DNA mutations, resistance mechanisms and disease progression. Thus there is a strong case for systematic analysis of such events in

cells expressing leukaemogenic PTKs and their normal counterpart. New technologies that have been applied to such systematic analysis are described in the following section.

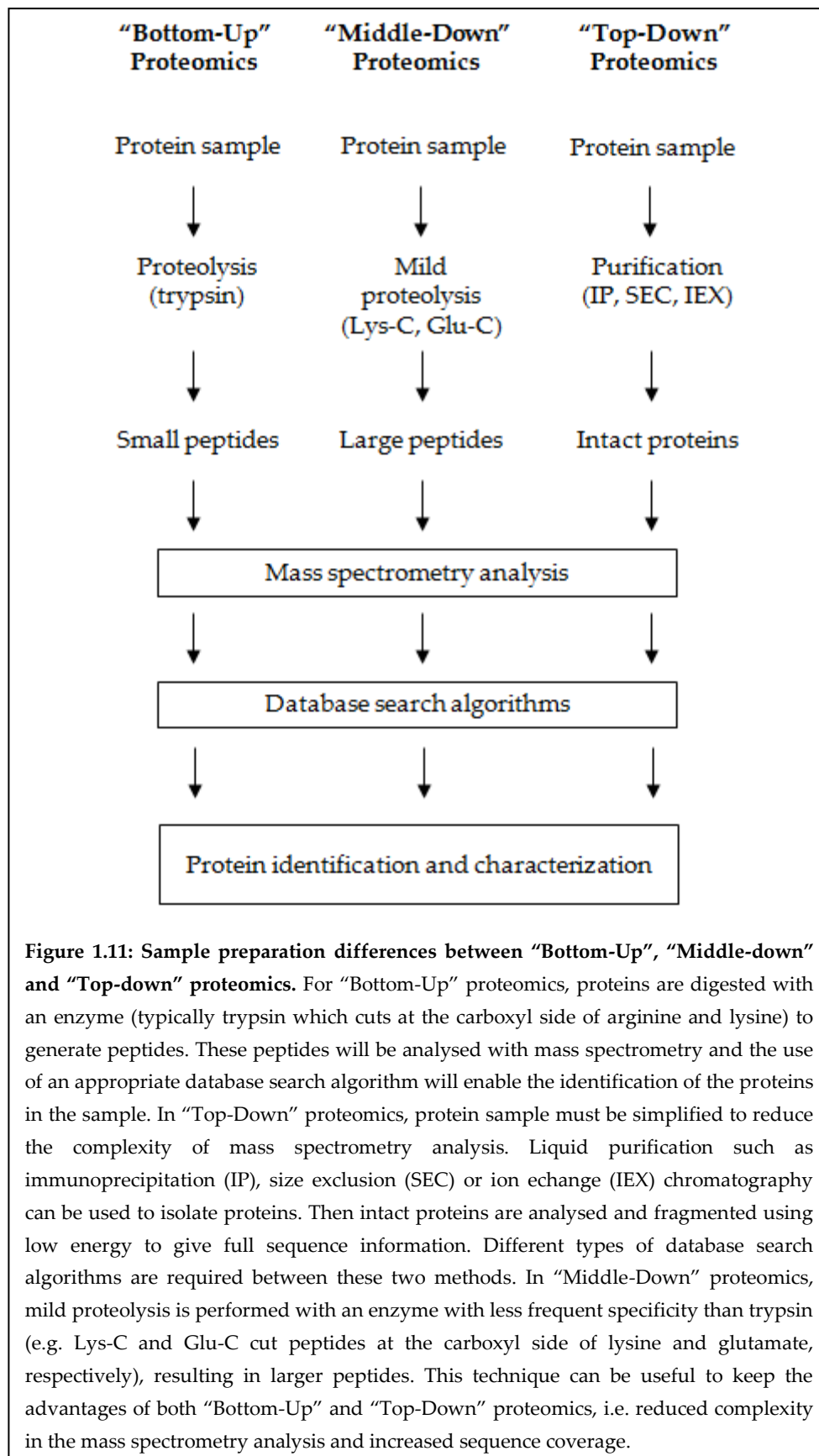
1.6. Approaches and technologies in proteomics

Proteomics is a post-genomic science which encapsulates all proteins expressed in organisms, also known as the proteome (Kahn 1995, Wasinger, *et al* 1995). This definition of proteomics was first introduced by Marc Wilkins in 1994 at the symposium “2D electrophoresis: from protein maps to genomes”. Proteomic research has advantages over transcriptomic analysis (the study of mRNA transcripts instead of proteins) by defining the cells functional entities and their modifications as well as their sub-cellular localization (Gygi, *et al* 1999b, Pierce, *et al* 2008b, Unwin, *et al* 2005a, Unwin, *et al* 2005b, Unwin and Whetton 2006). The human genome sequencing project was complete to a first draft in 2003 and the concomitant development of peptide ionization methods after their inception in the late 1980's (Fenn, *et al* 1989, Karas and Hillenkamp 1988, Whitehouse, *et al* 1985), aided the development of the field. Prior to this, protein identification was performed by *de novo* peptide sequencing with sequential Edman degradation (Steen and Mann 2004). Proteomics is composed of protein and/or peptide separation techniques as well as identification methods and encompasses the study of protein post-translational modifications, protein interactions and turnover. Mass spectrometry based quantitative proteomics is a penetrating new technology used to identify proteins at very low concentrations and identify their modifications involved in cellular processes.

1.6.1. Approaches to the proteome definition

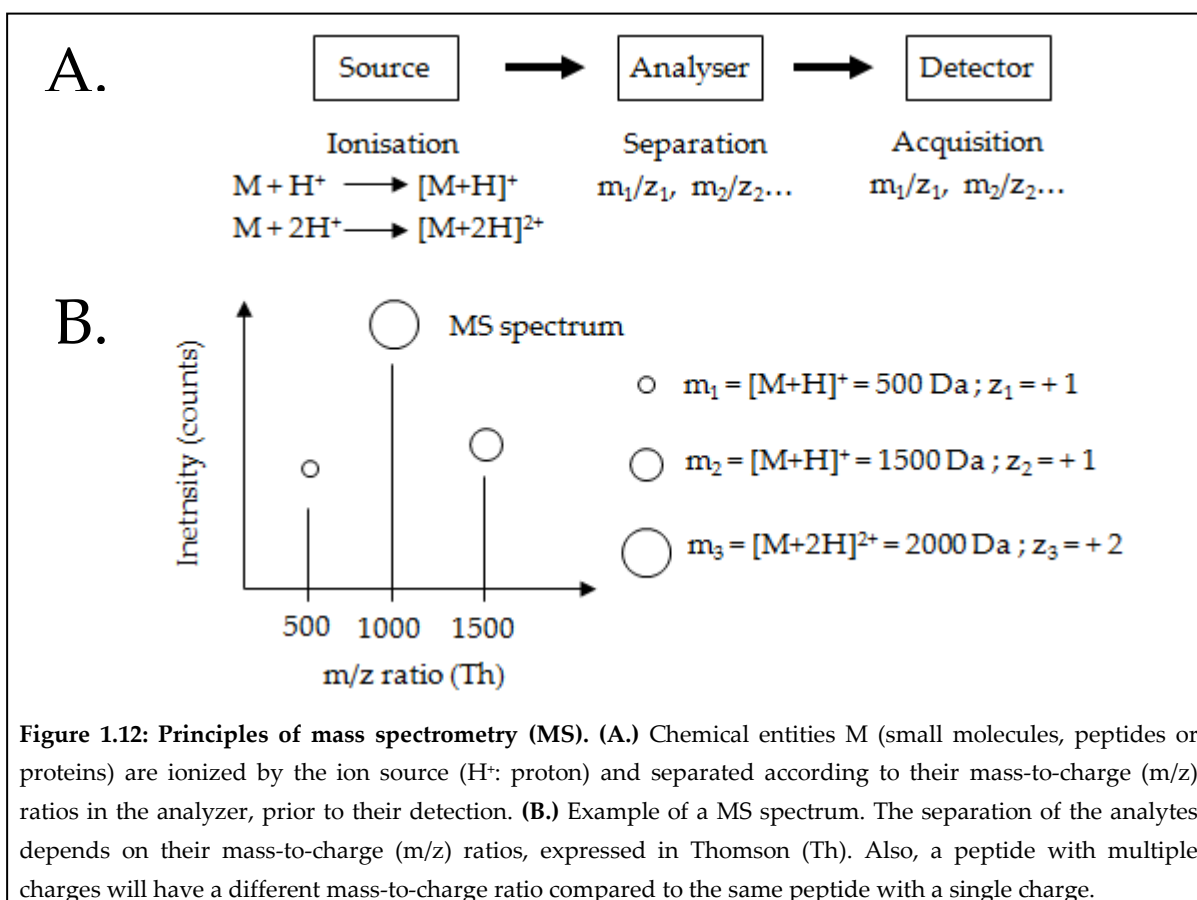
In so called “Bottom-Up” proteomics, the identification of peptides will give the identity of original proteins. First, proteins or protein complexes are purified by conventional biochemical methods and digested enzymatically to obtain specifically cleaved peptides before mass analysis using mass spectrometry (Figure 1.11). Experimental spectra are compared to theoretical spectra, obtained from *in silico* protein database digestion, giving protein identifications (Steen and Mann 2004). For this reason, protein identification depends on the comprehensive nature of sequence databases (Aebersold and Mann 2003, Tyers and Mann 2003). Trypsin, the most widely used enzyme in proteomics, cleaves at C-terminal side of arginine (R) and lysine (K) residues within proteins.

Alternatively, it is possible to derive partial sequence information using intact or partially digested proteins in processes called respectively “Top-Down” and “Middle-Down” protein identification (Steen and Mann 2004, Young, *et al* 2010). Mass spectrometry on intact proteins is improved by preliminary purification using chromatography and requires high resolution instruments such as FTICR and orbitrap. However, intact proteins retain multiple charges and the ion distribution of a protein reduces the sensitivity of “Top-Down” proteomics, although chemical entities can be used to manipulate protein charge state (Armirotti and Damonte 2010). The principal advantage of “Top-Down” proteomic strategy over “Bottom-Up” proteomics is the ability to cover the full sequence of the protein while only few peptides are usually detected with the peptide-centric methodology (Figure 1.11). Thus “Top-Down” proteomics appears to be useful to access sequence information in proteins containing repeated cleavage sites, i.e. generating small tryptic peptides, and to understand the combination of protein post-translational modifications, in the Histone code for example (Garcia, *et al* 2008, Plazas-Mayorca, *et al* 2010).



1.6.2. Principle of mass spectrometry

Mass spectrometry is an analytical technique which enables the separation and the structural analysis of chemical or biological compounds by accurately measuring their mass-to-charge (m/z) ratios (Aebersold and Mann 2003). Modifications in such mass-to-charge ratios can also highlight and identify the addition or removal of functional groups. Mass spectrometers consist of three regions, called the source, the analyzer and the detector. The source region is where analytes such as peptides are desolvated and ionized at atmospheric pressure. Analytes are then steered at low pressure towards the analyzer region using electric fields and electrostatic lenses. When ions reach the analyzer they are separated according to their stability within an electric field or their velocity in a flight tube. First, this separation depends on the peptide mass hence promoting preferentially the movement of small peptides instead of large peptides. Second, peptides can be singly or multiply charged so that separation also depends on this charge state (Figure 1.12).



1.6.3. Sources in mass spectrometry

Matrix-assisted laser desorption ionization (MALDI) and electrospray (ESI) sources are the most widely used for peptide or protein ionization. Laser ionization time-of-flight mass spectrometry was introduced in 1988 by Tanaka who won the Nobel prize in Chemistry and further developed by Karas and Hillenkamp into MALDI (Karas, *et al* 1990, Karas and Hillenkamp 1988, Karas, *et al* 1989). Samples are co-crystallized on a metal surface (MALDI target) with a matrix, which contains a particular small organic molecule such as α -cyano-4-hydroxycinnamic acid, dihydroxybenzoic acid or sinapinic acid, depending on whether peptides or proteins will be analysed. Matrix molecules can absorb LASER radiation at a specific wavelength and desorb from the MALDI target with the analytes so that they will be ionized predominantly by the transfer of a single proton (H^+) from the matrix molecules (de Hoffmann and Stroobant 2007). These ions then enter the mass analyser for analysis. The sample preparation is quite simple and is relatively tolerant to contaminants such as salts or buffers. Nevertheless, this technique cannot be coupled directly with liquid chromatography (LC) although it remains possible to spot drops on MALDI targets off-line.

The ESI source was developed by J.B. Fenn who was awarded the Nobel prize in Chemistry for this achievement (Fenn, *et al* 1989, Whitehouse, *et al* 1985). This technique is now widely used to ionize peptides because of the ease of coupling it with capillary chromatography systems (Figure 1.13). In this technique peptides become positively charged in a buffer at low pH. Peptides are eluted at low flow rate (typically 300 nL/min) from reversed phase (RP) LC and are transferred to gas phase at atmospheric pressure by applying heat and a high voltage difference between the LC capillary and the mass spectrometer. The mechanism of individual gas-phase ion formation is explained by liquid evaporation and coulombic fission of liquid droplets when electrostatic repulsion between positively charged ions occurs at the Rayleigh charge limit (Kearle and Peschke 2000, Taflin, *et al* 1989, Tang and Smith 2001)

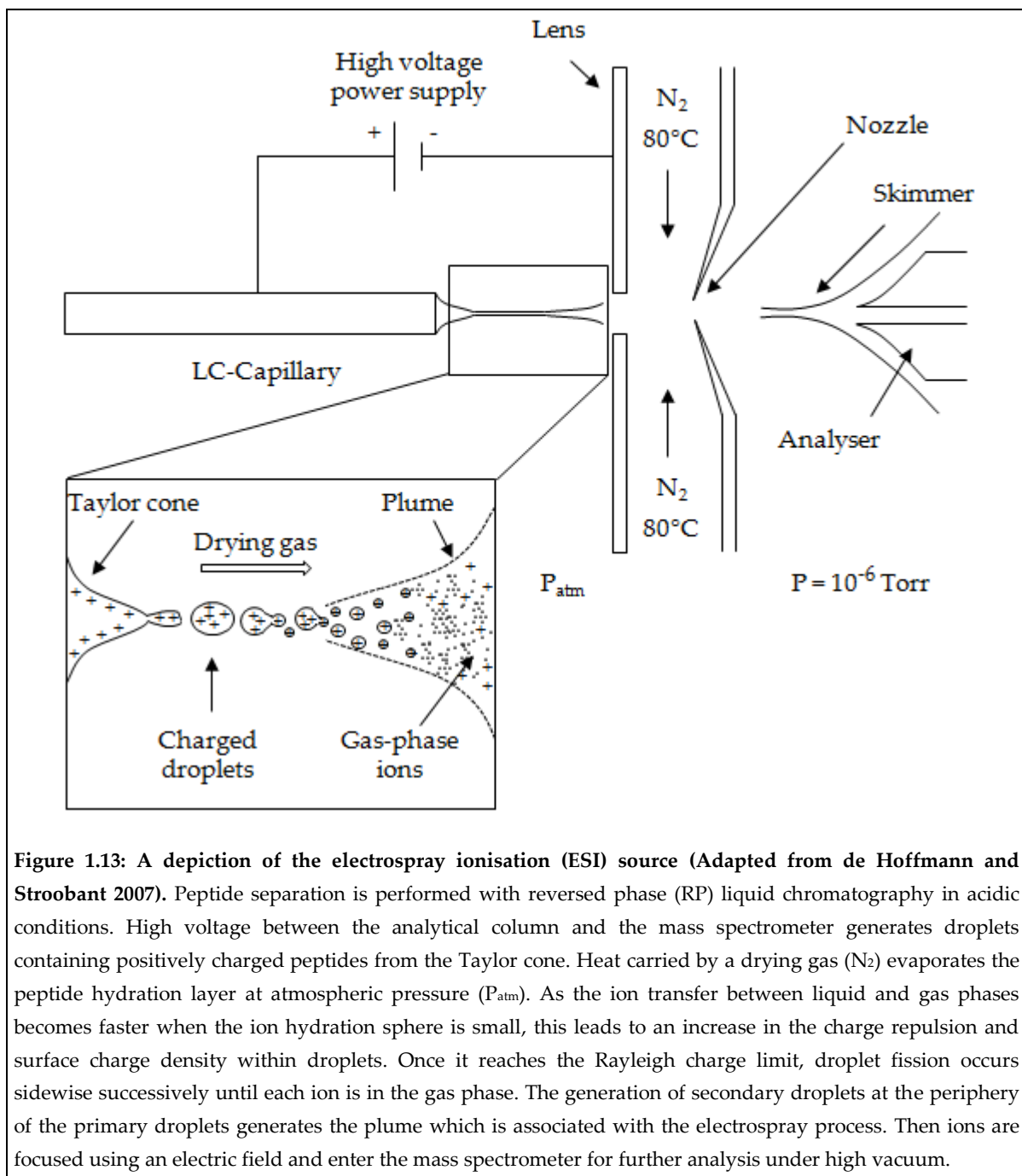


Figure 1.13: A depiction of the electrospray ionisation (ESI) source (Adapted from de Hoffmann and Stroobant 2007). Peptide separation is performed with reversed phase (RP) liquid chromatography in acidic conditions. High voltage between the analytical column and the mass spectrometer generates droplets containing positively charged peptides from the Taylor cone. Heat carried by a drying gas (N₂) evaporates the peptide hydration layer at atmospheric pressure (P_{atm}). As the ion transfer between liquid and gas phases becomes faster when the ion hydration sphere is small, this leads to an increase in the charge repulsion and surface charge density within droplets. Once it reaches the Rayleigh charge limit, droplet fission occurs sidewise successively until each ion is in the gas phase. The generation of secondary droplets at the periphery of the primary droplets generates the plume which is associated with the electrospray process. Then ions are focused using an electric field and enter the mass spectrometer for further analysis under high vacuum.

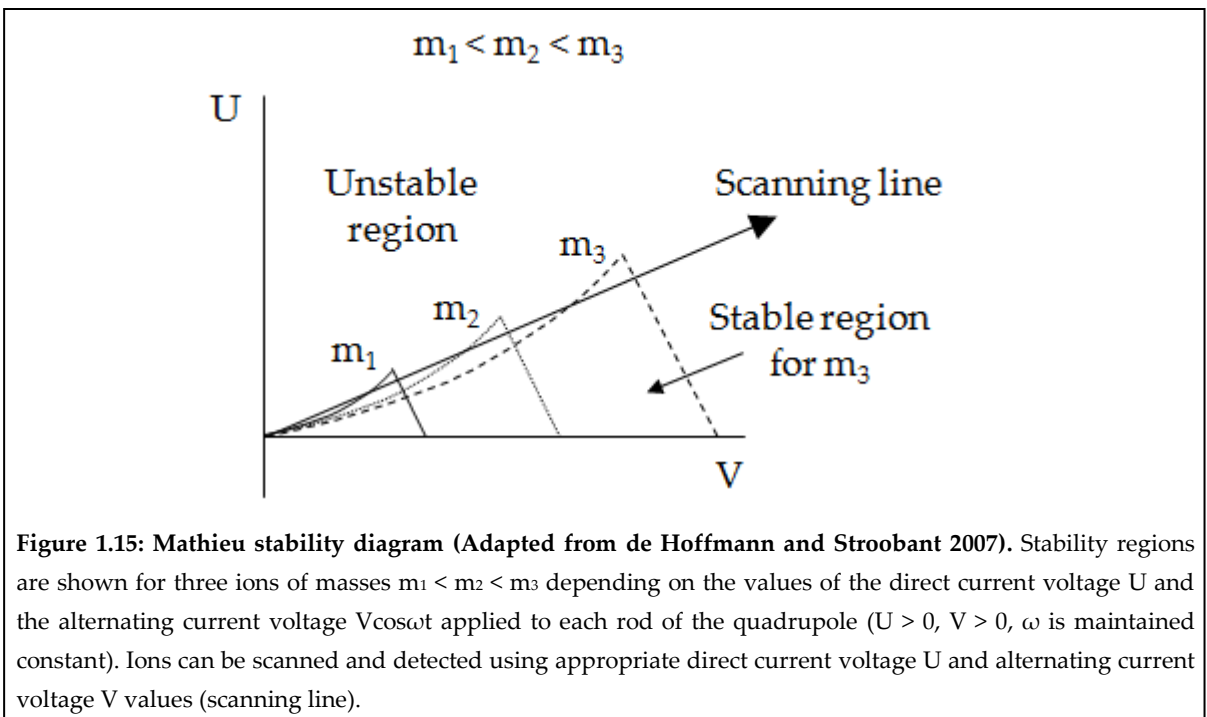
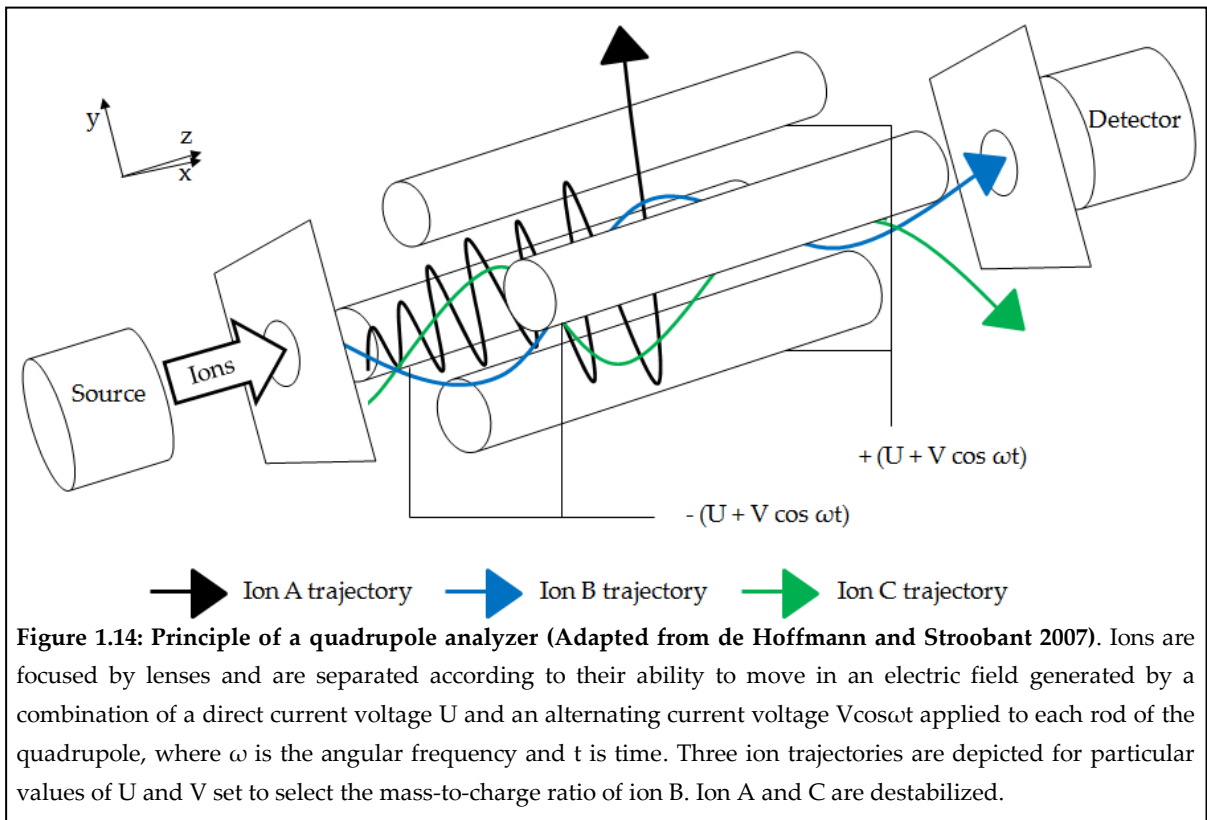
1.6.4. Analysers in mass spectrometry

Following ionization of peptides in the gas phase, mass analysis takes place. There are several different analysers which are used for this purpose with their own advantages and limitations. Below, some of the most widely used mass analysers are presented.

1.6.4.a. Quadrupole analyser

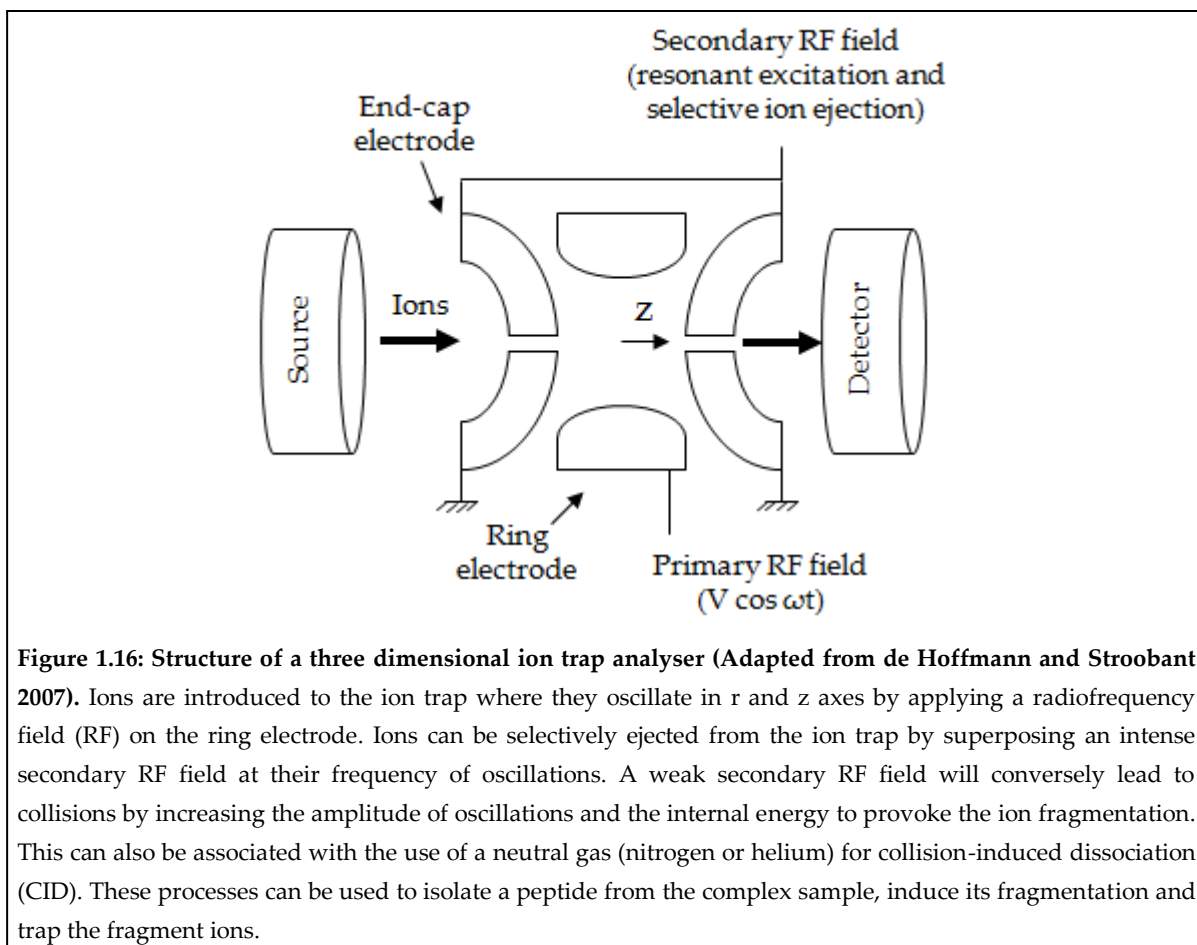
Quadrupoles consist of 4 metallic hyperbolic rods which can isolate and separate ions in 2 dimensions (x and y axes) according to their ability to pass through an electric field (Figure 1.14). This electric field is generated by applying a radiofrequency (RF) / alternating current (AC) voltage ($V\cos\omega t$), where ω is the angular frequency and t is time, and a direct current (DC) voltage U on each of the rod. Thus ions are alternately attracted then repelled by the rods and stably oscillate along the z axis towards the detector (Figure 1.14). However, peptide trajectories are stable only for specific values of U and V , as ω is maintained constant, while the stability region increases with the mass-to-charge ratio of the analyte (Figure 1.15). Indeed, the larger the peptide, the lower its capacity to move and the more the energy required to destabilize it. To separate the different chemical entities, the stability of ions with different mass-to-charge ratios is promoted by screening specific values of U and V . For this reason, the ratio between U and V is kept constant at the top of each stability region to separate different analytes from low electric field and kinetic energy (small peptides) to high electric field and kinetic energy (larger peptides). Importantly, mass-to-charge values can be determined from specific U and V values. The principle of quadrupole action was originally described by Paul and Steinwedel in 1953.

The mass accuracy of quadrupoles is about 100 ppm, the resolution R of 4,000 and the mass range approximately 4,000 m/z (these values depend on the instrument manufacturer).



1.6.4.b. Ion trap analyser

Three dimensional (3D) ion trap analysers have also been developed by Paul and Steinwedel. In this type of analyser, ions are introduced into a 3D chamber and move around a central point by the application of a RF field to ring electrodes, while end-cap electrodes are grounded ($U = 0$) (Figure 1.16). In the ion trap, ions are selected to leave the ion trap by destabilization in order to be detected (de Hoffmann and Stroobant 2007). For example, an ion of a specific mass-to-charge ratio oscillates continuously in r and z axes at its own frequency, different from the RF field. By applying an intense secondary RF field in the z axis at the same frequency, it is possible to selectively transfer energy to this ion only. Thus its trajectory will be destabilized in the z axis and this particular ion will leave the ion trap in a process called selective ion ejection. Large band of frequencies can be used to selectively eject multiple ions with different mass-to-charge ratios whilst trapping others (Figure 1.17). However, when the energy transferred using the same principle is low, a particular ion can increase the amplitude of its oscillations, collide with other particles and fragment. This is called resonant excitation. It is also possible to use a neutral gas such as helium or nitrogen to promote collision-induced dissociation (CID) which will lead to the ion fragmentation. In the Mathieu stability diagram, it is interesting to note the importance of a complex number β , whose values must be between 0 and 1 to ensure the stability of ion oscillations (Figure 1.17). It is thus possible to destabilize, scan and detect ions from the low mass to the high mass ranges by increasing V (Figure 1.17). However, low mass fragment ions below the third of the precursor mass will be lost as the value of V is not adequate for their stabilization. This phenomenon is called the low mass cut-off, or the "third cut-off" rule of the ion trap.



It is interesting to note that the frequency of oscillations in the z axis f_z depends on β_z . This last term is in relationship with U, V, m and z so that it is possible to associate the mass-to-charge (m/z) ratio of a particular ion to a particular oscillation frequency (de Hoffmann and Stroobant 2007).

$$f_z = \beta_z \left(\frac{\omega}{4\pi} \right)$$

Ion traps offer similar performances to quadrupoles, although they tend to be significantly more sensitive due to their ability to trap and accumulate a population of ions prior to mass analysis. Moreover, a linear ion trap (LIT) has been recently developed. This instrument can store 40 times more ions in the trap without problematic space-charge effects, resulting in an improvement in sensitivity and a better stability of the fragment ions (de Hoffmann and Stroobant 2007).

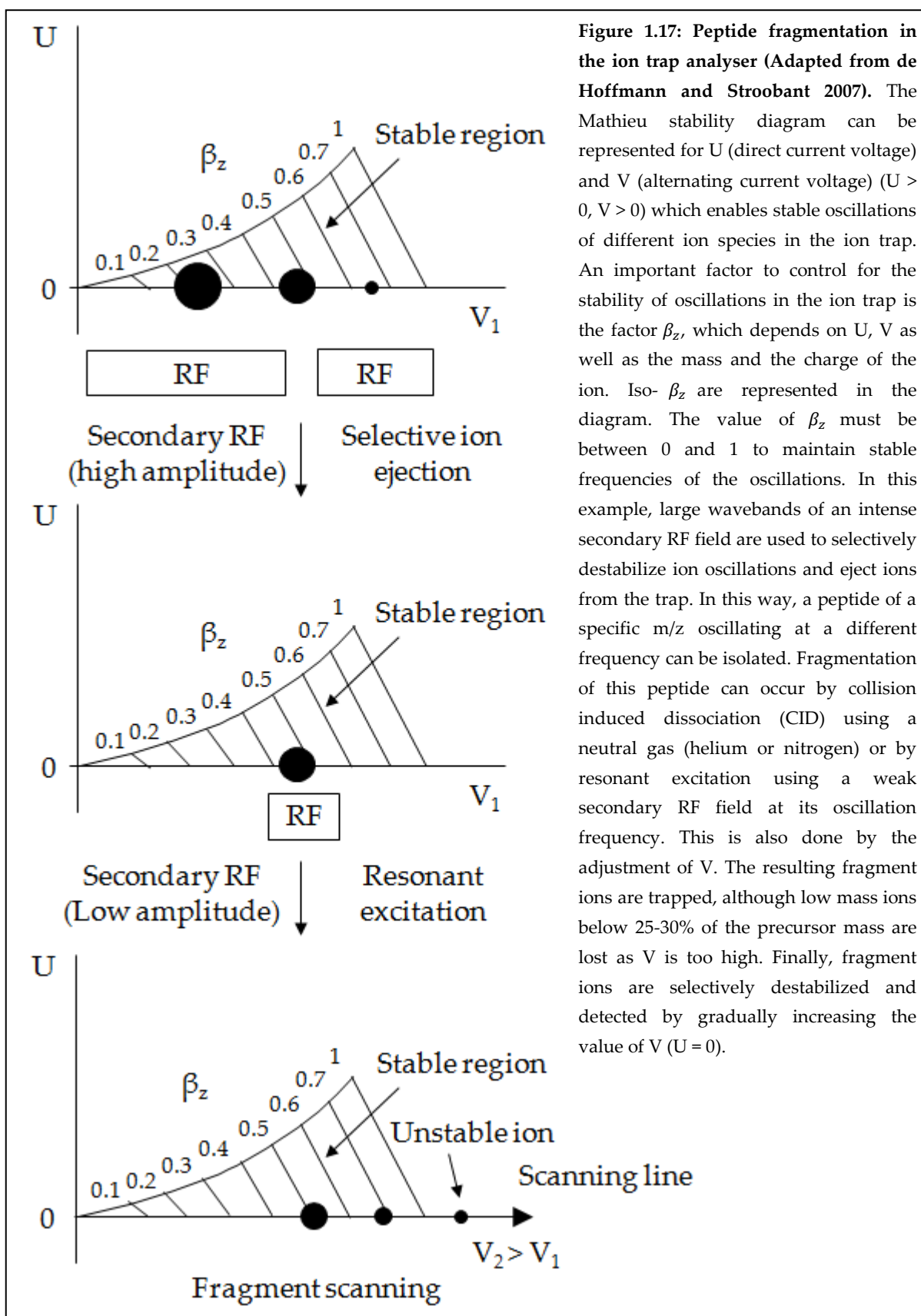


Figure 1.17: Peptide fragmentation in the ion trap analyser (Adapted from de Hoffmann and Stroobant 2007). The Mathieu stability diagram can be represented for U (direct current voltage) and V (alternating current voltage) ($U > 0, V > 0$) which enables stable oscillations of different ion species in the ion trap. An important factor to control for the stability of oscillations in the ion trap is the factor β_z , which depends on U, V as well as the mass and the charge of the ion. Iso- β_z are represented in the diagram. The value of β_z must be between 0 and 1 to maintain stable frequencies of the oscillations. In this example, large wavebands of an intense secondary RF field are used to selectively destabilize ion oscillations and eject ions from the trap. In this way, a peptide of a specific m/z oscillating at a different frequency can be isolated. Fragmentation of this peptide can occur by collision induced dissociation (CID) using a neutral gas (helium or nitrogen) or by resonant excitation using a weak secondary RF field at its oscillation frequency. This is also done by the adjustment of V. The resulting fragment ions are trapped, although low mass ions below 25-30% of the precursor mass are lost as V is too high. Finally, fragment ions are selectively destabilized and detected by gradually increasing the value of V ($U = 0$).

1.6.4.c. Time-of-flight (TOF) analyser

The principle of time-of-flight (TOF) analyser was first described by Stephens in 1946. Ionized peptides are allowed to enter into a flight tube, after preliminary ion acceleration and the increase of their kinetic energy by the application of an electric potential. In the flight tube, no electric potential is applied, thus ions can separate according to their mass-to-charge ratio only (Figure 1.18). The longer the flight tube, the better the resolution of the separation. However there are practical limitations to the maximum size it can be. There is a correlation between the mass-to-charge ratio (m/z) and the time (t) that an ion takes to travel the distance L , as shown in the following equation (de Hoffmann and Stroobant 2007).

$$t^2 = \frac{m}{z} \left(\frac{L^2}{2 e V_s} \right)$$

Where t represents the time, m the ion mass, z the ion charge, L the flight tube length, e the electron charge (1.6×10^{-19} C) and V_s the electric potential used to accelerate the ion from the source.

The advantage of the TOF analyser is that there is no theoretical limit for the mass range ($> 300,000$ m/z), as all ions are detected. This feature also results in very high sensitivity. Modern TOF analyzers are capable of achieving resolution of 40,000 with sub 2 ppm mass accuracy.

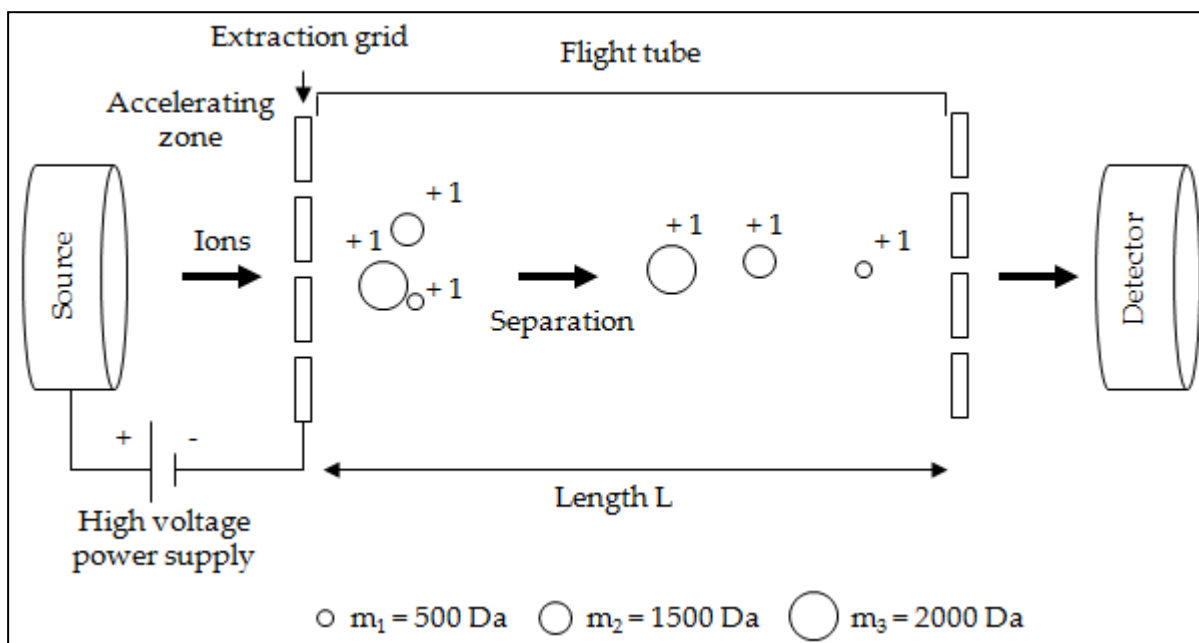


Figure 1.18: Principle of the time-of-flight (TOF) analyser (Adapted from de Hoffmann and Stroobant 2007). Ions are accelerated by an electric potential which gives them kinetic energy $E_k = zeV_s = mv^2/2$, where z is the ion charge, e the electron charge, V_s the electric potential, m the ion mass and v the velocity of the ion. Thus all singly charged peptides ($z = 1$) for example have the same kinetic energy at the time of extraction, but their speed in the flight tube where there is no electric potential, will vary upon their mass only. In this case, the slowest and last ions to reach the detector at the end of the flight tube will be the largest.

1.6.4.d. Fourier transform ion cyclotron resonance (FTICR) analyser

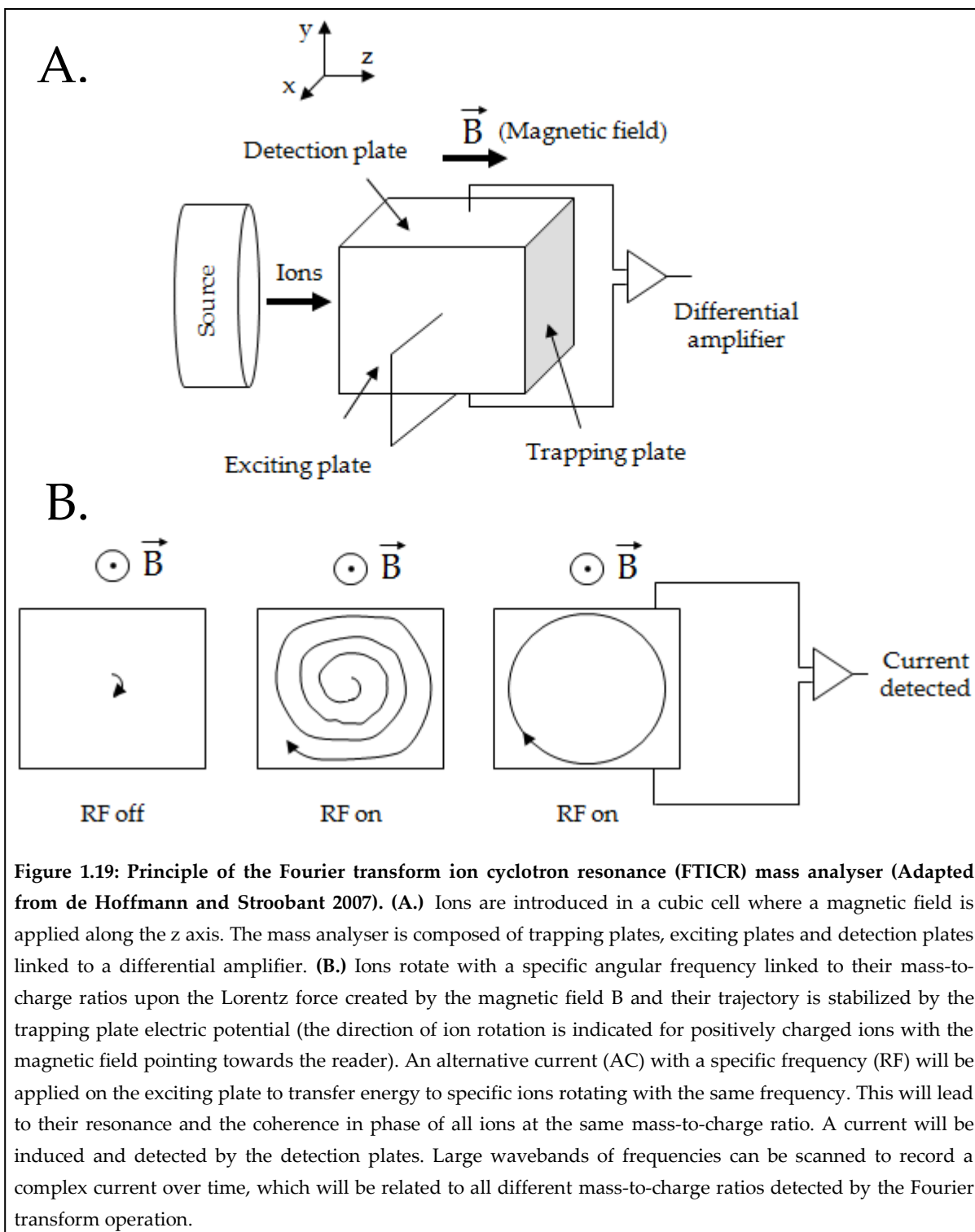
In the Fourier transform ion cyclotron resonance (FTICR) mass analyser, ions are introduced into a cubic cell. A magnetic field B along the axis z submits ions to the Lorentz force which will induce ion rotation with a specific angular frequency ω_c depending on the inverse of the mass-to-charge ratio as shown in the following equation (de Hoffmann and Stroobant 2007).

$$\omega_c = 2\pi f = \frac{v}{r} = \left(\frac{z}{m}\right) eB$$

Where f is the frequency of rotation, v represents the ion velocity, r the circular trajectory radius, z is the ion charge, m the ion mass, e the electron charge and B the magnetic field.

One of the possible methods to detect ions is to excite ions of a specific mass-to-charge ratio rotating at a particular frequency using a brief electromagnetic wave impulse at the same frequency. This will lead to the cyclotronic resonance of these ions in a coherent phase as well as an increase in the trajectory radius. An induced current, called the image current, can then be detected with the detection plates for each frequency (Figure 1.19). Importantly, it is possible to excite all ions by scanning a large waveband of frequencies, leading to their resonance. The complex intensity signal of the induced current acquired during time can then be correlated to the mass-to-charge (m/z) ratio using the Fourier transform mathematical operation.

This analyser enables very high resolution between different ions ($R > 1,000,000$) with a mass range of 30,000 m/z and excellent mass accuracy below 1 ppm. However a limited number of different chemical species can be detected due to space charge effects, similarly with the ion trap. Thus low abundant ions will be detected with reduced precision. Also, this instrument is particularly expensive due to the cost of the supraconducting magnet as well as the cost of the liquid nitrogen and liquid helium required to cool them.



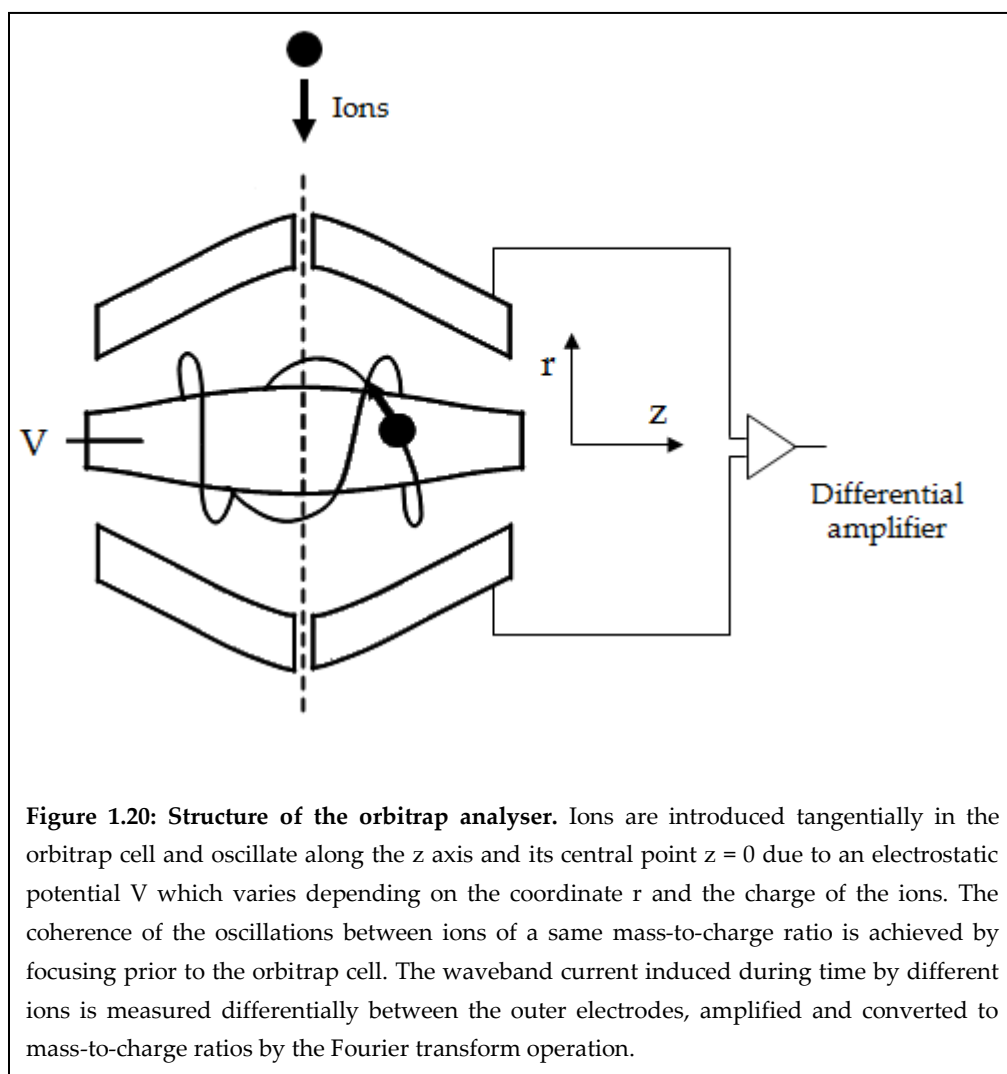
1.6.4.e. Orbitrap analyser

The Orbitrap analyser is the most recent analyser, patented in 1999 by Aleksander Makarov and commercialized in 2005 by ThermoFischer Scientific (Hu, *et al* 2005, Makarov 2000). Ions are injected tangentially into a trap containing a central electrode with an electric potential (V). The electrostatic attraction of the ions towards the inner electrode is balanced by centrifugal forces, resulting in an orbital movement of the ions around the electrode (Figure 1.20). The frequency of the harmonic oscillations around the inner electrode depends on the inverse of the mass-to-charge ratio of the ions, as described in the following equation (de Hoffmann and Stroobant 2007).

$$\omega = \sqrt{\left(\frac{z}{m}\right) k}$$

Where ω is the angular frequency, z the charge of the ion, m the mass of the ion and k a constant. Coherence of the oscillation is achieved by focusing ion bunches prior to the introduction into the Orbitrap and does not require further excitation. Detectors at the outer electrodes will then detect an image current in a similar way as in FTICR and the correlation with mass-to-charge ratios requires the use of the Fourier transform operation.

As the Orbitrap is much less affected by space-charge effects, it is very sensitive. There is very little background due to the lack of coherent oscillations generated by contaminants. It enables very good resolution between different masses ($R > 240,000$), a high dynamic range (5,000 m/z) and high mass accuracy (sub 1 ppm).



1.6.5. Detectors in mass spectrometry

Once separated, ions must be detected and transformed into a meaningful signal. Detection is performed by measuring the charge, mass or ion velocity. Faraday cups, electron multipliers and microchannel plate detectors are widely used in mass spectrometry. In Faraday cups, ions discharge when they hit the detector surface. This discharge is then amplified and measured. They are most used to measure isotopic ratios. Electron multipliers can be discrete or continuous, called channeltrons. Channeltrons are composed of glass dynodes covered with lead or semi-conductors so that each particle which hits the surface provokes an exponential electron cascade amplifying the final collected signal (de Hoffmann and Stroobant 2007).

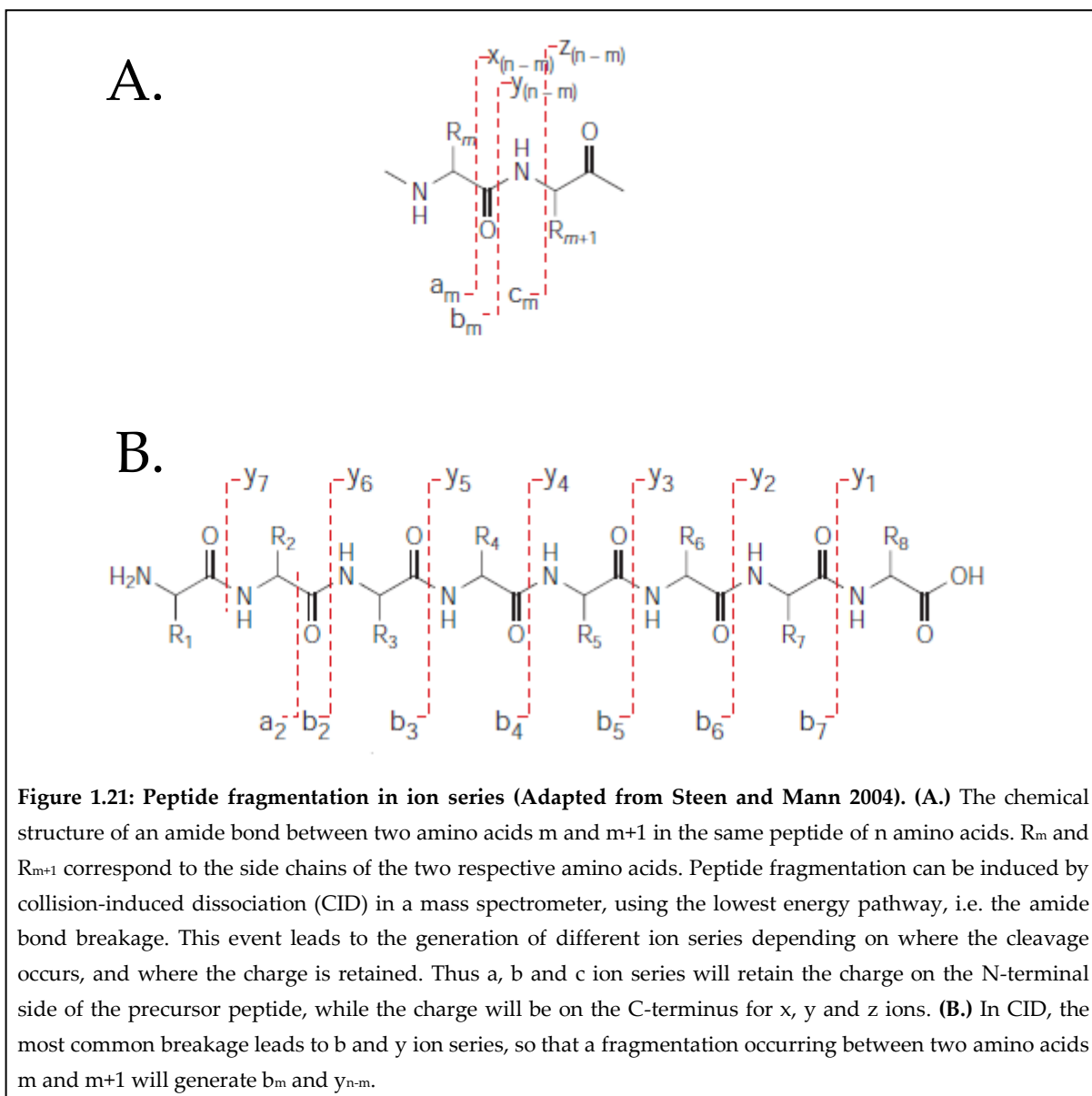
1.6.6. Tandem mass spectrometry

Mass spectrometry (MS) can in some cases be used to identify proteins in simple and well-characterised mixtures by peptide mass fingerprinting. However, the peptide sequence is often required information when dealing with complex mixtures. To address this issue, tandem mass spectrometers have been employed in proteomics to pursue in-depth structural analysis of a peptide by spatial or temporal tandem spectrometry.

Peptides can be fragmented to amino acids by MS^n steps in a collision cell (MS^2 : MS/MS) using different methods of fragmentation such as collision-induced dissociation (CID) using a neutral gas (helium, nitrogen or argon) or electron transfer dissociation (ETD). Fragmentation can occur in every bond of the peptide but the most common cleavage, requiring the lowest energy, occurs between amino acids just at the amide bond (Figure 1.21). In CID, this breakage leads mainly to the formation of b (charge is carried by the N-terminal side of the precursor peptide) and y ions (charge is carried by the C-terminal side of the precursor peptide), while ETD will mainly lead to the generation of c (charge at N-terminus) and z (charge at C-terminus) ions (Boersema, *et al* 2009, Roepstorff and Fohlman 1984, Steen and Mann 2004).

Fragmentation can be performed in both 3D and linear ion traps in the time rather than space domain as it requires the isolation of a peptide precursor (MS), its activation and the scanning of its fragment ions (MS/MS) in the same space. Spatial tandem mass spectrometers have also been designed such as the combination of quadrupole and TOF analysers (QqTOF), or triple quadrupoles (QqQ). In the triple quadrupole instrument, the two scanning quadrupoles are dedicated to peptide analysis whereas the middle one is used as the collision cell. QqTOF mass spectrometers are more accurate than triple quadrupoles due to the nature of time-of-flight detection. The recent 5600 TripleTOF™ (AB Sciex) can detect peptides with high mass accuracy (2 ppm) and high resolution ($R >$

40,000) which is invaluable for the separation of low mass ions such as iTRAQ™ reporter ions (Wolf-Yadlin, *et al* 2007).



However, the triple quadrupole features have been combined with the linear ion trap (LIT) to produce a novel hybrid instrument called the QTRAP™ (AB Sciex) (Hager 2002, Hopfgartner, *et al* 2004). These instruments enable different configuration possibilities depending on the research objectives (Figure 1.22). Neutral loss scanning as well as selected/multiple reaction monitoring (SRM/MRM) coupled to a product ion scan in the LIT (MIDAS™ workflow) can be alternatively used for phosphorylation site mapping,

while SRM is also used for protein quantification (Gerber, *et al* 2003, Unwin, *et al* 2005a, Unwin, *et al* 2009). The orbitrap mass analyser can be combined with the linear ion trap for tandem mass spectrometry (LTQ Orbitrap XL or Velos, ThermoFischer Scientific) to achieve high mass accuracy (1 ppm) and sensitivity but also with a quadrupole (Q Exactive, ThermoFischer Scientific) to achieve faster scan rates (12 Hz compared to 5 Hz).

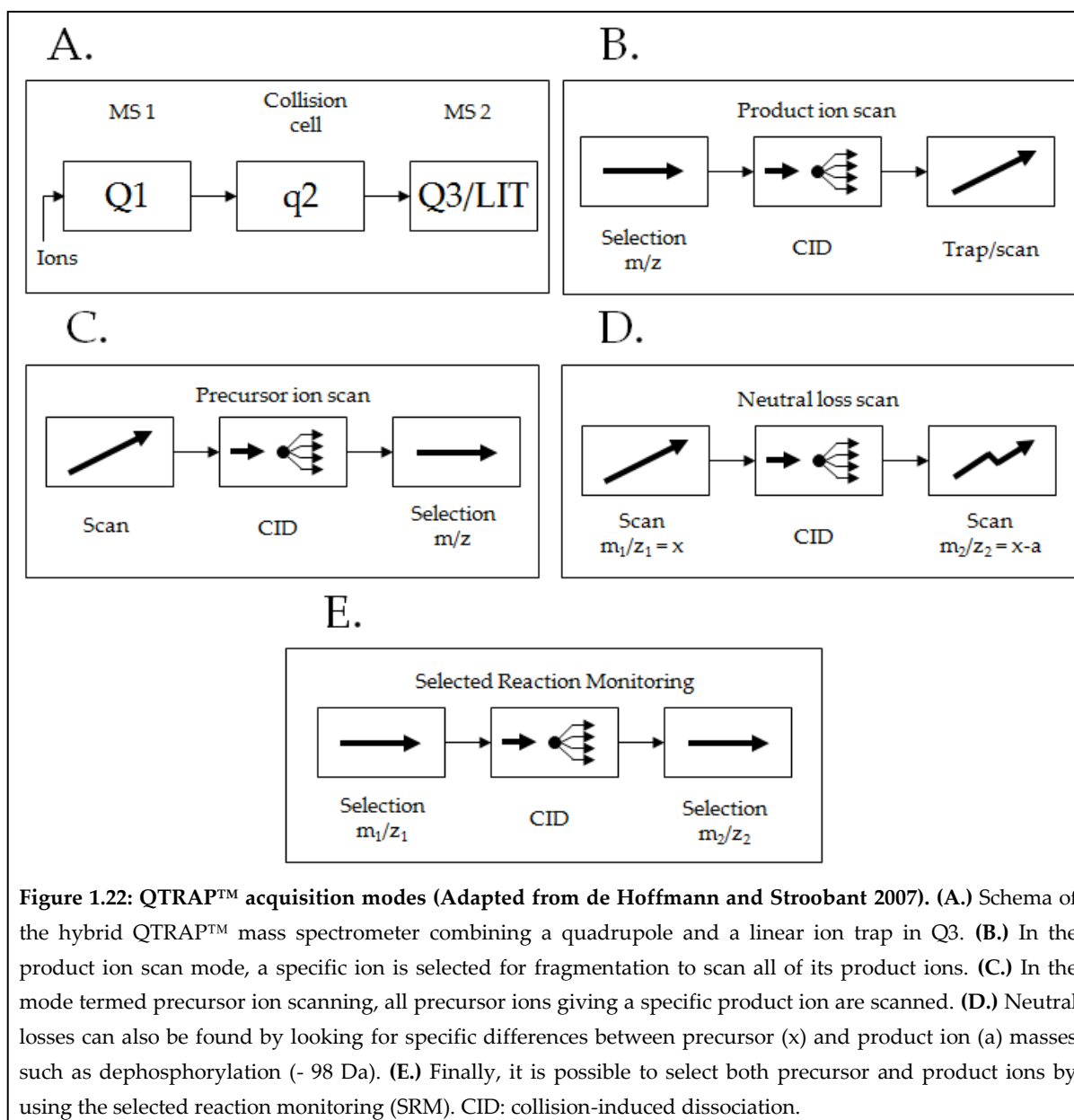


Figure 1.22: QTRAP™ acquisition modes (Adapted from de Hoffmann and Stroobant 2007). (A.) Schema of the hybrid QTRAP™ mass spectrometer combining a quadrupole and a linear ion trap in Q3. (B.) In the product ion scan mode, a specific ion is selected for fragmentation to scan all of its product ions. (C.) In the mode termed precursor ion scanning, all precursor ions giving a specific product ion are scanned. (D.) Neutral losses can also be found by looking for specific differences between precursor (x) and product ion (a) masses such as dephosphorylation (- 98 Da). (E.) Finally, it is possible to select both precursor and product ions by using the selected reaction monitoring (SRM). CID: collision-induced dissociation.

1.6.7. Sequence databases and proteomic software

Protein sequences can be obtained either from protein databases such as SwissProt and MSDB, or from translated coding DNA sequences compiled in Ensembl, Genbank or EMBL nucleotide sequence database. These databases can be interrogated by different proteomic software to identify peptides from experimental evidence (peptide mass, enzyme used for protein hydrolysis, MS and MS/MS spectra) and generate a list of peptides and therefore protein candidates.

ProteinPilot™ software (Applied Biosystems) (Shilov, *et al* 2007), and the original PeptideSearch software (Mann and Wilm 1994), uses a readily interpretable region of the MS/MS spectrum to define a “peptide sequence tag”, composed of a short identified amino-acid sequence and the masses of its two flanking unknown sequences. Then the software will scan peptide sequences generated from protein databases to match the “peptide sequence tag” in peptides of the same mass (Figure 1.23). By contrast, Mascot (Matrix Science) and Sequest (["http://fields.scripps.edu"](http://fields.scripps.edu)) software use respectively statistical and descriptive algorithms to match experimental MS/MS spectra with theoretical MS/MS spectra generated *in silico* from peptides of the same mass (Figure 1.23). In the “probability based scoring” approach used by Mascot, a match between an experimental MS/MS spectrum and a theoretical MS/MS spectrum is scored according to its absolute probability to occur by chance. In the “cross-correlation method” used by Sequest, top preliminary matches between theoretical and experimental MS/MS spectra are cross-correlated to give the best match.

First based on the differences between algorithms to identify peptides, the size of the final protein list also depends on the choice of qualitative constraints (e.g. post-translational modifications, oxidation, sample preparation) and quantitative parameters (error in % or ppm, number of identified peptides for a protein) defined by the analyst. If more than one peptide for a protein is identified, then the protein score increases as well as the confidence in this protein identification (Steen and Mann 2004).

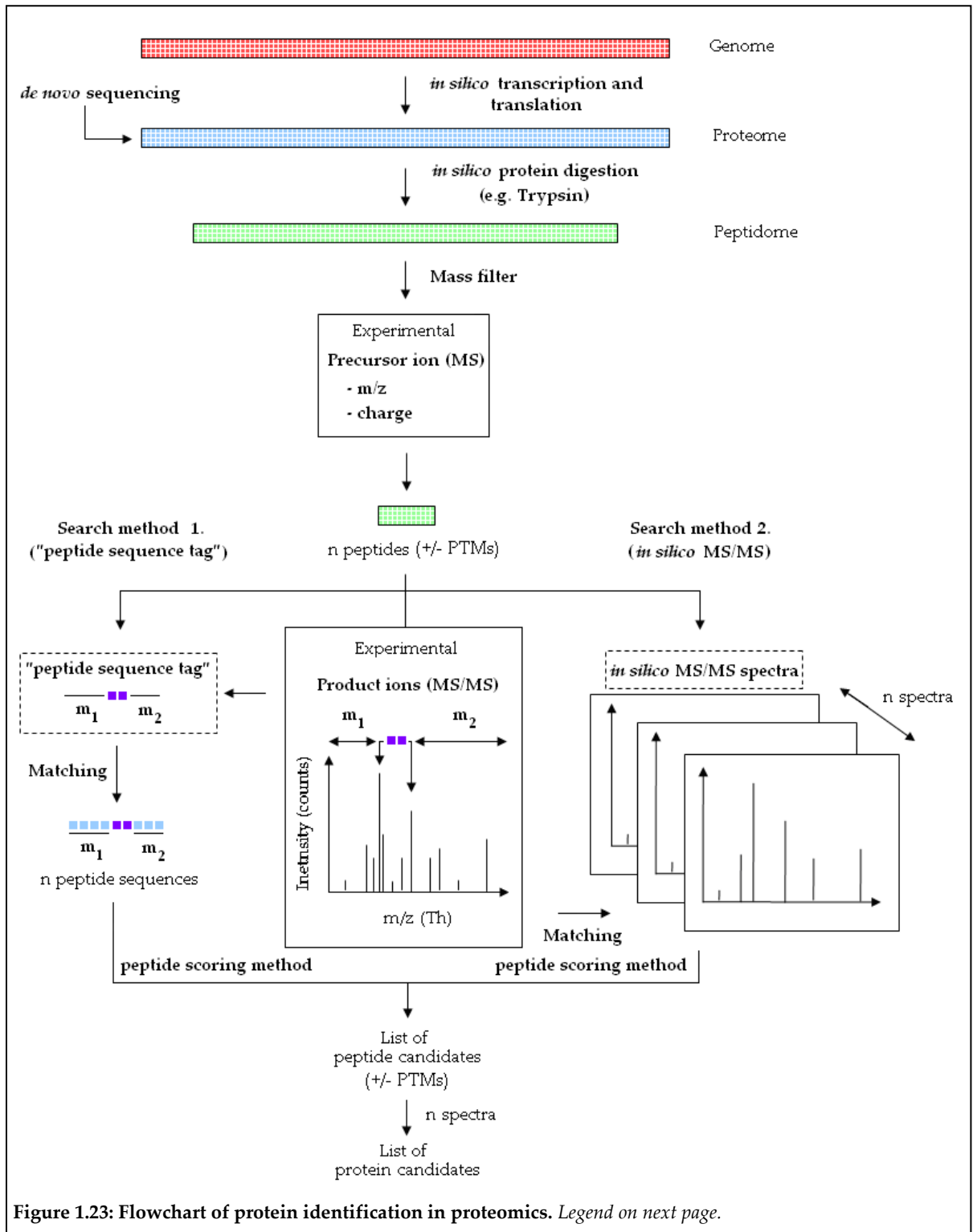


Figure 1.23: Flowchart of protein identification in proteomics. Legend on next page.

Figure 1.23: Flowchart of protein identification in proteomics (Figure on previous page). Gene open reading frame (ORF), obtained from genome sequencing, and/or protein *de novo* sequencing data are used to build proteome databases, containing protein sequences. Experimental evidence (peptide mass, MS and MS/MS spectra) can be used by different algorithms to identify a peptide and its post-translational modifications (PTMs). In the search method 1, some region of an experimental MS/MS spectrum can be easily interpreted to determine a short amino-acid sequence and masses of unknown sequences. The “peptide sequence tag” of the peptide is searched against peptides of the same mass using constraints such as the enzyme used (e.g. trypsin) and biological modifications. Peptides can then be scored according to their ability to fit the peptide sequence tag and further ions from the MS/MS spectrum. By contrast, the search method 2 uses theoretical MS/MS spectra resulting from *in silico* fragmentation of peptide of the same masses resulting from specific cleavage (e.g. trypsin) used for the experiment. Then both experimental and theoretical product ion masses are compared to identify a peptide with a score which depends on the chosen method. In the “probability based scoring” approach, a match between an experimental spectrum and a theoretical peptide MS/MS spectrum is scored according to its absolute probability to occur by chance. In the “cross-correlation method”, top preliminary matches between theoretical and experimental spectra are cross-correlated to give the best match. Finally, significantly identified peptides are used to build a list of protein candidates, which can also be sorted according to their respective scores to give the best estimation of proteins present in a sample (Aebersold and Mann 2003, Steen and Mann 2004).

1.7. Strategies for phosphoproteomics

1.7.1. Function, control and identification of protein phosphorylation

Three hundred distinct post-translational protein modifications (PTMs) are known to occur in biological processes (Witze, *et al* 2007). One of these, phosphorylation, is a key functional modulator of the protein activity found in major cellular pathways such as DNA damage response signalling pathways (Cohn and D'Andrea 2008, Lee, *et al* 2010b, Matsuoka, *et al* 2007, van Attikum and Gasser 2009). Indeed, a phosphoryl group adds a -2 charge to the amino acid residue thus leading to major changes in the conformation of specific protein domains required for the regulation of the protein function (Groban, *et al* 2006). Phosphorylation regulates important cellular processes such as protein kinase activation (e.g. ATM and Src), protein-protein interactions (eg SH2 and PTB domains), protein intracellular transport (e.g. ERK2 and NF- κ B) as well as protein degradation (e.g. I κ B and β -catenin) (Bakkenist and Kastan 2003, Deribe, *et al* 2010, Khokhlatchev, *et al* 1998,

Liu, *et al* 2002, Roskoski 2005, Takada, *et al* 2003). One third of the eukaryotic protein activity could be regulated by addition or removal of phosphorylation by kinases and phosphatases respectively (Witze, *et al* 2007). Protein phosphorylation is a dynamic, reversible modification, which is controlled by fine-tuned regulatory mechanisms. Protein kinases and phosphatases are integrated in regulatory networks controlling the amplitude, the duration and the rate of signalling systems (Heinrich, *et al* 2002). Mathematical modelling of cellular signal transduction composed of multiple components is highly complex, and depends on the strength of the pathway activation. The amplitude of the signal is mostly influenced by kinases while phosphatases have much more impact on signalling rate, signal duration as well as biological outcome of weakly activated pathways (Heinrich, *et al* 2002). However, permanently active oncogenic protein tyrosine kinases will also increase signalling duration. Pathways composed of multiple steps have longer signalling time, longer duration and more flexible distribution of the signal amplification over each step. Importantly, multiple steps enable signal to travel faster with a shorter duration (Heinrich, *et al* 2002). It is also worth considering that protein dephosphorylation can be described as a first order reaction kinetics while protein phosphorylation, which depends on the concentrations of the upstream activated kinase and the unphosphorylated form of the protein substrate, follows a second order reaction kinetics. As rate constants of phosphatases are generally higher than rate constants of kinases, phosphatase inhibition is primordial to have sufficient signal amplification, especially at early steps of the signalling cascade (Heinrich, *et al* 2002). For this particular reason, the study of protein phosphorylation requires the inhibition of protein phosphatases.

Enrichment of phosphoproteins and the determination of their relative abundance between samples are a possible way to infer a regulation *via* protein phosphorylation. However, methods enabling phosphosite assignment have shown that proteins contain generally multiple phosphosites. It has been shown that proteins can be phosphorylated on specific amino acids, such as serine (90% of total phosphosites found), threonine (10%) and tyrosine (< 0,05%) (Nita-Lazar, *et al* 2008). Presently, however it is quite possible that many phosphosites remain to be found and characterized on these amino acids and others such as

histidine (Hess, *et al* 1988, Puttick, *et al* 2008, Robertson, *et al* 1988). Protein phosphorylation corresponds to a mass increase of 80 Da (HPO_3), which of itself has diagnostic value in MS/MS. Phosphorylation on tyrosine is tracked by the loss of a phosphotyrosine-specific immonium ion at 216.043 m/z whereas serine and threonine phosphorylation can be detected by the neutral loss of 98 Da corresponding to phosphoric acid (H_3PO_4). This loss is usually not present for phosphotyrosine which is a more stable protein modification. However, phosphopeptide ionization is lower than seen with non-modified peptides while the phosphosite assignment is a challenge and an area of some concern (Witze, *et al* 2007). Below, some of the recent phosphopeptide enrichment methods to enhance the coverage of phosphopeptides identified in phosphoproteomic analysis are briefly described.

1.7.2. Phosphoprotein and phosphopeptide immunoprecipitation

Immunoprecipitation (IP) can be used to specifically pull-down proteins or phosphopeptides using phospho-specific antibodies targeting modified tyrosine, serine or threonine (Boersema, *et al* 2010, Gronborg, *et al* 2002, Lee, *et al* 2010a, Zhang, *et al* 2005). Antibodies have also been developed to bind specific phosphorylated peptide motifs to enrich substrates of specific kinases (Matsuoka, *et al* 2007). Phosphopeptides are incubated with the antibody bound to protein A or protein G agarose beads and the material is recovered in one elution step following centrifugation. The phospho-specific antibody can also be coupled to protein A or protein G agarose beads after the incubation to avoid non-specific binding between the phosphopeptides, the protein A or G and the agarose beads. Protein A is a cell wall protein of *Staphylococcus aureus* which binds to the Fc region of specific human and mouse antibody isotypes. Protein G is a streptococcal bacteria protein which has similar characteristics (Nita-Lazar, *et al* 2008).

1.7.3. Ion metal affinity chromatography (IMAC)

Ion metal affinity chromatography (IMAC) is a chromatographic technique broadly used to enrich phosphoproteins and phosphopeptides on the basis of the interaction between a negatively charged phosphate group and cations (e.g. Fe^{3+} , Ga^{3+} , Zn^{2+}) chelated on the IMAC resin (Andersson and Porath 1986, Nita-Lazar, *et al* 2008, Unwin and Whetton 2007, Witze, *et al* 2007). Unfortunately, acidic nonphosphorylated peptides, negatively charged at neutral pH, may non-specifically bind to cations and compete with phosphorylated peptides. Loss of phosphopeptides can also happen from poor binding and poor recovery. Thus between 30 and 50 % of the total phosphopeptide sequence population is estimated to be recovered with IMAC enrichment (Witze, *et al* 2007). IMAC shows strong selectivity for multiply phosphorylated peptides (Jensen and Larsen 2007), thus making it an ideal enrichment step prior to other methods such as titanium dioxide affinity chromatography (Thingholm, *et al* 2009, Thingholm, *et al* 2008).

1.7.4. TiO_2 and ZrO_2 affinity chromatography

Titanium dioxide (TiO_2) affinity chromatography demonstrates better capacity for phosphopeptide enrichment than IMAC with the same bed volume (Nita-Lazar, *et al* 2008). This technique is based on the same principle as IMAC, i.e. the interaction between the phosphate group of a phosphopeptide and the TiO_2 particles. It has a greater specificity for phosphopeptides than IMAC, but can also bind non specific peptides in non-acidic conditions (Thingholm, *et al* 2008). Originally developed with 2,5-dihydroxybenzoic acid (DHB) to compete with non-phosphorylated peptides and remove ion suppression of multi-phosphorylated peptides, enrichment with TiO_2 affinity chromatography is now preferably performed with aliphatic acids, such as lactic acid, which improve specificity towards phosphorylated peptides as well as LC/MS system stability (Larsen, *et al* 2005, Rappsilber, *et al* 2007, Sugiyama, *et al* 2007). Also, this method tolerates most biological buffers (Jensen and Larsen 2007). Zirconium dioxide (ZrO_2) has also been investigated in

metal oxide chromatography for phosphopeptide enrichment with similar selectivity to TiO₂/lactic acid affinity chromatography when used with β -Hydroxypropanoic acid (Sugiyama, *et al* 2007, Witze, *et al* 2007).

1.7.5. Sequential elution from IMAC (SIMAC)

Sequential elution from IMAC (SIMAC) has been developed to take advantage of both IMAC and TiO₂ enrichment procedures, as they enable the identification of different phosphopeptide populations (Bodenmiller, *et al* 2007, Thingholm, *et al* 2008). Although multiply phosphorylated peptides can bind to TiO₂ particles, they are difficult to elute. Thus SIMAC combines a first enrichment step with IMAC and the sequential elution of phosphopeptides at low and high pH, to recover both monophosphorylated and multiply phosphorylated peptides. The acidic peptide eluate, the unbound material as well as wash volumes are then passed through TiO₂ particles to enhance the recovery of monophosphorylated peptides. The IMAC eluate obtained at high pH contains multiply phosphorylated peptides and is analysed separately (Thingholm, *et al* 2009, Thingholm, *et al* 2008).

1.7.6. Strong cation exchange chromatography (SCX)

Negatively charged strong cation exchange (SCX) resins bind peptides charged positively so that the columns retain non-phosphorylated peptides at low pH conditions. Multiply and singly phosphorylated peptides elute in the flow-through and at low salt concentrations respectively. However, the elution of phosphopeptides also depends on their sequences and presence of arginine, lysine and histidine residues (Thingholm, *et al* 2009) as it is the case that some phosphopeptides can elute at high salt concentrations. The online combination of SCX with reversed phase (RP) is referred as multi-dimensional protein identification technology (MudPIT) and has been applied to phosphopeptide enrichment (Beausoleil, *et al* 2004, Mohammed and Heck 2011, Schirmer, *et al* 2003). SCX is

often used as a prefractionation technique coupled with IMAC or TiO₂ affinity chromatography to increase selectivity of the phosphopeptide enrichment (Thingholm, *et al* 2009). Nevertheless, coupling methodologies may require a large amount of material which reduces their utility. SCX has also been associated with a weak anion exchange (WAX) resin in a MudPIT mixed-mode ion exchange chromatography to enhance the separation of different populations of phosphopeptides (Motoyama, *et al* 2007)

1.7.7. Phosphosite tagging by chemical derivatization

A nucleophilic tag (e.g. ethanedithiol) can be coupled to the phosphorylation site by Michael addition (Witze, *et al* 2007). β -elimination stabilizes these forms prior to the coupling with a biotin tag on threonine and serine (but not tyrosine) phosphosites to perform avidin affinity purification. Another tag can also be obtained between phosphosites and phosphoramidate (Bodenmiller, *et al* 2007). Both of these methods can be useful to enhance both the capacity and the selectivity of the enrichment procedure (Witze, *et al* 2007).

1.7.8. Experimental approaches for dissecting functional roles of protein phosphorylation

Since the introduction of phosphoproteomics has enabled global phosphosite mapping leading to the discovery of thousands of protein phosphosites, the next and possibly more important challenge that will face biologists is to assign a cellular function to each of them. Matching a phosphorylation event with a particular function or signalling pathway is not a trivial task, particularly if little is known about a protein function and upstream/downstream regulatory pathways. Screening of protein kinase inhibitors and agonists can be a starting point to identify the pathway(s) in which a protein is integrated. Once a putative kinase has been identified, *in vitro* kinase assays may be used for further validation (Ramachandran, *et al* 2011). Important insights into the function of a

phosphosite may be obtained from the generation of genetically engineered *in vivo* models, such as mice expressing a mutated copy of the protein or knock-in mice in which the original gene is replaced with a copy lacking the phosphosite (Deribe, *et al* 2010). Substitutions of tyrosine (Y) to phenylalanine (F) and serine (S) to alanine (A) will prevent protein phosphorylation on a particular residue. Phospho-mimetic amino acid substitutions may also be used such as serine (S) to aspartic acid (D) or glutamic acid (E), although these may not always mimic conformational changes resulting from phosphorylation (Groban, *et al* 2006). However, this strategy may be impracticable for the functional analysis of thousands of phosphosites. Thus the use of computational modelling and bioinformatic tools may support the identification of kinases and relevant pathways by predicting kinase docking sites and appropriate phosphorylated domain conformations (Grewal, *et al* 2006, Groban, *et al* 2006, Obenauer, *et al* 2003).

1.8. Strategies for quantitative proteomics

Several methods can be used to assess the difference in abundance of protein or phosphorylation between biological conditions. Label-free peptide and phosphopeptide quantification has been attempted, based on the direct comparison of multiple independent sets of data (Montoya, *et al* 2011). However, it remains a potentially error-prone method because of differences in ionization efficiency and liquid chromatography reproducibility between mass spectrometry runs (Bantscheff, *et al* 2007, Nita-Lazar, *et al* 2008). Metabolic and chemical labelling strategies should be preferred to compare samples.

1.8.1. Strategies for label free quantification

The cost and the possible limitations of several labelling strategies have led to the development of label-free peptide quantification. The method termed “spectral counting” infers the abundance of a given peptide from the number of MS/MS spectra from which it has been identified. However this method relies on the reproducibility of the selection and fragmentation of this particular peptide, condition not satisfied with highly complex material. Another technique uses the extracted ion chromatogram (XIC) of a peptide which plots the intensity detected for a particular mass-to-charge ratio during MS analysis. The intensity or the area under the peak is proportional with the quantity of chemical entities with this particular mass-to-charge ratio and can be compared between samples. However care must be taken to avoid non-specific background from multiple peptides and substantial loss of the phosphopeptide during enrichment (Montoya, *et al* 2011). Another approach compares all peptide MS signals between different runs using the mass-to-charge ratio and retention time. This approach requires high mass accuracy instruments such as QqTOF or LTQ Orbitrap and the development of bioinformatic software to correct for technical variability. The normalized spectral index (S_N) method corrects for such variability by comparing spectral count, peptide count and the intensity of fragment ions between experiments (Palmisano and Thingholm 2010).

1.8.2. Isotope-coded affinity tags (ICAT)

Isotope-coded affinity tags (ICAT) methodology was developed in 1999 to label different samples at the peptide level using deuterium (Gygi, *et al* 1999a). However, such tags interfered with chromatographic steps as well as the peptide quantification because deuterium hydrophobicity shifts the peptide retention time (Bantscheff, *et al* 2007). Furthermore, the tags only react with cysteines and only proteins containing this amino acid can be identified (Unwin and Whetton 2007). Therefore this method has not gained wide usage even with the shift to ¹³C isotope labelling (Yi, *et al* 2005).

1.8.3. Stable isotope labelling by amino acids in cell culture (SILAC)

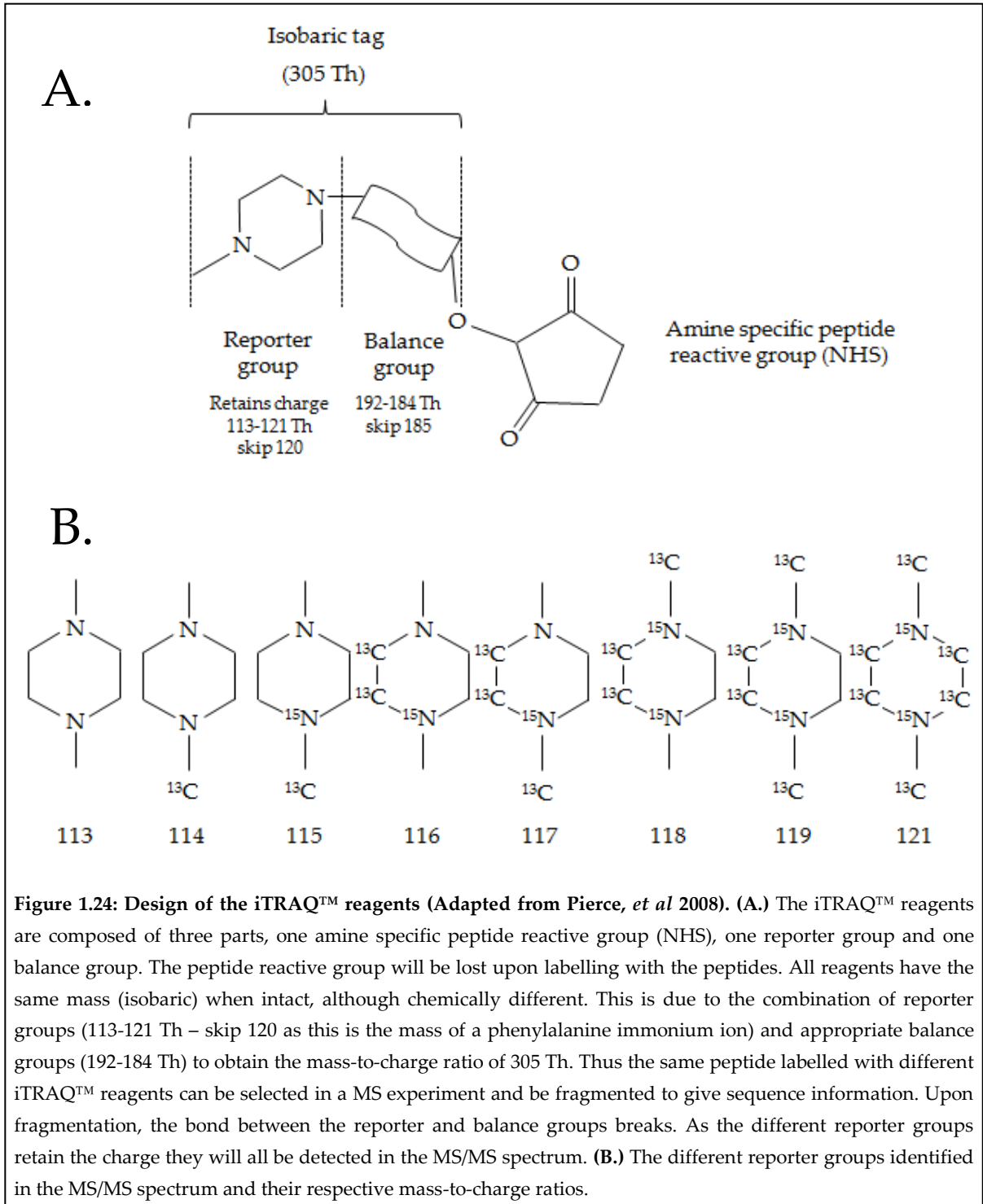
Stable isotope labelling by amino acids in cell culture (SILAC), developed by Ong and Mann in 2002 (Ong, *et al* 2002), has been a real breakthrough for quantitative proteomics. This method consists in differentially labelling cellular protein contents with different combinations of “light” and “heavy” amino acids (e.g. arginine and lysine so that each tryptic peptide can be quantified) containing ^{13}C and ^{15}N stable isotopes in separate culture media. Consequently, cells will metabolically incorporate these elements into newly synthesized proteins after a number of cell divisions so that they will contain either “light” or “heavy” forms of the isotopes in their proteins. The considerable advantage this offers is the pooling of up to five different culture samples at the protein level before enzymatic digestion thus reducing technical variability generated with downstream enrichment procedures (Molina, *et al* 2009). However, this very sensitive method is only suitable for cell lines which can be grown with stable labelled amino acids in culture. It also needs some effort in cell culture development to avoid metabolic conversion between distinct amino acids and the production of multiple labelled amino acids in proteins (Bicho, *et al* 2010), rendering quantitative analysis difficult and time-consuming. Arginine conversion to proline can lead to 10-25% of proline labelling. Correction methods have been tested to compensate the quantitation of proline-containing peptides, while adjustment of arginine concentration or even deletion of arginases and ornithine transaminase can prevent or reduce the conversion, depending on cell types (Bicho, *et al* 2010). Moreover, metabolic labelling requires the presence of the stable labelled amino acid in the peptide sequence for quantification and it requires generally 5 passages to achieve isotopic equilibrium (Unwin, *et al* 2006a). Although primary human samples for medical analysis cannot be processed with SILAC labelling, human material can be compared to protein samples labelled with SILAC. Recently, the super-SILAC technology has been introduced where various human cancer materials can be compared to mixtures of SILAC labelled tissue-specific cancer cell lines (Geiger, *et al* 2010, Geiger, *et al* 2011). However chemical labelling of peptides still remains a worthwhile strategy to develop for this purpose.

1.8.4. Isobaric tags for relative and absolute quantification (iTRAQ™)

Isobaric tags for relative and absolute quantification (iTRAQ™) is a relatively new technology introduced by the company Applied Biosystems in 2005 which has the advantage of being applicable to cell lysates, tissues or serum (Unwin and Whetton 2007). This technology available in 4-plex and 8-plex allowed the relative peptide quantification between up to 8 different samples in a single MS/MS run (Pierce, *et al* 2008b). iTRAQ™ reagents chemically label each free amine of peptides generated during protein enzymatic digestion so that all peptides are theoretically labelled at least once (Unwin and Whetton 2007). iTRAQ™ reagents are composed of a reactive group by which the labelling of a peptide is achieved *via* a *N*-hydroxysuccinimide (NHS) ester, a balance group and a reporter group. For the 8-plex, the mass difference between the reporter and the balance group is designed with different contents of ¹³C and ¹⁵N to reach an isobaric mass of 305 Da before fragmentation. Thus peptides labelled with different iTRAQ™ labels are isobaric and behave similarly during chromatography (Figure 1.24).

As the reporter masses are different, they produce different ions after fragmentation at the MS/MS step, readily detected in the mass spectrum with relatively few other ions present in that region. They are referred as reporter 113-119 and 121 for their respective mass-to-charge ratio in Thompson (Bantscheff, *et al* 2007). The mass-to-charge ratio 120 is missing as it is the mass of a phenylalanine immonium ion (Pierce, *et al* 2008b). As mentioned earlier, reporter groups differ in mass, thus a balance group is used to equilibrate the total mass of the iTRAQ™ reagent. This balance group is not charged after peptide fragmentation and is not present in the MS/MS spectrum. The isobaric property of these tags allows one to select the same peptide from 8 samples at the MS stage with high sensitivity because of the signal amplification of the precursor ion. Moreover, at the MS/MS stage, product ion intensity amplification from sample combination helps for more confident peptide identification, although quantification is primarily dependent on each sample. Protein quantification derives from relative quantification obtained by all its

peptides identified. The 8-plex option of the iTRAQ™ reagent offers more flexibility in the design of studies and may be used for achieving technical and biological replicates thereby increasing quantification confidence (Figure 1.25).



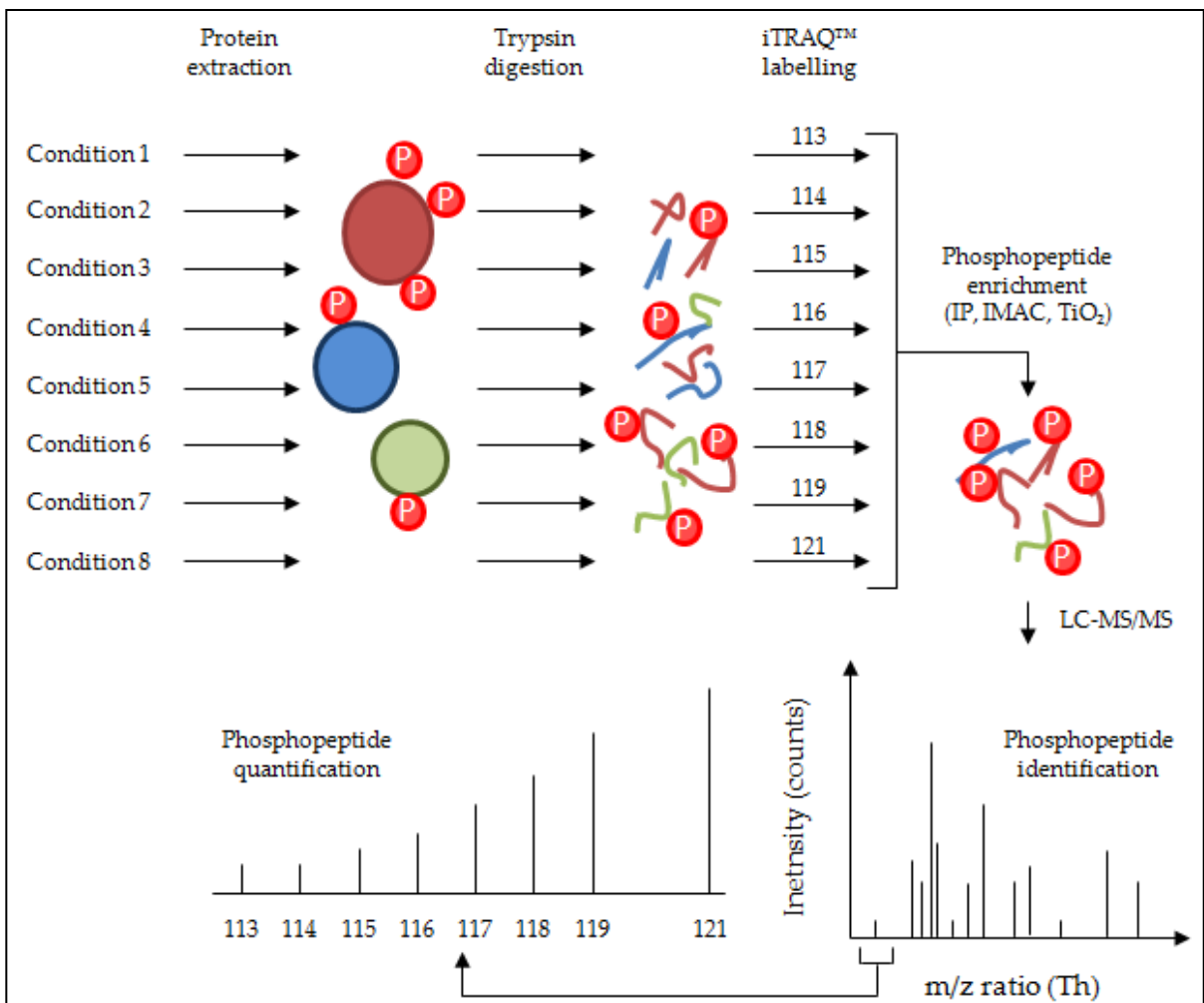


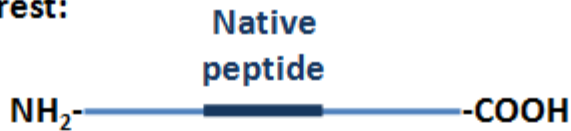
Figure 1.25: Workflow for relative quantification of phosphopeptides with iTRAQ™ peptide labelling. iTRAQ™ labelling strategy can be used easily to compare protein quantities in cell, tissue or serum samples. It also can be used to relatively quantify phosphorylation changes involved in signalling pathways with the relative abundance of phosphorylated peptides in different conditions. Up to 8 samples can be labelled with iTRAQ™ reagents then pooled, enriched and analysed together by mass spectrometry. Phosphorylated proteins can be extracted from whole cells or organelles. Their tryptic digestion generates both phosphorylated and non-phosphorylated peptides. Depending on selectivity of phosphopeptide enrichment methods (IP: immunoprecipitation, IMAC: ion metal affinity chromatography, TiO₂: titanium dioxide affinity chromatography), only phosphorylated peptides should be recovered, then separated by liquid chromatography (LC) and analysed by tandem mass spectrometry (MS/MS). Both protein identification and phosphorylation quantification are achieved at the MS/MS level. Ion reporters are found in a stable spectral window and their relative intensities indicate relative changes in phosphorylation at a particular phosphosite.

1.8.5. Absolute quantification in peptide mass spectrometry (AQUA™)

Peptide absolute quantification can be theoretically achieved using selected reaction monitoring (SRM) with triple quadrupole and hybrid triple quadrupole / linear ion trap mass spectrometers. The method, which can be applied to protein as well as phosphopeptide quantification, is a targeted analysis and requires the design of a stable isotope for a peptide of interest and its introduction in a sample at a known quantity (Gerber, *et al* 2003). Such synthetic peptide has an increment in mass (typically 6-10 Da) which enables the specific selection of either the native peptide (light peptide) or synthetic peptide (heavy or AQUA™ peptide) for a SRM assay along with an ideally intense specific product ion following peptide fragmentation. Comparison of each extracted ion chromatograms (XIC) allows absolute quantification of the native peptide relatively to the known amount of the synthetic peptide (Figure 1.26). This is possible as native and synthetic peptides co-elute during chromatographic steps and produce fragment ions with the same efficiency. The synthetic peptide should be introduced in the sample preparation as early as possible to ensure reliable and accurate results, as the impact of material loss prior to the addition cannot be estimated, affecting the final quantification. Protein quantification should be performed with at least two peptides while peptide and phosphopeptide quantification should be performed using 2-3 SRM transitions to confirm peptide identity and SRM assay specificity (Gallien, *et al* 2011, Gerber, *et al* 2003, Kirkpatrick, *et al* 2005, Sherman, *et al* 2009).

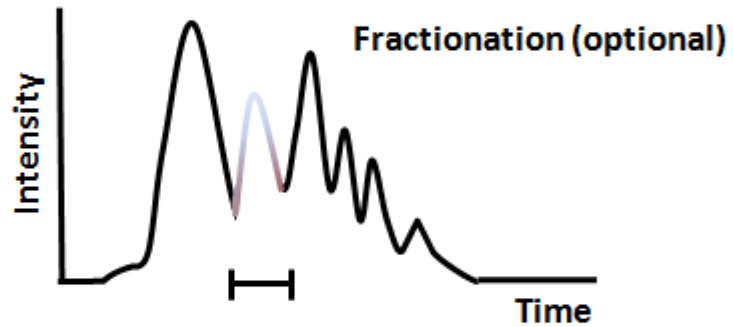
Figure 1.26 Principle of the absolute quantification (AQUA™) method (Figure on next page). A synthetic peptide (AQUA™ peptide) containing stable isotopes of one or more amino acids is designed to match the sequence of a native peptide of interest. After protein preparation, separation with SDS-PAGE (optional) and digestion, a known amount of the AQUA™ peptide is added to the mixture. Further sample preparation could be performed at this stage such as off-line fractionation to reduce sample complexity. Selected reaction monitoring (SRM) is then performed using a triple quadrupole to select specific Q1 and Q3 masses. The masses set at Q1 and Q3 mass analysers enable the specific detection of a fragment product from either the native or the heavy peptide with increased sensitivity. Although heavy and native peptides must elute at the exact same time, this criterion is not enough to ensure the specificity of the assay (identity of the peptide), thus several SRM should be performed for each peptide. Extracted ion chromatograms (XIC) of corresponding Q1/Q3 transitions are then used to determine the relative and absolute amount of the native peptide in comparison with the heavy peptide known quantity. Protein quantification should be performed using several peptides.

Protein of interest:



Cell extraction, SDS-PAGE or other enrichment procedures and protein digestion

Synthetic "AQUA™" peptide
Heavy (e.g. + 8 Da)



LC-SRM

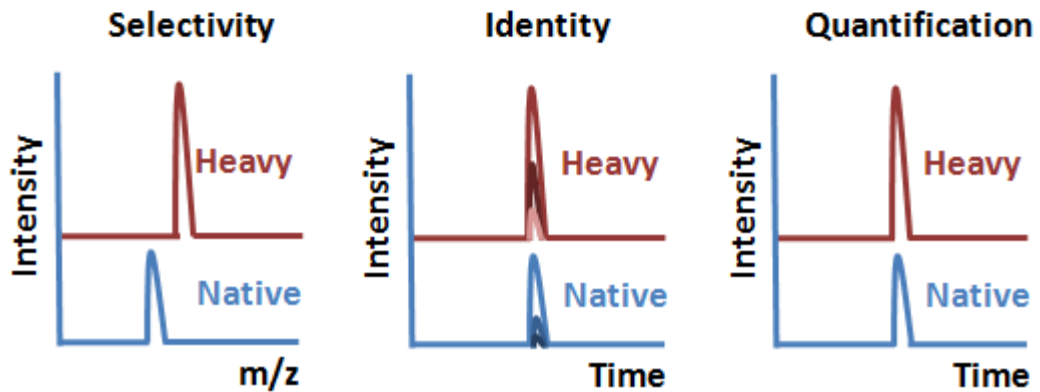


Figure 1.26: Principle of the absolute quantification (AQUA™) method. Legend on previous page.

1.9. Aims and objectives

As previously outlined, leukaemias are related to oncogene expression. Some of these oncogenes are leukaemogenic PTKs. Kinase inhibitors exist to treat patients with chronic myeloid leukaemia (CML) but resistance may occur, especially in advanced stages of the disease. As growing evidence suggests that BCR/ABL PTK, the hallmark of the disease, promotes a mutator phenotype by which it may precipitate disease progression, a global analysis of protein post-translational modifications involved in genotoxic stress is required to delineate the range of dynamic changes modulated by BCR/ABL PTK. As the DNA damage response is mediated by protein kinases a phosphoproteomic approach is appropriate. The hypothesis to be tested in this thesis is that protein phosphorylation related to the DNA damage sensing/repair signalling and/or genotoxic stress signalling pathways would be altered by BCR/ABL and other leukaemogenic PTKs.

The aim of this project is to demonstrate that BCR/ABL PTK expression can affect the DNA damage response and/or genotoxic stress signalling on phosphoproteins which could be involved in leukaemia progression. The objectives of the thesis are as follows:

- To define induced DNA damage in the presence and absence of BCR/ABL PTK with etoposide.
- To use quantitative phosphoproteomics methodology to study changes in phosphorylation status in nuclear proteins in the presence and absence of genotoxic stress and BCR/ABL PTK respectively.
- To identify phosphorylation sites or phosphoproteins, modulated by both the DNA damage response and BCR/ABL PTK expression using appropriate bioinformatic tools.
- To validate one or more modulations of protein phosphorylation identified using complementary techniques such as SRM or phospho-antibodies.
- To further study previously identified phosphosites modulated by BCR/ABL PTK in the context of genotoxic stress.

Chapter 2.

Materials and Methods

2.1. Cell culture

2.1.1. Ba/F3 cell culture

Ba/F3 cells are murine interleukin-3 dependent pro-B cells isolated from BALB/c mouse bone marrow (Palacios and Steinmetz 1985). Ba/F3 cell lines available for this PhD project were obtained from Dr. D. G. Gilliland and Dr. D. W. Sternberg, prepared as previously described (Schwaller, *et al* 1998). Ba/F3 cells were transduced with the retroviral expression vector murine stem cell virus (MSCV), either empty or containing an appropriate oncogene cDNA. BCR/ABL-expressing cells refer to p210^{BCR/ABL}-expressing cells. After 5 passages in selection medium containing Gibco® Genitacin 0.5 mg/mL (Invitrogen, Paisley, UK), Ba/F3 MSCV were grown in Gibco® Fischer's medium 85 % (v/v) (Invitrogen, Paisley, UK), Gibco® horse serum 10 % (v/v) (Invitrogen, Paisley, UK), murine IL-3 5 % (v/v) (mIL-3), Gibco® L-Glutamine 2 mM (Invitrogen, Paisley, UK) while Ba/F3 cells expressing oncogenes were grown without mIL-3 addition but with Fischer's medium 90% (v/v) and Gibco® horse serum 10 % (v/v). Cells were subcultured to 1×10⁵ cells/mL when they reached a cell density of approximately 1×10⁶ cells/mL. Cells were used for experiments in mid-log growth phase, corresponding to a doubling time of approximately 15 h. Murine IL-3 was produced by X63-Ag-653 cells grown in Gibco® McCoy's 5A medium (Invitrogen, Paisley, UK) and 10% (v/v) fetal bovine serum (Sigma-Aldrich, Poole, UK).

2.1.2. Ba/F3 cell stable gene transfection

Stable transfection of Ba/F3 cells with different protein sequences of Thoc5/Fmip was performed by Dr. Maria Belen Gonzalez Sanchez. Thus, Ba/F3 expressing GFP (control),

Myc-tagged Thoc5/Fmip WT-IRES-GFP and Myc-tagged Thoc5/Fmip Y225F-IRES-GFP were used for this project. Briefly, GP+envAm12 (GPAM) packaging cells, corresponding to NIH 3T3 cells expressing Moloney murine leukaemia retroviral proteins gag, pol and env (Markowitz, *et al* 1988) were grown in Dulbecco's modified eagle medium (DMEM) supplemented with 2 mM L-Glutamine (Sigma-Aldrich, Poole, UK) with 10% (v/v) in Gibco® fetal Bovine Serum (Invitrogen, Paisley, UK) and passages were performed by addition of trypsin-EDTA (Sigma-Aldrich, Poole, UK). GPAM cells were prepared in a six well plate (2 mL per well) to around 70% confluency at the time of transfection. DNA was prepared in Opti-MEM® (Invitrogen, Paisley, UK) and micelles were created with lipofectamine according to manufacturer's instructions and incubated with GPAM packaging cells for 6 hours. DMEM supplemented with 20% (v/v) NBS was added for overnight incubation. Replication-defective viruses were then used to infect Ba/F3 cells at $2-4 \times 10^5$ cells/mL for 2 days. Ba/F3 cells were then recovered, washed twice and prepared in cold PBS for sorting with a FACS Vantage SE (BD Biosciences, Oxford, UK) based on GFP expression.

2.1.3. Ba/F3 cell transient gene transfection

Ba/F3-MSCV cells were transfected with different Src plasmids, kind gifts of Dr. Simon Woodcock and Dr. Angeliki Malliri from the University of Manchester (Woodcock, *et al* 2009), using Amaxa® Cell Line Nucleofector® (Lonza, Cologne, Germany) protocol and reagents optimized for this cell line (Kit V). MScV cells were grown at mid-log phase and 2×10^6 cells were centrifuged at 100 RCF for 10 minutes for each condition at room temperature. Cell pellets were resuspended in 100 μ L of Nucleofector solution V supplemented as required. Then 2 μ g of DNA (pBI Src WT, pcDNA3 vSrc, pmaxGFP and no vector as a viability control) were added to the cell suspension and electroporation was performed with the Amaxa® Nucleofector® II device using the Program X-001 optimized for Ba/F3 cells [DSMZ ACC-300 cryopreserved]. Shortly after voltage burst, cells were gently resuspended in 500 μ L Gibco® Fischer's medium supplemented with 10% (v/v) Gibco® horse serum and mIL-3 5% (v/v) and transferred into a 6-well plate containing 1.5

mL of the same medium, pre-incubated at 37°C and 5% (v/v) CO₂ in air. Samples for western blotting were prepared after 24h incubation, centrifuged at 3,000 RCF for 3 min, washed with PBS, centrifuged at 12,000 RCF for 2 min and snap frozen in liquid nitrogen.

2.1.4. Preparation of Lin⁻ cells and mast cells (CD45 WT/null)

PTPRC/CD45 null B6.129 mice were obtained from the Jackson Laboratory (Bar Harbor, ME, USA) then bred with C57BL/6 mice at the animal facility of the Paterson Institute for Cancer Research to obtain homozygous null CD45 mice. Lineage negative (Lin⁻) cell preparation was performed in this laboratory by Dr. Elaine Spooncer as described previously (Spooncer, *et al* 2008). Briefly, haemopoietic cells were recovered from bone marrow femora and tibiae with a syringe and collected in PBS supplemented with 3-5% (v/v) fetal calf serum (FCS). The cell suspension was then incubated with the StemSep[®] cocktail of biotinylated antibodies against cell surface antigens specific to mouse haemopoietic cell lineages [CD5 (Ly-1), CD11b (Mac-1), CD45R/B220, Ly-6G/C (Gr-1), Neutrophils (7-4), TER119] (Stemcell Technologies, Grenoble, France). Bispecific tetrameric antibody complexes (TAC) against both biotin and dextran as well as dextran-coated magnetic nanoparticles were added to the cell suspension. Cells were passed through a magnetic separation column and flow through containing Lin⁻ cells was collected. Lin⁻ cells were then grown in Gibco[®] Fischer's medium supplemented with 20% (v/v) Gibco[®] horse serum, 5% (v/v) mIL-3, recombinant Human FLT3-Ligand 10 ng/mL (PeproTech, London, UK), recombinant mouse stem cell factor SCF 10 ng/mL (AbD Serotec, Oxford, UK) and subcultured at 1×10⁵ cells/mL every 2 days. Mast cells were obtained from bone marrow without above negative selection and were cultured in Gibco[®] Fischer's medium supplemented with 20% (v/v) Gibco[®] horse serum.

2.1.5. Human primary cell culture

All human primary samples were obtained with written informed consent from patients with either newly diagnosed CML in chronic phase or lymphoma (used for control stem cells). Briefly, these samples were enriched for CD34+ cells using CliniMACS (Miltenyi Biotec Ltd., Bisley, UK) and cryopreserved as previously described (Graham, *et al* 2002). After thawing, cells were cultured overnight in complete serum-free medium [Iscove's modified Dulbecco's medium (Sigma-Aldrich, Poole, UK), BSA/Insulin/Transferrin (StemCell Technologies, Vancouver, Canada), 40 µg/mL low-density lipoproteins (Sigma-Aldrich, Poole, UK), and 10⁻⁴ M 2-mercaptoethanol] as described by Graham and colleagues and supplemented with physiological concentrations of growth factors (SCF 0.2 ng/ml, G-CSF 1 ng/ml, GM-CSF 0.2 ng/ml, IL-6 1 ng/ml, LIF 0.05 ng/ml, MIP-α 0.2 ng/ml from StemCell Technologies, Vancouver, Canada).

2.1.6. K562 cell culture

CML blast crisis cell line K562 (ATCC) were cultured in RPMI 1640 Gibco® with 10% (v/v) fetal bovine serum (FBS) Gibco® (Invitrogen, Paisley, UK). Medium was supplemented with 2mM glutamine Gibco®, 100 units/ml of penicillin and 0.1mg/ml of streptomycin (Penstrep, Gibco®) (Invitrogen, Paisley, UK). Cultures were maintained at 37°C, 95% humidity and 5% (v/v) CO₂.

2.1.7. Chemicals and inhibitors

Inhibitors of protein kinase cell signalling as well as several other chemicals were used to treat cells in various experiments. Ba/F3 cells were treated with ATM inhibitor KU-55933 (Tocris Bioscience, Bristol, UK), MEK 1/2 inhibitor U0126 (Cell signalling, Beverly, MA, USA), etoposide VP-16 (PCH Pharmachemie, Haarlem, The Netherlands), SDF-1, leptomycin B, Src inhibitor SU6656, PI3K inhibitor LY294002 and Casein Kinase 2 inhibitor

V Quinalizarin (Calbiochem, Nottingham, UK), N-acetylcysteine and hydrogen peroxide (Sigma-Aldrich, Poole, UK), imatinib mesylate STI571 (Selleck Chemicals, Shanghai, China), 4-Hydroxynonenal (Cayman Chemical from Cambridge Bioscience, Cambridge, UK).

K562 and CML CD34+ primary cells were treated with imatinib (LC Laboratories, Woburn, USA), nilotinib (Novartis, Basel, Switzerland) and dasatinib, kindly provided by Dr. Lee, Bristol-Myers Squibb (Princeton, USA).

2.1.8. γ H2AX assay

A BD FACSCalibur™ flow cytometry system (Becton Dickinson Biosciences, Franklin Lakes, NJ, USA) was used to determine the relative amount of DNA double strand breaks (DSBs) with γ H2AX assay. Binding of anti- γ H2AX antibody, targeting H2AX phosphorylated on serine 139, was used to monitor DNA DSBs by fluoresceine isothiocyanate (FITC) fluorescence intensity (Millipore, Temecula, CA, USA). Cells at $3-5 \times 10^5$ cells/mL were treated for different times with appropriate etoposide concentrations prepared in Gibco® Fischer's medium 10% (v/v) Gibco® horse serum. After centrifugation at 14,000 RCF for 3 min, cells were fixed in Fixation solution 1X [Formaldehyde 2.3% (v/v) / Methanol 0.6-0.9% (v/v)] (50 μ L per 1×10^5 cells) for 20 minutes on ice, washed once in PBS, then lysed in 50 μ L per 1×10^5 cells of Permeabilisation solution 1X [0.5% (v/v) saponin, 10 mM HEPES (pH 7.4), 0.14 M NaCl, 2.5 mM CaCl₂] and incubated with 3.5 μ L per 1×10^5 cells of anti- γ H2AX antibody coupled to FITC or IgG isotype control coupled to FITC for 20 minutes at 4°C with gentle agitation. Finally, the excess of antibody was removed with 100 μ L per 1×10^5 cells of Wash solution 1X [0.1% (v/v) saponin, PBS] and cells were centrifuged at 14,000 RCF for 3 min then resuspended in PBS for flow cytometry analysis within 1 hour.

2.1.9. Apoptosis assay

Samples at $3\text{-}5 \times 10^5$ cells/mL were treated with etoposide or hydrogen peroxide at appropriate concentrations for indicated times. Cells were then centrifuged at 14,000 RCF for 3 min, washed in warm culture medium, centrifuged again at 14,000 RCF for 3 min and replated into complete Fischer's medium supplemented with mIL-3 5% (v/v) for 24h recovery. After approximately 24h, samples were taken and processed with an apoptosis assay kit containing a binding Buffer 10X [0.1 M HEPES (pH 7.4), 1.4 M NaCl, 25 mM CaCl_2], Annexin V coupled with phycoerythrin (PE) and 7-amino-actinomycin D (7-AAD) (BD Pharmingen, BD Biosciences, San Diego, CA, USA). Cells were centrifuged at 14,000 RCF for 3 min, washed in PBS and resuspended at 1×10^6 cells/mL in binding buffer 1X. Then 100 μL of these samples (approximately 1×10^5 cells) were incubated with 5 μL of both Annexin V - PE and 7-AAD for 15 minutes in the dark. Samples were then kept on ice and analysed by flow cytometry within 1 hour with a BD FACSCalibur™.

2.1.10. Flow cytometry analysis of Thoc5/Fmip tyrosine phosphorylation

For cell surface staining of different stem cell populations, CML and non-CML CD34+ cells were incubated with the appropriate antibodies coupled to fluorescent labels for 20 minutes in the dark in the presence of 2% FCS/PBS. Antibodies used were anti CD34-APC, CD38-PerCP, CD90-PE (BD Biosciences, Oxford, UK). The different cell populations, e.g. CD34+CD38+, CD34+CD38-, or K562 cells were fixed and permeabilised using FIX & PERM® kit manufacturer's instructions (Merck Chemicals Ltd., Nottingham, UK). Primary antibodies employed were anti-Thoc5/Fmip pY225 and anti-Src pY416 or rabbit IgG isotype control (Cell Signalling Technology, Beverly, MA, USA) and these were used at 1/100 dilution for 1h at RT. The secondary anti-rabbit FITC antibody (Sigma-Aldrich, Poole, UK) was diluted 100 times and incubated for 30 min at RT.

2.1.11. Immunofluorescence of Thoc5/Fmip tyrosine phosphorylation

K562 cells were spotted on poly-L-lysine coated slides and allowed to adhere for approximately 90 min before being fixed with 3.7% (w/v) formaldehyde/PBS for 15 min at RT. Cells were washed twice with PBS, permeabilised in 0.25% (w/v) Triton X-100 in PBS for 15 min, washed again twice with PBS and blocked with 5% (w/v) BSA in PBS for 30-60 min. Cells were incubated 90 min or overnight with anti-Thoc5/Fmip pY225 antibody, applied at a 1/100 dilution in 5% (w/v) BSA/PBS, or isotype control at the same concentration. Cells were washed three times with 5% (w/v) BSA/PBS and incubated with a secondary antibody coupled to Alexa Fluor® 488 (Invitrogen, Paisley, UK) for 1 hr at RT, also applied at 1/100 dilution in 5% (w/v) BSA/PBS. Cells were washed three times with 5% (w/v) BSA/PBS then once with PBS before mounting and nuclei staining with DAPI (Vectashield, Burlingame, USA). Images were analyzed with Confocal Zeiss Axio Imager M1 fluorescence microscope (Carl Zeiss, Jena, Germany). Images captured were subjected to deconvolution (AxioVision software, Carl Zeiss). Fluorescent signal was measured in 3D by Image Processing and Analysis in Java (Image J) program.

2.2. Sample preparation for protein and proteomic analysis

2.2.1. Whole cell lysis

Cells ($> 1 \times 10^6$ cells) were washed once in cold HBSS buffer [136.7 mM NaCl, 5.35 mM KCl, 0.812 mM MgSO₄, 1.28 mM CaCl₂, 5.5 mM Glucose, 24 mM Hepes, pH 7.4] or cold PBS prior to being quick frozen in liquid nitrogen and then stored at -80°C. Pellets were resuspended in RIPA buffer [Tris-HCl 50 mM, pH 7.4, NP-40 1% (v/v), Na-deoxycholate 0.25% (v/v), NaCl 150 mM EDTA 1 mM] (50 µL per 1×10^6 cells) supplemented with cocktails of phosphatase inhibitors, protease inhibitor and orthovanadate (10 µL/mL each) (Sigma-Aldrich Chemie GmbH, Steinheim, Germany).

2.2.2. Nuclear preparation

Nuclear preparation was performed according to the Nuclear Extract Kit manufacturer's protocol (Active Motif Europe, Rixensart, Belgium). Twenty mL of cells at $4\text{-}5 \times 10^5$ cells/mL were prepared after treatment with etoposide (20 μM) if appropriate. Samples were centrifuged at 4,000 RCF for 5 min at 4°C, washed once in 20 mL of HBSS buffer and then resuspended in 1 mL HBSS buffer supplemented with Nuclear Extract Kit's phosphatase inhibitor. Cells were centrifuged once at 14,000 RCF 3 min at 4°C. Cell pellets were resuspended in 500 μL of manufacturer's hypotonic buffer and incubated on ice for 15 minutes. Then 25 μL of detergent solution were added, samples vortexed for 10s then centrifuged at 14,000 RCF for 30s. Supernatants (cytoplasmic fractions) were collected and pellets (nuclei) were lysed in an iTRAQ™-compatible lysis buffer [TEAB 1M pH 8.5, SDS 0.05% (v/v), protease inhibitor cocktail 10 $\mu\text{L}/\text{mL}$, Benzonase 2 $\mu\text{L}/\text{mL}$ (Novagen, Darmstadt, Germany)], vortexed for 10s and incubated from 20 min to 1h on ice. Finally, lysates were vortexed 30s and insoluble fraction pelleted at 14,000 RCF for 10 min. Supernatants were removed from debris and kept at -80°C.

2.2.3. Protein assay

Proteins were quantified with a Bradford-based protein assay (Bio-Rad Laboratories GmbH, München, Germany). BSA at 0.25 mg/mL was used for the calibration curve with 8 concentrations ranging from 0 to 3.5 μg of protein per well in a 96-well plate format. Each dilution was distributed in triplicate (80 μL). Samples were diluted ten to twenty times in water and 3 \times 5 μL of diluted samples were distributed in three wells previously filled with 75 μL of milli-Q water. Bradford reagent was added to each well (20 μL) which were gently mixed without making air bubbles before UV reading with a Multiskan Ascent V1.22 spectrophotometer (Labsystems Affinity Sensors, Cambridge, UK). Measures were performed at 620 nm and were automatically compared with a reference at 405 nm.

2.2.4. Western blot analysis

Samples were prepared with Laemmli Buffer 4X [Tris-HCl 250 mM pH 6.8, SDS 4% (w/v), Glycerol 60% (v/v), 2-mercaptoethanol 10% (v/v)] and taken for SDS-polyAcrylamide gel electrophoresis (SDS-PAGE) after boiling for 5 min at 100°C to denature protein. Gels were prepared with ProtoFLOWGel™ solution [30% acrylamide (w/v) / 0.8% (w/v) bis-acrylamide] purchased from Flowgen Bioscience Ltd (Nottingham, UK), ammonium peroxydisulfate (APS) 10% (w/v), prepared fresh daily from powder supplied by BDH Laboratory supplies (Poole, UK) and N,N,N',N'-Tetramethylethylenediamine (TEMED), purchased from Sigma-Aldrich (Poole, UK). The upper stacking gel layer was prepared at fixed acrylamide concentration [4% acrylamide (w/v) / 0.11% (w/v) bis-acrylamide, Tris-HCl 125 mM pH 6.8, SDS 0.1% (w/v), TEMED 0.07% (v/v), APS 0.06% (w/v)], while the acrylamide percentage of the lower resolving gel layer varied upon application from 6 to 15% [Tris-HCl 375 mM pH 8.8, SDS 0.1% (w/v), TEMED 0.07% (v/v), APS 0.1% (w/v)]. After running the gel in running buffer [Tris-base 25 mM, Glycine 192 mM, SDS 0.1% (w/v)], proteins were transferred onto a nitrocellulose membrane (GE Healthcare, Little Chalfont, Buckinghamshire, UK) for 45 min at 100 V in transfer buffer [Tris-base 25 mM, Glycine 192 mM, Methanol 20% (v/v)]. The concentration of methanol in the transfer buffer was reduced when investigating proteins with high molecular weight (> 100 kDa). The membrane was then incubated with a solution of dry milk powder at 3% (w/v) in PBS Tween 20 [0,05% (v/v)] for 20 min to 1h to block the membrane with aspecific proteins. The membrane was then incubated with an appropriate primary antibody probing a specific protein such as Thoc5/Fmip (F6d11) (LR Immunodiagnosics Unit, John Radcliffe Hospital, Oxford, UK), Thoc5/Fmip pY225 (Eurogentec, Liège, Belgium), Actin (Sigma-Aldrich, Poole, UK), α -Tubulin (B-7), Hemogen (M-180 and T-20), I κ B- α (C-21) and NF- κ B p65 (C-20) (Santa Cruz Biotechnology, Santa Cruz, Ca, USA), pCRKL, GAPDH, Hsp90, Histone H3, Src, Src pY416, MycTag (9B11) (Cell Signalling Technology, Beverly, MA, USA), CD45 (BD Transduction Laboratories, BD Biosciences, Oxford, UK) MEK1 [32G3], Hsp40, Hsp70 [5A5] (Abcam, Cambridge, UK) and H2AX pY142 (Millipore, Temecula, CA, USA). These antibodies were diluted in PBS Tween 20 [0,05-0,1% (v/v)] containing either BSA or dry

milk at 1% (w/v). The membrane was incubated from 1h at room temperature or overnight at 4°C, depending on the antibody. The membrane was washed for 15 min three times in PBS Tween 20 [0,05-0,1% (v/v)] before incubation with anti-mouse or anti-rabbit secondary antibodies (GE Healthcare, Little Chalfont, Buckinghamshire, UK) coupled with horseradish peroxidase (HRP) diluted 1:10000 in PBS Tween 20 [0,05% (v/v)] containing dry milk powder at 3% (w/v). After incubation, the membrane was washed for 15 min three times in PBS Tween 20 [0,05-0,1% (v/v)]. Finally, proteins or phosphorylation motifs of interest were revealed on the membrane by the HRP enhanced chemiluminescence activity according to manufacturer's instructions (Pierce, Rockford, IL, USA).

2.2.5. Study of the etoposide-induced genotoxic stress with iTRAQ™ peptide labelling

Ba/F3 MSCV and BCR/ABL-expressing cells were grown in complete Fischer's medium supplemented with mIL3 5% (v/v) for 16h. Twenty mL of cells at $4-5 \times 10^5$ cells/mL were exposed to etoposide (20 μ M) for 20 min, then centrifuged at 2,000 RCF for 5 min. Supernatant was discarded and cells were washed with 20 mL of warm medium before centrifugation at 2,000 RCF for 5 min. Cells were resuspended in 20 mL of fresh Fischer's medium supplemented with mIL3 5% (v/v) and incubated for 1h. The level of DNA damage was assessed using the γ H2AX assay described previously. Nuclear preparations were performed as described above. Biological replicates were prepared to obtain eight nuclear extracts suitable for 8-plex iTRAQ™ labelling (AB Sciex, Warrington, UK). An aliquot of each nuclear enriched sample was used to check quality and reproducibility of the preparation by western blot of Histone H3 and Tubulin, as markers of the nucleus and cytosol, respectively. A hundred μ g of nuclear proteins was prepared in TEAB 1M pH 8.5 (20 μ L final volume) and reduced with 0.1 volume of Tris(2-carboxy-ethyl)phosphine hydrochloride (TCEP) 50 mM (Sigma-Aldrich, Poole, UK). Samples were vortexed and spun before incubation at 60°C for 1h. Free cysteines were blocked with 0.05 vol of 200 mM methylmethanethiosulphate (MMTS) in isopropanol, vortexed, spun and incubated at room temperature for 10 minutes. Finally, each sample was digested with 5 μ L of trypsin

reconstituted at 2 g/L (Promega, Madison, WI, USA) overnight at 37°C. After trypsin digestion, samples were spun and incubated with the full content of one iTRAQ™ reagent pack (AB Sciex, Warrington, UK) resuspended in 50 µL isopropanol (Sigma-Aldrich, Poole, UK) at pH ≥ 8 for 2h. Samples were then dried down separately until about 15 µL was remaining then samples were pooled and dried down to completeness and a dark brown pellet was formed.

2.2.6. Phosphopeptide enrichment with TiO₂ affinity chromatography

The iTRAQ™-labelled peptide mixture was resuspended in 150 µL of lactate loading buffer [240 mg/mL Lactate, 80% (v/v) Acetonitrile, 5% (v/v) TFA] and loaded onto a TopTip TiO₂ resin (Glygen Corp., Columbia, MA, USA supplied by Chromatography Consulting International Limited, Liverpool, UK) pre-equilibrated with 2 × 75 µL of the same buffer. Lactate buffer was purchased from Fluka Chemicals Ltd, Gillingham, UK. The flow-through was kept and reloaded onto a new tip. After sample loading, the tip was washed twice with 60 µL of lactate buffer then four times with 60 µL of washing buffer [80%(v/v) Acetonitrile, 5% (v/v) TFA]. Phosphopeptides were eluted with 60 µL of elution buffer containing ammonium hydroxide purchased from Sigma-Aldrich, Poole, UK [0.56% (v/v) ammonium hydroxide in water, pH 10.5]. The procedure was repeated with the first flow-through and eluates were combined and concentrated with a speed-vac for 1h prior to peptide fractionation.

2.2.7. Phosphopeptide fractionation with high-pH reversed phase (RP) chromatography

Peptides were fractionated off-line using a high pH chromatography system. Peptides were resuspended in 1 mL of buffer A [0.1% (v/v) ammonium hydroxide in H₂O, adjusted to pH 10.5 with formic acid] and loaded onto a C₁₈ reversed phase (RP) column such as Fortis C₁₈ (3 µm, 100 × 4.6 mm) or Agilent Zorbax Extend-C₁₈ (3.5 µm, 150 × 4.6 mm)

operated by Dionex/LC Packings Ultimate LC system ICS-3000 SP and Chromeleon software 6.60 SP6 Build 1518 (Dionex UK Ltd., Leeds, UK). Phosphopeptides were eluted at 700 $\mu\text{L}/\text{min}$ with a 30 min linear gradient of acetonitrile (Fischer Scientific, Loughborough, UK) starting from 0.5% (v/v) buffer B [0.1% (v/v) ammonium hydroxide in acetonitrile, pH 10.5] to 50% (v/v). Buffer B percentage was increased to 75% (v/v) in 4 minutes and maintained at this value for another 4 minutes before being reduced to 0.5% (v/v). Fifteen second fractions were taken for 30 min. Peptides were then concentrated with a speed-vac and stored at -80°C .

For absolute quantification (AQUA™) of Hemogen pS380, 2 μg (1.5 nmol) of the Hemogen synthetic (AQUA™) phosphopeptide (EFTVPIVSpSQK* with K*: K + 8 Da) (New England Peptide LLC, Gardner, MA, USA) were prepared in 100 μL of buffer A to determine its elution time on the C₁₈ RP column. A hundred μg of nuclear extracts from MSCV and BCR/ABL-expressing cells treated or untreated with etoposide and prepared as in section 2.2.5 were digested with trypsin at 2 g/L (Promega, Madison, WI, USA) overnight at 37°C . Three biological replicates of each sample were prepared. Peptides were dried for 1h under vacuum. Dried peptides were resuspended in 1 mL of buffer A and 250 fmol of the Hemogen (AQUA™) peptide was spiked in before off-line fractionation. Peptides were collected in a 2 min window comprising the Hemogen (AQUA™) peptide elution time and were concentrated under vacuum before LC-SRM analysis.

2.3. Mass spectrometry

2.3.1. Study of the etoposide-induced genotoxic stress

Peptides for isobaric tagging experiments were analysed using a QSTAR® XL or QSTAR® Elite (AB Sciex, Warrington, UK). For the QSTAR® XL, appropriate fractions from off-line fractionation were resuspended in 180 μL of buffer A [Acetonitrile 2% (v/v), Formic Acid 0.1% (v/v)] and 60 μL was loaded onto an on-line column (15 cm length ; 75 μm inner diameter) packed with RP C₁₈ PepMap100 (3 μm , 100 Å) using a UltiMate™ pump (LC

Packings, Amsterdam, Netherlands) and separated at 250 nL/min over a 90 min solvent gradient from 5.9% (v/v) acetonitrile / 0.1% (v/v) formic acid to 41% (v/v) acetonitrile / 0.1% (v/v) formic acid coupled to a QSTAR® XL mass spectrometer (AB Sciex, Warrington, UK), followed by 30 min of washing and column re-equilibration. Data were acquired using an information dependent acquisition (IDA), designed with Analyst QS 2.0 (AB Sciex, Warrington, UK) which selected in the MS scan the two most abundant multiply charged peptides (2+ to 4+) above a 20 count threshold with m/z between 400 and 2000 for MS/MS and this for each cycle of the acquisition. Each ion was selected a maximum of two times and was then dynamically excluded (± 50 mmu) for 1 min.

Some fractions were dried down and reanalyzed using a QSTAR® Elite (AB Sciex, Warrington, UK). Fractions were resuspended in 10 μ L of 3 % (v/v) acetonitrile, 0.1 % (v/v) formic acid and 20 mM citric acid to reduce binding between metallic parts of the chromatographic system and phosphopeptides (Winter, *et al* 2009). Five μ L of these fractions were loaded for 5 minutes at 15 μ L/min onto a nanoACQUITY UPLC Symmetry C₁₈ Trap (5 μ m, 180 μ m x 20 mm) piloted with MassLynx™ (Waters, Manchester, UK). Analytical separation of the peptides was performed at 300 nL/min using a nanoACQUITY UPLC BEH C₁₈ Column (1.7 μ m, 75 μ m x 250 mm) over a 91 min solvent gradient from 3% (v/v) acetonitrile, 0.1% (v/v) formic acid to 40% (v/v) acetonitrile, 0.1% (v/v) formic acid. Data was acquired using an information dependant acquisition (IDA) designed with Analyst® software QS 2.0 Build 1446 (AB Sciex, Warrington, UK) which selected for each cycle the four most abundant multiply charged peptides (2+ to 4+) in the MS scan above a 10 count threshold with m/z between 400 and 2000. Each ion was selected a maximum of two times and was dynamically excluded (± 50 mmu) for 90 seconds thereafter.

2.3.2. Data analysis

Spectra from QSTAR® XL and Elite were searched separately using ProteinPilot™ v3 software (Paragon version 3.0.0.0, 113442 with default settings, AB SCIEX, Framingham,

USA) to identify and quantify peptides as well as proteins from the Ensembl (FIXME reference, www.ensembl.org) murine “ens_mus_musculus_core_58.fasta” database containing 115,658 protein entries (species *Mus musculus* and “Thorough” search effort). Identification focus was on biological modifications with phosphorylation emphasis as a special factor. Search parameters included iTRAQ™ 8plex modification at peptide level, cysteine alkylation with MMTS, trypsin digestion, QSTAR® Elite ESI as instrument for the QSTAR® Elite ESI and QSTAR® ESI for the QSTAR® XL. A global false discovery rate (FDR) was performed using a decoy database and determined at 1.3% at the peptide level for a 20% confidence level. We used the peptide confidence of 20% as threshold for the valid identification of phosphoentities. Ratio values for each phosphoentity were obtained from weighted averages of multiple spectra when appropriate, similarly to the way ProteinPilot™ calculate ratios for proteins. The minimum iTRAQ™ reporter ion area used for quantification was set at 20 (arbitrary units). Weighted ratios were log-averaged for the 244 phosphoentities identified with both QSTAR® XL and QSTAR® Elite. ProteinPilot™ biases were used to correct for any sampling error so that the median value of $\log_2(\text{ratios})$ of the phosphoentity distribution is equal to 0 for each pair of iTRAQ™ reagents. The distribution of the biological replicates Control(2):Control(1) was used to determine the biological variability of the procedure by combining the 4 control ratios MSCV(2):MSCV(1), MSCV+Etoposide(2):MSCV+Etoposide(1), BCR/ABL(2):BCR/ABL(1) and BCR/ABL+Etoposide(2):BCR/ABL+Etoposide(1) obtained for the QSTAR® XL and QSTAR® Elite instruments. Student’s t-test was performed between the values of 2 biological replicates for each appropriate ratio and the gaussian distribution of the biological replicates Control(2):Control(1) (see below). Phosphoentities determined as potentially changing had a Student’s t-test p-value < 0.05 in appropriate ratiometric analysis. Phosphoentities changing between the two controls, i.e. for Control(2):Control(1) ratio, with a p-value < 0.05 were manually removed from the analysis. Clustering was performed with Cluster 3.0 version 1.50 (de Hoon, *et al* 2004) on phosphoentities having full quantification information. No further filtering, centering or normalization was performed. The k-means method was used using 8 clusters with 100 repeats using the

Euclidian distance as the similarity metric and the resulting heatmap was visualized using Java Treeview 1.1.6 (Saldanha 2004).

2.3.3. Validation with selected reaction monitoring (SRM)

Absolute quantification (AQUA™) experiments were performed with a 4000 QTRAP® (Applied Biosystems, Foster City, CA) mass spectrometer coupled to a liquid chromatography system consisting of a Famos autosampler, a Switchos trap system and an Ultimate Plus dual pump (LC Packings, Dionex, Sunnyvale, CA). Peptides were resuspended in buffer A [97.9% (v/v) water, 2% (v/v) acetonitrile and 0.1% (v/v) formic acid] and washed onto a trap C₁₈ column (LC Packings, Dionex, Sunnyvale, CA). Peptide elution was then performed using a gradient of buffer B [79.9% (v/v) acetonitrile, 20% (v/v) water and 0.1% (v/v) formic acid] and passed through an analytical C₁₈ column (Acclaim pepmap 100, 15 cm, pore size 100 Å) from Dionex (LC Packings, Dionex, Sunnyvale, CA). The LC system and the mass spectrometer were piloted with Chromeleon 6.50 SP4 Build 1000 and Analyst 1.5.1 (Applied Biosystems, Foster City, CA), respectively. A calibration curve was performed with the AQUA™ peptide by injecting in triplicate on the system 0, 1, 5, 10, 50, 100 and 500 fmol prepared in 55 µL of buffer A. Quantification was performed with the maximum intensity in counts per second (cps) of the extracted ion chromatogram (XIC) of the transition 662.0/846.5, while two other transitions were used to confirm peptide identity, i.e. 662.0/748.5 and 662.0/1046.6. The equivalent transitions were created for the native peptide (Table II).

Table II: Parameters used for selected reaction monitoring for the native and the AQUA™ Hemogen peptides

Peptide	Sequence (K*: K + 8 Da)	Precursor ion charge state	Q1 m/z (Th)	Q3 m/z (Th)	Fragment (1+)	Dwell time (ms)	CE (V)
AQUA™	EFTVPIVSpSQK*	2+	662.0	846.5	y ₇	400	32.1
	EFTVPIVSpSQK*	2+	662.0	1046.6	y ₉	200	32.1
	EFTVPIVSpSQK*	2+	662.0	748.5	y ₇ - H ₃ PO ₄	200	32.1
Native	EFTVPIVSpSQK	2+	658.0	838.5	y ₇	400	32
	EFTVPIVSpSQK	2+	658.0	1038.6	y ₉	200	32
	EFTVPIVSpSQK	2+	658.0	740.5	y ₇ - H ₃ PO ₄	200	32

The method had a total cycle time of 1.6401 s, the ion source voltage was 2300.0 V, the curtain gas was 20.0 and the interface heater temperature was 155.0°C. Collision energies (CE) for both the native and AQUA™ peptides were calculated using the following equation:

$$CE = [a \times (m/z)] + b$$

Where a = 0.044 and b = 3.000 are parameters for a doubly charged peptide optimized for this particular instrument by Drs. John Griffiths, Richard Unwin and Duncan Smith (unpublished work). The method was tested with 100% buffer A and 500 ng of trypsinized nuclear material to assess the level of different backgrounds for all transitions. Additionally, the AQUA™ peptide did not trigger the transitions of the native peptide for the range of quantities injected for each sample (< 50 fmol of AQUA™ peptide). Dried peptides were resuspended in 165 µL of buffer A and analysis was performed with 55 µL. Q1 mass resolution was set at “low” and Q3 at “unit”.

2.4. Statistical methods

2.4.1. Parametric tests

For the analysis of the phosphoproteomics dataset, a two-sided unpaired two-sample Student’s t-test was performed under the assumptions of data normality and equal variance

between the biological control distribution Control(2):Control(1) and the ratio values of the 2 independent biological replicates, for each ratio of interest. The null hypothesis of the test was that the mean of the 2 independent ratio values was not different than the mean of the biological control distribution Control(2):Control(1). The null hypothesis was rejected when the Student's t-test p-value was < 0.05 . R project software (www.r-project.org/) version 2.13.1 (2011-07-08) and the function TTEST in Microsoft© Excel were used to compute p-values.

For the analysis of γ H2AX and apoptosis assays under the assumption of data normality and unequal variances, paired and/or unpaired two-sided Student's t-test were performed when appropriate. The null hypothesis was that the mean of data from sample 1 was not different from the mean of data from sample 2. The null hypothesis was rejected when the Student's t-test p-value was < 0.05 . The function TTEST in Microsoft® Excel was used to compute p-values.

2.4.2. Non-parametric tests

R project software (www.r-project.org/) version 2.13.1 (2011-07-08) and StatsDirect statistical software Version 1.9.7 (Iain E. Buchan. All rights reserved) were used to perform Wilcoxon signed-rank test and Mann-Whitney U test, also called Wilcoxon rank-sum test, to compare paired and unpaired data, respectively. These statistical tests do not require the assumption that the sample data belong to a Gaussian distribution. Type I error (α) was chosen at 0.05 for two-sided tests. The null hypothesis was that there was no difference between the mean of data from sample 1 and the mean of data from sample 2. The null hypothesis was rejected when the p-value was < 0.05 .

2.4.3. Standard error of the mean

The error bars shown in graphics (histograms and scatter plots) represent the standard error of the mean (SEM) calculated from replicate observations (Cumming, *et al* 2007). It is defined by:

$$SEM = SE_{\bar{x}} = \frac{s}{\sqrt{n}}$$

Where s is the sample standard deviation as follows:

$$s = \sqrt{\frac{1}{n-1} \sum_{i=1}^n (x_i - \bar{x})^2}$$

Chapter 3.

Site-specific quantitative phosphoproteomic analysis of BCR/ABL PTK crosstalk on etoposide-induced DNA damage response identifies a synergistic phosphorylation change on developmental protein Hemogen

3.1. Introduction

BCR/ABL PTK has been shown to cause genomic instability which may be involved in disease progression to blast crisis if untreated, and this may be associated with unfaithful DNA damage sensing/repair signalling (Calabretta and Perrotti 2004, Nowicki, *et al* 2004, Skorski 2002, Slupianek, *et al* 2002). However, previous studies have assessed the effects of BCR/ABL PTK on specific proteins of DNA repair pathways with potentially partial information on their phosphosites (Rink, *et al* 2007, Slupianek, *et al* 2009, Slupianek, *et al* 2001). It remains the case that proteins with as yet unmapped phosphorylation sites could be regulated by both DNA damage and BCR/ABL PTK to be the source of genomic instability and disease progression. Thus nuclear protein phosphorylation changes were investigated after inducing DNA damage with etoposide, a chemotherapeutic agent which promotes DNA double strand breaks (DSBs). However, DNA repair and apoptosis pathways are differentially initiated after DNA damage induction by etoposide depending on the amount of DNA DSBs generated (Abe, *et al* 2008, Bree, *et al* 2004). Also, leukaemogenic PTKs like BCR/ABL PTK can resist apoptosis by promoting multiple anti-apoptotic signals such as modulating Bcl-2 family member expression (Skorski 2002). The experiments performed therefore required the establishment of conditions for DNA damage mediated DNA repair signalling with minimal apoptosis in the absence and presence of BCR/ABL PTK. This chapter reports the development of such a system and

analysis of the proteomic datasets acquired in control and BCR/ABL PTK-expressing Ba/F3 cells.

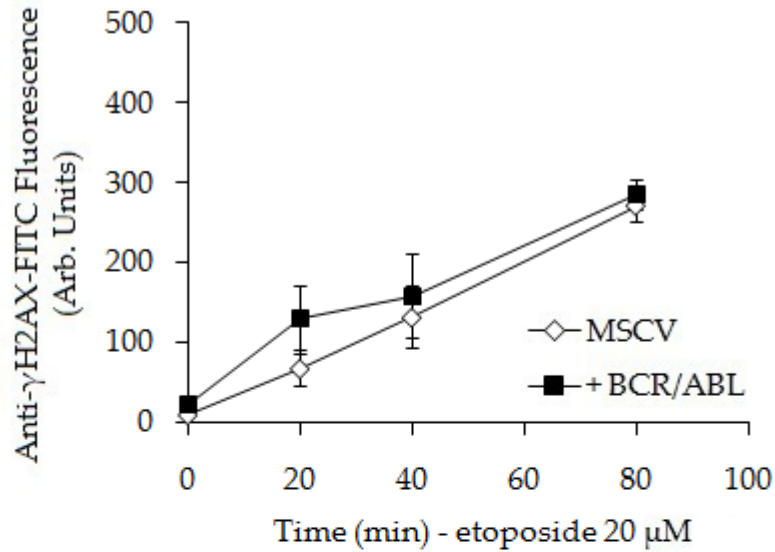
3.2. Results

3.2.1. Induction of DNA damage and DNA repair with etoposide

Etoposide, a topoisomerase 2 inhibitor, was used to induce DNA damage in Ba/F3 cells as measured using a DNA double strand break (DSB) assay. It has been shown that this drug can create predominantly DNA DSBs as both topoisomerase 2 subunits are saturated with the inhibitor and each blocked subunit disrupts one DNA strand (Montecucco and Biamonti 2007). To assess whether etoposide can induce DNA DSBs in control and BCR/ABL PTK-expressing Ba/F3 cells, the DNA DSB-specific phosphorylation of the histone H2AX on serine 139 (γ H2AX) was monitored using flow cytometry.

Differential incubation times and etoposide concentrations were screened to establish a dose which induces sufficient DNA DSBs. Cells were prepared in exponential growth phase, as etoposide is more efficient when cells are replicating and are transcriptionally active (Burden and Osheroff 1998). DNA DSBs increased with etoposide incubation time (Figure 3.1-A) and etoposide concentration (Figure 3.1-B) in both MSCV and BCR/ABL PTK-expressing cells. Nearly the entire population of MSCV and BCR/ABL PTK-expressing cells were positive for γ H2AX phosphorylation within 20 minutes of treatment with etoposide at high concentrations such as 40 and 80 μ M, for which median fluorescence also seemed to saturate and be similar for both cell populations (data not shown).

A.



B.

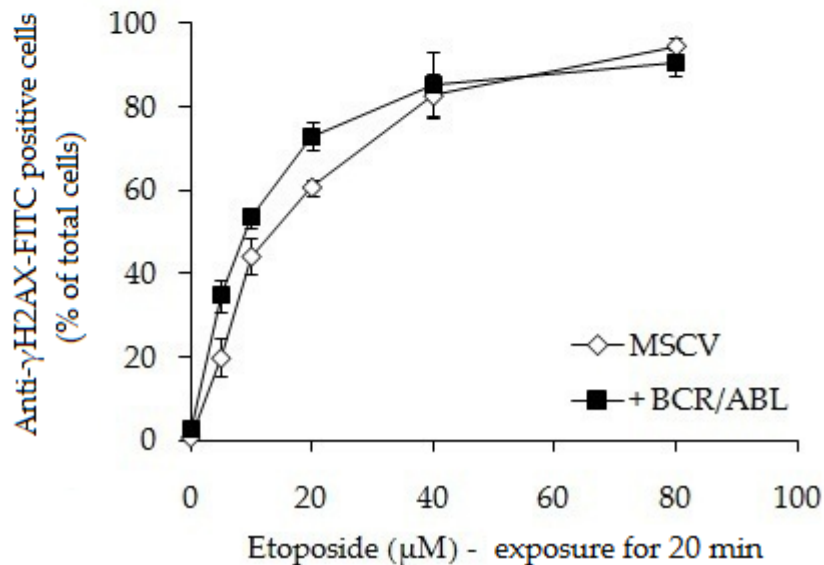


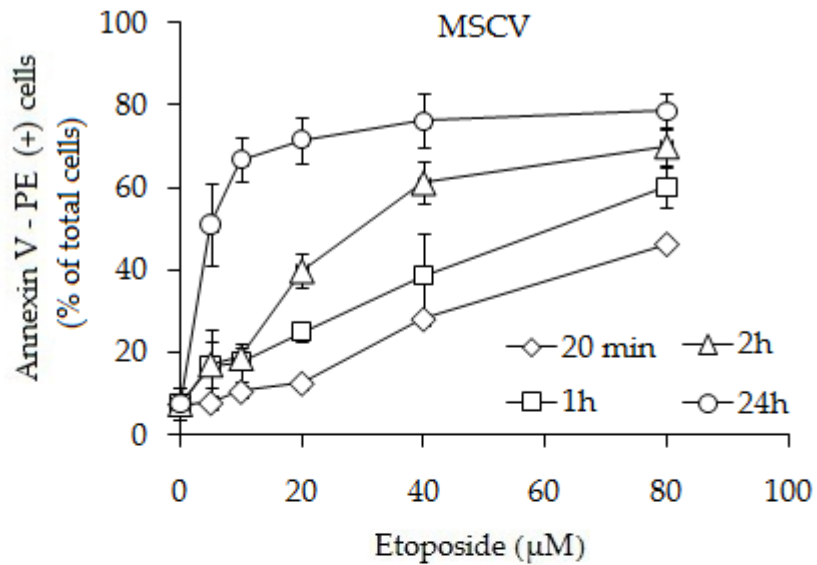
Figure 3.1: Etoposide-induced DNA double strand breaks in Ba/F3 cells in the presence or absence of BCR/ABL PTK. (A.) DNA double strand breaks (DSBs) were induced in MSCV and BCR/ABL PTK-expressing cells by etoposide at 20 μM for 20, 40 and 80 min and were quantified (median fluorescence) by flow cytometry using the anti-γH2AX-FITC assay **(B.)** DNA DSBs were induced with etoposide at 5, 10, 20, 40 and 80 μM for 20 min in MSCV and BCR/ABL PTK-expressing cells. The percentage of anti-γH2AX-FITC positive cells was determined above the fluorescence of the control population. Data displayed correspond to average values of three independent biological replicates. Error bars correspond to standard error of the mean (SEM). A representative histogram overlay for control cells and cells exposed to etoposide (80 μM) for 20 min is shown in Appendix 7.1.

No significant difference was observed between the levels of H2AX phospho-antibody binding between MSCV and BCR/ABL PTK-expressing treated and untreated cells, although the anti- γ H2AX binding was marginally higher in the presence of BCR/ABL PTK. To ensure this study concentrates on DNA repair, etoposide-dependent apoptosis was studied using Annexin V binding and the vital dye 7-Amino-actinomycin D (7-AAD) (Balasubramanian, *et al* 2007). The cells did not show Annexin V positivity increase after 2h incubation with etoposide 80 μ M (data not shown). Thus, Ba/F3 cells were washed after etoposide treatment and replated in fresh medium containing mIL-3 to support growth and survival for 24h.

The percentage of Annexin V positive (+) cells increased with etoposide incubation time and etoposide concentration (Figure 3.2) in both MSCV and BCR/ABL PTK-expressing Ba/F3 cells. However, while apoptosis increased to maximal values in control cells with etoposide at 40 to 80 μ M (exposure for 20 min), the same level of apoptosis was already seen in BCR/ABL PTK-expressing cells for lower etoposide concentrations such as 10 and 20 μ M (Figure 3.3). This difference was on further examination not significant using a Student's t-test under the assumption of data normality (P-values of 0.252 and 0.130 for 10 and 20 μ M respectively). Prolongation of the incubation with etoposide up to 24h did reveal an anti-apoptotic effect promoted by the PTK (P-values of 0.041, 0.041 and 0.004 for 20, 40 and 80 μ M respectively) (Figure 3.3). Such anti-apoptotic effects can also be seen with 1h and 2h exposure to etoposide for the highest etoposide concentrations like 40 and 80 μ M (Figure 3.2). Thus BCR/ABL PTK-expressing cells undergo apoptosis at low etoposide dose exposures and this difference with control cells could be explained by the increase in DNA DSBs compared to control Ba/F3 cells previously observed at 20 μ M for 20 min.

In conclusion, apoptosis remained at low levels after 20 min exposure to etoposide (20 μ M) despite 60 to 70% of cells being DNA damage-positive using γ H2AX assay (Figure 3.1). It was thus possible to infer that cells were able to predominantly direct signalling towards DNA repair and this concentration was used for proteomic analysis.

A.



B.

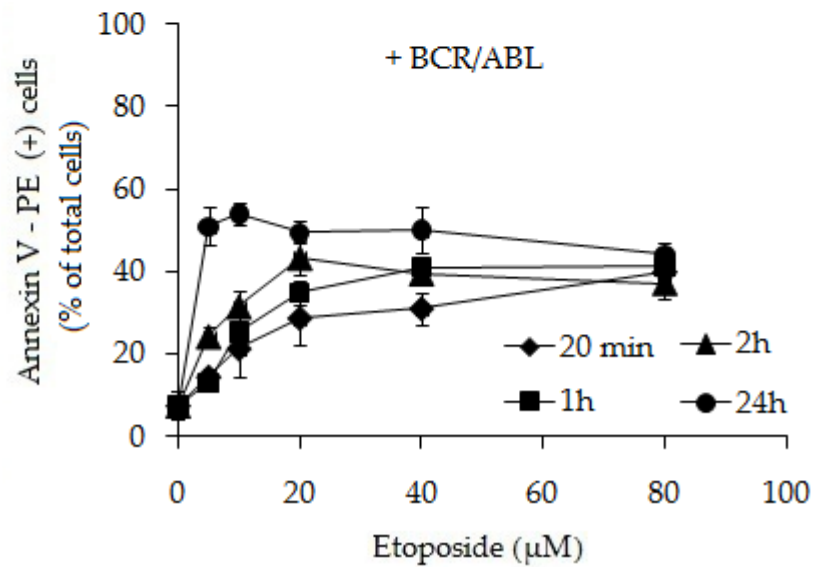
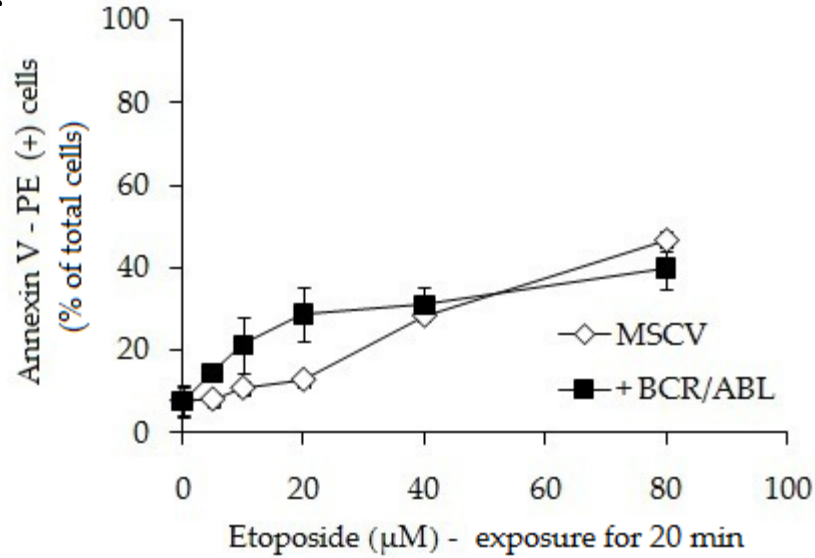


Figure 3.2: Etoposide-induced apoptosis in Ba/F3 cells in the presence or absence of BCR/ABL PTK (1). DNA double strand breaks (DSBs) were induced in MSCV (A.) and BCR/ABL PTK-expressing Ba/F3 cells (B.) for times indicated by etoposide at 5, 10, 20, 40 and 80 µM for 20 min, 1h and 2h then cells were washed and left for 24h in fresh medium supplemented with mIL-3. A positive control was performed with 24h incubation with etoposide. Apoptosis was quantified by flow cytometry using Annexin V - PE and 7-AAD. Percentages of total Annexin V - PE positive (+) cells, i.e. total apoptotic cells, were averaged from three independent biological replicates. Error bars correspond to standard error of the mean (SEM). Representative bivariate dot plots for control cells and cells incubated with etoposide (80 µM) for 24h are shown in Appendix 7.2.

A.



B.

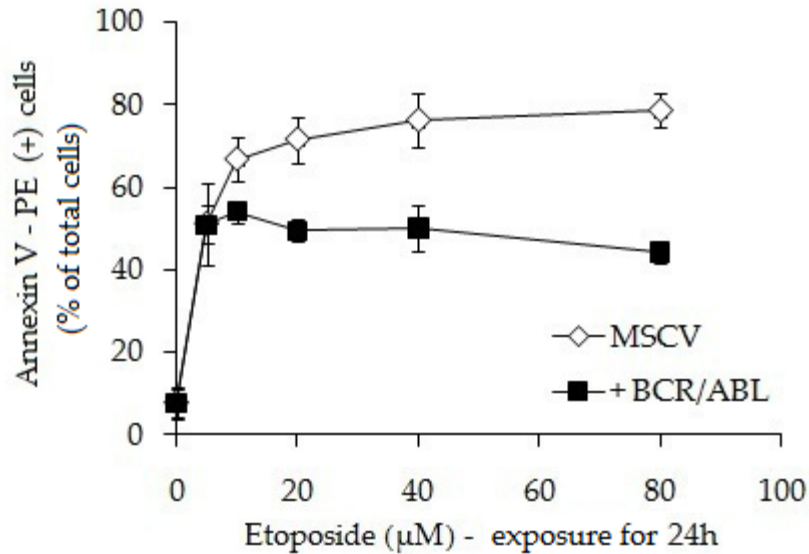
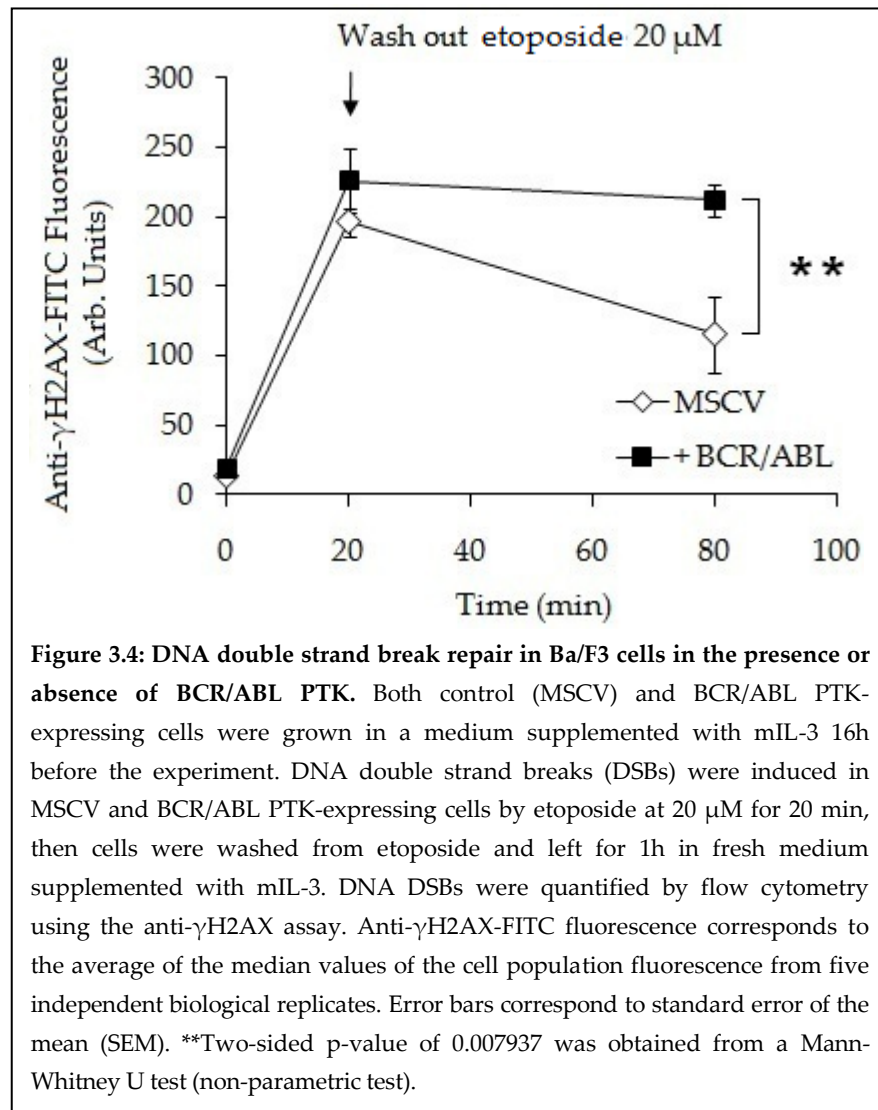


Figure 3.3: Etoposide-induced apoptosis in Ba/F3 cells in the presence or absence of BCR/ABL PTK (2). (A.) DNA double strand breaks (DSBs) were induced in MSCV and BCR/ABL PTK-expressing cells by etoposide at 5, 10, 20, 40 and 80 μM for 20 min, then cells were washed and left for 24h in fresh medium supplemented with mIL-3. (B.) Ba/F3 cells were exposed to etoposide at 5, 10, 20, 40 and 80 μM for 24h. Apoptosis was quantified by flow cytometry using Annexin V - PE and 7-AAD. Percentages of total Annexin V - PE positive (+) cells, i.e. total apoptotic cells, were averaged from three independent biological replicates. Error bars correspond to standard error of the mean (SEM). Representative bivariate dot plots for control cells and cells incubated with etoposide (80 μM) for 24h are shown in Appendix 7.2.

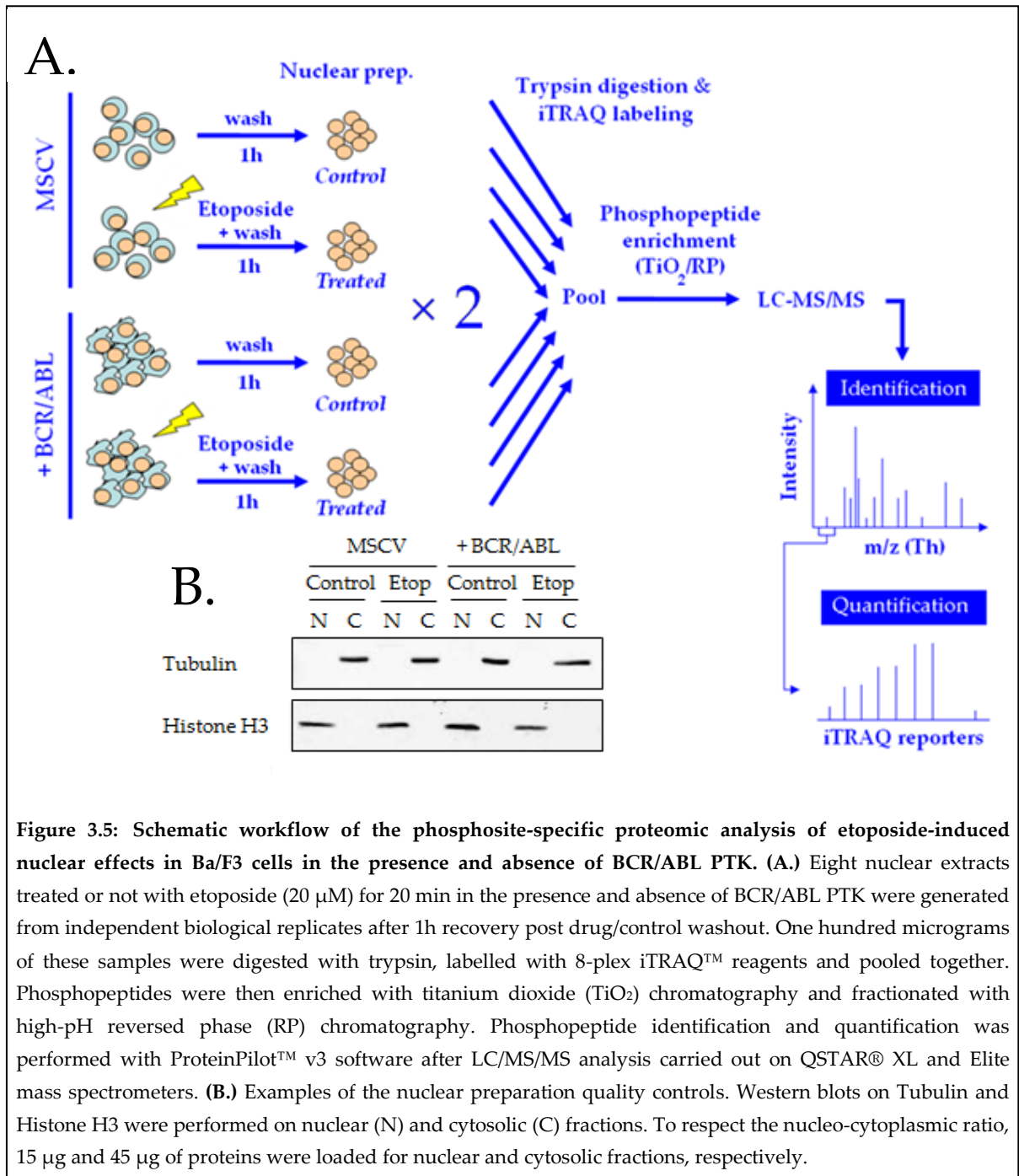
To characterize potential DNA DSB repair, a kinetic study was performed to evaluate the decrease of γ H2AX phosphorylation. After DNA DSBs induction by etoposide (20 μ M) for 20 min, control and BCR/ABL PTK-expressing Ba/F3 cells were washed, replated into fresh medium and left for recovery for 1h. Over this period of time, some DNA DSBs were repaired in control cells, as shown by the decrease of anti- γ H2AX median fluorescence (Figure 3.4), while the amount of DNA DSBs was steady and remained high in the presence of BCR/ABL PTK. The difference in DNA DSBs between control and BCR/ABL-expressing cells was found to be significant (p-value = 0.0079) using the non-parametric Mann-Whitney U test (no assumption of data normality required). These observations suggested that either the recruitment of DNA repair proteins at the site of DNA DSBs may be modulated by BCR/ABL PTK or that this leukaemogenic PTK could modulate DNA damage response signalling including serine/threonine kinase action (e.g. ATM, ATR, DNA PKcs) and/or phosphatases (e.g. PP2A, WIP1). This led us to examine phosphopeptide changes in response to etoposide in the presence and absence of BCR/ABL PTK.



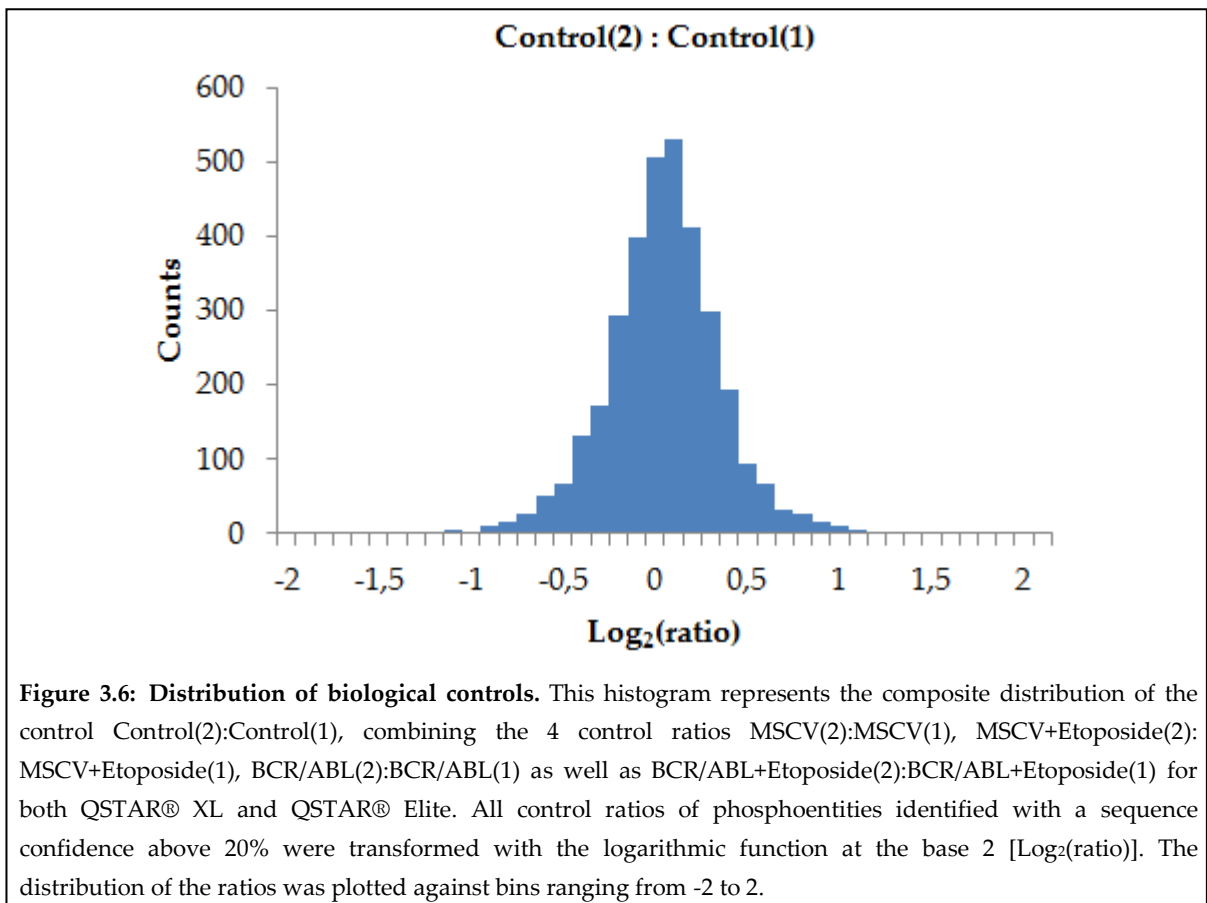
3.2.2. Phosphoproteomic analysis of etoposide-induced events in the presence and absence of BCR/ABL PTK

MSCV and BCR/ABL PTK-expressing Ba/F3 cells were prepared with or without a 20 min exposure to etoposide (20 μ M) followed by a 1h period in fresh medium supplemented with mIL-3 to enable DNA damage response signalling to occur. Then, nuclear extraction was performed on these four samples. Biological replicates were prepared to obtain eight nuclear extracts in total suitable for 8-channel iTRAQ™ labelling following trypsin digestion. Labelled nuclear peptides were then pooled and phosphopeptides were enriched with titanium dioxide (TiO₂) chromatography and fractionated with high-pH reversed phase (RP) chromatography to reduce peptide complexity before LC/MS/MS analysis performed with QSTAR® XL and Elite high resolution mass spectrometers (see Figure 3.5 for workflow).

Mass spectra from QSTAR® XL and Elite mass spectrometers were searched separately against a mouse protein database to identify and quantify peptides using the Paragon search engine from ProteinPilot™ v3 software. Calculation of single ratio values for each phosphoentity as well as data handling was enhanced with in-house software developed in the group by Dr. Samuel Taylor. Approximately 950 protein identifications reached the 95% confidence score of 1.3, while around 1115 phosphoentities were identified. Phosphoentities corresponded to phosphopeptides and their additional modifications, which were taken into account separately as they may influence quantification. Approximately 240 phosphoentities were identified with both instruments for which $\log_2(\text{ratio})$ values were averaged (Appendix 7.4). To remove erroneous data, iTRAQ™ reporter ions having weak signal intensities were not included in the analysis. Therefore 703 phosphoentities were fully quantified.



As shown in Figure 3.6, the histogram distribution of the $\text{Log}_2(\text{ratio})$ values of all phosphoentities for the control Control(2):Control(1) showed a Gaussian distribution centred around 0. This demonstrated that iTRAQ™ labelling had been performed efficiently between replicate samples (isobaric labelling exceeded 99.9% of all peptides identified). To determine if etoposide exposure and/or BCR/ABL PTK expression resulted in a change for each phosphoentity, the mean of 2 independent replicates was compared to the mean of this control distribution for each appropriate ratio (see Figure 3.7) in a two-sample Student's t-test, assuming equal variance between these two samples. Therefore, the mean of 2 independent replicates was different from the control distribution if outside the ratio interval [- 0.44 ; 0.44] with a Student's t-test p-value < 0.05.



Response to both BCR/ABL PTK and/or etoposide could be identified by clustering the average response of the two biological replicates for each phosphoentity (Figure 3.7), assuming that the regulation of the protein level remained minimal within the time interval of the study. BCR/ABL PTK could affect the response of Ba/F3 cells to etoposide by modulating the intensity of the response (potentially clusters 1, 2 and 4), by blocking or creating a phosphorylation change in response to etoposide (potentially clusters 3, 5 and 6) or by sustaining a stress signal similar to the one induced by etoposide (potentially clusters 1, 2, 5 and 6). The analysis concentrated on the changes reproduced between biological replicates downstream of the DNA damage response initiation. Approximately 110 phosphoentities showed consistent changes for either BCR/ABL PTK and/or etoposide action (Student's t-test p-value < 0.05 for all appropriate ratios). Among them 41 phosphoentities were regulated by etoposide but not BCR/ABL PTK and 27 by BCR/ABL PTK but not etoposide (Figure 3.8). Finally, 44 phosphoentities, corresponding to 33 protein phosphosites, were regulated by both etoposide and BCR/ABL PTK, this observation suggesting that phosphosite-specific overlap between BCR/ABL and genotoxic stress signalling may exist. In total, evidence of regulation by etoposide and BCR/ABL PTK on single and/or multiple phosphosites was obtained for 21 proteins whereas phosphorylation modulation by BCR/ABL PTK signalling only and etoposide response only could be detected on 20 and 21 proteins, respectively. The complete list of consistent phosphorylation changes are shown in Appendices 7.5-7.12.

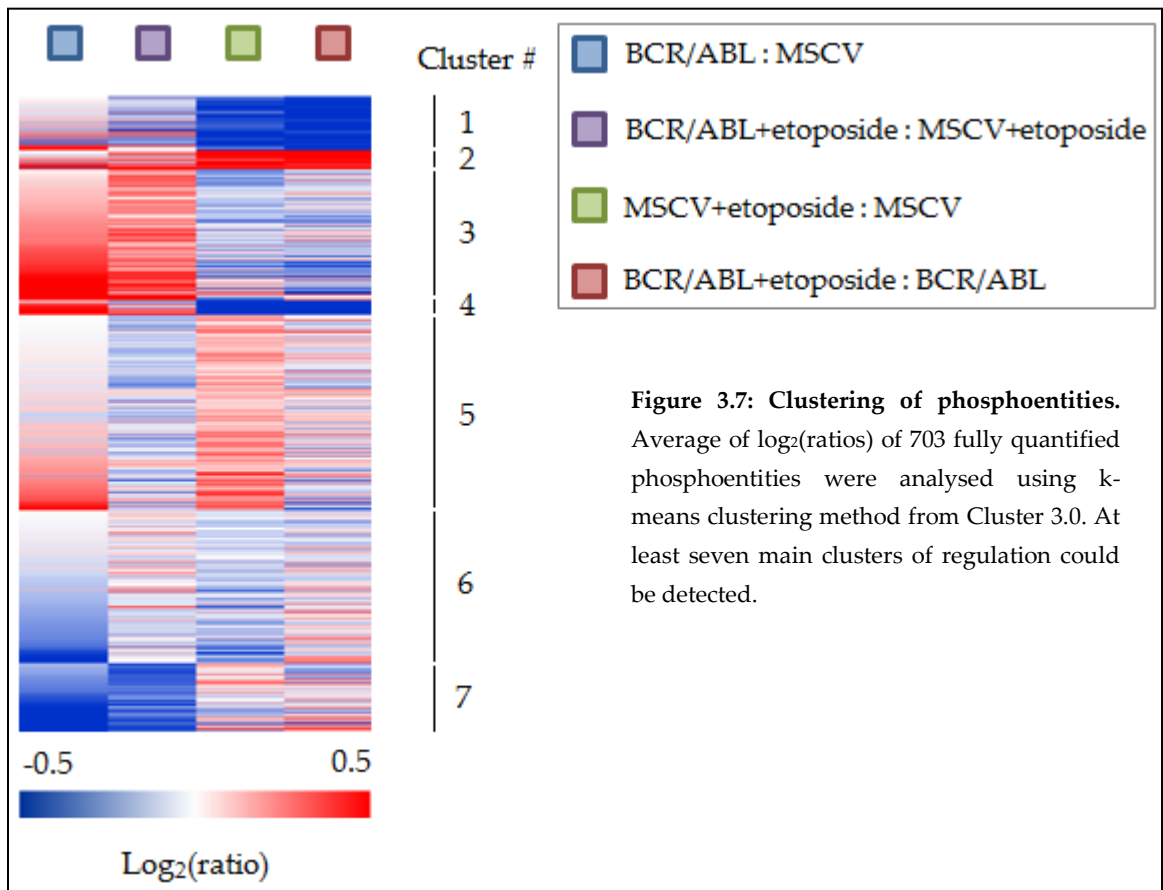
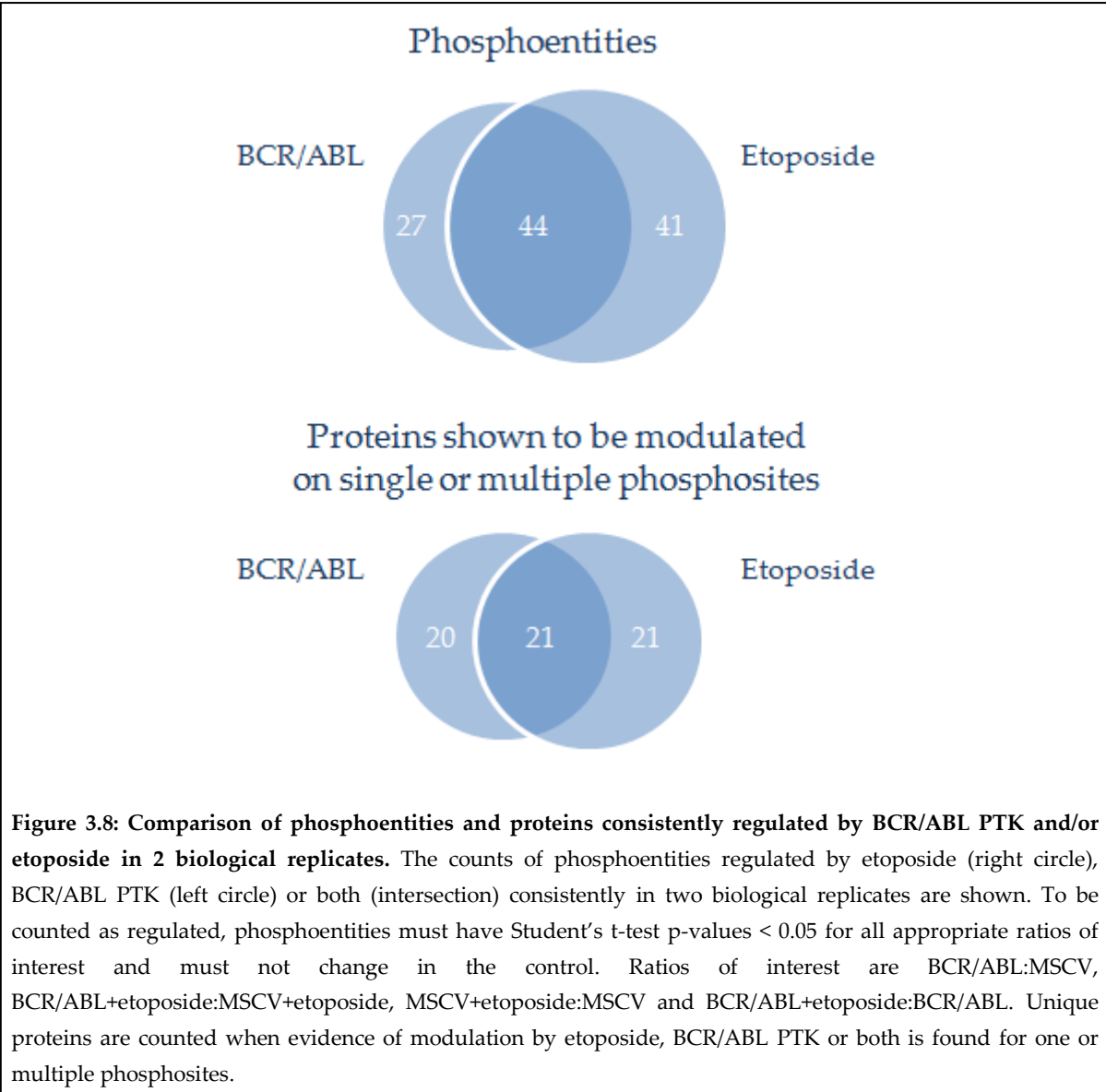


Figure 3.7: Clustering of phosphoentities. Average of $\log_2(\text{ratios})$ of 703 fully quantified phosphoentities were analysed using k-means clustering method from Cluster 3.0. At least seven main clusters of regulation could be detected.



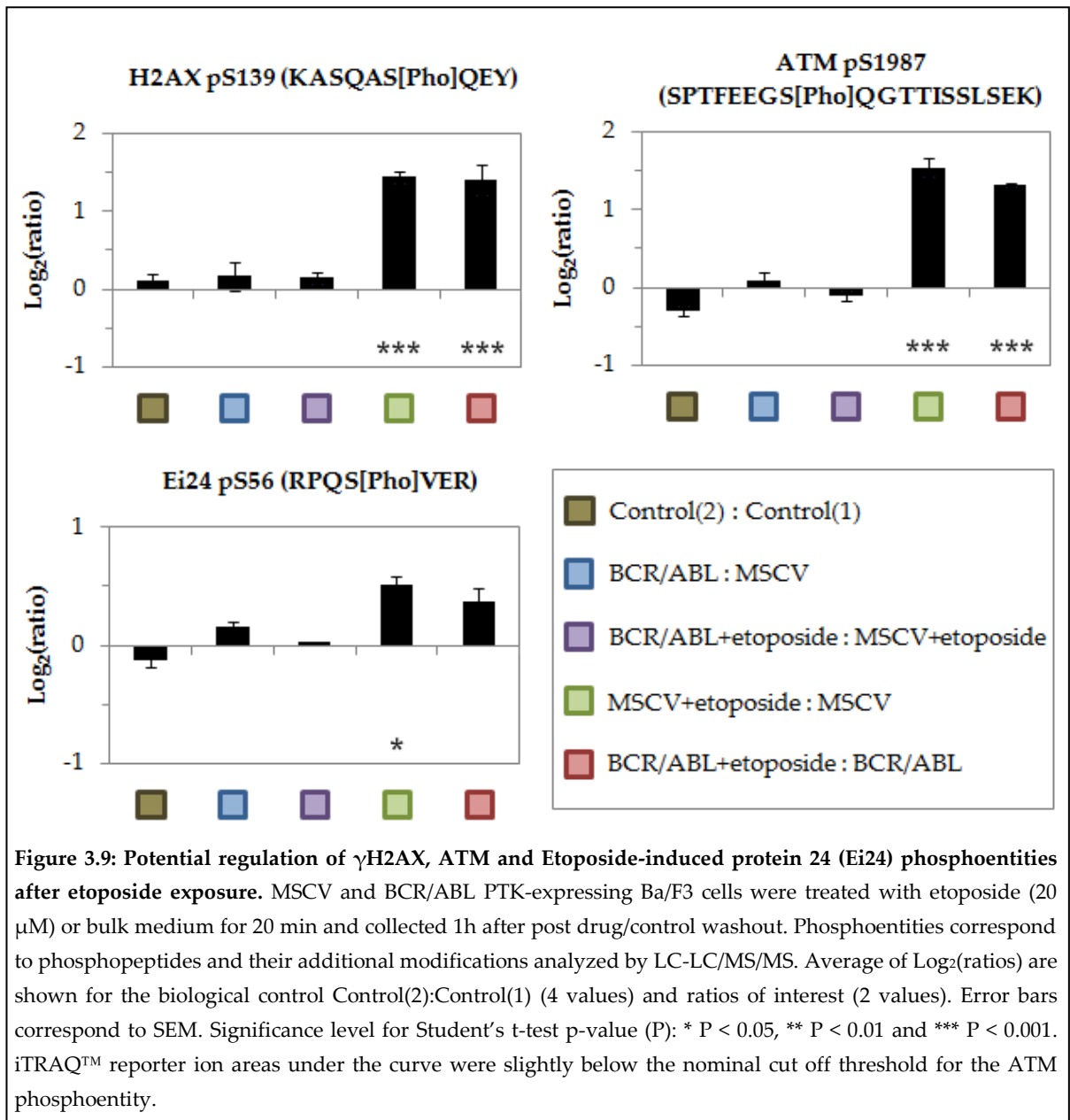
3.2.3. γ H2AX, ATM and 53BP1 respond to etoposide

Several markers of DNA damage could be identified among the 41 phosphoentities regulated by etoposide exposure. The histone H2AX was phosphorylated on serine 139 by etoposide both in the presence and absence of the BCR/ABL PTK (Figure 3.9).

Two proteins that have been previously shown to be modulated by etoposide failed to pass our selective criteria. Given the pivotal role of ATM, its autophosphorylation on serine 1987 mediated by MRN complex binding is of interest (Riches, *et al* 2008), although the iTRAQ™ reporter ions were low for this phosphoentity. Nonetheless a similar level of phosphorylation could be measured in response to etoposide for both cells. Use of weaker iTRAQ™ reporter ions was not suitable for our discovery purpose concerning unknown phosphoentities, therefore the following analysis excluded them. Of note, Etoposide-induced protein 24 (Ei24), was potentially regulated by etoposide here. Ei24 acts downstream of p53-mediated pathway by binding Bcl-2 and negatively regulates cell growth (Gu, *et al* 2000, Lehar, *et al* 1996).

Interestingly, the component of the DNA damage response 53BP1 was found regulated at different phosphosites following etoposide treatment (Figure 3.10). Indeed, while threonine 906 was hyperphosphorylated similarly in both the absence and presence of BCR/ABL PTK, serine 549 and potentially serine 546 were dephosphorylated after etoposide exposure. Several other phosphoentities of 53BP1 were not altered in response to BCR/ABL PTK expression or etoposide addition, indicating that threonine 906 as well as serines 546 and 549 were specifically regulated. Other phosphoentities from proteins linked to DNA repair such as RAB22 (Rad51 associated protein 1), BRCA1, Rad50 and Xrcc1 were also identified but no change in phosphorylation could be detected (Figure 3.11).

Details of other proteins and phosphoentities regulated by etoposide can be found in following sections or in Appendices 7.10-7.12.



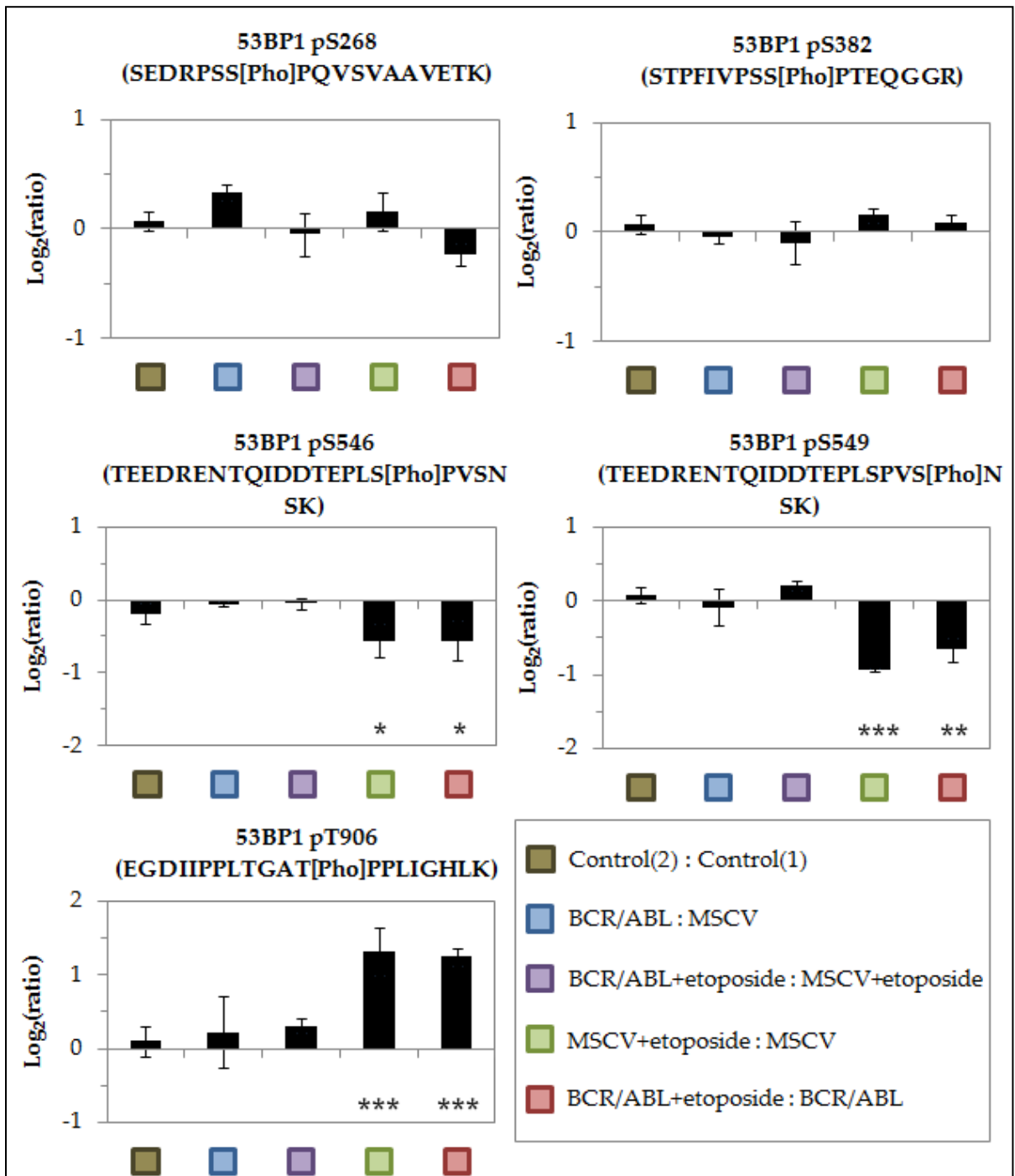
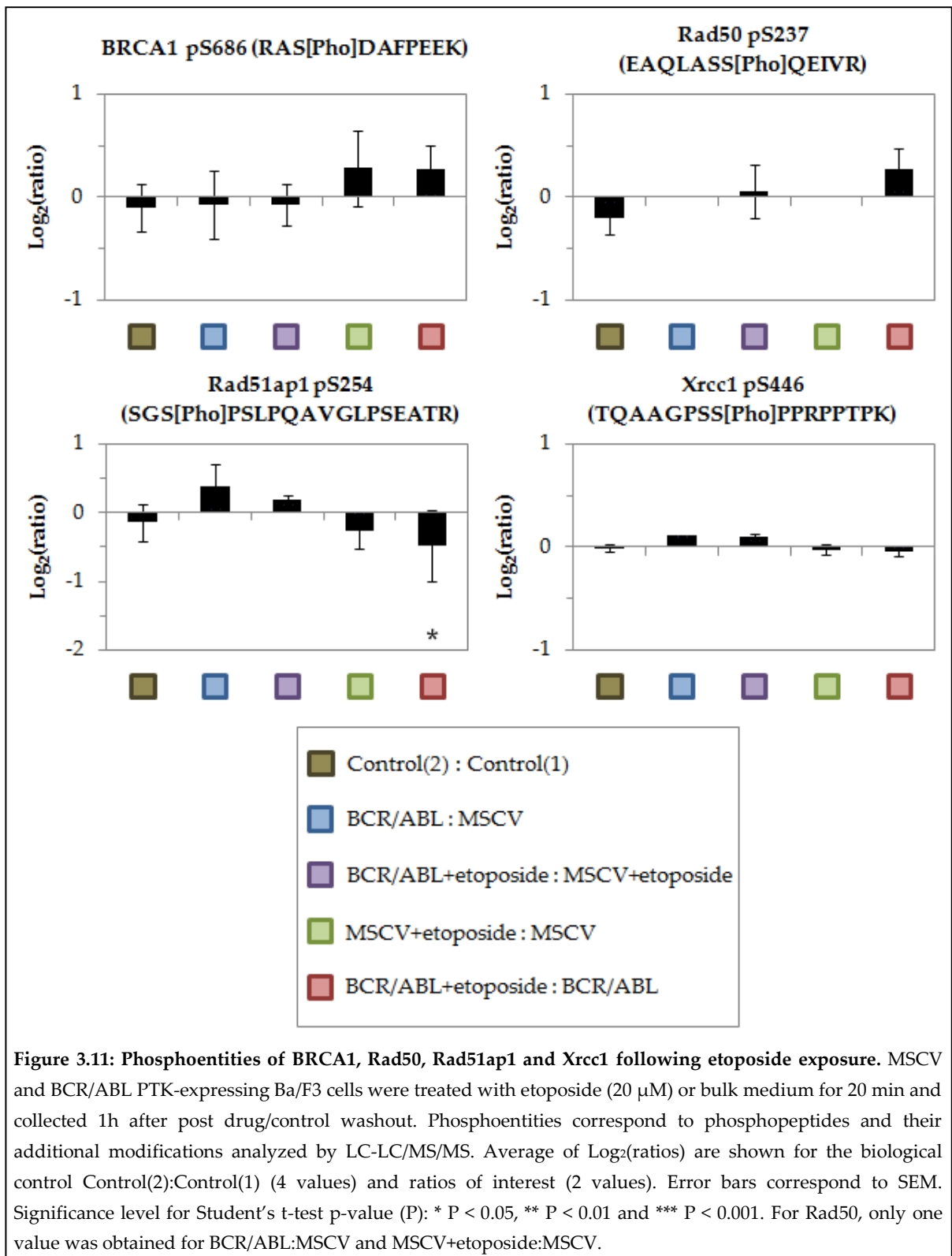


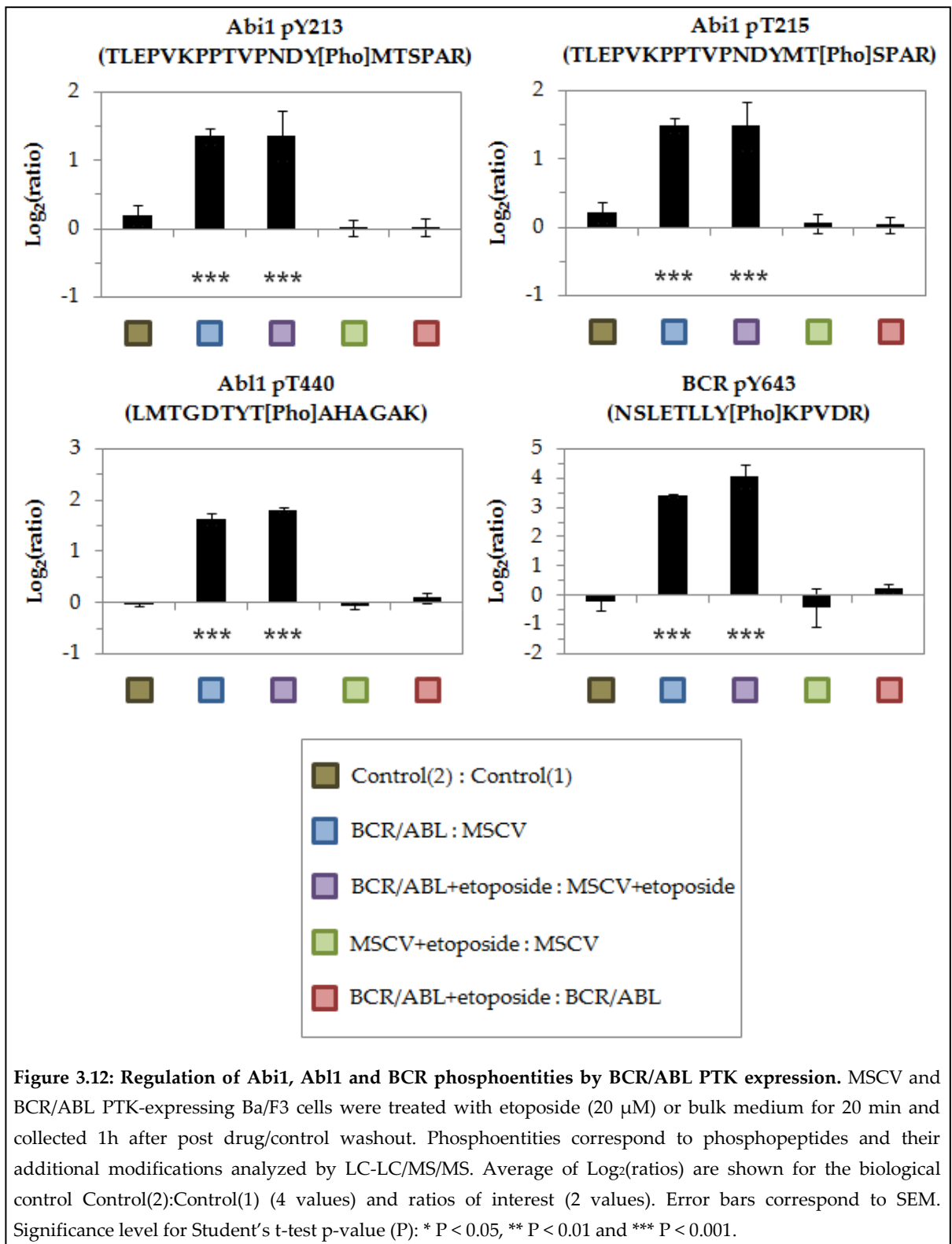
Figure 3.10: Dynamics of 53BP1 phosphoresidues after etoposide exposure. MSCV and BCR/ABL PTK-expressing Ba/F3 cells were treated with etoposide (20 μ M) or bulk medium for 20 min and collected 1h after post drug/control washout. Phosphoentities correspond to phosphopeptides and their additional modifications analyzed by LC-LC/MS/MS. Average of $\text{Log}_2(\text{ratios})$ are shown for the biological control Control(2):Control(1) (4 values) and ratios of interest (2 values). Error bars correspond to SEM. Significance level for Student's t-test p-value (P): * $P < 0.05$, ** $P < 0.01$ and *** $P < 0.001$.

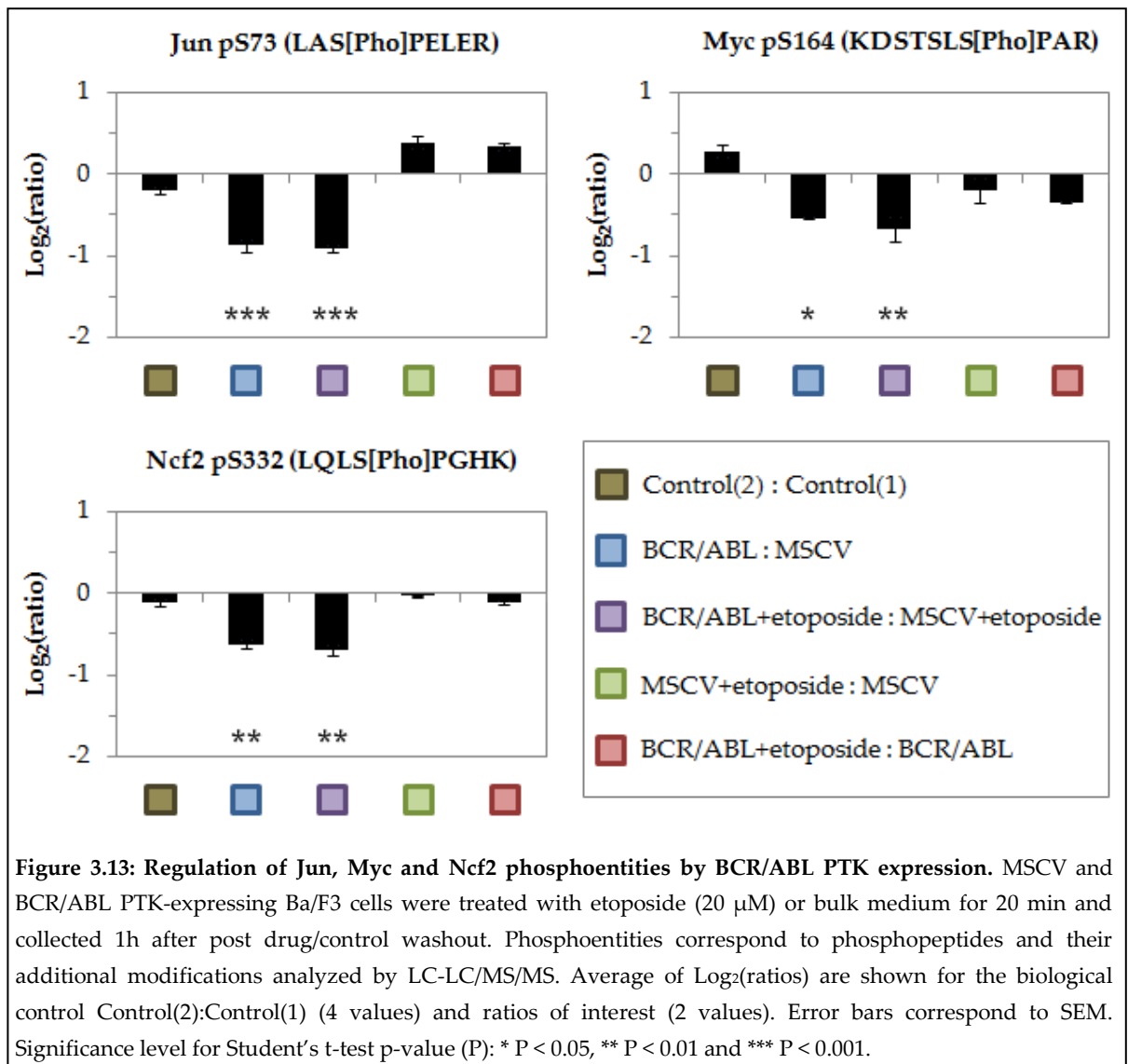


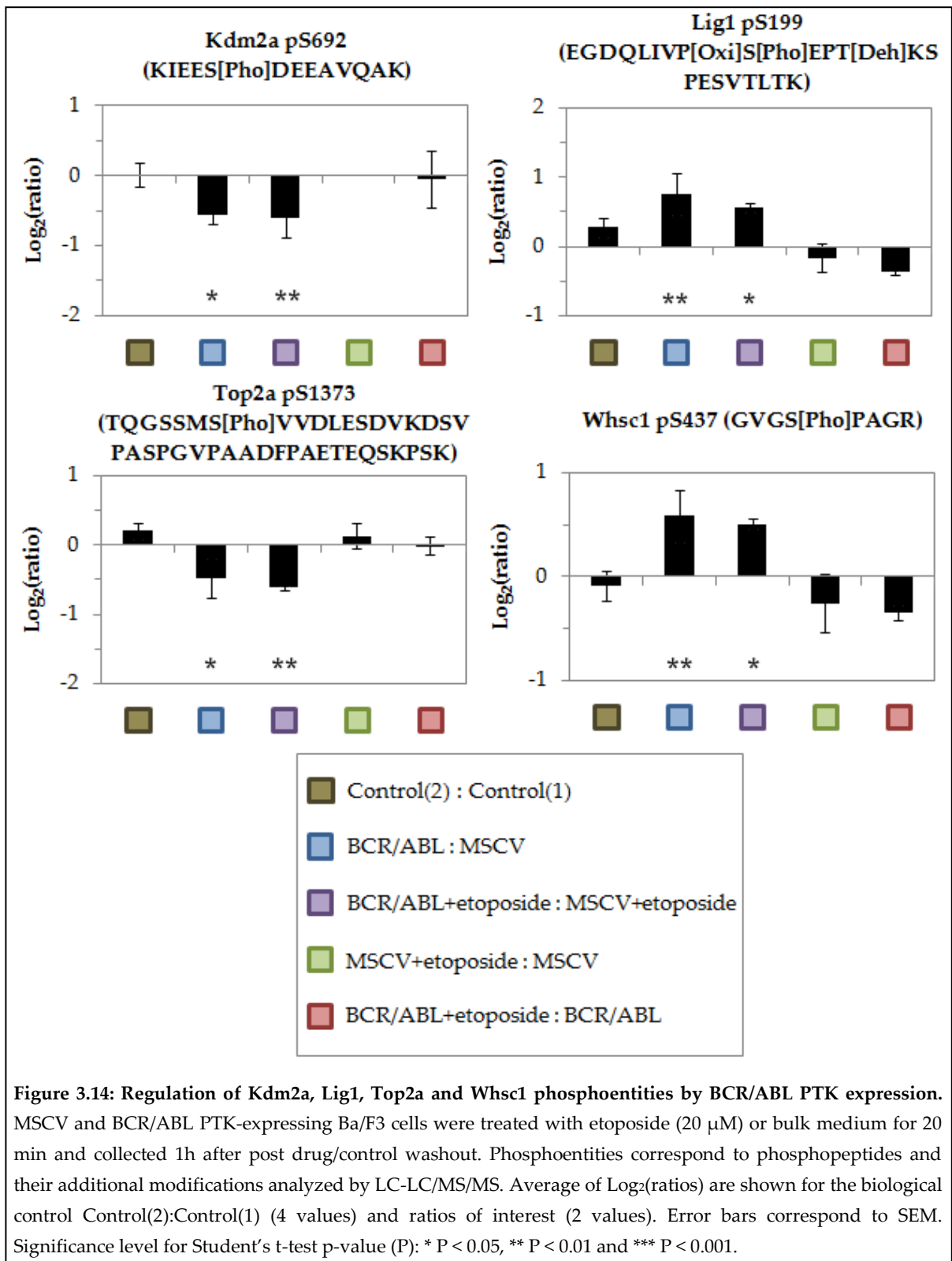
3.2.4. BCR/ABL PTK signalling acts on proteins within multiple pathways

Twenty-seven phosphoentities were found to be regulated in both replicates by BCR/ABL PTK without any direct association with etoposide exposure. Among them, positive controls like Abl interactor 1 and BCR peptides were present due to overexpression of the leukaemogenic PTK (Figure 3.12). BCR/ABL PTK may regulate proteins involved in transcription (Myc, Jun) (Figure 3.13), RNA processing/splicing (Pabpn1, Hnrnp), ribosome biogenesis (Dkc1, Nop56), translation initiation (Eif5b), nuclear trafficking (Nup35, Ranbp2), PI3K pathway (Inpp5d, Dok1) and superoxide production (Ncf2) (Figure 3.13) (Appendices 7.5-7.6). Interestingly, DNA ligase1, which acts on DNA nicks during DNA replication, recombination and repair was phosphorylated upon BCR/ABL PTK expression on serine 199 (Figure 3.14). Also histone demethylase Kdm2a was found dephosphorylated on serine 692 in the presence of the oncogene. Conversely, the putative histone methyltransferase Whsc1 was phosphorylated on serine 437 in the presence of the oncogene. Finally, topoisomerase 2 alpha serine 1373 was dephosphorylated in the presence of BCR/ABL PTK. Top2a controls the topology of DNA during DNA replication and DNA repair and it is the protein target of etoposide to induce DNA double strand breaks (Montecucco and Biamonti 2007).

The complete list of phosphoentities changing upon BCR/ABL expression is shown in Appendices 7.5-7.6.







3.2.5. Phosphosite-specific overlap of etoposide and BCR/ABL PTK signalling

As described previously, 44 phosphoentities were found to be regulated by BCR/ABL PTK and etoposide (including where positive and negative effects respectively were recorded). Thirty-one of these phosphoentities were regulated by BCR/ABL PTK prior to their response to etoposide, while 13 showed a modified response to etoposide in the presence of the oncogene.

Twenty of these 44 phosphoentities were mapped to Histone H1 variants H1A (threonine 4 and serine 183), H1B (serine 18, threonine 135 and serine 186), H1D (threonine 4 and threonine 18) and H1E (threonine 4, threonine 18 and serine 187) (Figures 3.15-3.18). While it appeared that phosphorylation on serine/threonine 18 as well as serines 183, 186 and 187 seemed to be downregulated by etoposide, more phosphorylation at these sites was found in BCR/ABL PTK-expressing cells prior and/or after etoposide treatment. Conversely, Histone H1 threonine 4 was hyperphosphorylated both before and after etoposide treatment in the presence of the oncogene compared to control cells, this regulation being also associated with etoposide exposure. More potential regulations of Histone H1 can be found in Appendices 7.7-7.9.

Other proteins like the dual specificity protein kinase Clk3 or the p53 interactor Gnl3 could be differentially regulated between control and BCR/ABL PTK-expressing cells. Clk3 might be phosphorylated on serine 157 only in control cells while Gnl3 could be dephosphorylated on serine 95 only in control cells (Figure 3.19). Another modulation was observed on Serine/threonine kinase 10 (Stk10) or Lymphocyte-oriented kinase (Lok) on threonine 950. It appeared that the level of this phosphoentity was reduced with the expression of BCR/ABL PTK. This downregulation was also observed with etoposide but only in MSCV cells. Other phosphoentities presented a similar phosphorylation pattern such as Incenp pS284 or Anln pS318 (Figure 3.19). Conversely, Anln and Zfp828 were dephosphorylated upon etoposide exposure on serine 293 and serine 532 respectively only in the presence of the oncogene (Figure 3.20).

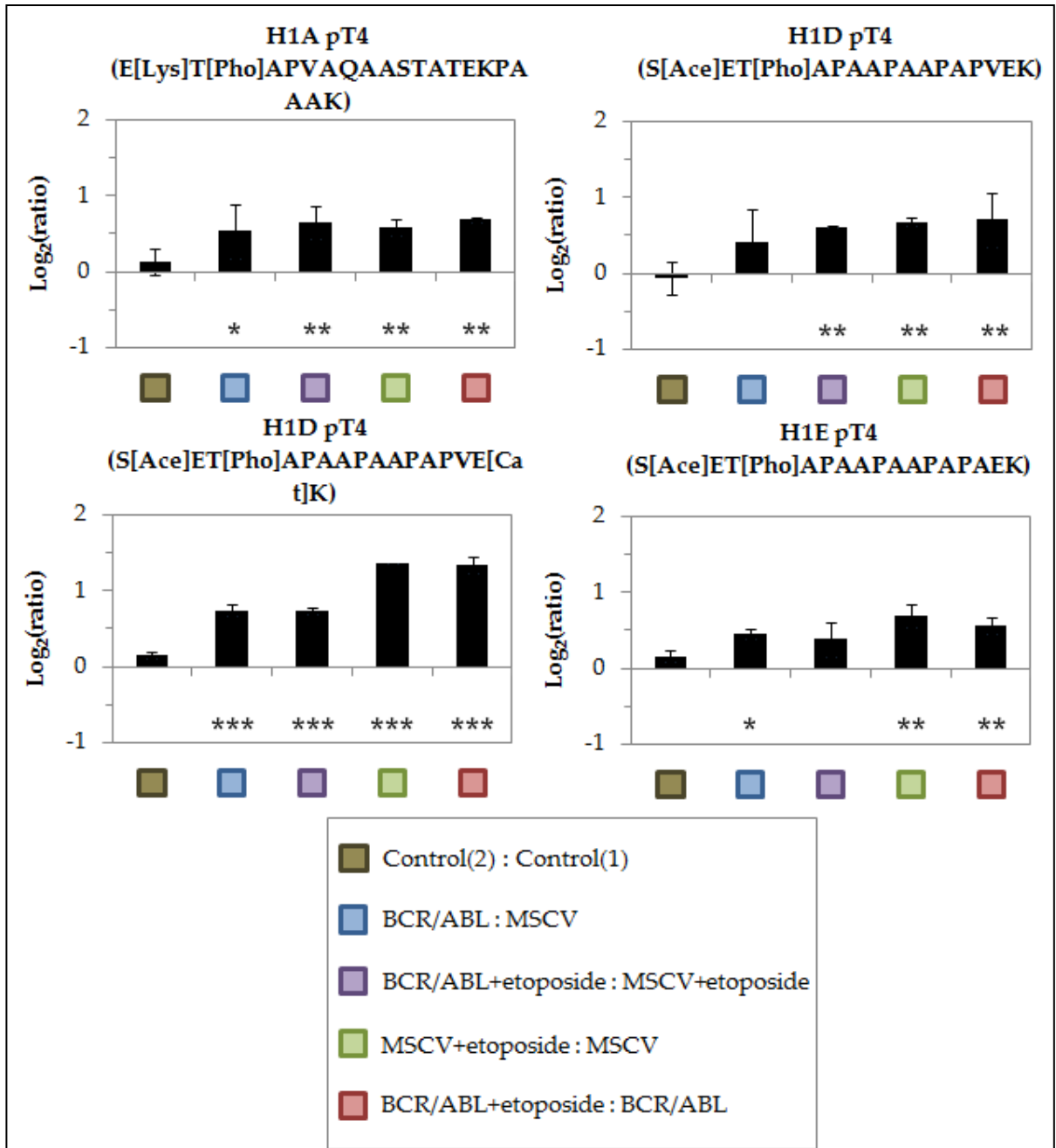
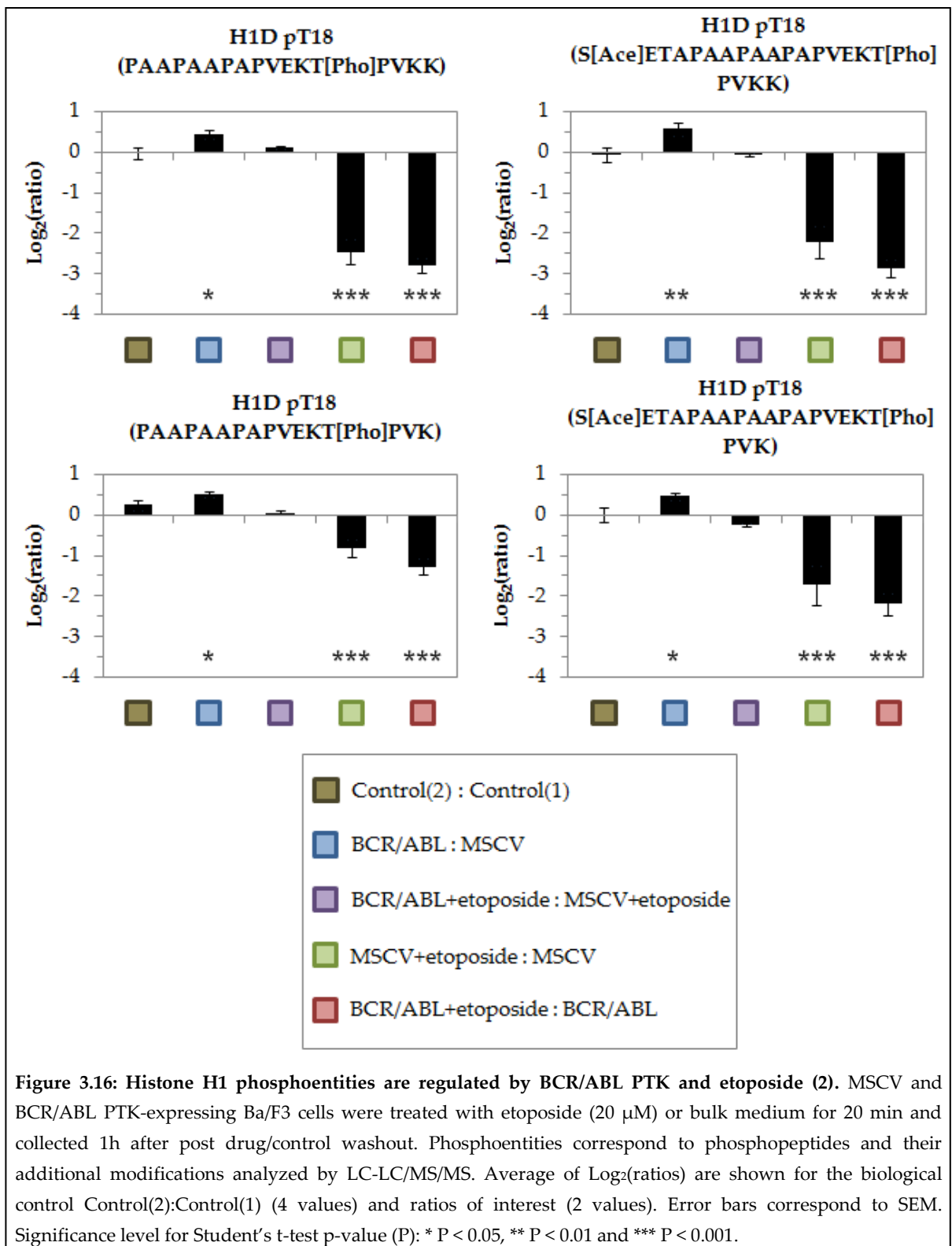


Figure 3.15: Histone H1 phosphoentities are regulated by BCR/ABL PTK and etoposide (1). MSCV and BCR/ABL PTK-expressing Ba/F3 cells were treated with etoposide (20 μ M) or bulk medium for 20 min and collected 1h after post drug/control washout. Phosphoentities correspond to phosphopeptides and their additional modifications analyzed by LC-LC/MS/MS. Average of $\text{Log}_2(\text{ratios})$ are shown for the biological control Control(2):Control(1) (4 values) and ratios of interest (2 values). Error bars correspond to SEM. Significance level for Student's t-test p-value (P): * $P < 0.05$, ** $P < 0.01$ and *** $P < 0.001$.



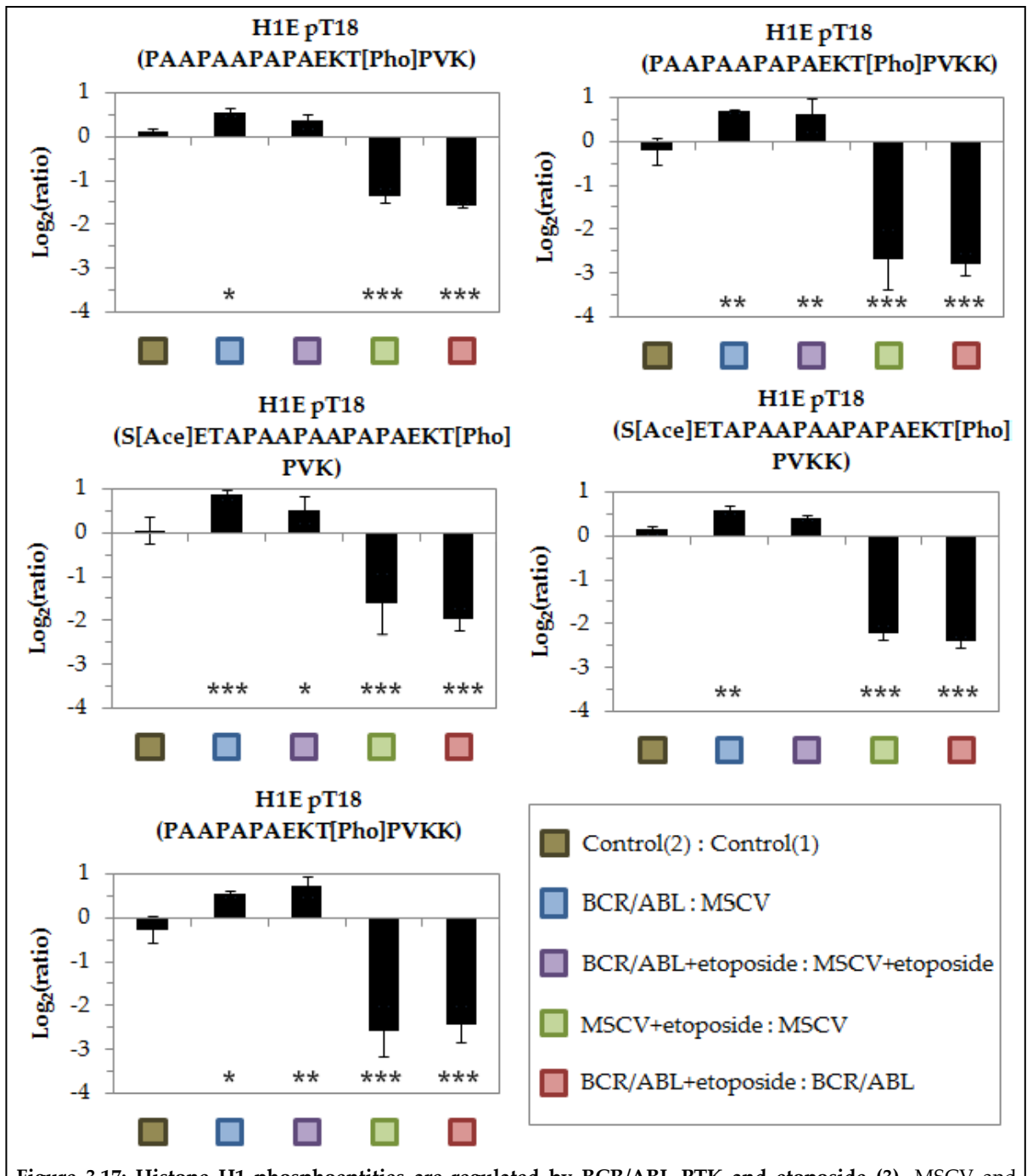


Figure 3.17: Histone H1 phosphoentities are regulated by BCR/ABL PTK and etoposide (3). MSCV and BCR/ABL PTK-expressing Ba/F3 cells were treated with etoposide (20 μ M) or bulk medium for 20 min and collected 1h after post drug/control washout. Phosphoentities correspond to phosphopeptides and their additional modifications analyzed by LC-LC/MS/MS. Average of Log₂(ratios) are shown for the biological control Control(2):Control(1) (4 values) and ratios of interest (2 values). Error bars correspond to SEM. Significance level for Student's t-test p-value (P): * P < 0.05, ** P < 0.01 and *** P < 0.001.

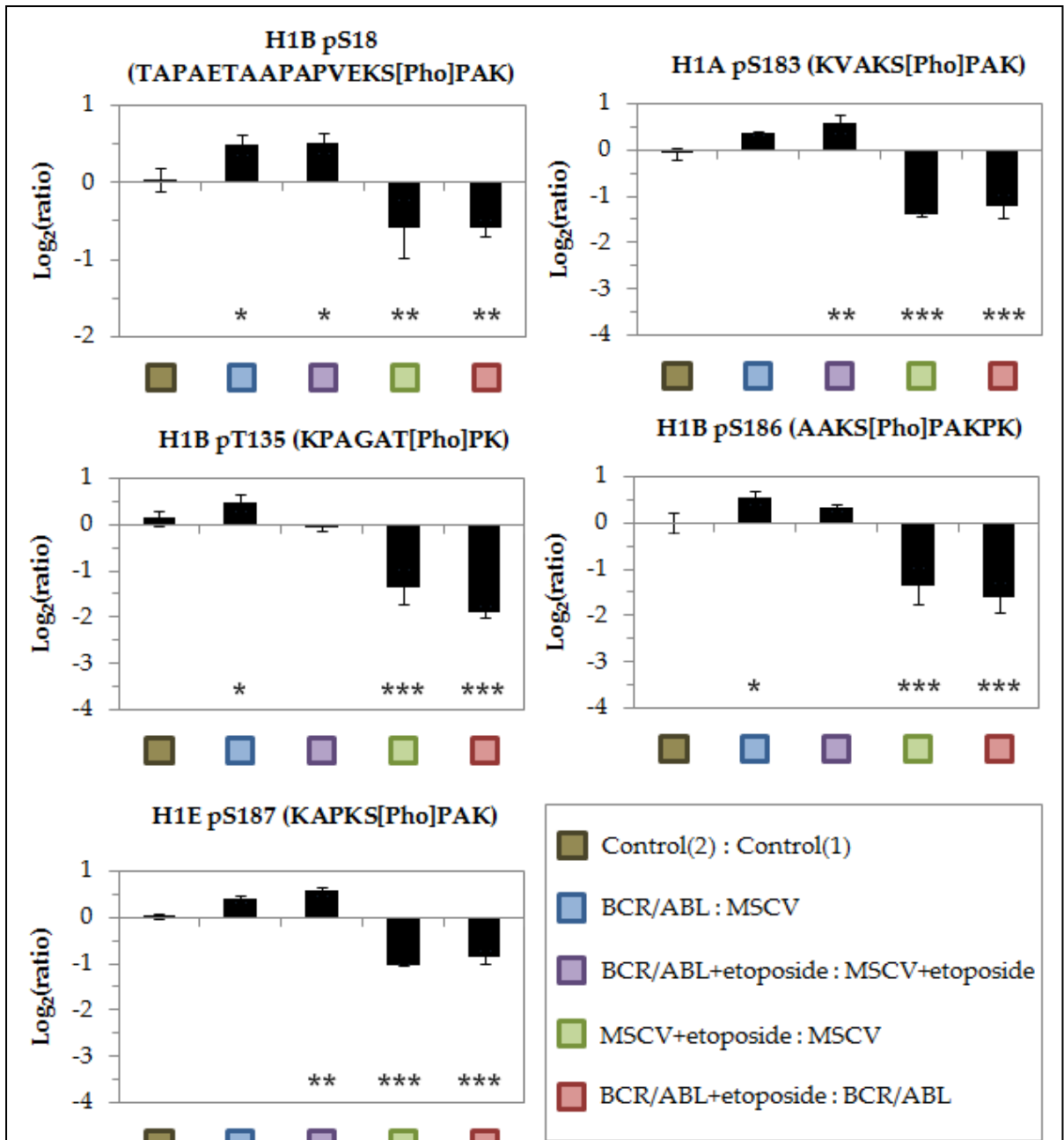


Figure 3.18: Histone H1 phosphoentities are regulated by BCR/ABL PTK and etoposide (4). MSCV and BCR/ABL PTK-expressing Ba/F3 cells were treated with etoposide (20 μ M) or bulk medium for 20 min and collected 1h after post drug/control washout. Phosphoentities correspond to phosphopeptides and their additional modifications analyzed by LC-LC/MS/MS. Average of Log₂(ratios) are shown for the biological control Control(2):Control(1) (4 values) and ratios of interest (2 values). Error bars correspond to SEM. Significance level for Student's t-test p-value (P): * P < 0.05, ** P < 0.01 and *** P < 0.001.

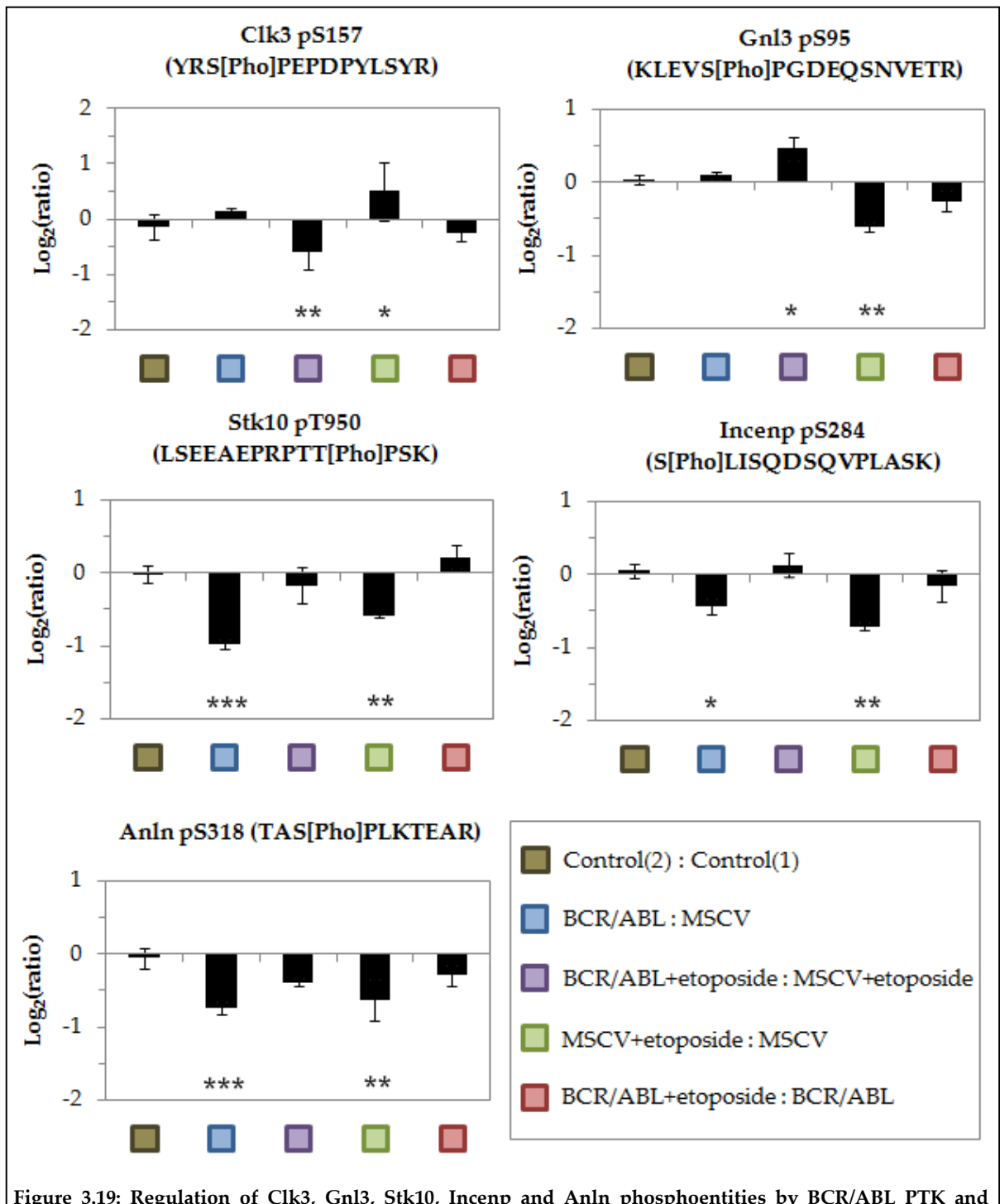
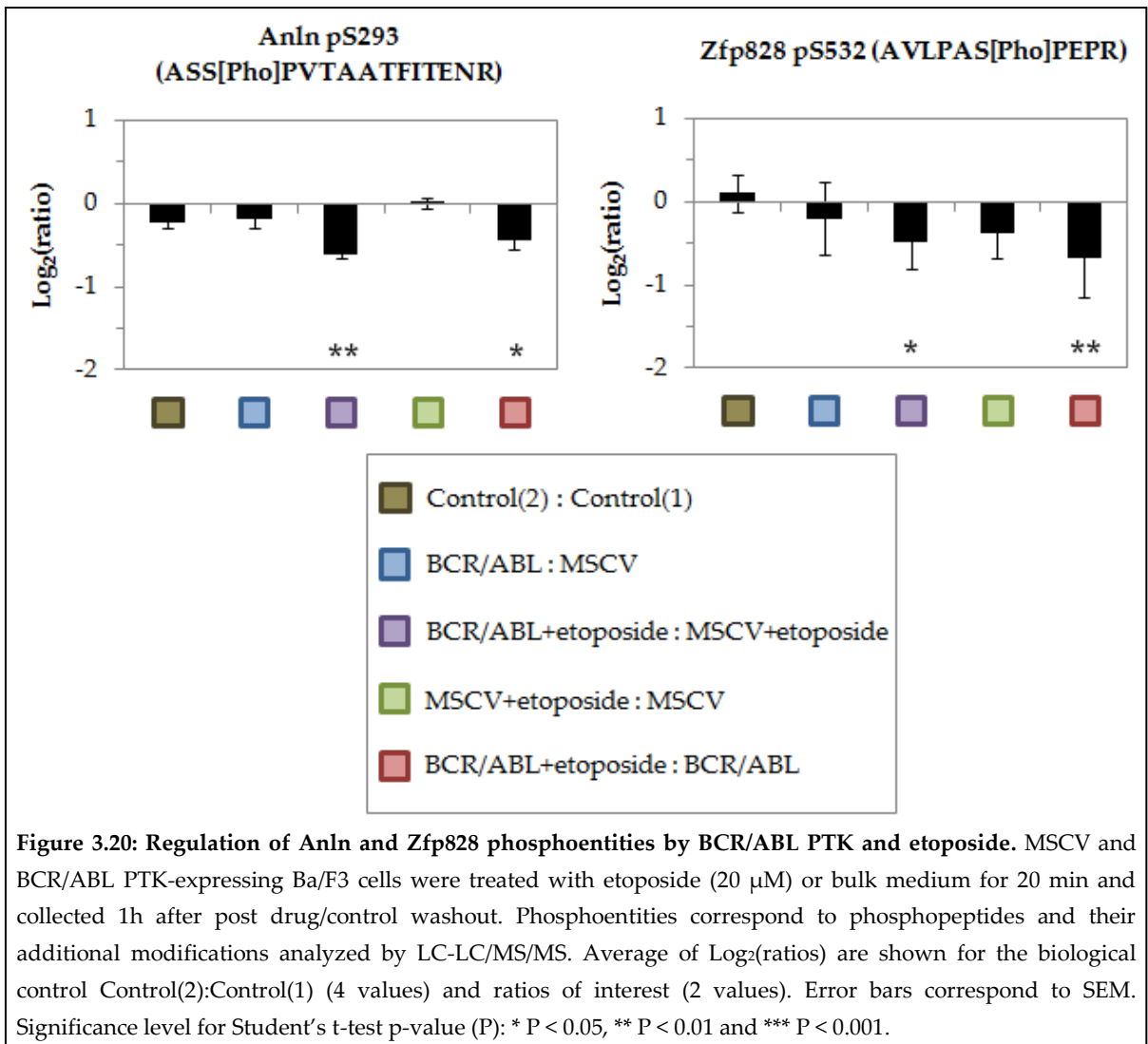


Figure 3.19: Regulation of Clk3, Gnl3, Stk10, Incenp and Anln phosphoentities by BCR/ABL PTK and etoposide. MSCV and BCR/ABL PTK-expressing Ba/F3 cells were treated with etoposide (20 μ M) or bulk medium for 20 min and collected 1h after post drug/control washout. Phosphoentities correspond to phosphopeptides and their additional modifications analyzed by LC-LC/MS/MS. Average of Log₂(ratios) are shown for the biological control Control(2):Control(1) (4 values) and ratios of interest (2 values). Error bars correspond to SEM. Significance level for Student's t-test p-value (P): * P < 0.05, ** P < 0.01 and *** P < 0.001.



Among the 31 phosphoentities which were regulated by BCR/ABL PTK signalling prior to their response to etoposide, B-cell chronic lymphocytic leukemia/lymphoma 7 C protein (Bcl7c) and DNA ligase 1 were dephosphorylated only in the presence of the oncogene on serine 126 and serine 67, respectively (Figure 3.21). Interestingly, Hmga1, a protein involved in transcription regulation and overexpressed in the presence of BCR/ABL and other leukaemogenic PTKs (Pierce, *et al* unpublished observations) was found dephosphorylated on serine 36 upon etoposide exposure but also on serines 99 and/or 103 with etoposide specifically in the presence of the oncogene (Figure 3.21).

The chromobox protein homolog 3 (Cbx3), involved in epigenetic repression, as well as the transcriptional repressor p66-alpha (Gatad2a) also responded to etoposide respectively on serines 93 and 181 but less phosphorylation was detected in treated samples in the presence of BCR/ABL PTK compared to control cells (Figure 3.22). Similarly less phosphorylation of Hnrnpc on serine 229 and Safb2 on threonine 344 was detected upon etoposide exposure with the oncogene (Figure 3.22). Interestingly, phosphoserine 301 of NFIL3 was also found regulated by etoposide, although no modulation was detected in BCR/ABL PTK-expressing cells compared to control cells, both cultured with IL-3.

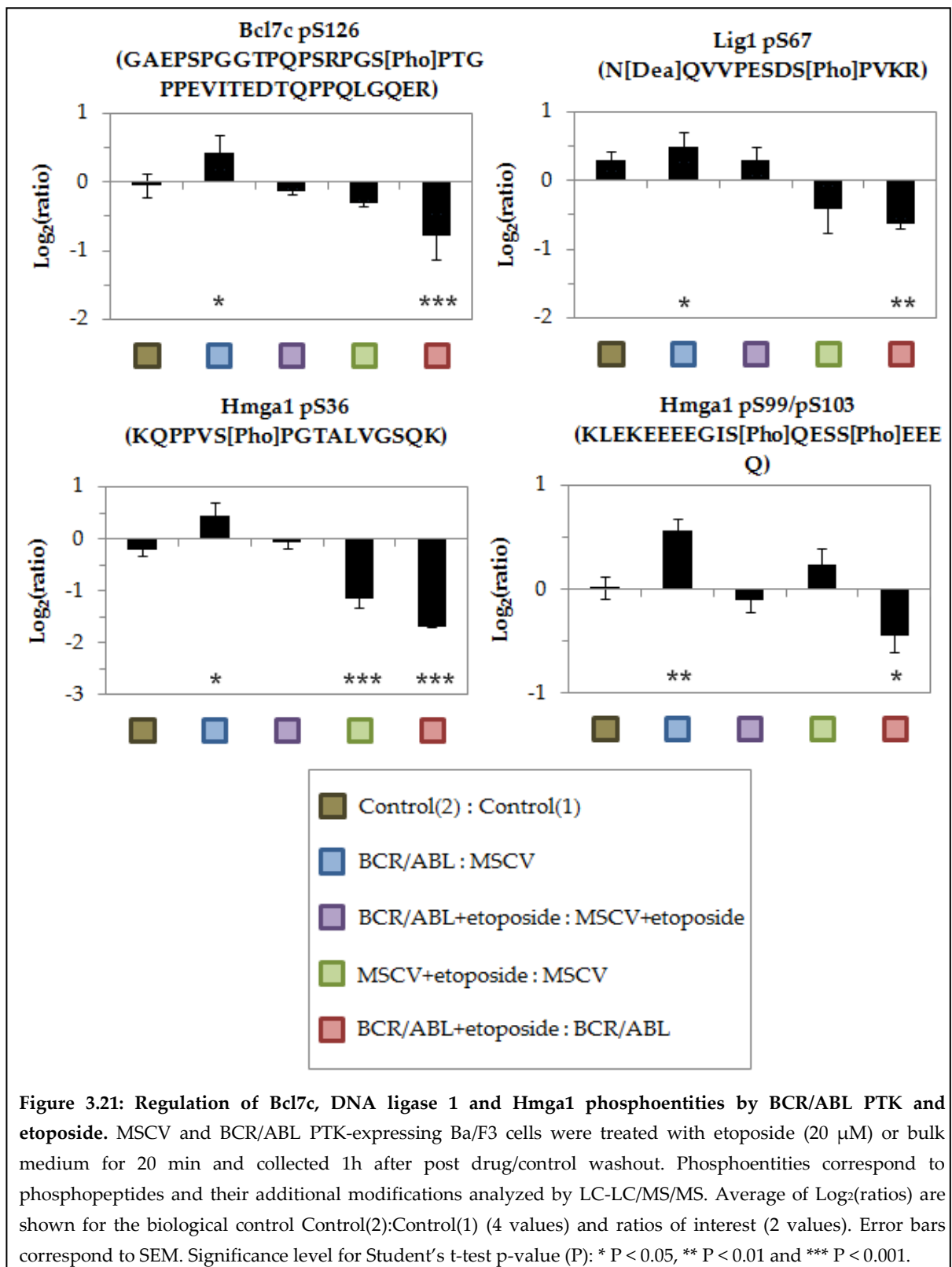


Figure 3.21: Regulation of Bcl7c, DNA ligase 1 and Hmga1 phosphoentities by BCR/ABL PTK and etoposide. MSCV and BCR/ABL PTK-expressing Ba/F3 cells were treated with etoposide (20 μ M) or bulk medium for 20 min and collected 1h after post drug/control washout. Phosphoentities correspond to phosphopeptides and their additional modifications analyzed by LC-LC/MS/MS. Average of Log₂(ratios) are shown for the biological control Control(2):Control(1) (4 values) and ratios of interest (2 values). Error bars correspond to SEM. Significance level for Student's t-test p-value (P): * P < 0.05, ** P < 0.01 and *** P < 0.001.

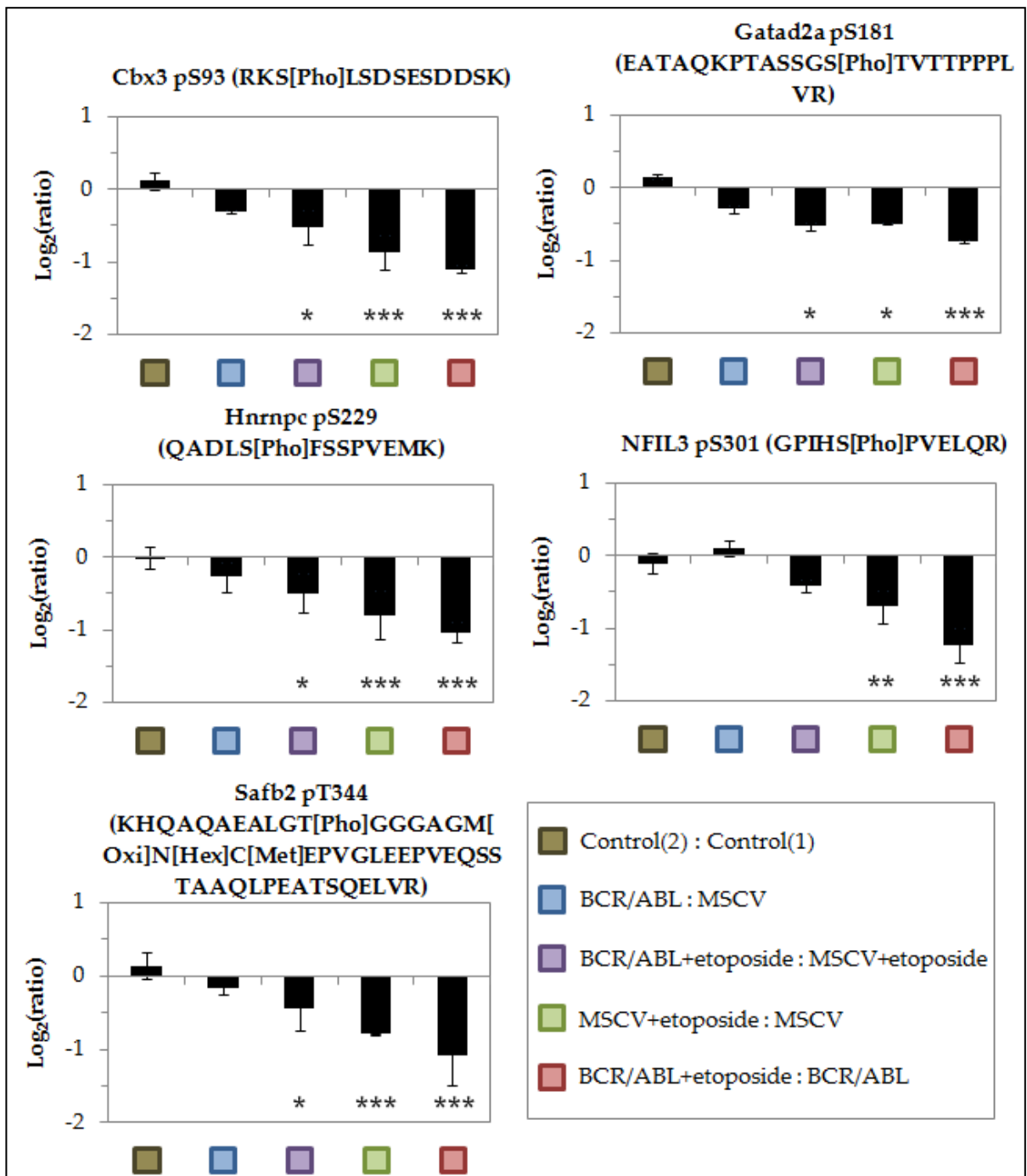
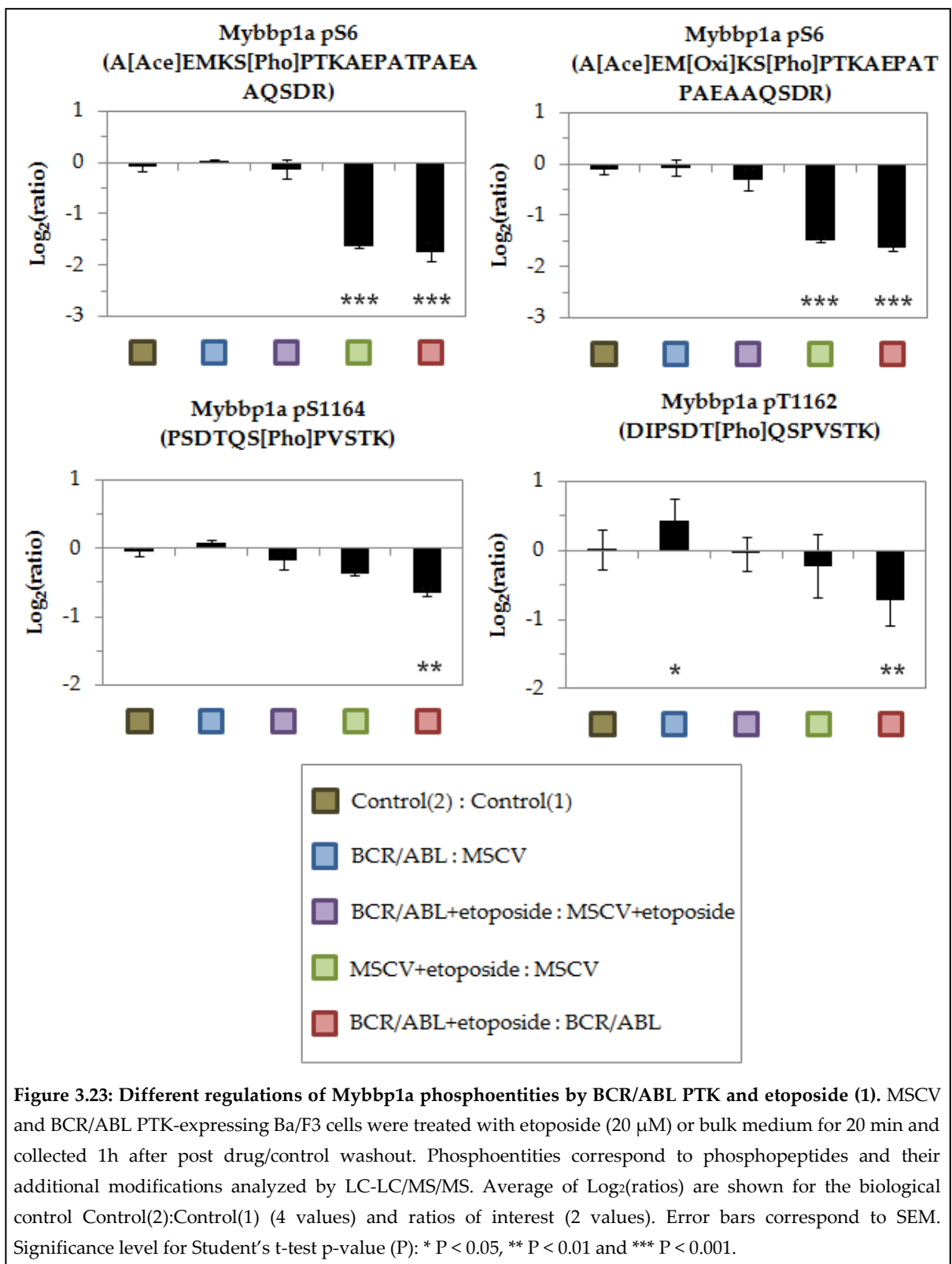
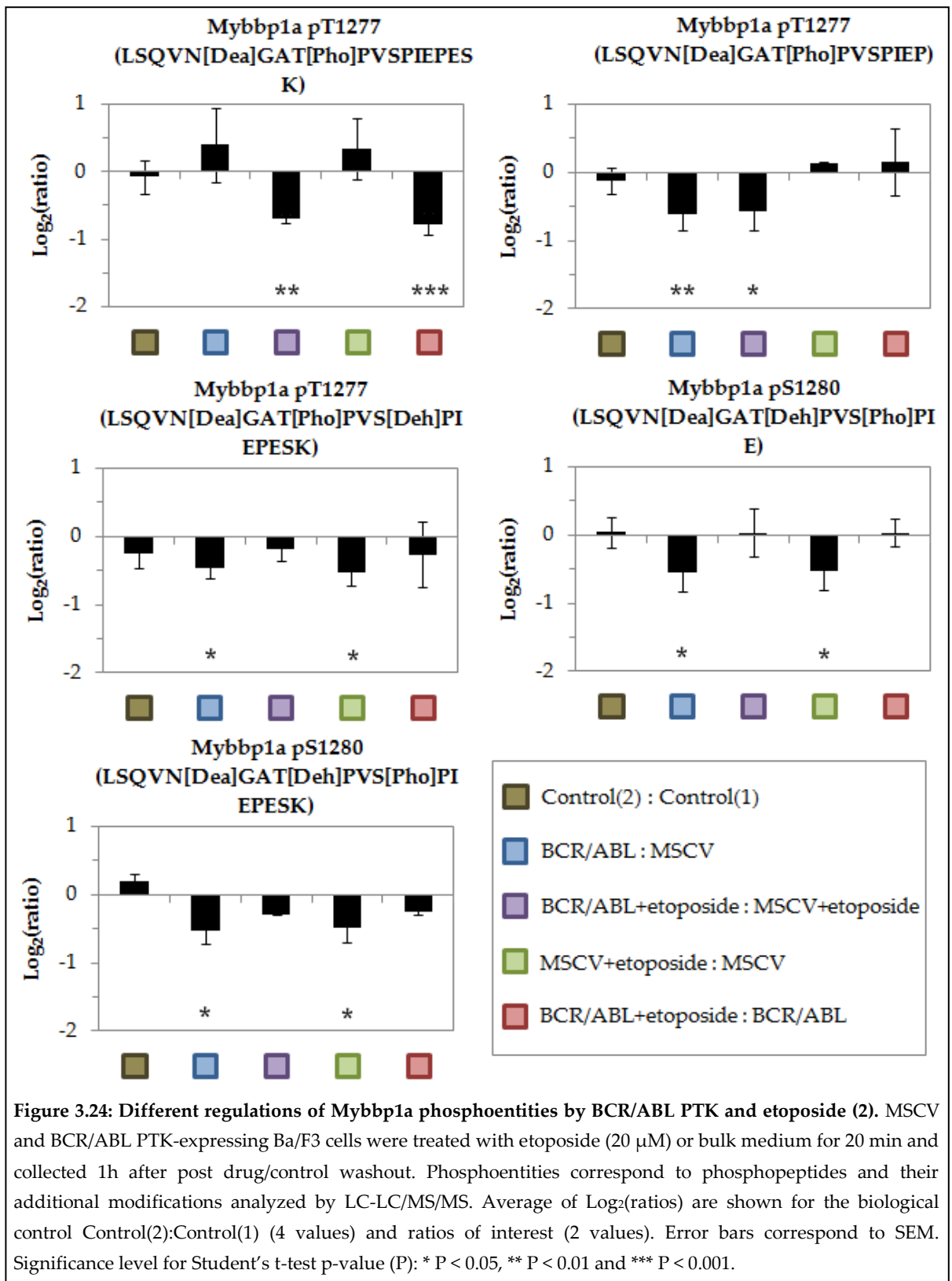


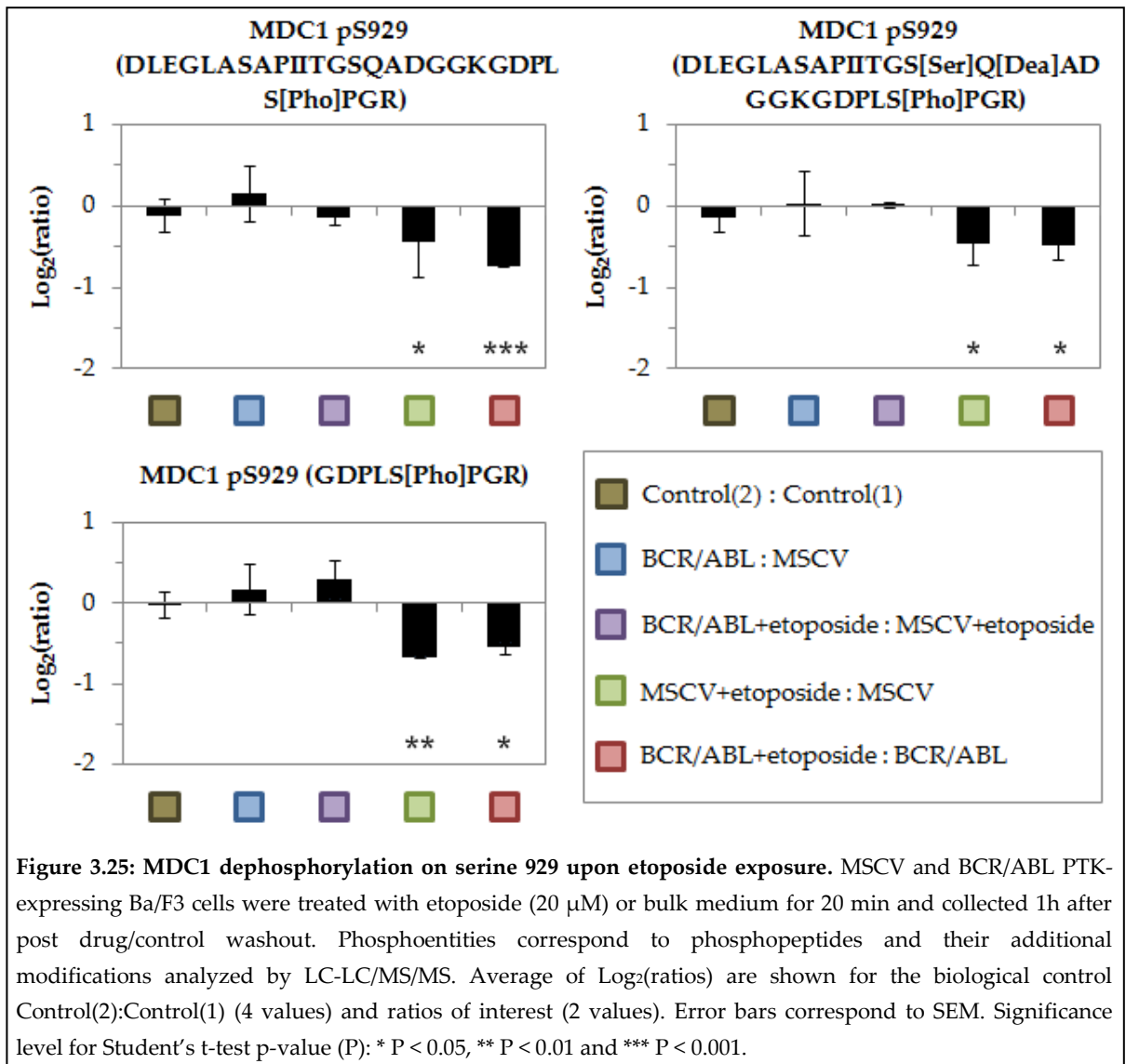
Figure 3.22: Regulation of Cbx3, Gatad2a, HnrnpC and Safb2 by BCR/ABL PTK and etoposide. MSCV and BCR/ABL PTK-expressing Ba/F3 cells were treated with etoposide (20 μ M) or bulk medium for 20 min and collected 1h after post drug/control washout. Phosphoentities correspond to phosphopeptides and their additional modifications analyzed by LC-LC/MS/MS. Average of Log₂(ratios) are shown for the biological control Control(2):Control(1) (4 values) and ratios of interest (2 values). Error bars correspond to SEM. Significance level for Student's t-test p-value (P): * P < 0.05, ** P < 0.01 and *** P < 0.001.

We reported above that Jun phosphorylation on serine 73 decreased upon BCR/ABL PTK expression. Interestingly, Jun binds Mybbp1a (Tavner, *et al* 1998), a member of the B-WICH complex, which was dephosphorylated on serine 6 following etoposide exposure similarly in both cells (Figure 3.23). Additionally, Mybbp1a appeared to be substantially affected by the presence of BCR/ABL PTK as well as etoposide treatment on other phosphosites. Indeed multiple phosphoentities were found regulated by both stresses, including threonine 1162, threonine 1277 and serine 1280, although no clear understanding of the modulation for these two last phosphosites could be confidently delineated from the comparison of independent observations (Figure 3.24).

Mediator of DNA damage checkpoint 1 (MDC1) was another protein regulated by BCR/ABL PTK and etoposide signalling on multiple phosphosites. Three phosphoentities suggested that serine 929 was dephosphorylated following etoposide exposure only (Figure 3.25), while serines 595 and 1053 were modulated by both stresses (Figure 3.26). Indeed, serine 595 was more phosphorylated in the presence of the oncogene compared to control cells both before and after its dephosphorylation upon etoposide addition. Conversely, serine 1053 was phosphorylated by etoposide exposure only in the presence of the oncogene. Serine 750 was not regulated by any stress while only partial evidence was obtained in favour of the regulation of threonine 782 by etoposide (Figure 3.26).







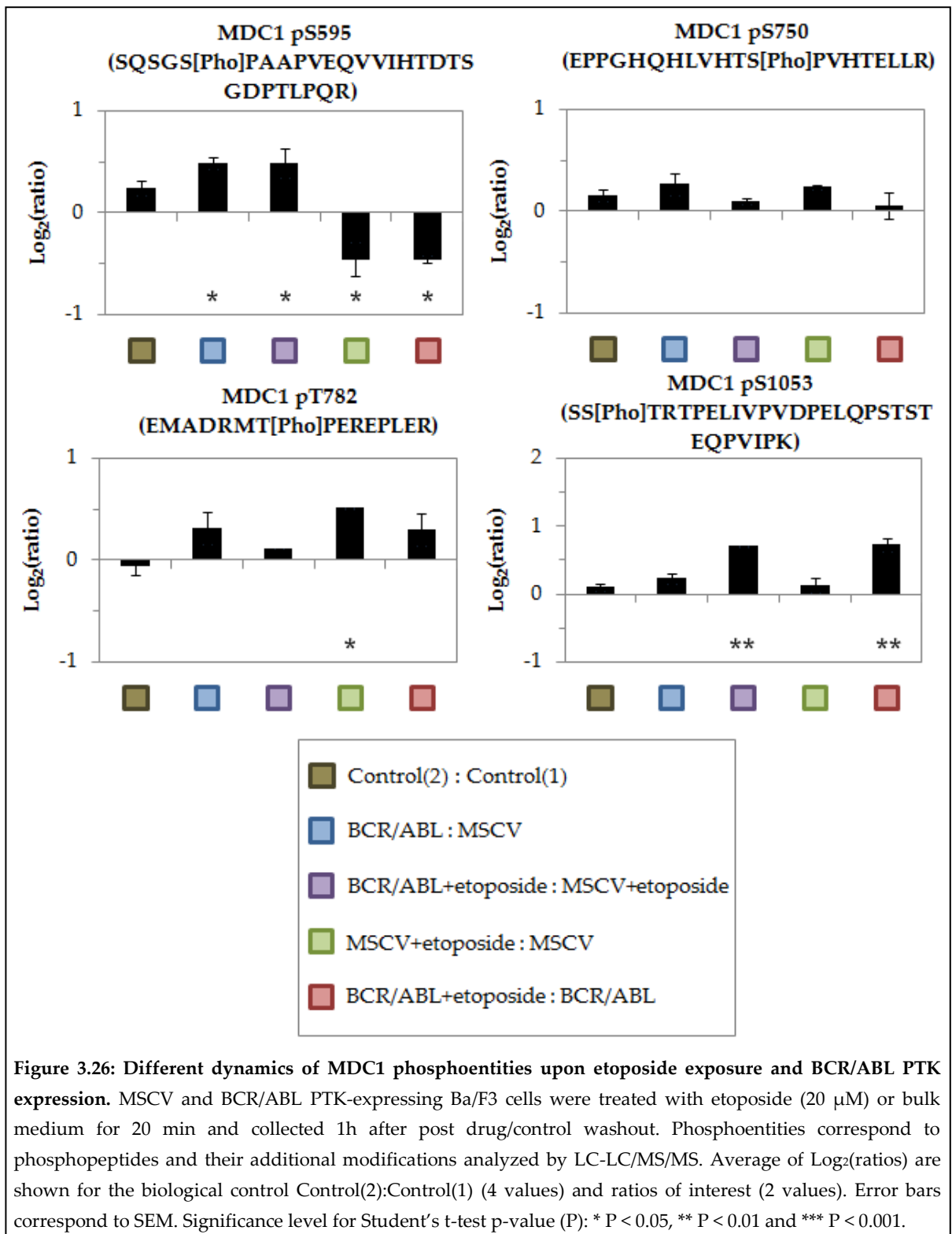
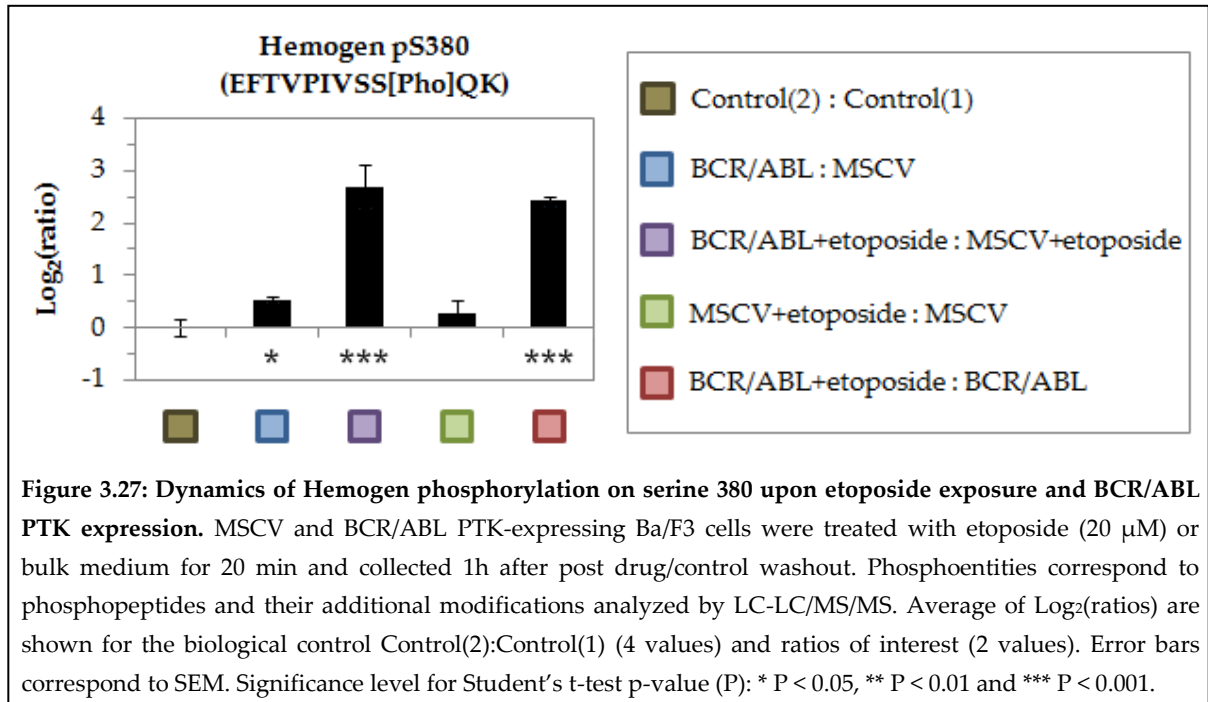


Figure 3.26: Different dynamics of MDC1 phosphoentities upon etoposide exposure and BCR/ABL PTK expression. MSCV and BCR/ABL PTK-expressing Ba/F3 cells were treated with etoposide (20 μ M) or bulk medium for 20 min and collected 1h after post drug/control washout. Phosphoentities correspond to phosphopeptides and their additional modifications analyzed by LC-LC/MS/MS. Average of Log₂(ratios) are shown for the biological control Control(2):Control(1) (4 values) and ratios of interest (2 values). Error bars correspond to SEM. Significance level for Student's t-test p-value (P): * P < 0.05, ** P < 0.01 and *** P < 0.001.

Finally, Hemogen phosphorylation on serine 380 was regulated by etoposide specifically with the presence of BCR/ABL PTK (Figure 3.27). Hemogen pS380 was also increased in BCR/ABL PTK-expressing cells compared to control Ba/F3 cells.



Hemogen is a transcriptional target of HOXB4 and GATA1, two transcription factors involved in haemopoietic development, and Hemogen expression itself can induce myelopoiesis and suppress lymphopoiesis in transgenic mice (Jiang, *et al* 2010, Li, *et al* 2007a, Yang, *et al* 2006). Its overexpression has also been related to differentiation blockade in K562 cells, NF-κB activation and with AML (An, *et al* 2005, Li, *et al* 2004, Liu, *et al* 2004) while high Hemogen expression correlated with ETS-related gene (ERG) expression and worse disease-free survival of AML patients (Marcucci, *et al* 2005). As etoposide seemed to have a considerable effect on Hemogen specifically at serine 380 in BCR/ABL PTK-expressing Ba/F3 cells, western blotting was used to confirm that Hemogen protein expression was not upregulated by this drug (Figure 3.28). No such increase in total protein was seen following etoposide treatment in both cells. However, Hemogen protein expression was higher with the expression of BCR/ABL PTK compared to control cells. Thus the more Hemogen pS380 seen in BCR/ABL PTK-expressing cells as compared to control cells before etoposide treatment could be due to Hemogen overexpression.

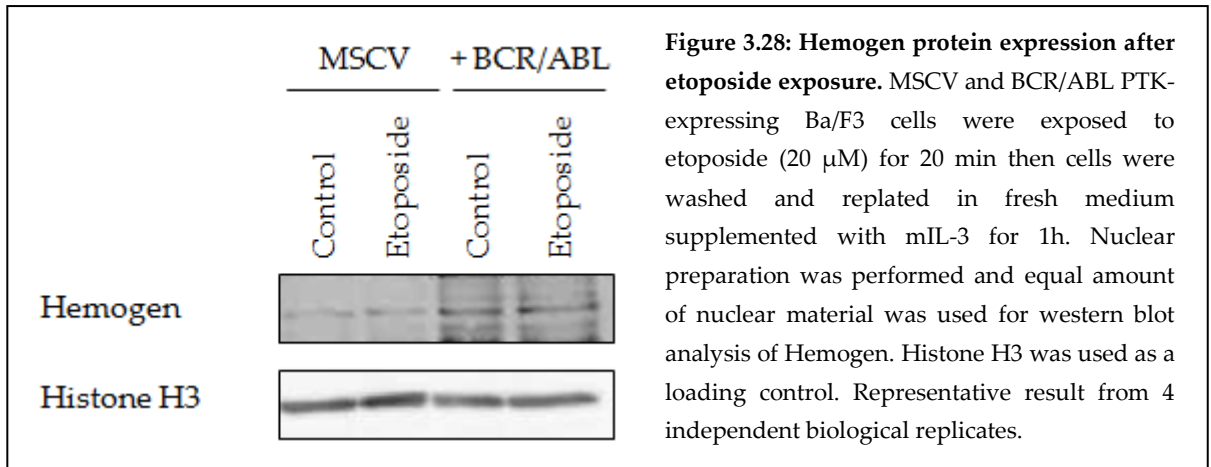


Figure 3.28: Hemogen protein expression after etoposide exposure. MSCV and BCR/ABL PTK-expressing Ba/F3 cells were exposed to etoposide (20 μ M) for 20 min then cells were washed and replated in fresh medium supplemented with mIL-3 for 1h. Nuclear preparation was performed and equal amount of nuclear material was used for western blot analysis of Hemogen. Histone H3 was used as a loading control. Representative result from 4 independent biological replicates.

3.2.6. Validation of Hemogen phosphorylation on serine 380 with AQUA™

Due to its relevance to leukaemia, the hyperphosphorylation of Hemogen at serine 380 with the presence of BCR/ABL PTK, was confirmed with absolute quantification (AQUA™). Phosphosite assignment by ProteinPilot™ software was first confirmed by manual mapping (Figure 3.29).

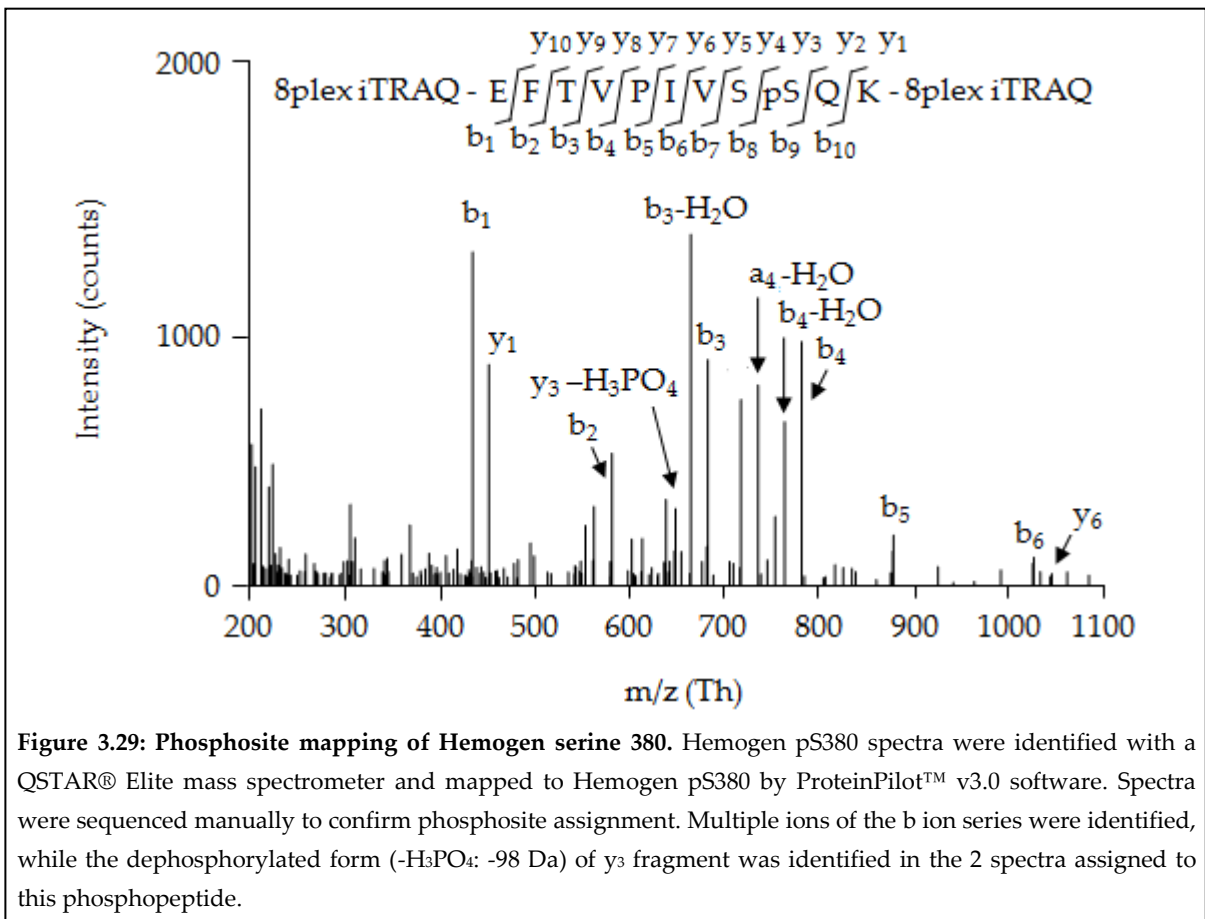


Figure 3.29: Phosphosite mapping of Hemogen serine 380. Hemogen pS380 spectra were identified with a QSTAR® Elite mass spectrometer and mapped to Hemogen pS380 by ProteinPilot™ v3.0 software. Spectra were sequenced manually to confirm phosphosite assignment. Multiple ions of the b ion series were identified, while the dephosphorylated form (-H₃PO₄: -98 Da) of y₃ fragment was identified in the 2 spectra assigned to this phosphopeptide.

Based on these hemogen data, a heavy-labelled version of the phosphopeptide (AQUA™ peptide) was designed with a mass increase of 8 Da compared to the native peptide. The same amount of the AQUA™ peptide was spiked in different tryptic digests of nuclear proteins from Ba/F3 cells (treated or not with etoposide and in the presence or not of BCR/ABL PTK). Three biological replicates for this sample set were prepared. Phosphopeptides were fractionated off-line for each condition (Figure 3.30). Then relevant

fractions were combined and analysed on a 4000 QTRAP® mass spectrometer using SRM transitions designed for both endogenous and heavy-labelled phosphoentity. Three pairs of SRM transitions were designed to identify either the native or the AQUA™ peptide and quantification was performed and improved for the most intense fragment ion (y_7). Linear response of the intensity was confirmed between 0 and 100 fmol of the AQUA™ peptide for this transition, comprising the range of injection for both the native and the AQUA™ peptide (< 50 fmol). Typical examples for each individual sample are shown in Figures 3.31-3.34 for one set of biological replicates and a summary of quantification is shown in Figure 3.35.

The use of AQUA™ technology enabled the confirmation of the increase in phosphorylation of Hemogen on serine 380 upon etoposide exposure with the expression of BCR/ABL PTK. Indeed, although a reproducible etoposide-dependent increase in control cells was observed, the levels of phosphorylation remained very low at approximately 1 fmol compared to more than 20 fmol in the presence of the oncogene (Figure 3.35).

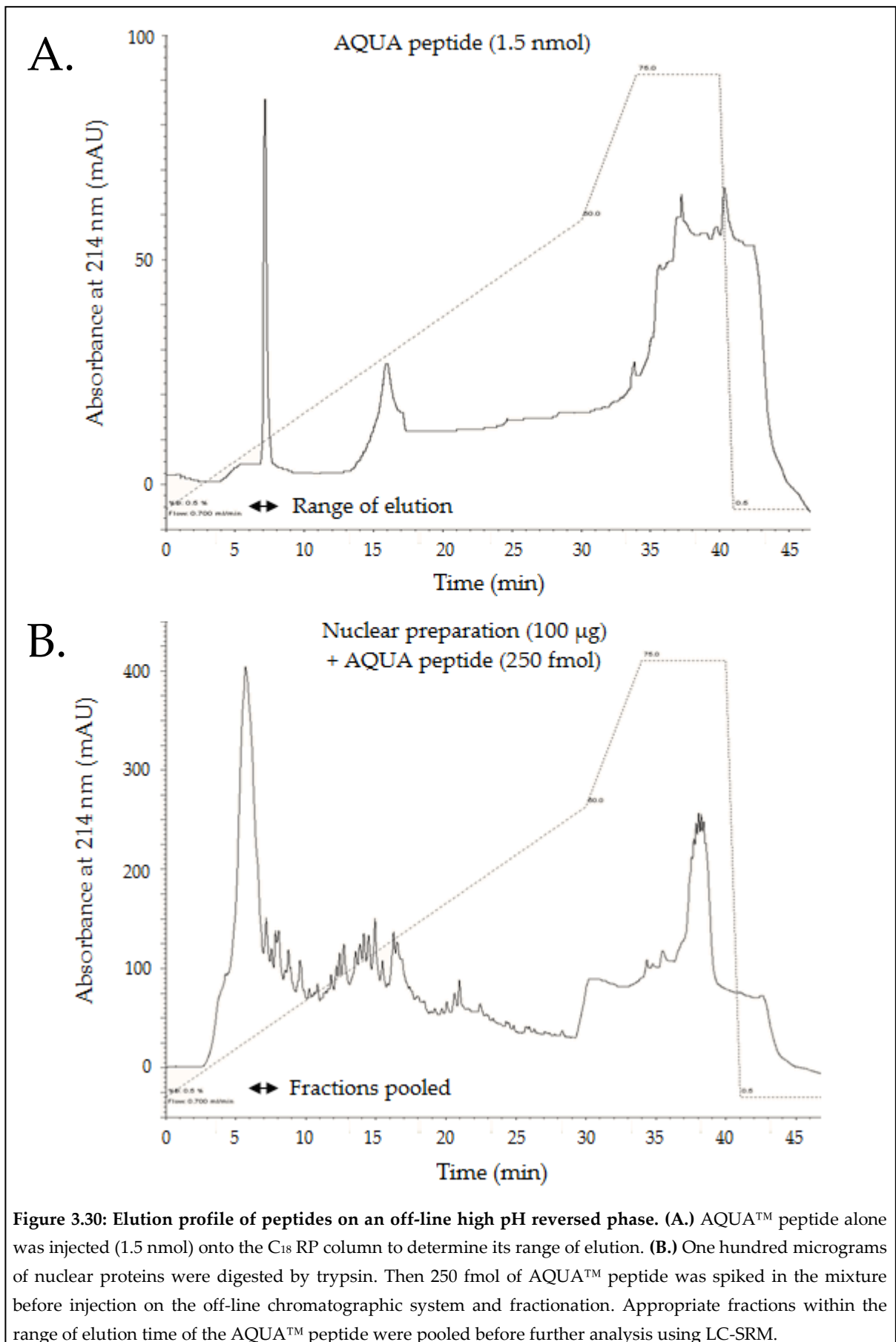
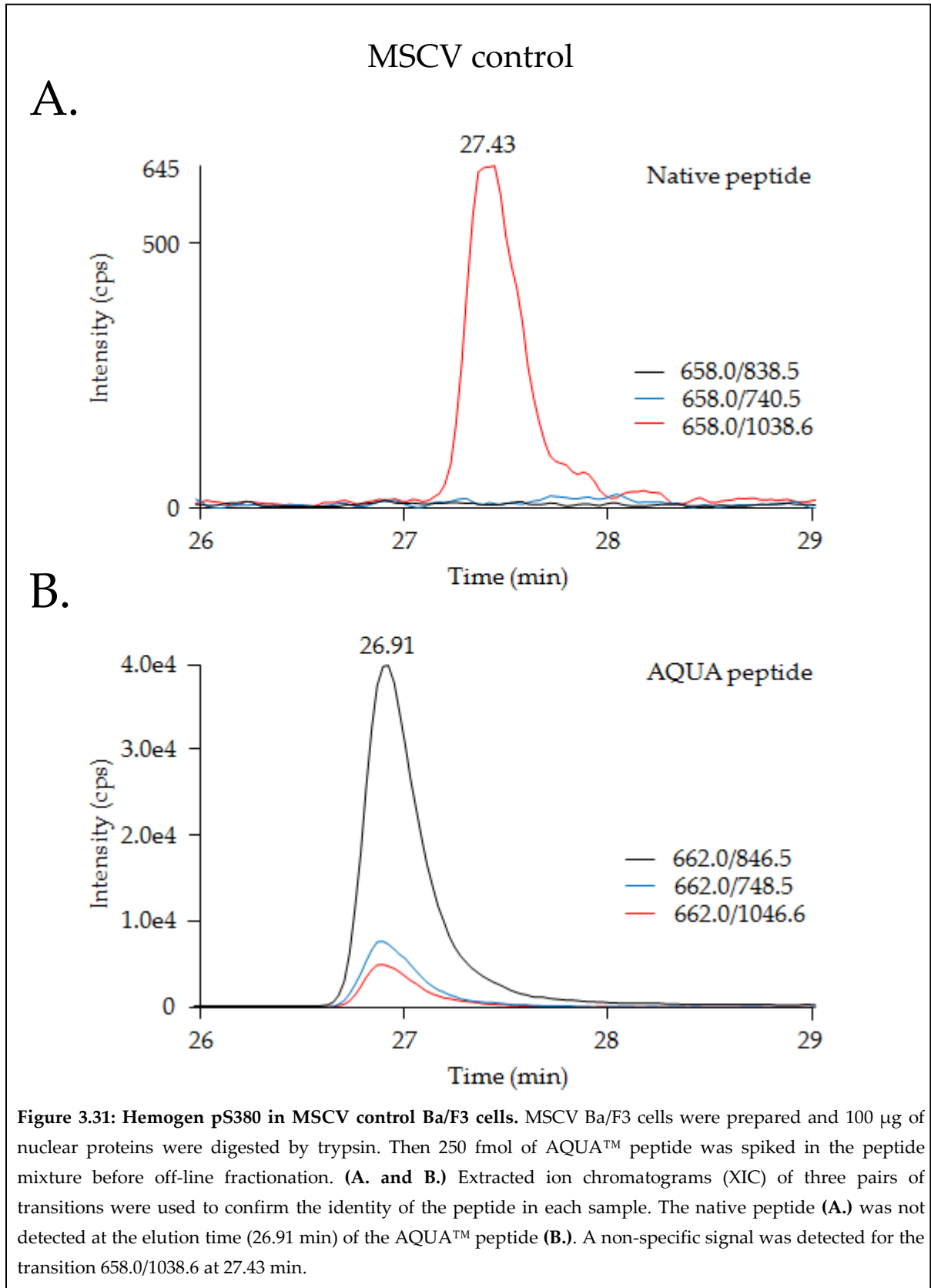
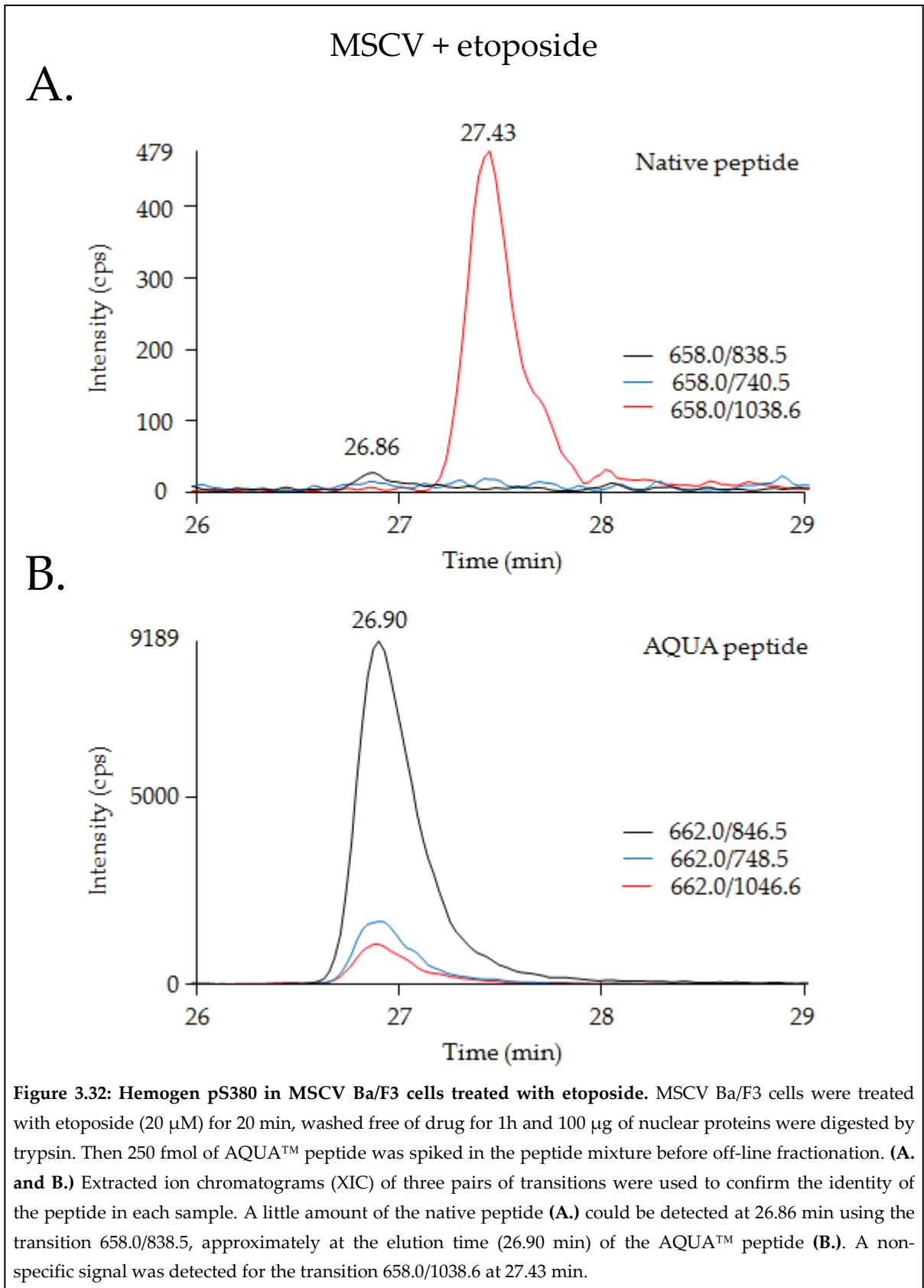
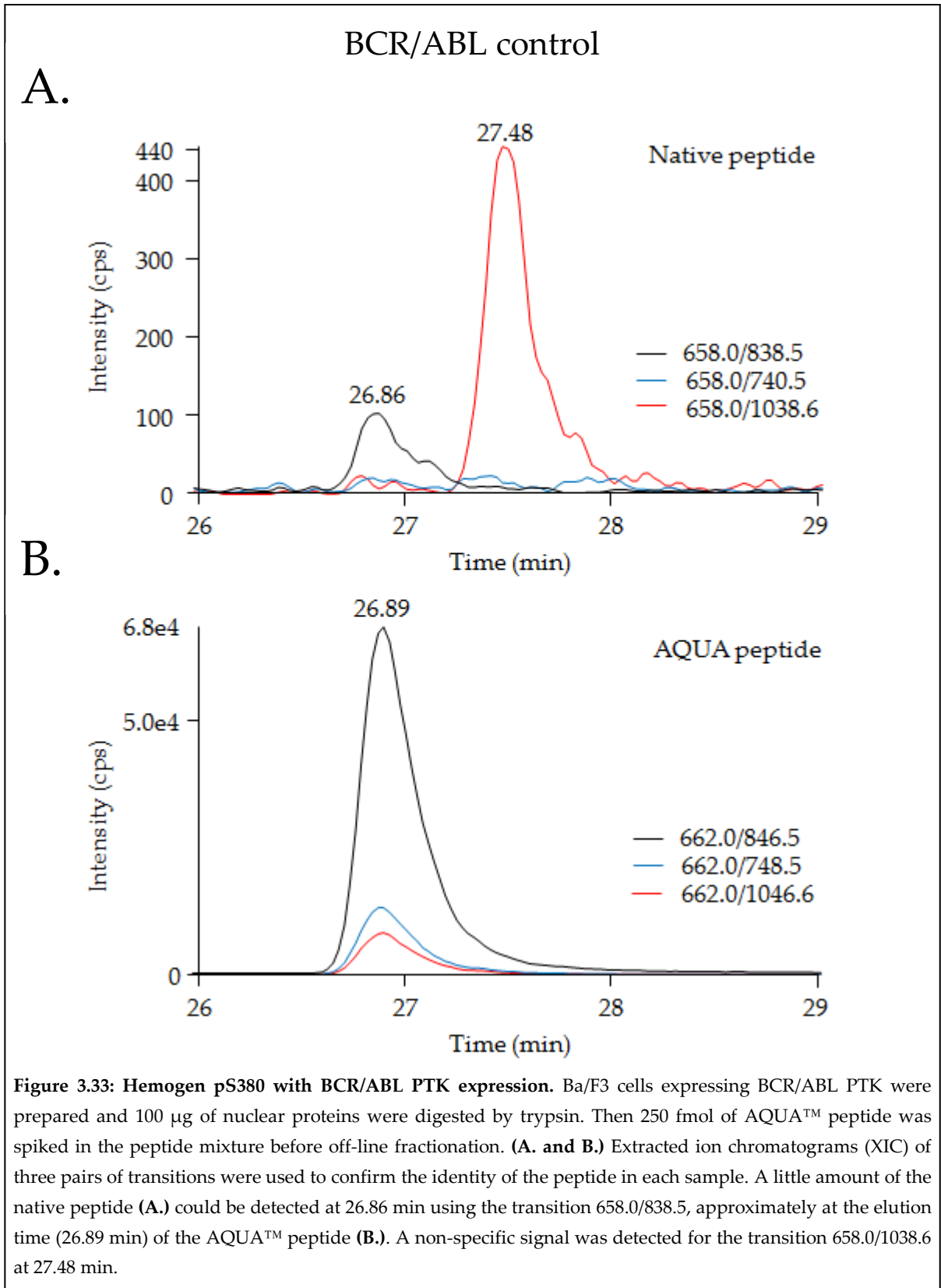
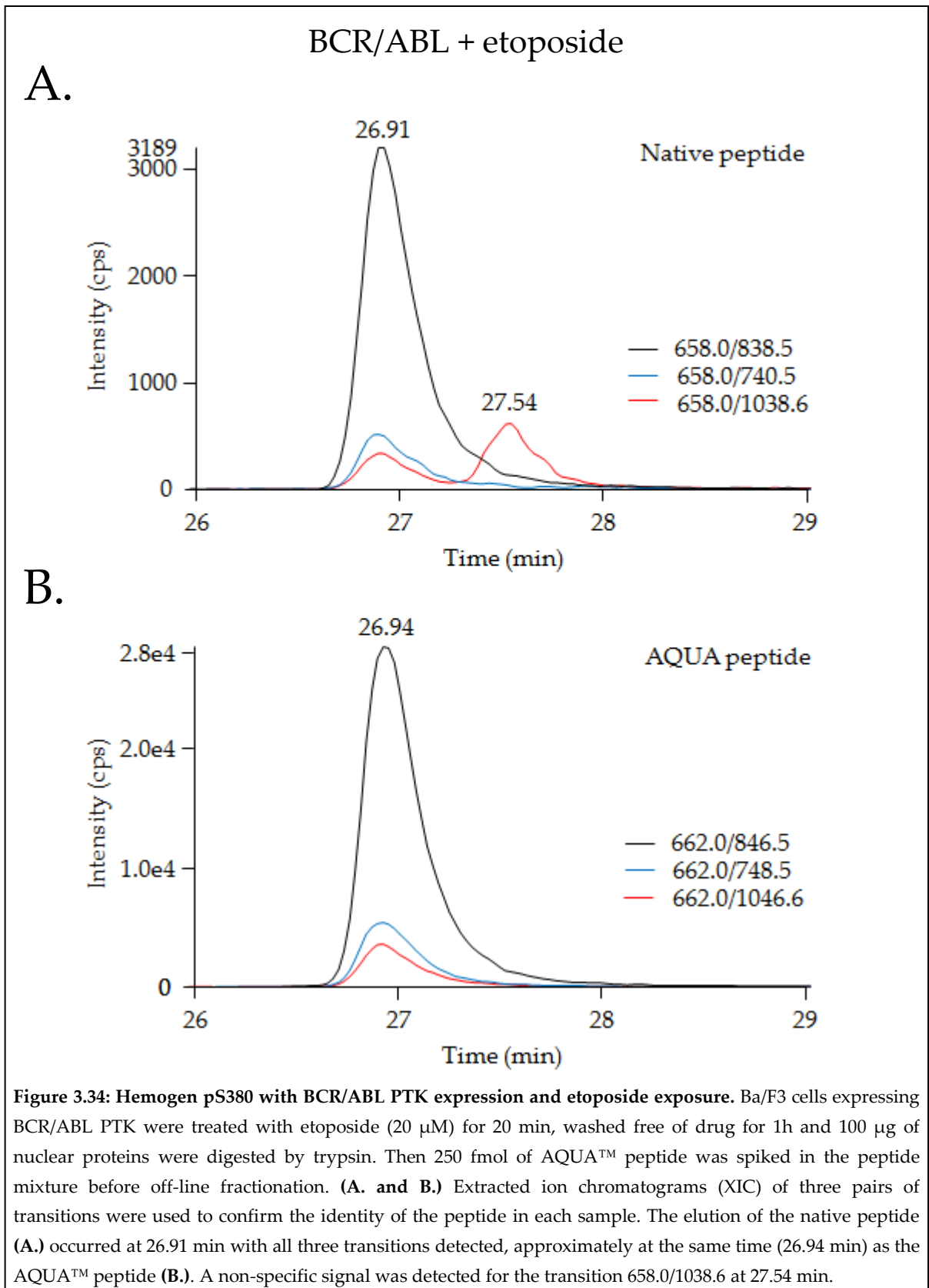


Figure 3.30: Elution profile of peptides on an off-line high pH reversed phase. (A.) AQUA™ peptide alone was injected (1.5 nmol) onto the C₁₈ RP column to determine its range of elution. **(B.)** One hundred micrograms of nuclear proteins were digested by trypsin. Then 250 fmol of AQUA™ peptide was spiked in the mixture before injection on the off-line chromatographic system and fractionation. Appropriate fractions within the range of elution time of the AQUA™ peptide were pooled before further analysis using LC-SRM.

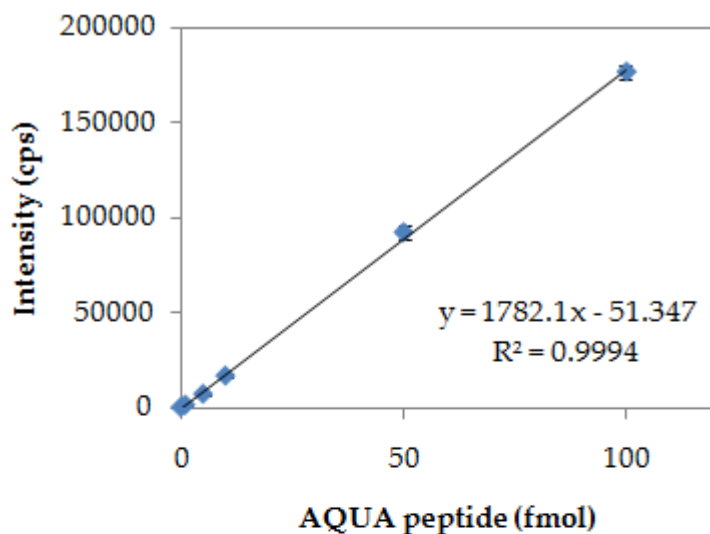








A.



B.

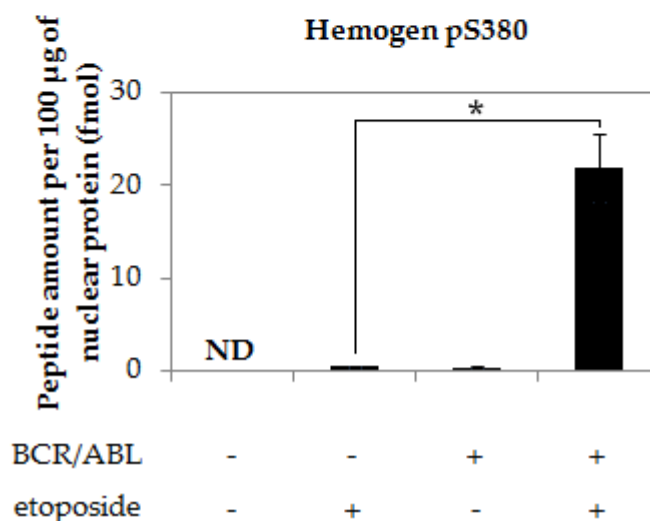
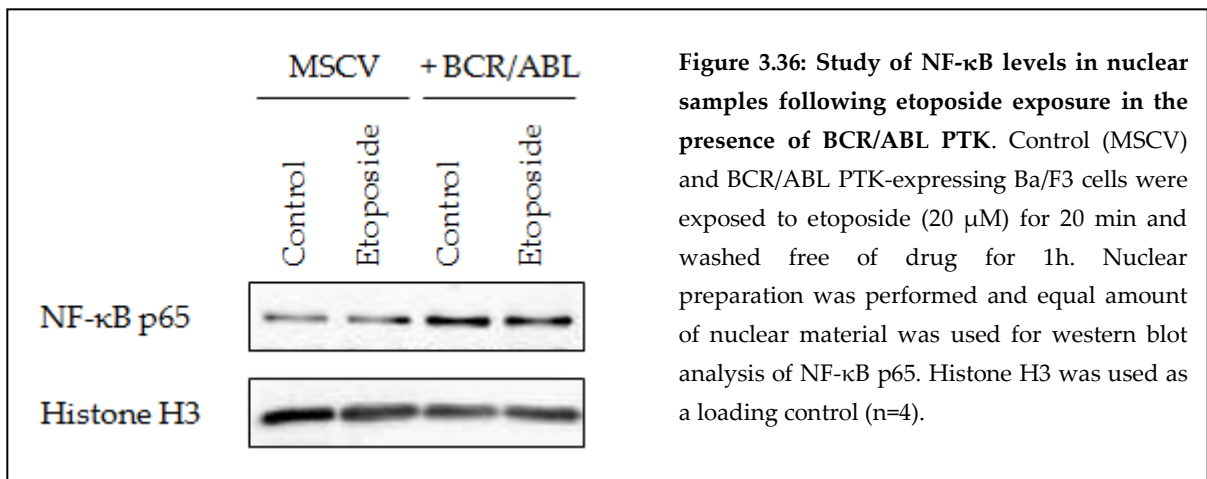


Figure 3.35: Absolute quantification of murine Hemogen pS380 upon etoposide exposure and in the presence of BCR/ABL PTK. Control MSCV and BCR/ABL PTK-expressing Ba/F3 cells were treated or not with etoposide (20 µM) for 20 min and washed free of drug for 1h. Nuclear preparation was performed and 100 µg of nuclear proteins were digested with trypsin. Peptides were fractionated using a reversed phase at high pH in the presence of 250 fmol of Hemogen pS380 AQUA™ peptide. Quantification was performed using a 4000 QTRAP® mass spectrometer. **(A.)** Linear regression of an isotopic dilution of the AQUA™ peptide using the maximum intensity of the extracted ion chromatogram (XIC) of the transition 662.0/846.5 (fragment ion y_7) from 100 to 0 fmol in buffer A in triplicate. **(B.)** The quantity of the native peptide was determined in each sample with the XIC maximum intensities for the pair of transitions 662.0/846.5 (AQUA™ peptide) and 658.0/838.5 (native peptide), each targeting the fragment ion y_7 , with 3 independent biological replicates. Error bars correspond to the standard error of the mean (SEM). *Unpaired two-sided Student's t-test p-value = 0.029 (assumption of unequal variances). ND: not detected.

3.2.7. Pathway analysis pinpoints the B-WICH and NF- κ B complexes as potential mediators of BCR/ABL PTK-mediated genomic instability

As Hemogen has been shown to activate the anti-apoptotic NF- κ B transcription factor to promote cell survival (Li, *et al* 2004), the level of activated NF- κ B p65 subunit following etoposide treatment was determined in nuclear fractions with western blot. As shown in cells expressing BCR/ABL PTK, NF- κ B was already activated as demonstrated by the increased amount of nuclear NF- κ B p65, previously described (Hamdane, *et al* 1997, Reuther, *et al* 1998), but no modulation of NF- κ B activation associated with etoposide addition was found in BCR/ABL PTK-expressing Ba/F3 cells (Figure 3.36).



Ingenuity pathway analysis was performed with the different proteins consistently regulated on phosphoentities between biological replicates by BCR/ABL PTK and/or etoposide addition. The connections between a subset of proteins are shown in Figure 3.37. Links between some of the proteins described above (Stk10, Myc, Jun, Ranbp2, Hmga1 and BCR) were noted with the NF- κ B complex. Interestingly, Mybbp1a has been shown to repress the NF- κ B transcription factor (Owen, *et al* 2007), and was found regulated at multiple phosphosites by BCR/ABL PTK and etoposide. This particular protein belongs to the B-WICH complex along with Smarca5/Snf2h, Baz1b/WSTF, Sf3b1, Dek, Myo1c, Ercc6 and DDX21. Phosphoentities of Baz1b/WSTF and DDX21 were identified in this study. DDX21 belongs to the DEAD box helicase family and may play a significant role in RNA

transcription and transport. As shown in Figure 3.38, DDX21 was regulated by etoposide on serine 144 and/or 181 in both cells but no modulation could be seen with BCR/ABL PTK. No change in phosphorylation could be detected for Baz1b/WSTF. Nevertheless, the responses of DDX21 and Mybbp1a to etoposide pinpointed the B-WICH complex as a potential node for the modulation of the DNA damage response. Baz1b/WSTF has been recently described as a new tyrosine kinase for H2AX on tyrosine 142 (Xiao, *et al* 2009), close to H2AX phosphorylation on serine 139 (γ H2AX). Conversely, H2AX is dephosphorylated on tyrosine 142 by the phosphatase Eyes absent (Krishnan, *et al* 2009), an event required for cell survival and DNA repair through the efficient recruitment of MDC1 (Cook, *et al* 2009), a protein found regulated in this study on serines 595 and 1053 by BCR/ABL PTK and etoposide. Therefore the level of H2AX phosphorylation on tyrosine 142 during etoposide exposure was determined using western blot analysis. The decrease of H2AX phosphorylation tyrosine 142 with etoposide was confirmed in the absence and presence of the oncogene, although less phosphorylation was detected in the presence of BCR/ABL PTK (Figure 3.39). Low H2AX tyrosine 142 phosphorylation associated with high H2AX serine 139 phosphorylation would be required for efficient MDC1 recruitment (Cook, *et al* 2009).

These observations would suggest that BCR/ABL PTK affects the etoposide-induced genotoxic stress signalling on proteins involved in the regulation of the activity of B-WICH and NF- κ B complexes as well as the DNA repair platform H2AX.

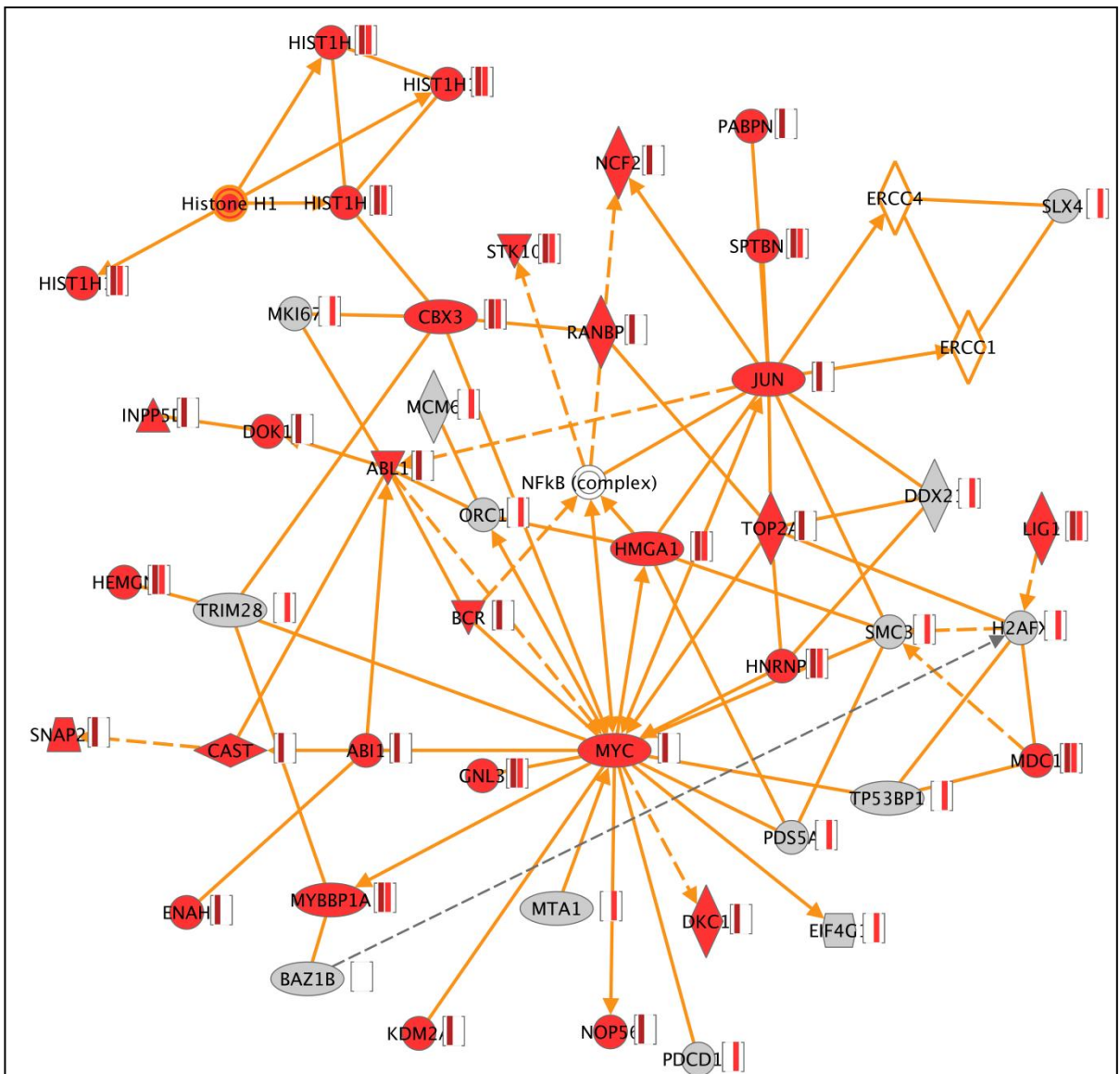
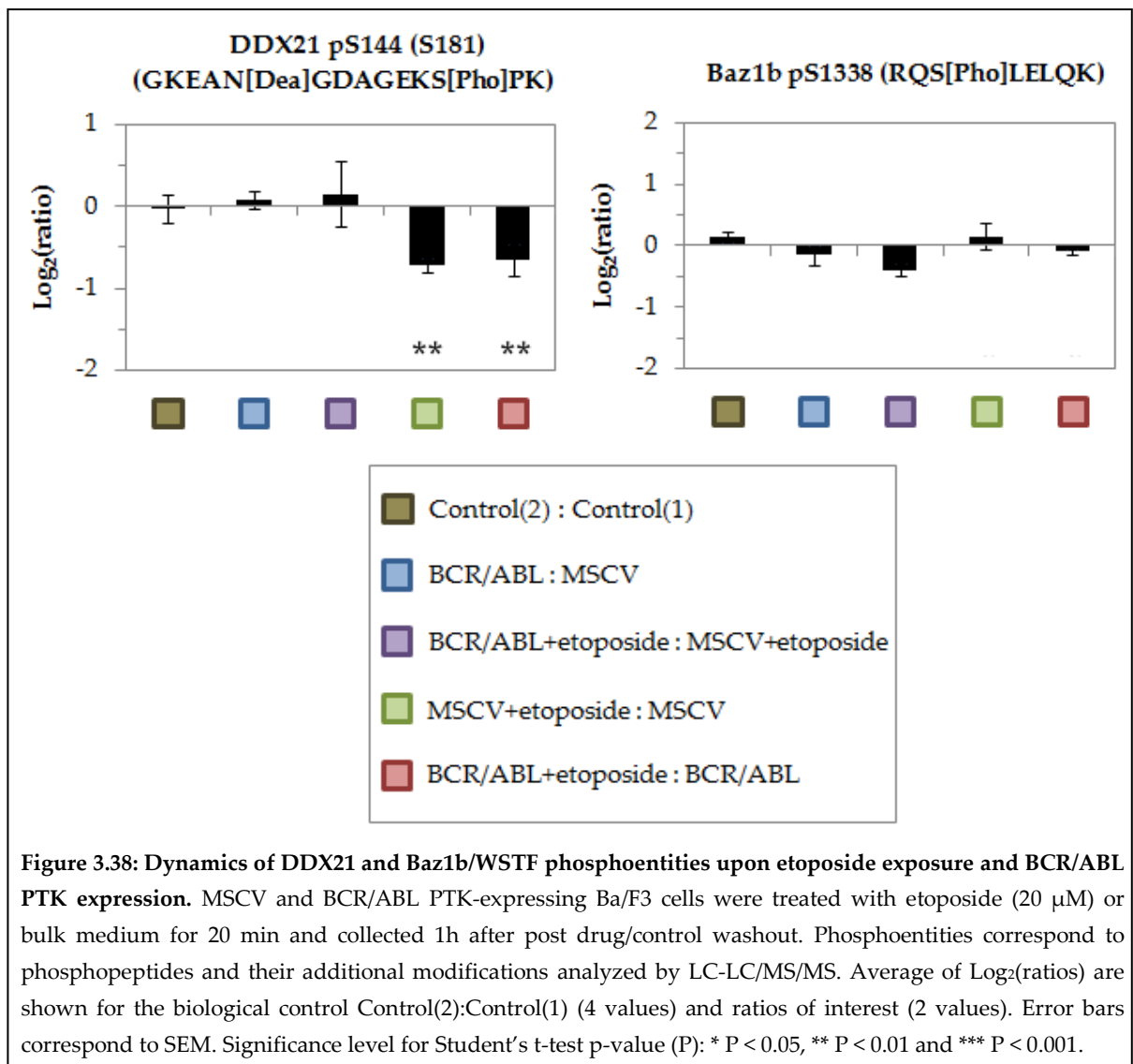
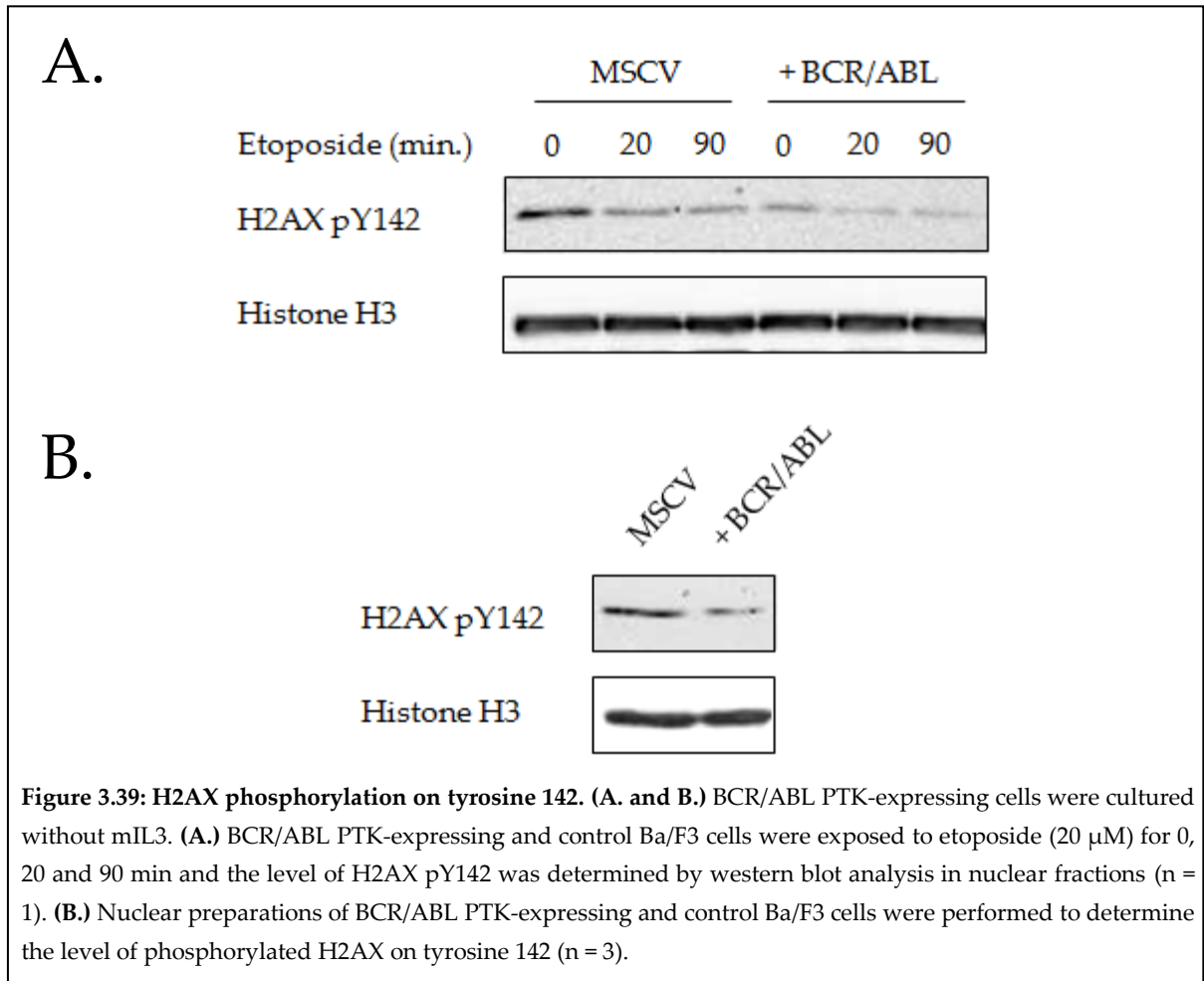


Figure 3.37: Annotated Ingenuity pathway analysis for a subset of proteins consistently modulated by BCR/ABL PTK and etoposide. This diagram was created using Ingenuity pathway analysis (connections in orange) (<http://www.ingenuity.com>). One connection was added in grey between the tyrosine kinase Baz1b and its substrate H2AFX based on literature (Cook, *et al* 2009, Xiao, *et al* 2009). Bars in brackets are shown whenever a protein is regulated on one or multiple phosphosites by BCR/ABL PTK (left bar) or etoposide (right bar). Proteins shown in red contain phosphoentities modulated by BCR/ABL PTK. Proteins in grey correspond to other proteins identified in this study. Proteins in white were added to build the network.





3.3. Discussion

The relationship between BCR/ABL PTK and genotoxic stress signalling remains poorly understood. Only a few modulations of protein phosphorylation have been described in relation to their relevance to disease progression, treatment resistance, DNA repair fidelity or cell cycle progression (Dierov, *et al* 2004, Rink, *et al* 2007, Slupianek, *et al* 2001).

In this study the dose of etoposide was assessed in order to generate DNA double strand breaks (DSBs) (60 to 70% of cells had an increase in H2AX phosphorylation on serine 139), which did not trigger substantial levels of apoptosis in the long term (15-30% compared to 8% of Annexin-V-positive cells when untreated, Figure 3.3-A). To recruit proteins involved in DNA double strand break repair and DNA processing, cells were washed free of etoposide for 1h following a 20 min exposure. Using flow cytometry, H2AX phosphorylation on serine 139 was found significantly higher with BCR/ABL PTK expression than in control cells after removal of etoposide and recovery for 1h, possibly due to ongoing DNA repair in control cells. This observation confirmed previous results showing that BCR/ABL PTK and other leukaemogenic PTKs generate DNA DSBs (Cramer, *et al* 2008, Slupianek, *et al* 2006). ATM autophosphorylation on serine 1987 is mediated after recognition of DNA DSBs by the MRN complex (Riches, *et al* 2008). ATM autophosphorylation on serine 1987 was induced similarly in control and BCR/ABL PTK-expressing cells in the presence of etoposide. To explain an increased H2AX phosphorylation on serine 139, phosphatases such as PP2A, PP4 and WIP1 could also be deregulated. Alternatively, enhancers of H2AX pS139 such as the SWI/SNF complex, WINAC and B-WICH complex could be modulated to sustain phosphorylation (Chowdhury, *et al* 2005, Macurek, *et al* 2010, Nakada, *et al* 2008, Oya, *et al* 2009, Park, *et al* 2009, Park, *et al* 2006, Xiao, *et al* 2009). Interestingly, topoisomerase 2a, the target of etoposide was dephosphorylated on serine 1373 with the expression of BCR/ABL PTK and this modulation might influence the topoisomerase efficiency to cleave DNA strands.

Our analysis of phosphoentities concentrated on significant changes across biological replicates to identify potential regulation by BCR/ABL PTK and/or etoposide (Figure 3.7). In total, 112 phosphoentities were found potentially regulated, among them 44 phosphoentities, corresponding to 33 protein phosphosites, responded to etoposide and were modulated by BCR/ABL PTK expression. Potential patterns of modulation by BCR/ABL PTK were discovered such as the ones found for Stk10 pT950, Incenp pS284 and Anln pS318 or Cbx3 pS93, Gatad2a pS181, Hnrnpc pS229 and Safb2 pT344 (Figures 3.19 and 3.22). Stk10 is a polo-like kinase highly expressed in haemopoietic tissues which has been shown to phosphorylate histone H2A on serine and threonine (Kuramochi, *et al* 1997, Walter, *et al* 2003). Its phosphorylation on threonine 950 was downregulated in the presence of BCR/ABL PTK in this study. Interestingly, this downregulation was also found in control cells when stressed by etoposide, suggesting that this modulation by BCR/ABL PTK correspond to a sustained stress signalling. Polo-like kinases are important in cell cycle regulation, spindle assembly, cytokinesis and recovery after DNA damage checkpoint and Polo-like kinase 1 is overexpressed in AML (Renner, *et al* 2009, Sumara, *et al* 2004). Interestingly, Incenp is also involved in the regulation of mitosis with Aurora B kinase, as a component of the chromosomal passenger complex (CPC), which ensures the mitotic spindle assembly, the sister chromatid cohesion as well as the correct alignment, the biorientation and the segregation of chromosomes (Resnick, *et al* 2006, Tanaka, *et al* 2002). Zfp828 is a zinc finger protein which was more dephosphorylated in the presence of the oncogene following etoposide treatment. Zfp828 is required for accurate chromosome segregation and sister chromatid biorientation too (Itoh, *et al* 2011). Defect in sister chromatid cohesion and chromosome segregation are potential sources of chromosomal instability and cancer (Dodson and Morrison 2009, Draviam, *et al* 2004, Morrison, *et al* 2003, Stephan, *et al* 2011), while sister chromatid exchange is increased upon BCR/ABL PTK expression after DNA damage (Deutsch, *et al* 2003). Among the other proteins similarly modulated Actin-binding protein Anln is overexpressed in CML cells (Affer, *et al* 2011) and has also a role in cytokinesis (Oegema, *et al* 2000). Anln pS293 and pS318 would be differentially regulated by BCR/ABL PTK expression in response to etoposide. Interestingly increasing evidence suggests that Actin has a crucial role in the nucleus in

the regulation of chromatin remodelling complexes as well as transcription and mRNA export and it would of interest to assess the impact of the modulation of Anln phosphoresidues on these processes (Bettinger, *et al* 2004).

Chromobox protein homolog 3 (Cbx3) binds to Zfp828 and Incenp, although these interactions were not detailed with Ingenuity pathway analysis (Ainsztein, *et al* 1998, Vermeulen, *et al* 2010). Cbx3 controls the formation of functional kinetochore and represses gene expression through binding with Histone H3 methylated at lysine 9 (Lachner, *et al* 2001). Cbx3 was dephosphorylated upon etoposide exposure to a greater extent in the presence of BCR/ABL PTK than in control cells. Cbx3 is also linked with Trim28/TIF-1beta/KAP-1 which was phosphorylated on serine 473 upon etoposide exposure (Appendix 7.12) while its phosphorylation on serine 824 has been shown to be required for DNA double strand break repair (Cammass, *et al* 2004, Noon, *et al* 2010). Cbx3 dephosphorylation in the presence of the oncogene may be associated with the regulation of gene expression. Similarly, a greater dephosphorylation of the transcriptional repressor p66-alpha (Gatad2a) on serine 181 was found in the presence of BCR/ABL PTK which might also suggest that the transcription programme in the presence of the oncogene is affected. The different response of Hnrnpc pS229, Safb2 pT344 and the dual specificity protein kinase Clk3 pS157 to etoposide in the presence of BCR/ABL PTK could also be linked to the modulation of gene expression by the mediation of RNA splicing or the attachment to the nuclear matrix (Duncan, *et al* 1998). Moreover, Gatad2a is found in complex with proteins binding methylated DNA to silence gene expression as well as with HDAC1 and HDAC2 histone deacetylases which promote NHEJ in the DNA damage response (Gong, *et al* 2006, Miller, *et al* 2010). Interestingly the histone demethylase Kdm2a and the histone methyltransferase Whsc1 were regulated in the presence of BCR/ABL PTK on serine 692 and serine 437, respectively, although these phosphosites did not respond to etoposide. However, Kdm2a and Whsc1 are potential targets of ATM/ATR at threonine 632 and serine 102, respectively (Matsuoka, *et al* 2007). Kdm2a is important to maintain genomic stability and to silence gene expression (Blackledge, *et al* 2010, Frescas, *et al* 2008), while Whsc1 may support cancer cell proliferation as well as gene repression along with

HDAC1 and HDAC2 in multiple myeloma (Lauring, *et al* 2008, Marango, *et al* 2008). Whsc1 gene has also been found to be fused to the IgH gene by the chromosomal translocation t(4;14)(p16;q32) in multiple myeloma and deleted in Wolf-Hirschhorn syndrome causing developmental abnormalities (Bergemann, *et al* 2005, Chesi, *et al* 1998, Malgeri, *et al* 2000, Santra, *et al* 2003, Stec, *et al* 1998).

Several proteins regulated by etoposide were previously linked to leukaemogenic PTK action. Hmga1 pS36 was dephosphorylated upon etoposide exposure in both cells while pS99/S103 was dephosphorylated only in the presence of the oncogene. The two corresponding phosphoentities were overrepresented in the presence of BCR/ABL PTK. Hmga1 protein is relevant to leukaemic development and DNA damage as it interacts with BRCA1 (Baldassarre, *et al* 2003), it is involved in chromatin condensation, RNA processing and nucleosome phasing (Downs 2007) and it is upregulated by 6 different leukaemogenic PTKs (Pierce, *et al* unpublished observations). Pds5a, involved in sister chromatid cohesion has been found regulated by 4 leukaemogenic PTKs and was also regulated here by etoposide on serine 1300 (Pierce, *et al* unpublished observations). Also, the dephosphorylation of nucleostemin/Gnl3 on serine 95 upon etoposide exposure could be related to its role in regulating the response to reactive oxygen species (ROS). However, this dephosphorylation was not found in the presence of BCR/ABL PTK. This interactor of p53 has been related to stem cell and cancer cell proliferation and the high amount of ROS produced by leukaemogenic PTKs could lead to its abnormal regulation (Han, *et al* 2005, Huang, *et al* 2011, Tsai and McKay 2002).

Here, we identified a regulated phosphoentity from Hemogen/EDAG/NDR, a protein overexpressed in AML patients and part of the ETS-related gene (ERG) overexpression gene signature, linked with poor prognosis (An, *et al* 2005, Marcucci, *et al* 2005). Hemogen expression has been shown to block differentiation in K562 cells (Liu, *et al* 2004) and is able to induce myelopoiesis and suppress lymphopoiesis in transgenic mice and it can promote cell survival via NF- κ B activation (Li, *et al* 2007a, Li, *et al* 2004). Also, Hemogen pS213 has been found to be increased with BCR/ABL and FIP/PDGFR α PTKs in the same model as

the one used here (Pierce, *et al* unpublished observations). Interestingly, Hemogen was identified in the Heterochromatin protein 1 α (HP1 α) – Chromatin-assembly factor 1 (CAF-1) complex along with Trim28/TIF-1beta/KAP-1 (Loyola, *et al* 2009). HP1 is a non histone protein which has multiple functions in sister chromatid cohesion, chromatin remodelling, gene transcription, DNA replication and repair (Ball and Yokomori 2009). HP1 protein isoforms are recruited to several types of DNA damage and their inactivation results in UV light and ionizing radiation hypersensitivity (Luijsterburg, *et al* 2009). Also, HP1 is phosphorylated on threonine 51, an event which is required for its release from chromatin and normal H2AX phosphorylation on serine 139, although HP1 is then recruited to the sites of DNA damage in a slow process independent of threonine 51 phosphorylation (Ayoub, *et al* 2008, Ayoub, *et al* 2009, Luijsterburg, *et al* 2009). Interestingly, Trim28 works downstream of ATM and 53BP1 in heterochromatin DNA double strand break repair (Goodarzi, *et al* 2008, Goodarzi, *et al* 2009, Noon, *et al* 2010). These observations would suggest that Hemogen might take part in some of HP1 functions, possibly in association with Trim28. Here, combining the results of iTRAQTM peptide labelling, AQUATM methodology and western blot analysis, Hemogen was found phosphorylated on serine 380 following etoposide exposure exclusively with BCR/ABL PTK expression, while its protein expression was increased with BCR/ABL PTK, but not etoposide. Correlation between this phosphorylation event and survival advantage will be a subject of further work. Importantly, this phosphosite is conserved in humans within a region of relatively high sequence variability. Murine Hemogen serine 380 (EFTVPIVSSQKTIQESP) would correspond to human serine 339 (EIIVPKAPSHKTIQETP). Although no motif for these sites were identified using Scansite Motif, PhosphoMotif Finder found kinases such as Chk1, PKA, PKC, DNA PKcs, Casein Kinase I, MAPKAPK2 and ATM kinase in mouse or human. Interestingly, PKC has been shown to mediate Hemogen downregulation during TPA-induced megakaryocytic differentiation of K562 cells (Liu, *et al* 2004).

The modulation of Histone H1 on threonine 4 is another example of how BCR/ABL PTK could sustain stress signalling *via* a particular phosphosite. Histone H1 is the linker

Histone as its binding to nucleosomes enables DNA compaction required to reach higher structures of the chromatin fiber during cell cycling. How the modulation of Histone H1 phosphorylation dynamics could affect its biological functions and how it could cause disease progression remains to be answered. The regulation of Histone H1 phosphosites by etoposide would suggest that DNA DSBs could lead to a change in chromatin conformation to create a platform so that DNA repair proteins could access the site of damage. Opening chromatin could also result in a change in transcriptional regulation so that DNA repair proteins and stress proteins could be expressed along with cell cycle arrest. The modulation of Histone H1 phosphorylation on threonine 4 (H1A/D/E), serine/threonine 18 (H1B/D/E), threonine 135 (H1B) and serines 183/186/187 (H1A/B/E) by BCR/ABL PTK suggests that the oncogene could interfere with the downstream response to etoposide. It has been demonstrated that all histone H1 variants are released from the chromatin and translocate to the cytoplasm in a p53 dependent manner after ionizing radiation but that only H1.2 (H1C) is required for cytochrome c release from mitochondria (Konishi, *et al* 2003). Indeed, such dynamics could be seen in a proteomics study using etoposide (50 μ M) for 1h (Boisvert, *et al* 2010). However, hyperphosphorylation of threonine 4 would suggest that no such translocation was observed under these conditions (nuclear preparations), although the translocation of specific phosphorylated forms could be differentially modulated. Nevertheless it remains the case that linker histones are important in DNA DSB repair for the regulation of chromatin condensation (Downs 2007).

Among the proteins found regulated by etoposide, 53BP1 is a key player in the determination of NHEJ (Xie, *et al* 2007) and was phosphorylated on threonine 906 and dephosphorylated on serines 546 and 549. 53BP1 works in concert with MDC1 which was regulated by etoposide on serine 929 similarly in control and BCR/ABL PTK-expressing cells. Phosphorylation of MDC1 on serine 595 was increased in the presence of the oncogene before and after the response of this phosphosite to etoposide. This BCR/ABL PTK-dependent effect, but not the etoposide response described here, was also identified in another study using BCR/ABL and FLT3/ITD PTK-expressing Ba/F3 cells (Pierce, *et al* unpublished observations). Also, MDC1 was phosphorylated on serine 1053 by etoposide

only in the presence of BCR/ABL PTK. This potential phosphosite is found at the beginning of MDC1 PST domain which has been shown to be involved in the regulation of both NHEJ and HR (Jungmichel and Stucki 2010). MDC1 and 53BP1 can bind to H2AX, although 53BP1 binding to H2AX may be not required for NHEJ (Xie, *et al* 2007). H2AX hyperphosphorylation by leukaemogenic PTKs on serine 139 was related here to less H2AX phosphorylation on tyrosine 142 in the presence of BCR/ABL PTK. This configuration has been shown to enhance the binding of MDC1 (Cook, *et al* 2009), which in turn is pivotal for the amplification of H2AX phosphorylation on serine 139 and the recruitment of DNA repair proteins in HR and cell survival (Cook, *et al* 2009, Xie, *et al* 2007). The modulation of MDC1 phosphosites by BCR/ABL PTK might affect its recruitment, H2AX post-translational modifications or DNA repair. BCR/ABL PTK has been shown to increase the rate of homologous recombination and alternative NHEJ through overexpression of Rad51, WRN and ligase III (Nowicki, *et al* 2004, Sallmyr, *et al* 2008c, Slupianek, *et al* 2002, Slupianek, *et al* 2011b, Slupianek, *et al* 2001) to promote unfaithful DNA repair. Conversely, MDC1 abnormal phosphorylation could be a consequence of unfaithful H2AX histone code to promote further DNA repair/cell survival. Moreover, a recent report demonstrates the role of H2AX as a tumour suppressor to avoid CML progression to blast crisis in transgenic mice (Nagamachi, *et al* 2009). To show this role, the investigators crossed p210^{BCR/ABL} transgenic mice in CML chronic phase with heterozygous H2AX^{+/-} mice. The progeny developed CML blast crisis and this outcome was concomitant with the loss of the other H2AX allele expression. These observations would suggest that post-translational modifications of this particular histone may also be relevant for leukaemia progression. Here, H2AX tyrosine 142 downregulation could be the result of increased DNA damage, although it may also promote cell survival in the presence of BCR/ABL PTK (Cook, *et al* 2009). The regulation of H2AX at tyrosine 142 could be due to modulation of the kinase Baz1b/WSTF or EYA1/3 phosphatase (Jungmichel and Stucki 2010). However, no modulation could be identified on the single Baz1b/WSTF phosphoentity identified in this study (Figure 3.38). Interestingly Baz1b/WSTF has been found deleted in Williams-Beuren syndrome, a rare neurodevelopmental disorder, so has Bcl7c which was found regulated on serine 126 by etoposide only in the presence of

BCR/ABL PTK. It has been proposed that Bcl7c may have anti-apoptotic role in chronic lymphocytic leukaemia (CLL) (Jadayel, *et al* 1998, McCarthy, *et al* 2004, Peoples, *et al* 1998). Baz1b/WSTF is part of the B-WICH complex, a chromatin remodelling complex considered to play a major role in DNA replication, but also in DNA repair (Oya, *et al* 2009, Poot, *et al* 2005, Xiao, *et al* 2009, Yoshimura, *et al* 2009), although Baz1b/WSTF activity itself promote apoptosis when damage is too high. Two other proteins from this complex, Mybbp1a and DDX21, were identified in this study. Mybbp1a serine 6 and DDX21 serine 181 were dephosphorylated following etoposide exposure and these regulations demonstrated that several members of the B-WICH complex are involved in the DNA damage response. Also, the responses of Mybbp1a threonine 1162, threonine 1277 and serine 1280 to etoposide may be changed with the expression of BCR/ABL PTK. Interestingly, Mybbp1a has been shown to repress the anti-apoptotic NF- κ B transcription factor (Owen, *et al* 2007), which is known to be modulated in many cancers and by multiple leukaemogenic PTKs to promote both chemotherapy and radiotherapy resistance (Baud and Karin 2009). Mybbp1a is a substrate for Aurora B kinase, a mitotic kinase (see above) which has been linked to tumorigenesis when its activity is misregulated (Perrera, *et al* 2010). Thus it would be interesting to see if the modulation seen on Mybbp1a phosphoresidues by BCR/ABL PTK would affect its repressing role on NF- κ B and also if Hemogen pS380 can activate it. Thus, NF- κ B activation and H2AX dephosphorylation on tyrosine 142 observed in BCR/ABL PTK-expressing cells would suggest that the B-WICH complex could be inactivated by BCR/ABL PTK. Moreover, a recent study identified that the B-WICH complex member Myo1c interacts with the BCR/ABL "core complex" *via* Shc1 (Brehme, *et al* 2009).

BCR/ABL PTK alone affected the phosphorylation status of several proteins. Some proteins were found dephosphorylated such as the proto-oncogenes Myc and Jun on serine 164 and serine 73 respectively or the negative regulator of cell survival/cell proliferation Inpp5d (Shp-1) on serine 935. Interestingly, Myc has been recently shown to induce aberrant DNA synthesis and may be linked to blast crisis progression in CML (Albajar, *et al* 2011). Also the protein Ncf2, which is required for the activation of NADPH oxidase and superoxide production was found dephosphorylated on serine 332 in the

presence of the oncogene. Conversely, the DNA ligase 1 Lig1 was phosphorylated on serine 199 in BCR/ABL-expressing cells where its role in mediating ligation of DNA double strand breaks during DNA replication, recombination and repair may be impaired. Also, its response to etoposide only in the presence of BCR/ABL PTK on serine 67 could affect its role in maintaining genome stability possibly through the alternative NHEJ pathway (Bentley, *et al* 2002, Gao, *et al* 2011, Simsek, *et al* 2011, Subramanian, *et al* 2005, Waterworth, *et al* 2009).

In conclusion, this study identified several phosphorylation sites that BCR/ABL PTK could modulate with respect to their response to DNA damage induced by etoposide. BCR/ABL PTK could sustain genotoxic stress signalling on several proteins and compromise the response of DNA repair proteins. MDC1, H2AX, Hemogen and members of the B-WICH complex could be the targets of BCR/ABL PTK (Figure 3.40) for the promotion of cell survival along with other proteins (e.g. NF- κ B) as well as DNA misrepair leading to genomic instability. Further study of the role of these modifications on genomic stability, DNA repair mechanisms and cell survival should be carried out to unravel the relevance of these crosstalks in leukaemia progression and chemotherapy resistance.

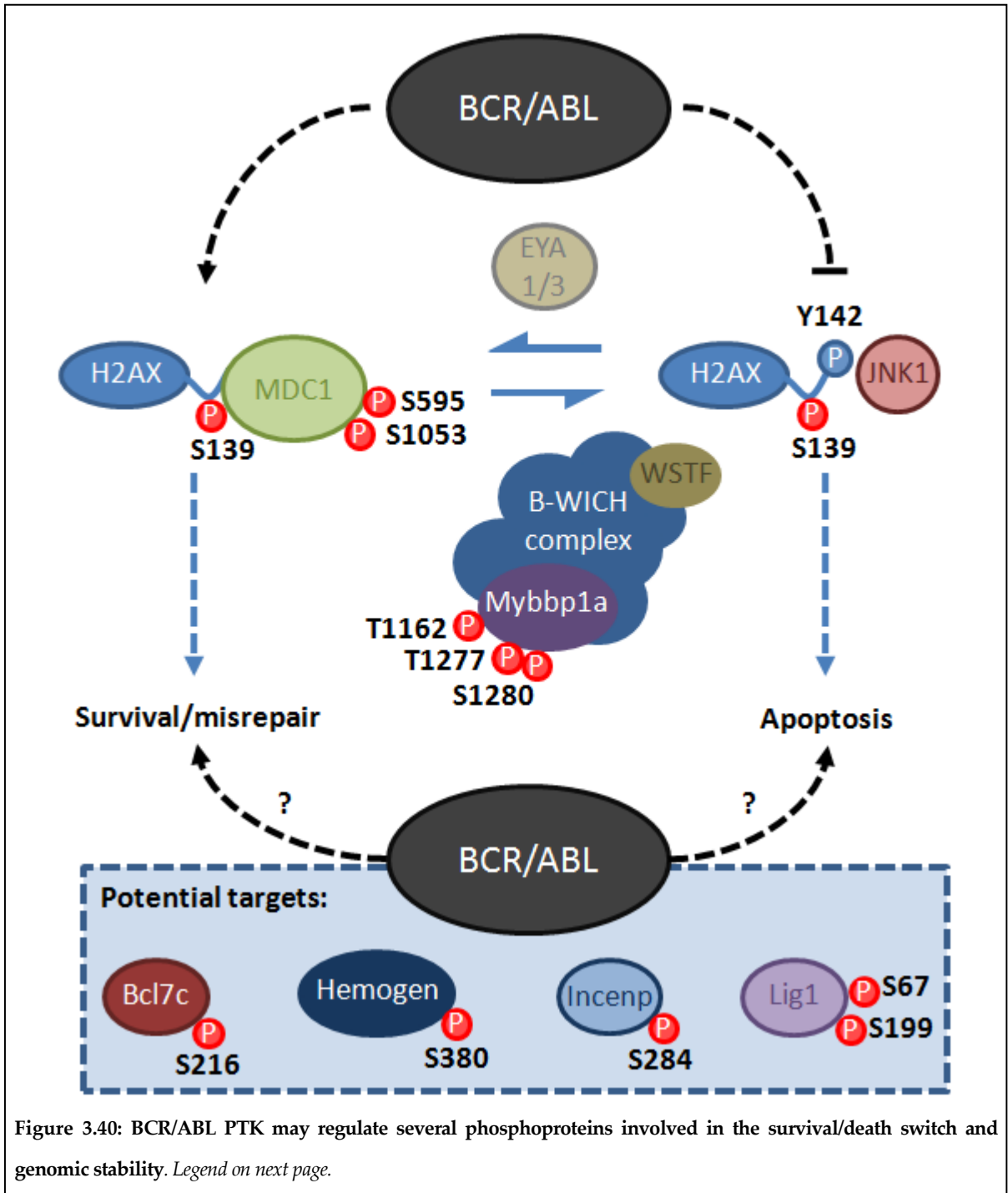


Figure 3.40: BCR/ABL PTK may regulate several phosphoproteins involved in the survival/death switch and genomic stability. Legend on next page.

Figure 3.40: BCR/ABL PTK may regulate several phosphoproteins involved in the survival/death switch and genomic stability (Figure on previous page). The phosphorylation of H2AX on serine 139 coupled with reduced phosphorylation on tyrosine 142 promoted by BCR/ABL PTK is linked to increased survival and DNA repair by recruitment of MDC1 to the site of DNA damage (Cook, *et al* 2009). H2AX tyrosine dephosphorylation is mediated by EYA1/3 phosphatase. Changes in H2AX post-translational modifications were associated with the modulation of several MDC1 and Mybbp1a phosphoresidues. Mybbp1a is part of the B-WICH complex, whose member Baz1b/WSTF is the kinase of H2AX tyrosine 142. BCR/ABL PTK may further orientate cell fate towards survival and unfaithful DNA repair after DNA damage by the modulation of specific proteins. Among the phosphoproteins found modulated by both BCR/ABL PTK expression and etoposide, Bcl7c and Hemogen have been shown to promote anti-apoptotic signalling. In contrast with Hemogen which can activate NF- κ B (not shown) to induce cell survival, Mybbp1a has been shown to repress NF- κ B. Thus NF- κ B activation and H2AX tyrosine 142 dephosphorylation observed in the presence of BCR/ABL PTK suggest that the B-WICH complex function is impaired with the oncogene. Hemogen might also play a role in heterochromatin DNA repair. Incenp is involved in sister chromatid cohesion, a process required for DNA double strand break repair by homologous recombination, while DNA ligation during homologous recombination might be impaired by the modulation of DNA ligase 1 by BCR/ABL PTK expression.

Chapter 4.

A signalling pathway from receptor activation and oxidative stress to THO complex phosphorylation potentiated by leukaemogenic protein tyrosine kinases and stem cell homing chemokines

4.1. Introduction

Thoc5/Fms interacting protein (FMIP) is a member of the THO complex along with Hpr1/Thoc1, Thoc2, Thoc6 and Thoc7. N-terminal region of Thoc5/Fmip is required for the binding and the nuclear localization of Thoc7 while the C-terminal region contains a putative leucine zipper like domain which weakly binds Thoc1 (El Bounkari, *et al* 2009, Guria, *et al* 2011). THO complex is a part of the TREX (Transcription/export) complex with the components Thoc3, Thoc4/Aly/REF1 and Uap56. TREX has been conserved from yeast to human and has been shown to be required for coupled transcription elongation and nuclear export of mRNAs. In *Drosophila melanogaster*, depletion of Thoc1 and Thoc2 affects 20 % of gene expression but reduces protein synthesis by approximately 50%. However there is an increase seen in DNA repair gene expression, including Ku80 and Mre11 which are particularly important in the regulation of NHEJ (Rehwinkel, *et al* 2004). Mutants of Thoc1 and Thoc2 show defects in nucleotide excision repair pathway in yeast (Gonzalez-Barrera, *et al* 2002) and THO mutants in general show a hyper-recombination phenotype linked to increased genetic instability (Jimeno, *et al* 2002, Luna, *et al* 2005). Also, THO mutants have been shown to stimulate the activity of activation-induced cytidine deaminase (AID) which generates DNA double strand breaks, genomic instability and drug resistance in the progression of CML to blast crisis (Feldhahn, *et al* 2007, Gomez-Gonzalez and Aguilera 2007, Gruber, *et al* 2010, Klemm, *et al* 2009, Ruiz, *et al* 2011).

Recent evidence suggests a relationship between the THO complex and the response to adverse changes in the cellular environment. THO complex components are not essential for bulk poly(A) RNA export in higher eukaryotes, but for the nuclear export of a subset of mRNAs. The THO complex is associated with the messenger ribonucleoparticle (mRNP) and nascent RNA and the (nuclear) exported RNA. Mutations in the THO complex can lead to decreased polyadenylation of RNAs and their enhanced rate of degradation, possibly associated with 3' end processing of RNA. A non-functional THO complex also adversely affects transcription elongation and mRNA export in lower eukaryotes (Aguilera 2005). Heat shock leads to the accumulation of nuclear poly(A) mRNA in the absence of THO complex in higher eukaryotes, although the majority of mRNA species produced are unaffected. Heat shock protein 70 (Hsp70) is one gene product that can be regulated by THO complex, specifically by Thoc5/Fmip which can bind Hsp70 mRNP particularly under heat shock and associates with the Tap/NXF1-p15/NXT1 poly(A) mRNA nuclear export system (Guria, *et al* 2011, Katahira, *et al* 2009, Rehwinkel, *et al* 2004). Hsp70 has a role in haemopoiesis, in resistance to imatinib and etoposide as well as CML disease progression (Guo, *et al* 2005b, Pocaly, *et al* 2007, Ribeil, *et al* 2007, Yeh, *et al* 2009). Moreover, Hsp72 gene knock out shows reduced H2AX phosphorylation on serine 139 (Gabai, *et al* 2010) which strongly links heat shock proteins to genotoxic stress and genetic stability.

Thoc5/Fmip is one of the THO complex proteins only expressed in mammals and *Drosophila melanogaster*, Thoc5/Fmip has been implicated in regulation of differentiation and development via modulation of transcription factor C/EBP α , a gene often mutated in human leukaemias and suppressed in CML blast crisis (Carney, *et al* 2009, Mancini, *et al* 2007, Melo and Barnes 2007, Somerville and Cleary 2009). This protein regulates adipocyte and neutrophil/macrophage development and modulates the level of PIP3 second messengers related to leukaemia transformation (Carney, *et al* 2009, Cully, *et al* 2006, Mancini, *et al* 2007, Mancini, *et al* 2004, Pierce, *et al* 2008a, Tamura, *et al* 1999). Indeed Thoc5/Fmip was originally named FMIP and identified as a substrate and binding partner of the macrophage colony-stimulating factor (M-CSF) receptor (Tamura, *et al* 1999).

Thoc5/Fmip is a 75 kDa phosphoprotein found both in the nucleus and cytoplasm and is phosphorylated on tyrosine by the M-CSF receptor tyrosine kinase. Its ectopic expression matures NFS60 myeloid cells similarly as M-CSF addition (Carney, *et al* 2009). It is also phosphorylated on tyrosine 225 as a consequence of leukaemogenic PTK action (Pierce, *et al* 2008a). Thoc5/Fmip expression modulation can also potentiate monocytic development (Mancini, *et al* 2004). Thoc5/Fmip gene knockouts are embryonic lethal in the mouse and it has been shown that inducible gene knockouts die from rapid hematopoietic failure due to primitive hematopoietic cell depletion (Mancini, *et al* 2010). This collapse is far swifter than observed with ATM null mice where self-renewal is compromised (Ito, *et al* 2004) and evidence from marrow samples suggests the decay in the primitive cell population on Thoc5/Fmip depletion is due to a requirement for this protein to suppress apoptosis (Mancini, *et al* 2010). Interestingly, depletion of its interactor Thoc1 has also been related to apoptosis, but only in transformed cells, in association with increased DNA damage. Remarkably, human cancer cells express more Thoc1 and cells depleted of Thoc1 are resistant to transformation by RAS and MYC, both suggesting that Thoc1 is required for oncogenic transformation (Li, *et al* 2007b). The functional role of Thoc5/Fmip gene knock down was investigated using mouse embryo fibroblast cell line (MEFs) (Guria, *et al* 2011). This study demonstrated that Thoc5/Fmip is required for the export of 2.9 % of all mRNAs, 45% of which are involved in cell differentiation and one fifth being crucial for haemopoiesis. Thus in hematopoietic terms Thoc5/Fmip is a protein implicated in stem cell survival, which is a target for downstream action of cytokine tyrosine kinase receptors and leukaemogenic PTKs (BCR/ABL, TEL/PDGFR β , NPM/ALK, KIT D816V), inferring its action on hematopoietic stem cell transcription factors is usurped or bypassed in leukaemias (Carney, *et al* 2009, Ribeil, *et al* 2007). Thoc5/Fmip has also been listed as a potential downstream target of ATM/ATR kinases on serine 307 following ionizing radiation (Matsuoka, *et al* 2007).

How these effects are achieved is not clear. Subcellular localization of Thoc5/Fmip has been shown to be in a dynamic equilibrium with the protein shuttling between the cytosol and nucleus (Mancini, *et al* 2004). This raises the possibility that Thoc5/Fmip protein could

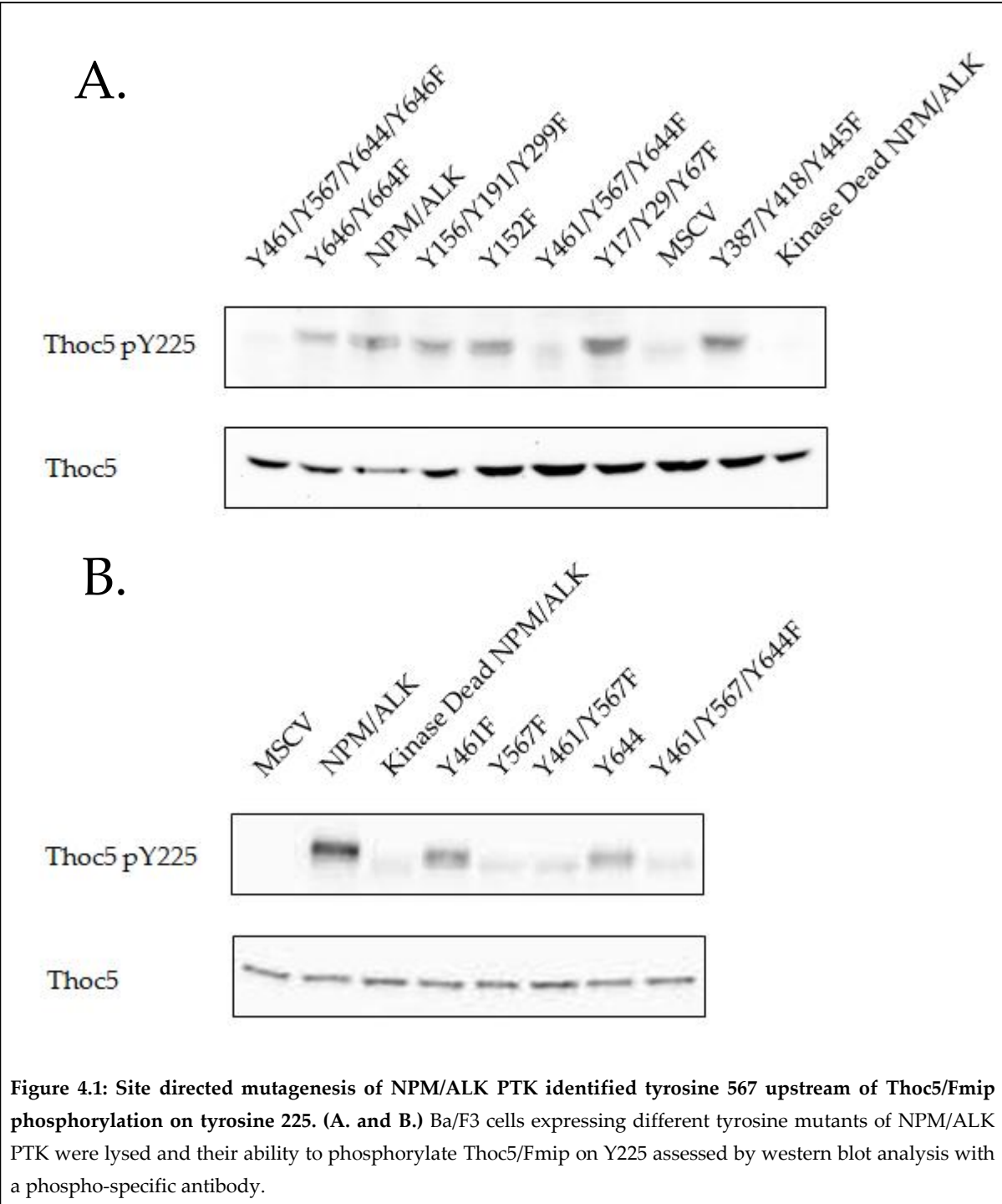
be critical in conveying survival/development signals, such as from the M-CSF receptor, to the spliceosome/mRNA export complex. As Thoc5/Fmip protein phosphorylation on tyrosine 225 by M-CSF receptor action likely occurs at the plasma membrane we have investigated potential pathways for Thoc5/Fmip phosphorylation, regarding its modulation by leukaemogenic PTKs, and thereby determination of its biological role. We demonstrated that the proto-oncogene Src signalling associated with cellular stress is responsible for Thoc5/Fmip phosphorylation on tyrosine 225.

4.2. Results

4.2.1. Structure/function analysis on NPM/ALK reveals the key residues for activation of Thoc5/Fmip tyrosine phosphorylation

It has been recently demonstrated that Thoc5/Fmip is a downstream target of the leukaemogenic PTKs BCR/ABL, KIT D816V, TEL/PDGFR β and NPM/ALK (Pierce, *et al* 2008a). To discover the potential biological pathways upstream from Thoc5/Fmip phosphorylation on tyrosine 225, site directed mutagenesis was performed on NPM/ALK PTK by Dr. Andrew Pierce and these NPM/ALK PTK mutants were expressed in Ba/F3 cells. NPM/ALK kinase dead demonstrated that the PTK activity of NPM/ALK is required for the increase in Thoc5/Fmip phosphorylation on tyrosine 225 (Figure 4.1).

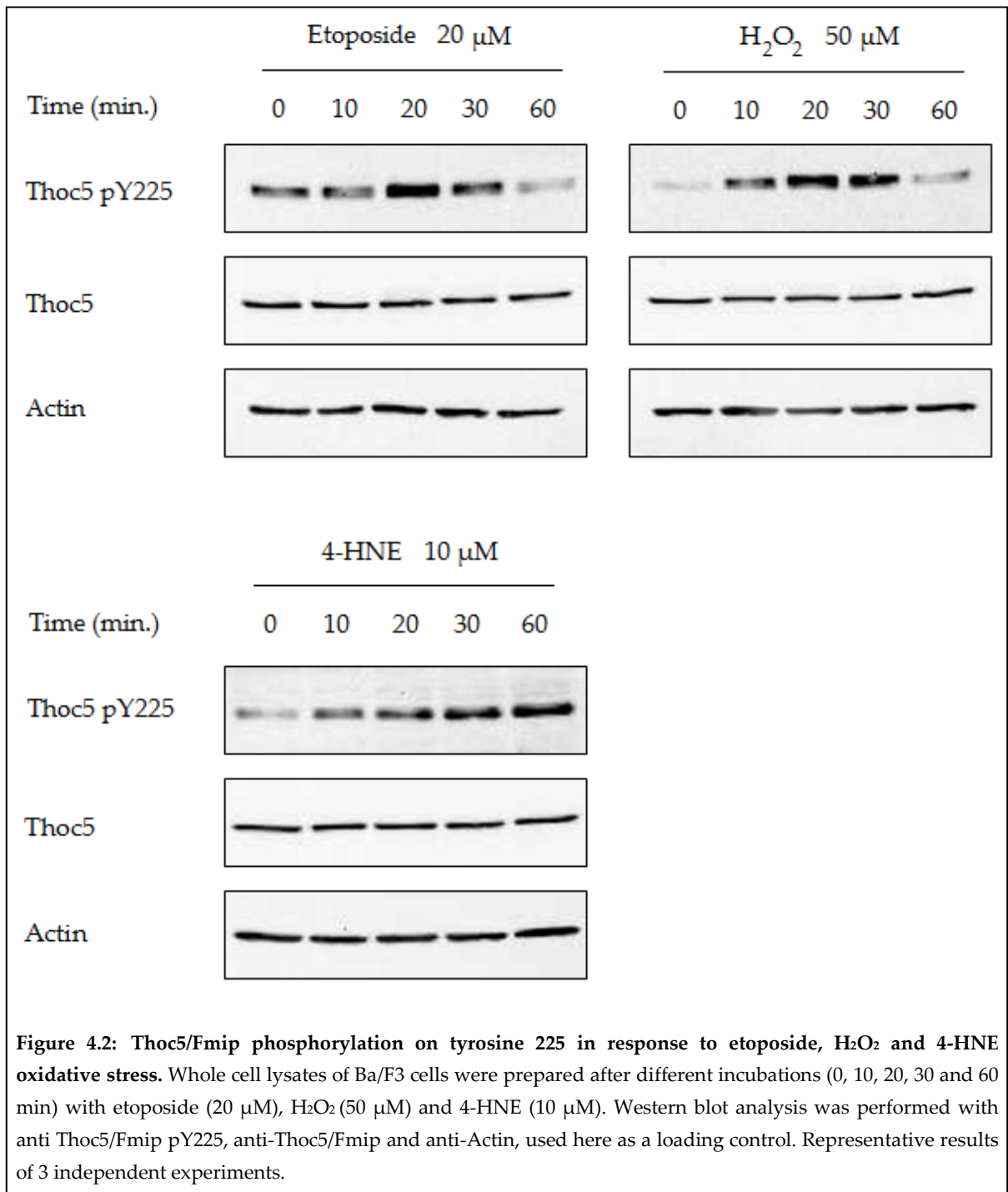
Initial analysis of point mutated NPM/ALK identified Y461F, Y567F, Y644F triple mutant as unable to promote Thoc5/Fmip phosphorylation on tyrosine 225 (Figure 4.1-A). Single mutation analysis then identified Y567F mutant as being deficient in this respect (Figure 4.1-B). NPM/ALK tyrosine 567 phospho-residue is known to bind Shc1 (Bai, *et al* 1998). All 3 isoforms of the Shc1 family are phosphorylated by PTKs including p66 Shc, and work as adaptor protein in response to growth factors/external stimuli from the cell membrane. This particular isoform can enhance reactive oxygen production by mitochondria and is implicated in oxidative stress-induced apoptosis in concert with p53. Its mutation is also linked to increased lifespan (Migliaccio, *et al* 1999, Pinton, *et al* 2007, Trinei, *et al* 2002).



4.2.2. Thoc5/Fmip phosphorylation on tyrosine 225 is increased by oxidative stress

To determine if oxidative stress, along with DNA damage, could be involved in Thoc5/Fmip phosphorylation on tyrosine 225, etoposide (20 μM), H_2O_2 (50 μM) and the peroxidated lipid 4-Hydroxynonenal (4-HNE) (10 μM), were used to treat cells. Indeed etoposide phenolic group is able to capture an electron, thus becoming a phenoxy radical, and etoposide has previously been reported to promote both anti-oxidative and pro-oxidative stress responses (Haim, *et al* 1986, Kagan, *et al* 2001, Ladner, *et al* 1989, Ritov, *et al* 1995, Siitonen, *et al* 1999, Sinha, *et al* 1985, Sinha, *et al* 1983). Phosphorylation on tyrosine 225 was transient with a maximum observed approximately at 20 min for etoposide and H_2O_2 , whereas the response to 4-HNE appeared to be linear over 1h (Figure 4.2). As shown previously by Pierce and colleagues (Pierce, *et al* 2008a), the permanent phosphorylation of tyrosine 225 by leukaemogenic PTKs contrasts with the transient nature of the oxidative stress generated effect with etoposide or H_2O_2 -mediated phosphorylation (Figure 4.3).

As leukaemogenic PTKs can stimulate the production of reactive oxygen species (ROS), high level of oxidative stress (Cramer, *et al* 2008) could interfere with a fine-tune stress response. The anti-oxidant N-acetylcysteine (NAC) was used at 10 mM for 4h to determine if Thoc5/Fmip basal tyrosine phosphorylation was only due to oxidative stress. Such treatment did not substantially affect Thoc5/Fmip phosphorylation on tyrosine 225 (Figure 4.4). There was a decrease in phosphorylation when NAC was added in NPM/ALK or TEL/PDGFR β PTK-expressing Ba/F3 cells.



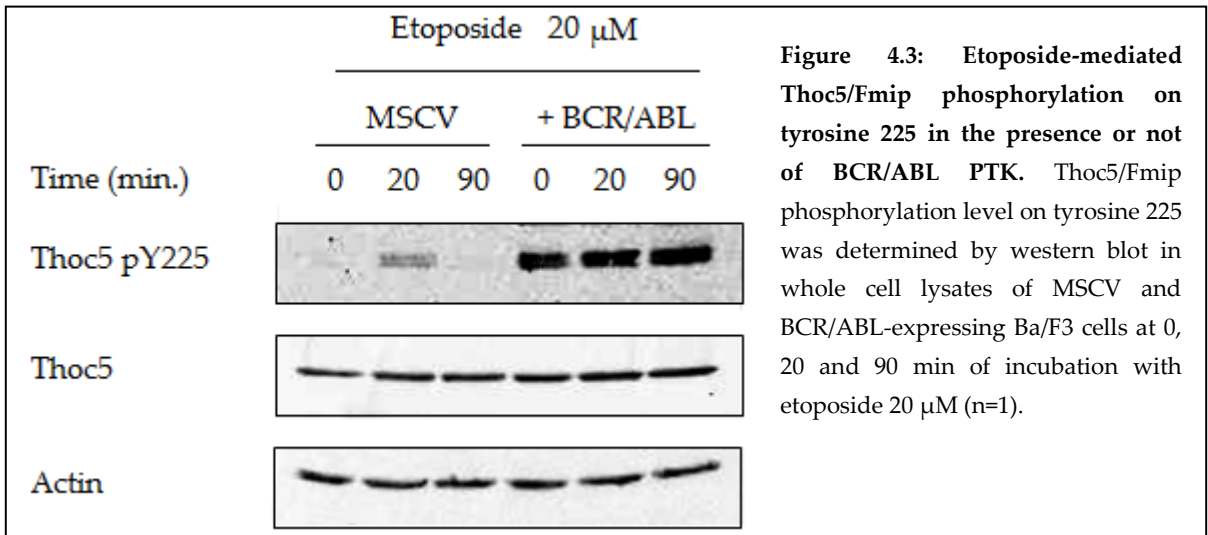


Figure 4.3: Etoposide-mediated Thoc5/Fmip phosphorylation on tyrosine 225 in the presence or not of BCR/ABL PTK. Thoc5/Fmip phosphorylation level on tyrosine 225 was determined by western blot in whole cell lysates of MSCV and BCR/ABL-expressing Ba/F3 cells at 0, 20 and 90 min of incubation with etoposide 20 μ M (n=1).

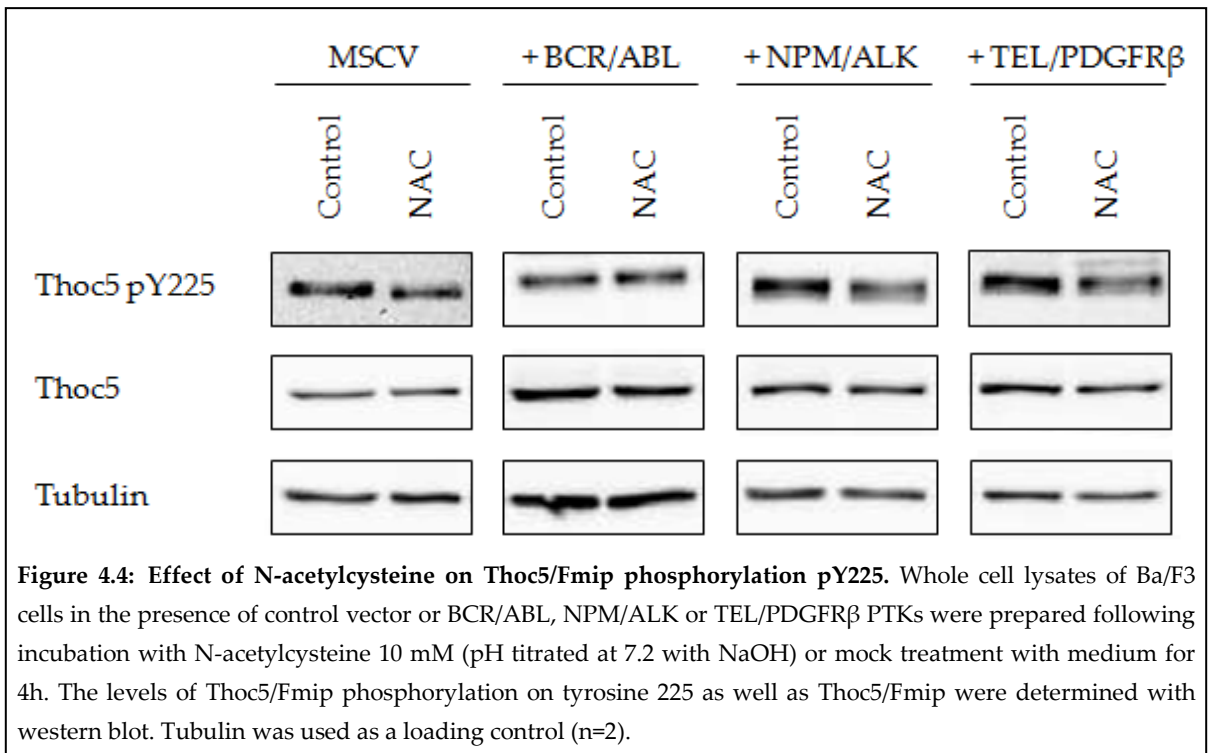


Figure 4.4: Effect of N-acetylcysteine on Thoc5/Fmip phosphorylation pY225. Whole cell lysates of Ba/F3 cells in the presence of control vector or BCR/ABL, NPM/ALK or TEL/PDGFR β PTKs were prepared following incubation with N-acetylcysteine 10 mM (pH titrated at 7.2 with NaOH) or mock treatment with medium for 4h. The levels of Thoc5/Fmip phosphorylation on tyrosine 225 as well as Thoc5/Fmip were determined with western blot. Tubulin was used as a loading control (n=2).

4.2.3. Nucleocytoplasmic distribution of Thoc5/Fmip tyrosine phosphorylation

Thoc5/Fmip is part of the THO complex that is critical for the processing and transport of RNA. Under normal conditions Thoc5/Fmip has a nucleocytoplasmic location and has been shown to shuttle between these two compartments (Mancini, *et al* 2004). Thoc5/Fmip has been shown not only to be phosphorylated as a consequence of M-CSF stimulation but indeed interact with its receptor c-fms, thus the phosphorylation of Thoc5/Fmip on tyrosine 225 could be a cytosolic event. However, Thoc5/Fmip response to etoposide might also suggest that it is a nuclear event following induction of DNA double strand breaks. Nuclear and cytosolic preparations were performed to further investigate the distribution of Thoc5/Fmip protein and phosphorylation on tyrosine 225. Western blot analysis of nuclear and cytosolic fractions showed that pY225 resides in the cytosol (Figure 4.5-A) and that mutation of this residue does not influence Thoc5/Fmip subcellular localization. The proportion of Y225F Thoc5/Fmip in the nucleus was the same as native Thoc5/Fmip (Figure 4.5-B).

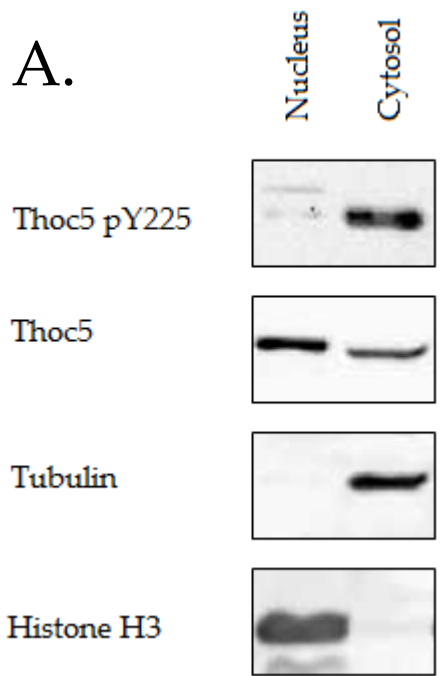
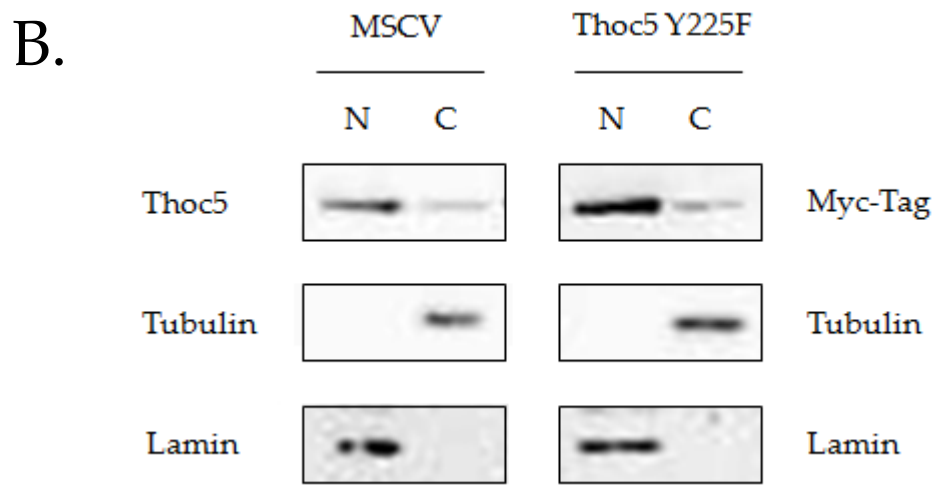


Figure 4.5: Nucleocytoplasmic distribution of Thoc5/Fmip and Thoc5/Fmip Y225F. (A.) Nuclear and cytosolic fractions of MSCV Ba/F3 cells were studied by western blot for Thoc5/Fmip protein and phosphorylation on tyrosine 225, using Tubulin and Histone H3 as cytosolic and nuclear controls, respectively. As three times more total proteins were recovered in the cytosol than the nucleus, three times more proteins were loaded for the cytosolic fraction than the nuclear fraction (n>3). **(B.)** Kind gift of Dr. Andrew Pierce. Control MSCV cells and Myc-Tagged Thoc5/Fmip Y225F mutant transfected cells were subjected to nuclear and cytoplasmic fractionation. Cellular distribution of endogenous and Myc-Tagged Thoc5/Fmip Y225F mutant was then assessed by western blot analysis with anti-Thoc5/Fmip and anti-Myc-Tag antibodies. Tubulin and Lamin were used to control the quality of the preparation.



However the cytosolic localization of Thoc5/Fmip tyrosine phosphorylation could be the result of its nuclear export following endogenous oxidative stress as well as etoposide-mediated genotoxic stress. Thoc5/Fmip has been recently shown to interact with Tap-p15 nuclear system for the export of a subset of mRNAs (Katahira, *et al* 2009), and such interactions may result in dynamic mobility of Thoc5/Fmip between the nucleus and the cytosol. Previous experiments have demonstrated that the export of overexpressed Thoc5/Fmip could be inhibited by leptomycin B (Mancini, *et al* 2004), an inhibitor of Crm1/Exportin1, a nuclear export system interacting with proteins containing a nuclear export signal (NES). It is noteworthy that a NES has been predicted in Thoc5/Fmip sequence using the NetNES 1.1 server located from leucine 622 to valine 631 with the sequence LTNQLQRLCV matching the NES motif [LIVFM]-x(2,3)-[LIVFM]-x(2,3)-[LIVFM]-x-[LIVFM] (Figure 4.6) (la Cour, *et al* 2004). These observations led to the investigation of the localization of Thoc5/Fmip phosphorylation following leptomycin B treatment (Figure 4.7).

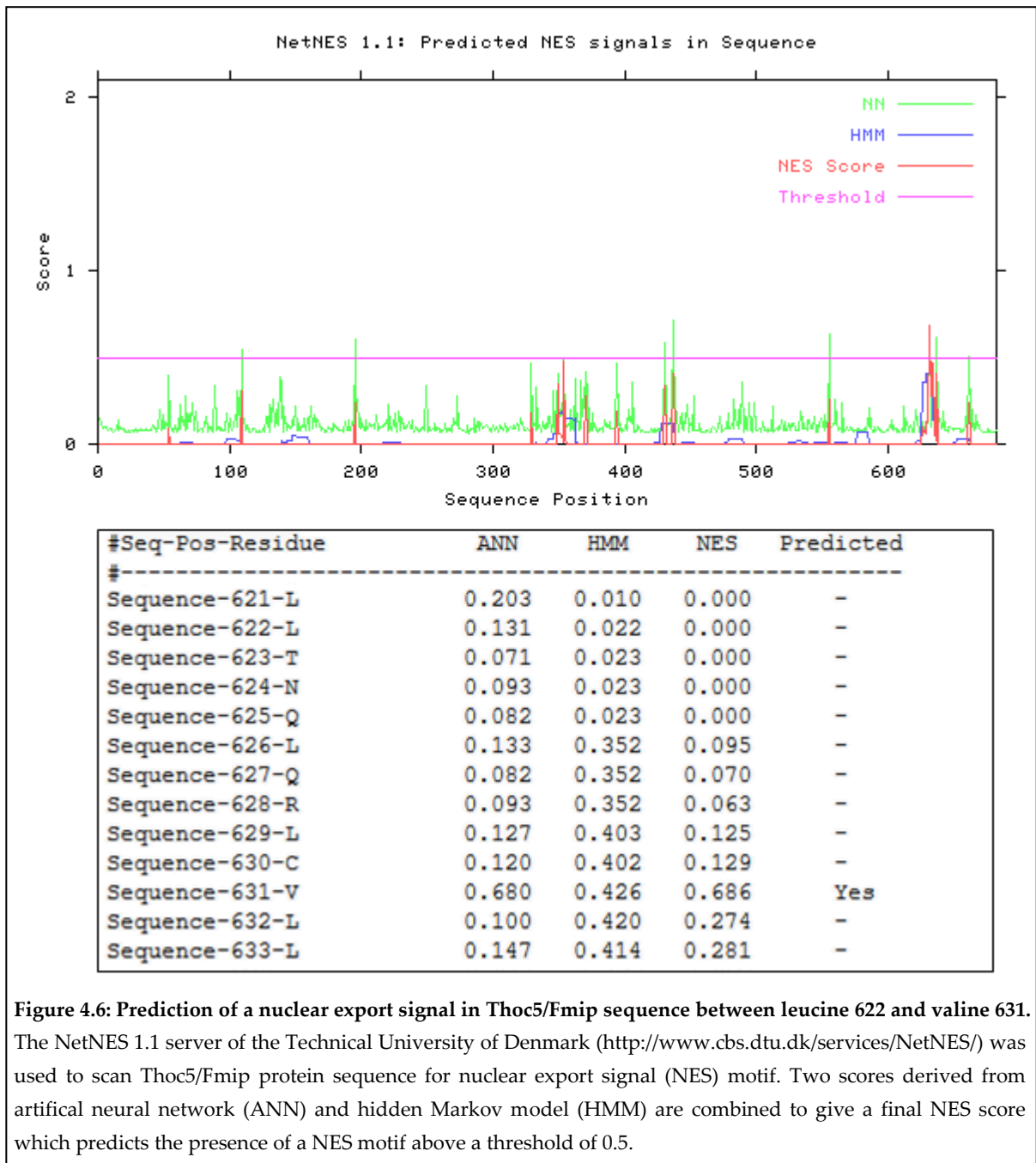


Figure 4.6: Prediction of a nuclear export signal in Thoc5/Fmip sequence between leucine 622 and valine 631. The NetNES 1.1 server of the Technical University of Denmark (<http://www.cbs.dtu.dk/services/NetNES/>) was used to scan Thoc5/Fmip protein sequence for nuclear export signal (NES) motif. Two scores derived from artificial neural network (ANN) and hidden Markov model (HMM) are combined to give a final NES score which predicts the presence of a NES motif above a threshold of 0.5.

While conditions of nuclear export inhibition were shown to prevail using the nuclear accumulation of MEK1, a NES motif-containing protein, as a control (Yao, *et al* 2001), no such event occurred in any scenario with Thoc5/Fmip. Thoc5/Fmip phosphorylation on tyrosine 225 was upregulated in the cytosol, with no concomitant accumulation in the nucleus. Unless Thoc5/Fmip export is also mediated by another activated system under stress, e.g. Tap-p15, this result would suggest that phosphorylation on tyrosine 225 is *stricto sensu* a cytosolic event.

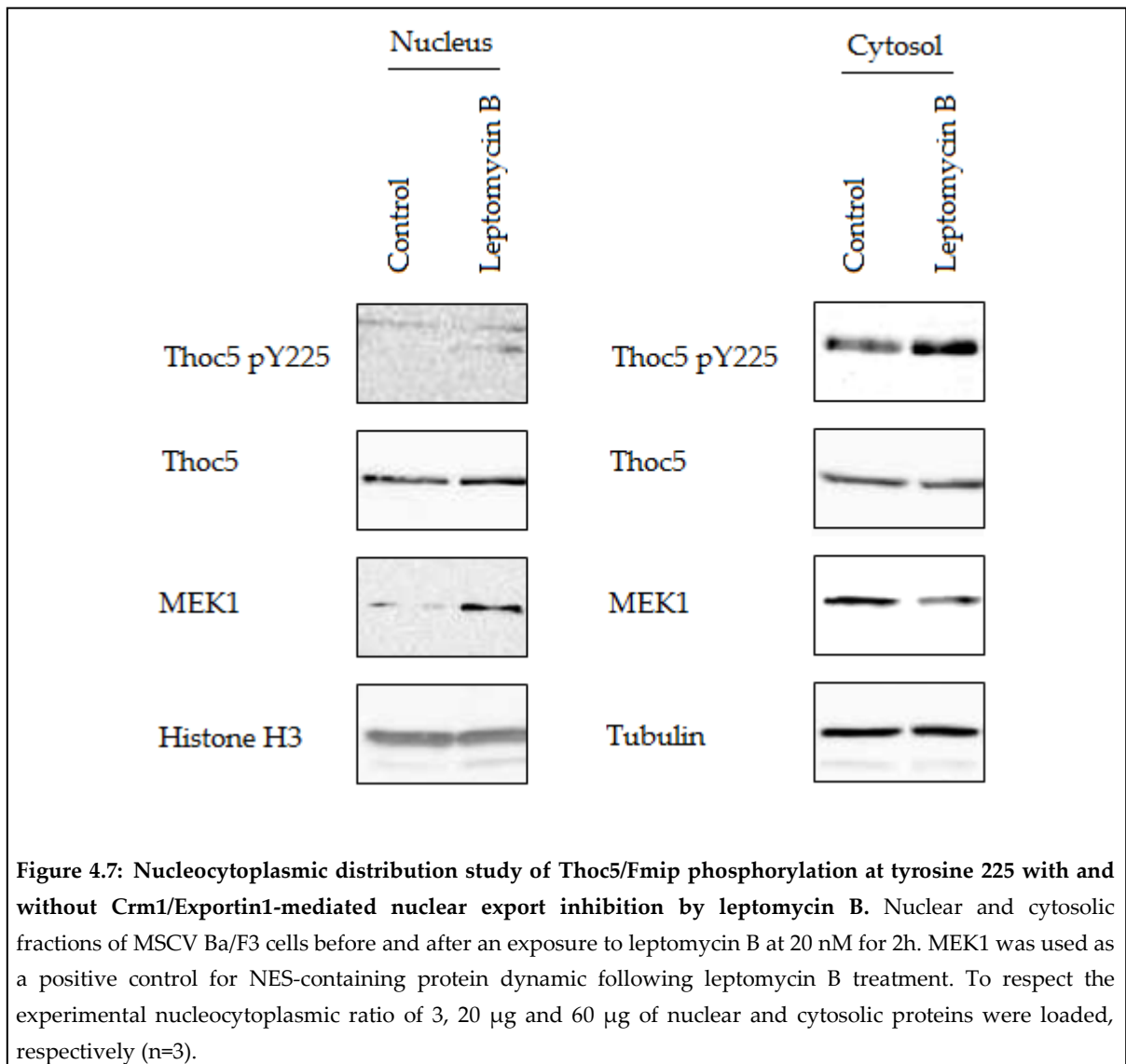


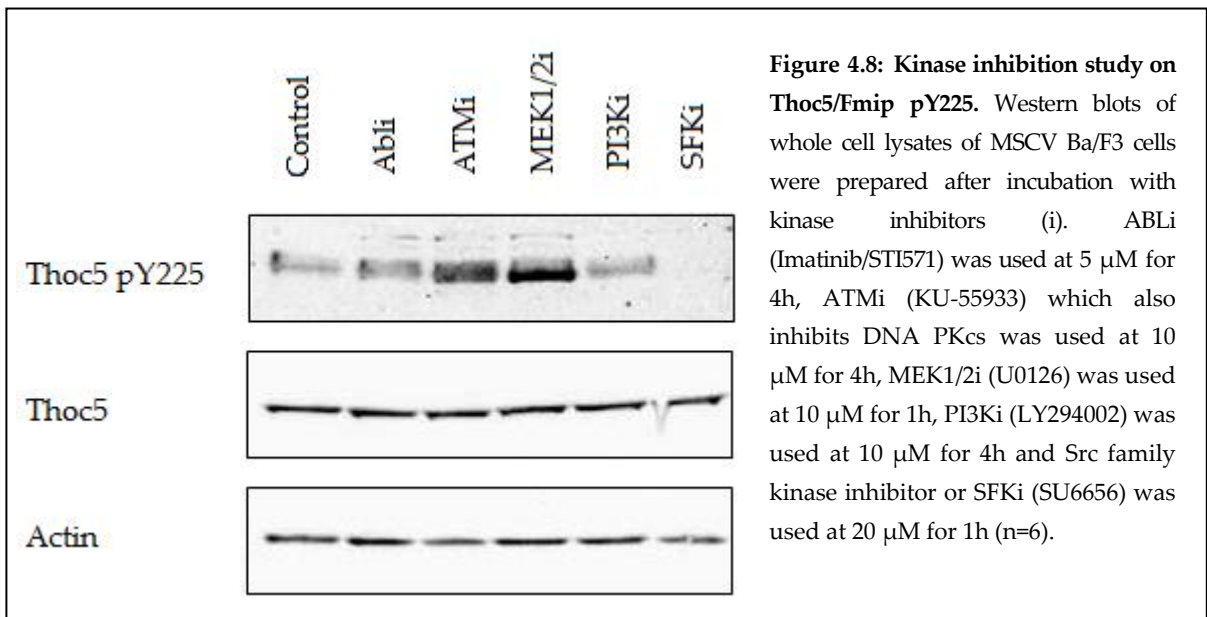
Figure 4.7: Nucleocytoplasmic distribution study of Thoc5/Fmip phosphorylation at tyrosine 225 with and without Crm1/Exportin1-mediated nuclear export inhibition by leptomycin B. Nuclear and cytosolic fractions of MSCV Ba/F3 cells before and after an exposure to leptomycin B at 20 nM for 2h. MEK1 was used as a positive control for NES-containing protein dynamic following leptomycin B treatment. To respect the experimental nucleocytoplasmic ratio of 3, 20 µg and 60 µg of nuclear and cytosolic proteins were loaded, respectively (n=3).

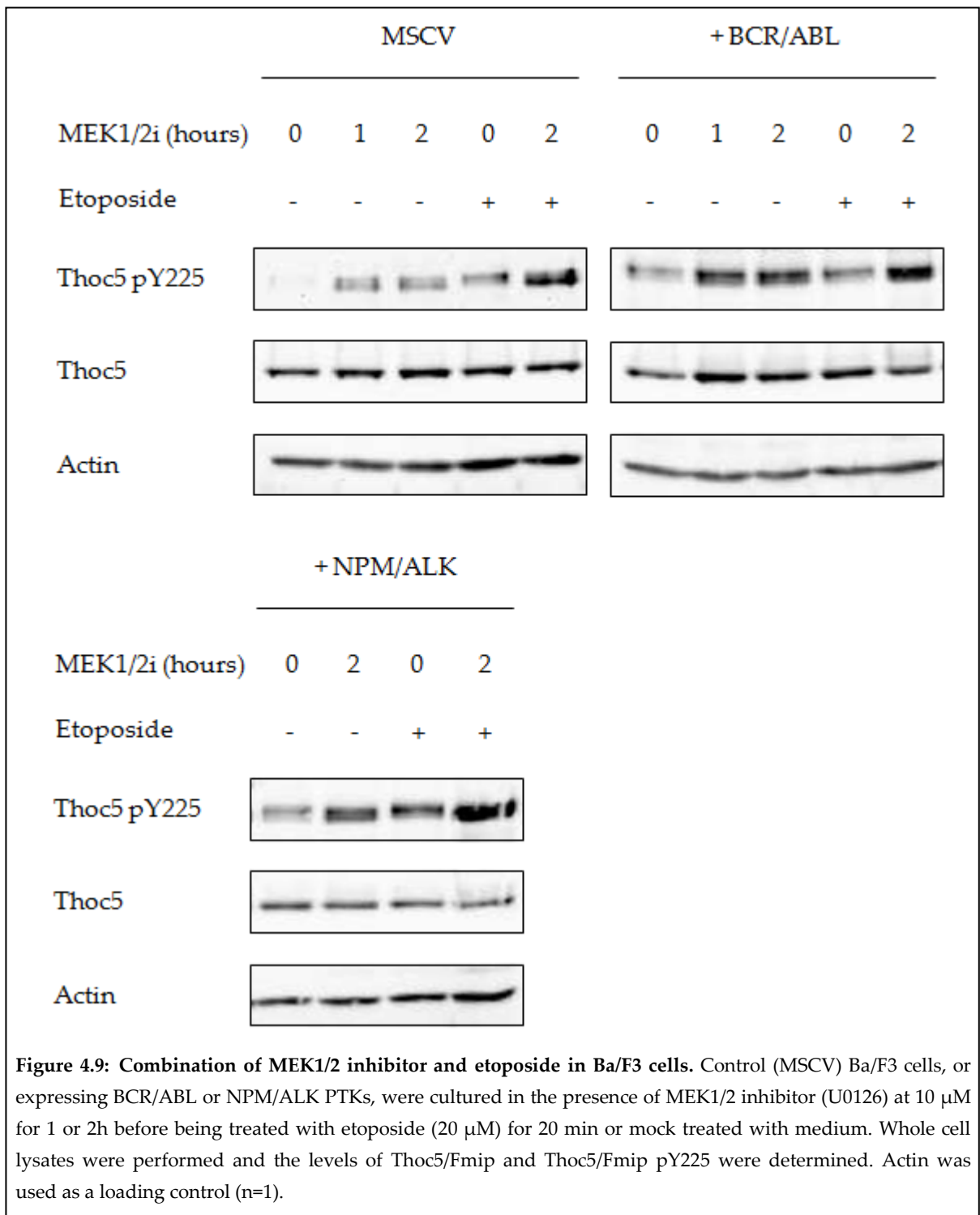
4.2.4. Thoc5/Fmip tyrosine phosphorylation relies on proto-oncogene Src

A screening of protein kinase inhibitors was performed to identify signalling pathways which could be involved in Thoc5/Fmip phosphorylation on tyrosine 225. Multiple pathways related to stress were targeted using inhibitors of ABL, ATM, PI3K, MEK1/2 and Src family kinases (SFKs). While ABL and PI3K inhibitors did not have any impact on tyrosine 225 phosphorylation in control MSCV Ba/F3 cells under these experimental conditions, MEK1/2, ATM and SFKs inhibitors did (Figure 4.8). Thoc5/Fmip phosphorylation on tyrosine 225 was strongly dependent on the Src Family as SU6656 inhibitor abolished pY225 phosphorylation. SFKs are known to be activated by oxidative

stress and some of them have been shown to be involved in BCR/ABL PTK transforming activity and other leukaemogenic PTKs signalling (Dittmann, *et al* 2009, Donato, *et al* 2003, Meyn, *et al* 2006, Rosado, *et al* 2004, Rubbi, *et al* 2011).

Conversely, a substantial increase in Thoc5/Fmip phosphorylation was obtained with the inhibition of MEK1/2 and ATM, both serine/threonine kinases. These increases were also detected in the presence of leukaemogenic PTKs, although only the inhibition of MEK1/2 let etoposide to further increase Thoc5/Fmip tyrosine phosphorylation (Figures 4.9 and 4.10). This ATM kinase-dependent reduction in tyrosine 225 phosphorylation might be the result of ATM ability in controlling the level of oxidative stress (Ito, *et al* 2004). Interestingly, imatinib (ABLi) reduced the etoposide-mediated phosphorylation on tyrosine 225 in control and BCR/ABL PTK-expressing Ba/F3 cells (Figure 4.10).





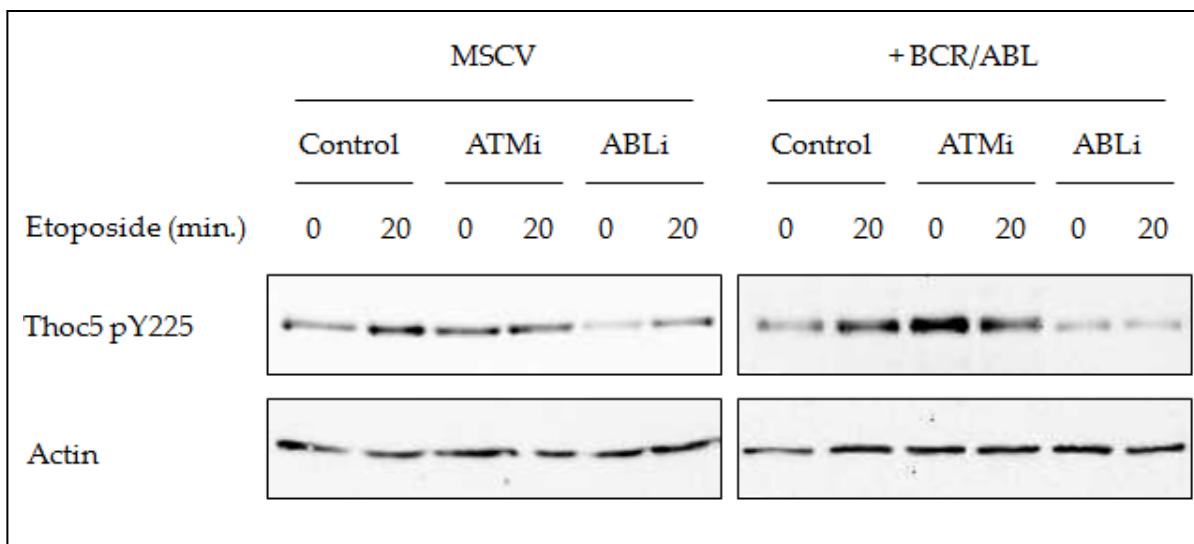


Figure 4.10: Combination of ATM or ABL inhibitors with etoposide in Ba/F3 cells. Control (MSCV) Ba/F3 cells, or expressing BCR/ABL PTK, were cultured in the presence of ATM inhibitor (KU-55933) at 10 μ M for 2h or ABL inhibitor (STI-571) at 5 μ M for 4h before being treated with etoposide (20 μ M) for 20 min or mock treated with medium. Whole cell lysates were performed and the level of Thoc5/Fmip pY225 was determined. Actin was used as a loading control (n=1).

Further investigation of SFK and MEK1/2 kinase inhibition was then performed in combination with different genotoxic stresses such as etoposide, H₂O₂ and 4-HNE. As previously shown MEK1/2 inhibition increased Thoc5/Fmip phosphorylation both before and after etoposide exposure, while SFK inhibition reduced the basal phosphorylation and abolished the genotoxic stress signalling induced by all three molecules tested (Figure 4.11). It would suggest that SFKs may be upstream of Thoc5/Fmip pY225 and are activated upon genotoxic stresses while MEK1/2 activity maintenance may reduce genotoxic stress signalling on tyrosine 225, like ATM.

Finally, SFK inhibition was studied under the same conditions with the presence of three oncogenic protein tyrosine kinases, BCR/ABL, NPM/ALK and TEL/PDGFR β PTKs. Similarly, SU6656 inhibitor reduced the amount of Thoc5/Fmip phosphorylation on tyrosine 225 (Figure 4.12). Therefore, it shows that leukaemogenic PTK downstream signalling activates SFKs which mediate Thoc5/Fmip tyrosine phosphorylation.

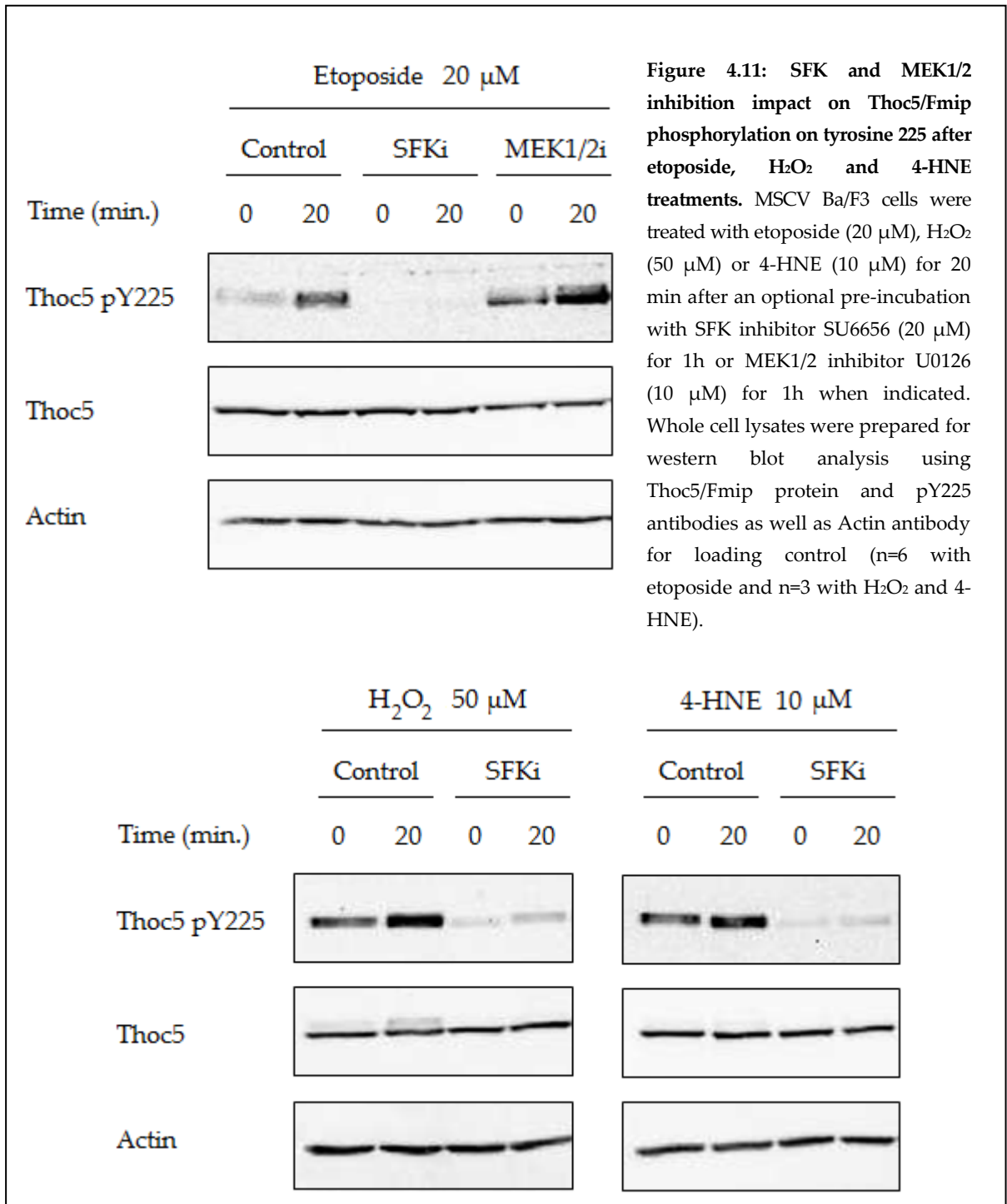
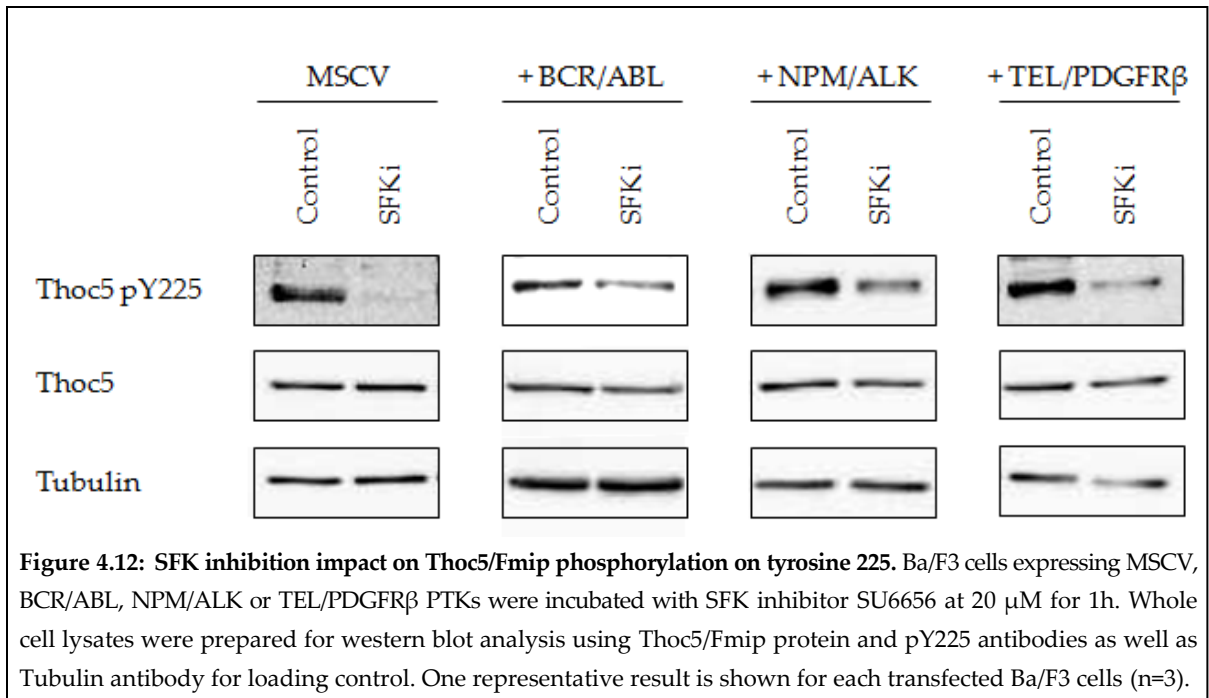
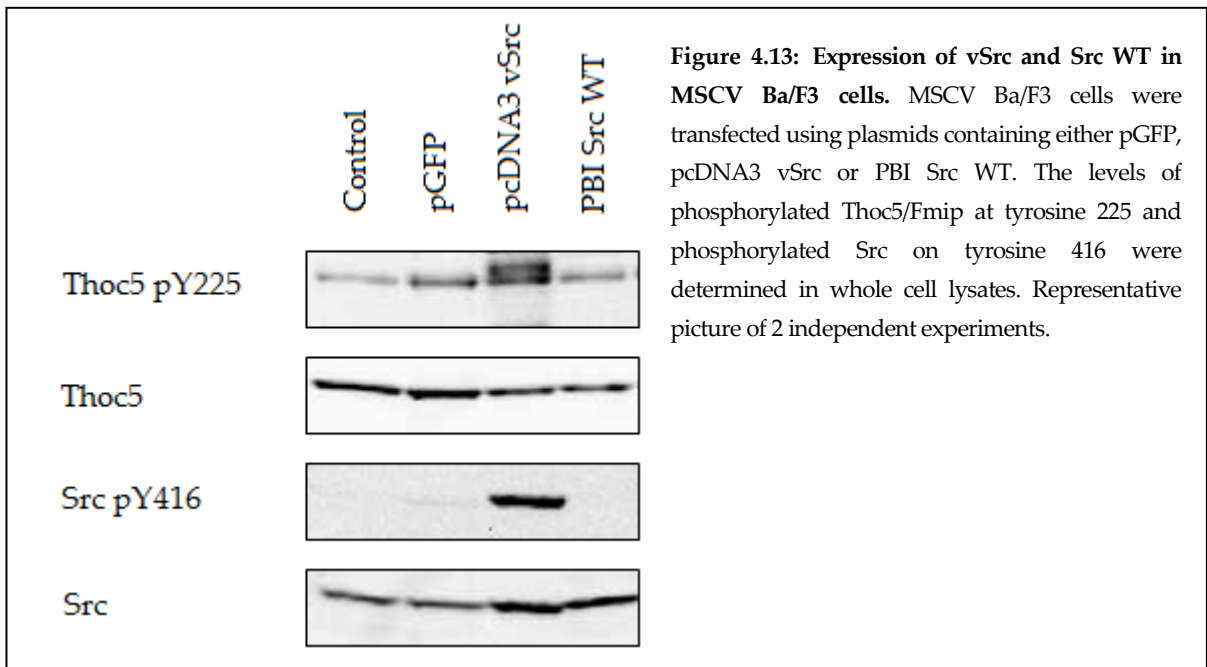


Figure 4.11: SFK and MEK1/2 inhibition impact on Thoc5/Fmip phosphorylation on tyrosine 225 after etoposide, H₂O₂ and 4-HNE treatments. MSCV Ba/F3 cells were treated with etoposide (20 μ M), H₂O₂ (50 μ M) or 4-HNE (10 μ M) for 20 min after an optional pre-incubation with SFK inhibitor SU6656 (20 μ M) for 1h or MEK1/2 inhibitor U0126 (10 μ M) for 1h when indicated. Whole cell lysates were prepared for western blot analysis using Thoc5/Fmip protein and pY225 antibodies as well as Actin antibody for loading control (n=6 with etoposide and n=3 with H₂O₂ and 4-HNE).



To further validate the role of SFKs in the upstream signalling of Thoc5/Fmip phosphorylation on tyrosine 225, a series of plasmids expressing Src kinase were used, kind gift of Drs. Simon Woodcock and Angeliki Malliri from The University of Manchester (Woodcock, *et al* 2009) and transfected into MSCV Ba/F3 cells. The level of Thoc5/Fmip phosphorylation on tyrosine 225 was determined in whole cell lysates using western blot. Strikingly, active vSrc kinase increased the level of phosphorylation while the non active Src WT kinase did not (Figure 4.13). The level of active Src kinase was determined with the amount of Src phosphorylation on tyrosine 416. This observation consolidated previous evidence, demonstrating that the proto-oncogene Src can be a potential upstream modulator of Thoc5/Fmip phosphorylation on tyrosine 225.

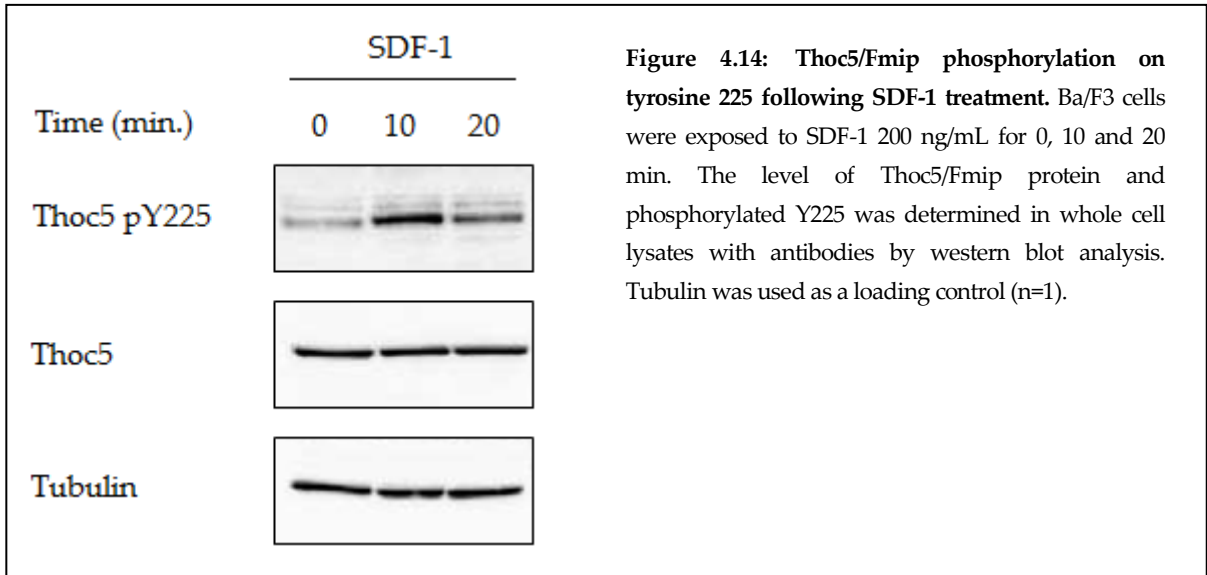


4.2.5. CD45/Src signalling pathway is upstream of Thoc5/Fmip tyrosine phosphorylation

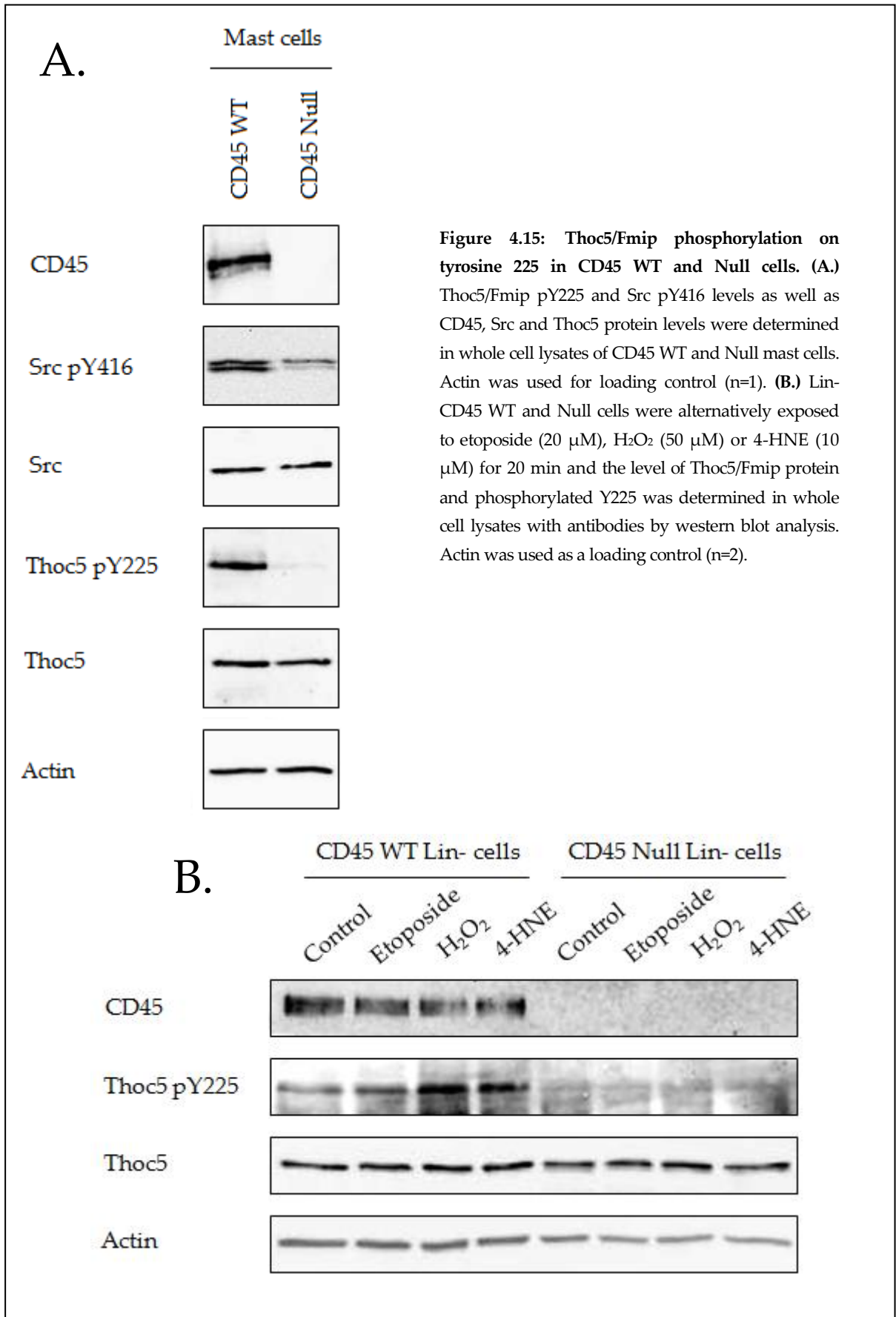
In hematopoietic cells there are several stimuli that can activate the Src family kinases. Therefore, it was investigated if Src-related upstream regulatory mechanisms could also be involved in Thoc5/Fmip phosphorylation. CD45 protein tyrosine phosphatase is a leukocyte marker which has a dual role in the activation of Src family kinases like Lck and Fyn. Indeed CD45 can dephosphorylate negative or positive regulatory phosphorylation, hence activating or inhibiting Src kinase activity (Roskoski 2005).

Moreover, CD45 could also play a regulatory role in H₂O₂ signalling (Qin and Chock 2002), which can be generated from multiple cellular mechanisms such as receptor signalling (Droge 2002). Previous work in this group investigated Src activation by CD45 phosphatase after the activation of the chemokine receptor CXCR4 with the addition of CXCL12/SDF-1 stem cell homing chemokine to the cells. The level of Thoc5/Fmip phosphorylation on tyrosine 225 was determined following SDF-1 exposure in Ba/F3 cells

(Figure 4.14). This indicated that CXCR4 signalling may potentiate Thoc5/Fmip with phosphorylation on tyrosine 225, possibly through CD45-Src activation.



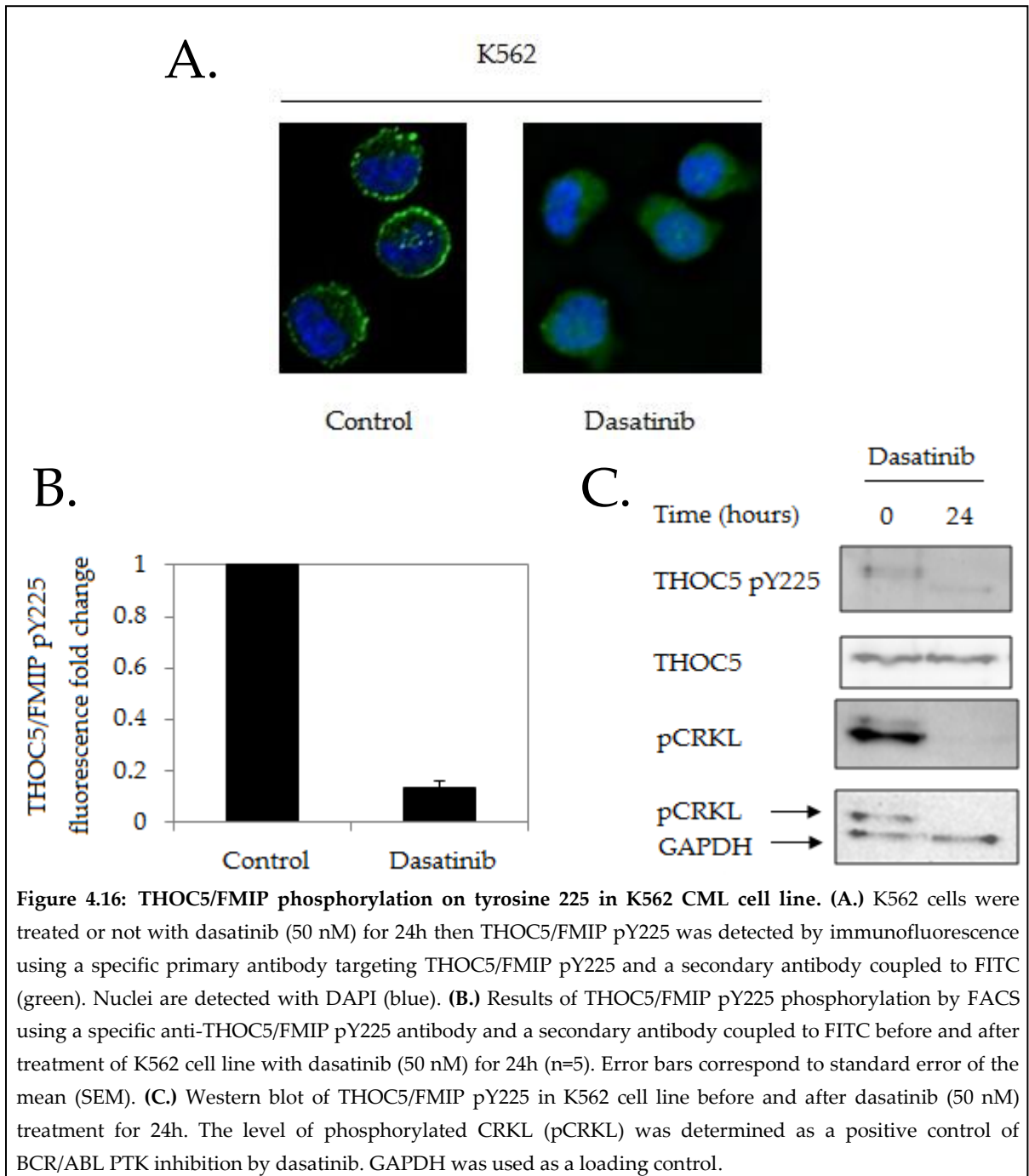
This observation led to further study on the CD45-Src-mediated Thoc5/Fmip tyrosine phosphorylation. CD45 null and WT mast cells were generated by Dr. Elaine Spooner from murine bone marrow and the level of Thoc5/Fmip phosphorylation on tyrosine 225 was determined in whole cell lysates. Strikingly, phosphorylation on tyrosine 225 was negligible in CD45 null cells compared to WT cells while decrease in Src activating autophosphorylation on tyrosine 416 was also observed in the absence of CD45. This demonstrated the dependence of CD45 for Src-mediated Thoc5/Fmip phosphorylation (Figure 4.15-A). Then, the requirement of CD45 for Thoc5/Fmip phosphorylation following genotoxic stresses, such as etoposide, H₂O₂ and 4-HNE was investigated. For this purpose, primitive lineage negative (Lin⁻) CD45 null and WT cells were produced as they represent a more suitable cell model for the study of Thoc5/Fmip, which is required for primitive haemopoietic cell survival (Mancini, *et al* 2010). As seen for the CD45 null mast cells, the level of Thoc5/Fmip phosphorylation was decreased in Lin⁻ CD45 null cells and the importance of CD45 for this phosphorylation was further confirmed by the absence of response to genotoxic stresses in these cells on tyrosine 225 (Figure 4.15-B).



4.2.6. THOC5/FMIP tyrosine phosphorylation is elevated in primary CML stem cells.

Having established the fact that pY225 was a target for numerous leukaemogenic PTKs we were keen to demonstrate that THOC5/FMIP phosphorylation played a role in leukaemogenesis in primary cells. This work was performed by Prof. Tessa Holyoake and Dr. Mary Scott from the Paul O'Gorman Leukaemia Research Centre at the University of Glasgow. To confirm this phosphorylation was not cell line dependent, the K562 CML patient derived cell line was used. K562 cells were treated with the BCR/ABL PTK inhibitor dasatinib then subjected to immunofluorescence microscopy using the THOC5/FMIP pY225 antibody (Figure 4.16-A). These data confirmed the cytoplasmic location of THOC5/FMIP pY225 and demonstrated that it is sensitive to dasatinib treatment. THOC5/FMIP subcellular localization could not be assessed in these cells as the THOC5/FMIP antibody did not work for immunofluorescence application. Flow cytometry measurements also demonstrated the sensitivity of THOC5/FMIP pY225 levels to dasatinib (Figure 4.16-B). The loss of pY225 following dasatinib treatment was further confirmed by western blot (Figure 4.16-C.). Modulation of phosphorylated CRKL was used to demonstrate successful inhibition of BCR/ABL PTK. These observations were then repeated in primary cells. First we assessed by flow cytometry (Figure 4.17-A) that the level of THOC5/FMIP phosphotyrosine 225 was increased in the bulk CD34+ cell population from patients with CML compared to controls, but also in the CML CD34+CD38- and CD34+CD38-CD90+ haemopoietic stem cells as well as the more developed CML CD34+CD38+ cells (Figure 4.17-A). All four cell populations showed a higher level of expression of THOC5/FMIP pY225 in CML than controls. However, high THOC5/FMIP tyrosine phosphorylation could be reduced upon treatment with dasatinib as demonstrated by western blot with 2 CML CD34+ samples (Figure 4.17-B). Dasatinib in addition to inhibiting BCR/ABL PTK also inhibits Src family kinases. We were therefore interested whether the other two drugs commonly used in the treatment of CML, namely imatinib and nilotinib, also inhibited THOC5/FMIP pY225 phosphorylation. Also, whilst all these drugs target BCR/ABL PTK, they have been shown to target slightly different cell

populations (Copland, *et al* 2006, Jorgensen, *et al* 2007). We therefore investigated the effects of these drugs on pY225 levels in CML CD34+, CD34+CD38+ and CD34+CD38- cells. Figure 4.17-C clearly shows that THOC5/FMIP pY225 levels are reduced by all three drugs in all three cell populations. However, preliminary data would suggest that the most primitive CML CD34+CD38-CD90+ cell population might be less responsive to imatinib compared to dasatinib and nilotinib with respect to THOC5/FMIP tyrosine phosphorylation (Figure 4.17-C.). Interestingly, preliminary data would suggest that the conditions used here for nilotinib treatment enable the inhibition of Src activation, as assessed by Src dephosphorylation on tyrosine 416, in a similar manner as dasatinib treatment, while nilotinib has previously been shown to inhibit the Src family kinase member Lck (Blake, *et al* 2009, Chen, *et al* 2008a, Chow, *et al* 2007).



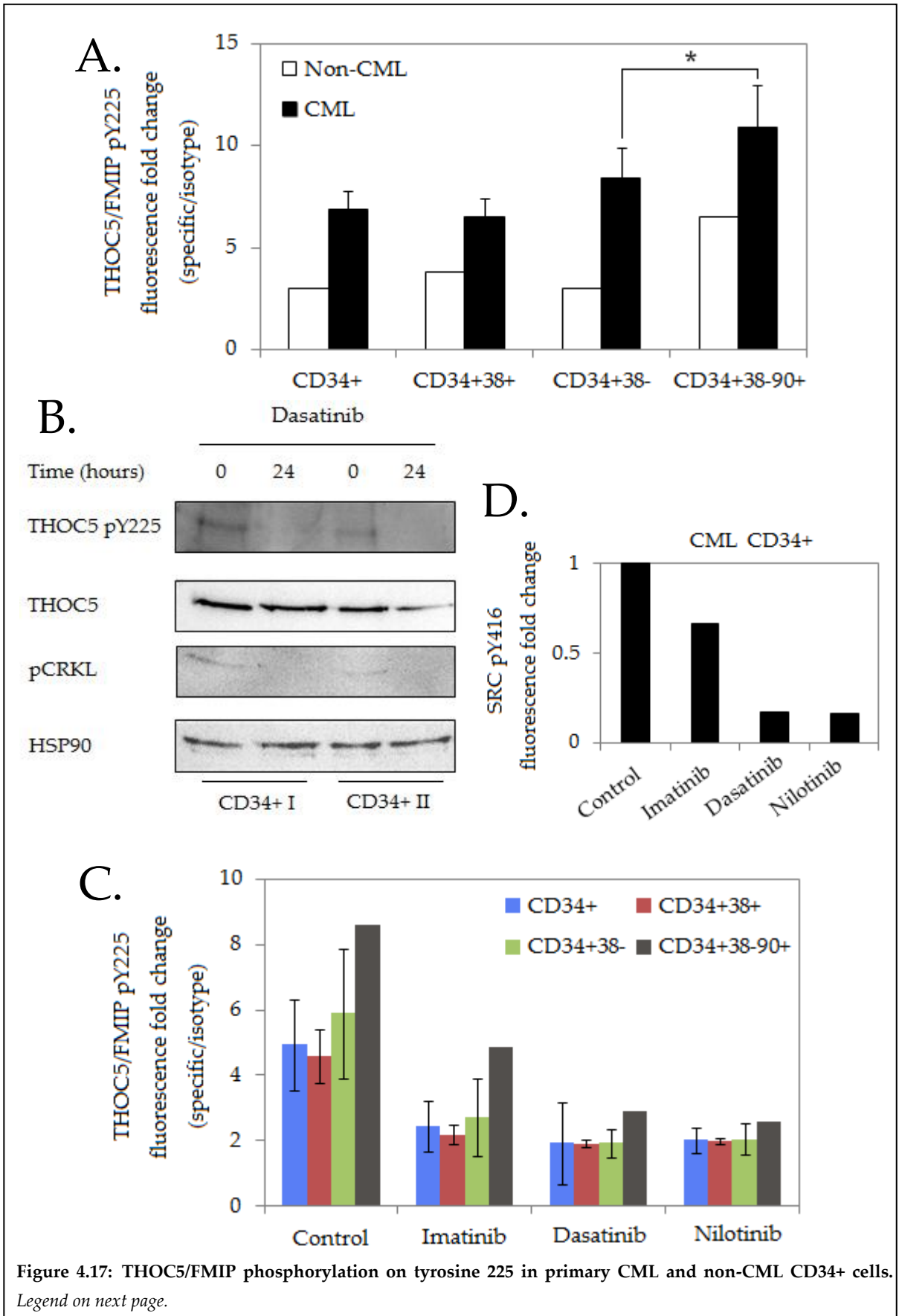


Figure 4.17: THOC5/FMIP phosphorylation on tyrosine 225 in primary CML and non-CML CD34+ cells. Legend on next page.

Figure 4.17: THOC5/FMIP phosphorylation on tyrosine 225 in primary CML and non-CML cells (Figure on previous page). (A.) CML and non-CML cells were stained with the different fluorescent labels CD34-APC, CD38-PerCP and CD90-PE for FACS analysis to identify each CD34+ sub-population i.e. CD34+CD38+, CD34+CD38- etc. Cells were fixed and permeabilised before intra-cellular staining with a specific primary anti-THOC5/FMIP pY225 antibody or the antibody isotype control before incubation with a secondary antibody coupled to FITC. FACS analysis enabled the quantification of the mean fluorescence intensity of THOC5/FMIP pY225 (specific) and its isotype control in each CD34+ sub-populations for CML (n = 4) and non-CML (n = 2 ; n = 1 for CD34+ CD38- CD90+) samples so that the specific/isotype fluorescence ratio could be calculated. Error bars corresponding to standard error of the mean (SEM) are shown when n = 3. Significance level for Student's t-test p-value (P): * P < 0.05. **(B.)** Western blot analysis of THOC5/FMIP pY225 and THOC5/FMIP in two CD34+ CML samples (I and II) before and after exposure to dasatinib at 150 nM for 24h. Phosphorylated form of CRKL (pCRKL) was used as a positive control of BCR/ABL PTK inhibition and Hsp90 was used as a loading control. **(C.)** CML bulk CD34+ cells were treated with tyrosine kinase inhibitors imatinib (5 µM), dasatinib (150 nM) and nilotinib (5 µM) for 24h, then cells were stained with the different fluorescent labels CD34-APC, CD38-PerCP and CD90-PE, fixed and permeabilised before intra-cellular staining with anti-THOC5/FMIP pY225 or the antibody isotype control and the secondary antibody coupled to FITC. FACS analysis was used to measure the mean fluorescence intensity and the specific/isotype fluorescence ratio was calculated for the different cell populations (n= 3; n=2 for CD34+CD38-CD90+) before and after each drug treatment. Error bars corresponding to standard error of the mean (SEM) are shown when n=3. **(D.)** Src phosphorylation on tyrosine 416 was determined in CML bulk CD34+ cells by FACS using a specific primary antibody targeting Src pY416 and a secondary antibody coupled to FITC, before and after each drug treatment as in (C.) (n = 1).

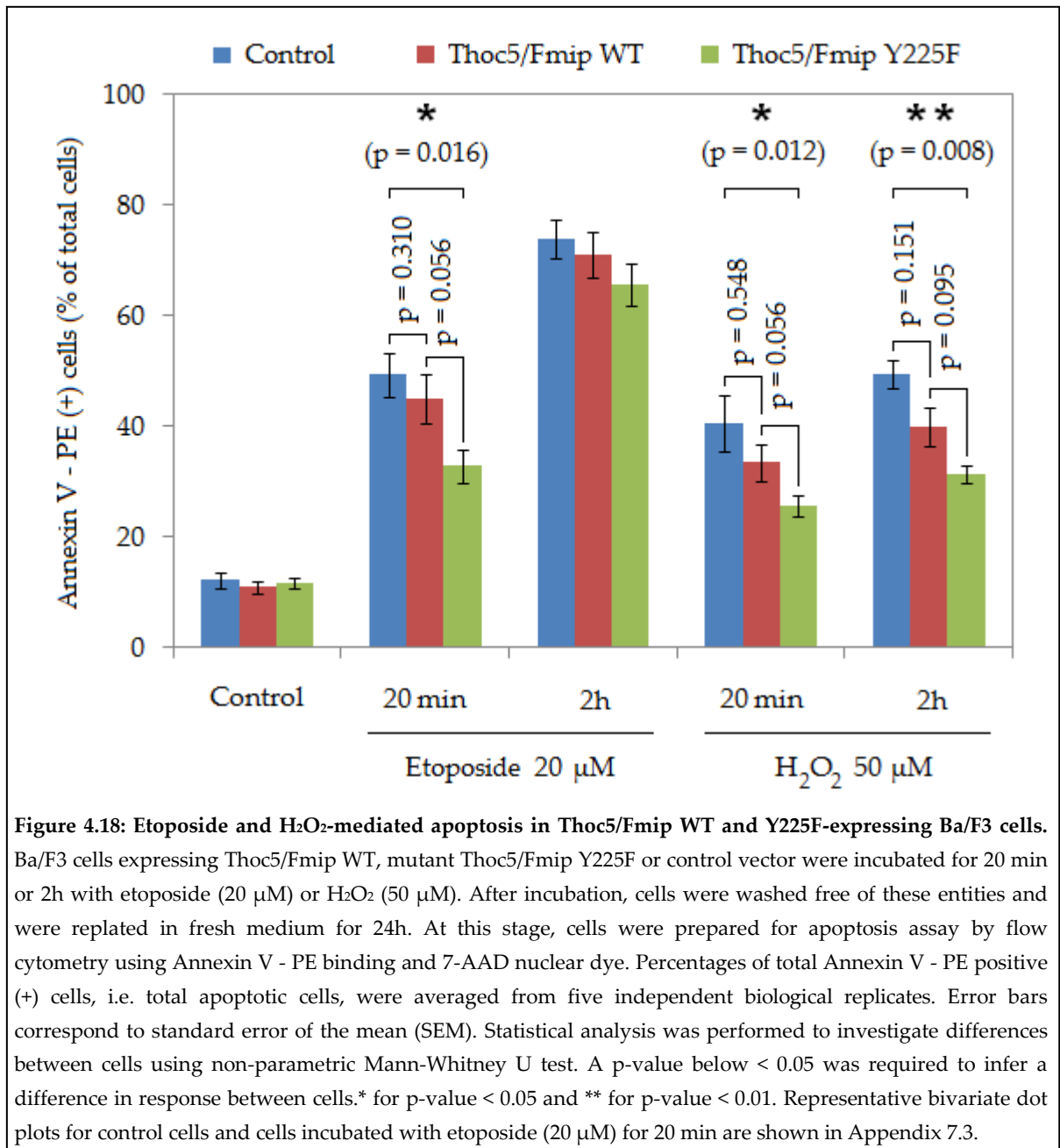
4.2.7. Thoc5/Fmip phosphorylation on tyrosine 225 in mediation of apoptosis in response to oxidative stress

Having demonstrated that Thoc5/Fmip is phosphorylated on tyrosine 225 after various genotoxic stresses, downstream of SDF-1 chemokine as well as CD45 protein phosphatase and the proto-oncogene Src, experiments were undertaken to determine the effects of this phosphorylation. Ba/F3 cells were transduced with a retrovirus containing either Myc-tagged Thoc5/Fmip WT-IRES-GFP, Myc-tagged mutant Thoc5/Fmip Y225F-IRES-GFP or GFP alone by Dr. Maria Belen Gonzalez Sanchez. These cells were exposed to etoposide (20 µM) and H₂O₂ (50 µM) for either 20 min or 2h before being washed free of drugs and replated in fresh medium. The level of apoptosis of these cells was determined for all the conditions tested after 24h recovery using Annexin V - PE and 7-AAD.

While apoptosis levels remained low without stress for control Ba/F3 cells as well as with the expression of Thoc5/Fmip WT and Y225F, it increased substantially from 20 min

exposure to etoposide or H₂O₂ (Figure 4.18). A small but significant (P-value = 0.01587 with a two-sided Mann-Whitney U test) difference in apoptosis levels existed between control and Thoc5/Fmip Y225F mutant-expressing cells after etoposide exposure of 20 min while no difference was seen between control and Thoc5/Fmip WT (P-value = 0.3095). Under these conditions, the expression of the mutant Y225F would reduce apoptosis. A direct comparison between Thoc5/Fmip WT and Y225F showed a difference close to significance (P-value = 0.05556). Additional evidence showing an anti-apoptotic action of Thoc5/Fmip Y225F was obtained when comparing the responses of control Ba/F3 cells and the expression of the mutant after treatment with H₂O₂ for 20 min and 2h (P-value = 0.01193 for 20 min and P-value = 0.007937 for 2h). Again, no significant differences could be seen between control and Thoc5/Fmip WT (P-value = 0.5476 for 20 min and P-value = 0.1508 for 2h), and a difference close to significance was obtained between Thoc5/Fmip WT and Y225F for 20 min exposure (P-value = 0.05556 for 20 min and P-value = 0.09524 for 2h).

Thus the overexpression of Thoc5/Fmip Y225F might be perceived in Ba/F3 cells as a reduced amount of stress and be able to limit stress downstream signalling and hypothetically apoptosis. These differences highlight the possibility that Thoc5/Fmip might be partially involved in mediating apoptosis following genotoxic stresses. Thoc5/Fmip mediates the export of mRNA involved in stress response, but it also regulates mRNAs involved in cell differentiation (Guria, *et al* 2011). In this sense, Ba/F3 cells are differentiation blocked and as such differentiation control should be studied in other cell populations (Guria, *et al* 2011). Thoc5/Fmip is known to be involved in the processing of Hsp70 mRNA following heat shock and Hsp70 expression has been shown to reduce etoposide-induced apoptosis by 40%, a decrease similar to our results (Guo, *et al* 2005a, Guo, *et al* 2005b, Katahira, *et al* 2009). Therefore the levels of Hsp70 and Hsp40 proteins, modulated by Thoc5/Fmip and the THO complex were investigated (Rehwinkel, *et al* 2004).

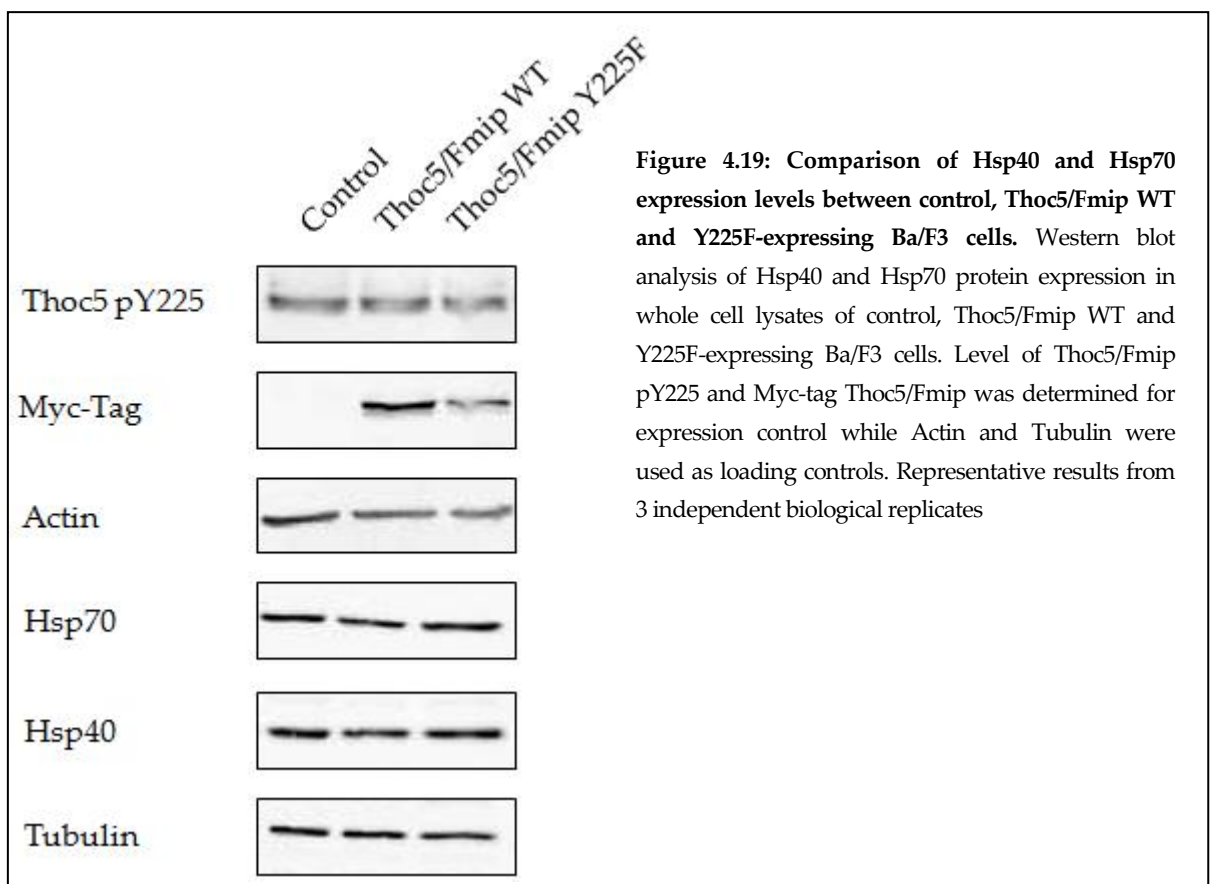


4.2.8. Thoc5/Fmip tyrosine phosphorylation does not mediate protein levels of Hsp40 and Hsp70 in response to etoposide and H₂O₂

There are numerous examples of Hsp70 and Hsp40 responding to genotoxic stresses and regulating apoptosis signalling (Jacobs and Marnett 2007, Kim, *et al* 2008, Mosser, *et al* 2000, Su, *et al* 1999, Su, *et al* 1998), while Hsp70 is also linked to resistance to imatinib in CML and resistance to etoposide in AML (Guo, *et al* 2005b, Pocaly, *et al* 2007).

The protein expression of Hsp70 and Hsp40, two proteins found to be regulated by the depletion of Thoc1 and Thoc2 subunits of the THO complex in *Drosophila melanogaster* (Rehwinkel, *et al* 2004), was determined by western blots in whole cell lysates of control, Thoc5/Fmip WT and Y225F-expressing Ba/F3 cells.

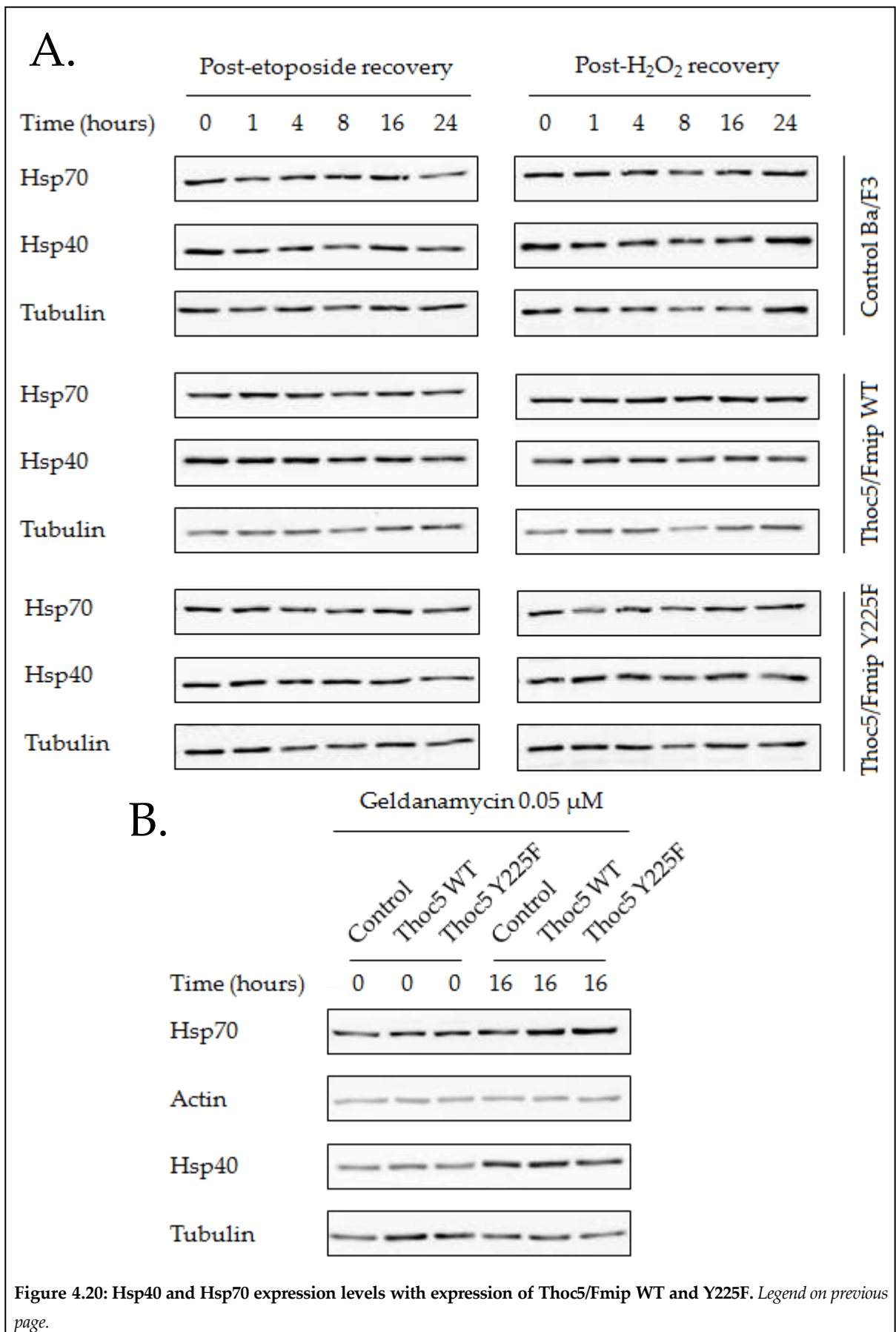
However, no consistent difference was observed between the levels of expression of Hsp40 or Hsp70 in these lysates (Figure 4.19), and the mutant Thoc5/Fmip Y225F expression did not reduce the amount of Thoc5/Fmip phosphorylation.



The responses of control, Thoc5/Fmip WT and Y225F-expressing Ba/F3 cells to 20 min exposure to etoposide (20 μ M) and H₂O₂ (50 μ M) were then determined over a 24h time course after washing cells free of these compounds and replating them in fresh medium (Figure 4.20). However, neither the amount of Hsp70 nor the level of Hsp40 reproducibly changed during this period in any of the cells tested in triplicate. To confirm that change in

Hsp70 and Hsp40 protein expression could be detected and to determine the degree of change that could be expected, we treated these cells with geldanamycin A. Geldanamycin A is an Hsp90 inhibitor which blocks the interaction between Hsp90 and Heat shock factor 1 (HSF1). Free HSF1 can then translocate to the nucleus and upregulate the heat shock response genes like Hsp40 and Hsp70. As shown in Figure 4.20, geldanamycin A treatment resulted in an increase in Hsp40 and Hsp70 in all cells.

Figure 4.20: Hsp40 and Hsp70 expression levels with expression of Thoc5/Fmip WT and Y225F (Figure on next page). (A.) Protein levels of Hsp40 and Hsp70 were determined by western blot analysis in whole cell lysates of control, Thoc5/Fmip WT and Y225F-expressing Ba/F3 cells at different times (0, 1, 4, 8, 16 and 24h) after a 20 min exposure to etoposide (20 μ M) or H₂O₂ (50 μ M). Cells were washed free of these compounds and replated in fresh medium for the times indicated. Tubulin was used as a loading control. (B.) Whole cell lysates of control, Thoc5/Fmip WT and Y225F-expressing Ba/F3 cells were prepared after treatment with Geldanamycin A (0.05 μ M) for 16h. Western blot analysis was performed to determine the level of Hsp70 and Hsp40. Actin and Tubulin were used as loading controls. A and B. Representative results from 3 independent biological replicates.



4.3. Discussion

Leukaemogenic PTKs have been shown to promote the phosphorylation of Thoc5/Fmip on tyrosine 225 (Pierce, *et al* 2008a). Thoc5/Fmip has been proven to be a key protein in the maintenance of haemopoiesis by controlling cell differentiation and apoptosis of primitive cells, thus making it a potential common target for leukaemogenic PTKs for the progression of leukaemias and related disorders (Mancini, *et al* 2010). The aims of this study were to identify the sources of the modulation of Thoc5/Fmip tyrosine phosphorylation that leukaemogenic PTKs commonly affect and its biological role. Here the use of a kinase inhibitor screen and vSrc expression enabled us to show that normal Thoc5/Fmip tyrosine phosphorylation and leukaemogenic PTK action on Thoc5/Fmip is Src-dependent. We also showed that Thoc5/Fmip tyrosine phosphorylation can be stimulated with multiple genotoxic stresses (etoposide, H₂O₂ and 4-HNE), while NPM/ALK PTK action is also correlated with oxidative stress potentially mediated by p66Shc, which controls organism lifespan (Migliaccio, *et al* 1999). Src family kinases are cytoplasmic non-receptor tyrosine kinases involved in cell growth, cell proliferation, embryo development as well as myeloid cell differentiation and myeloid malignancies (Johnson 2008, Molina, *et al* 1992). Src family kinases such as Lyn have been shown to have a role in CML progression to blast crisis as well as being a direct source of imatinib and nilotinib resistance (Donato, *et al* 2003, Gioia, *et al* 2011, Pene-Dumitrescu and Smithgall 2010, Rubbi, *et al* 2011), thus suggesting that Thoc5/Fmip tyrosine phosphorylation by multiple leukaemogenic PTKs might be involved in the pathogenesis of leukaemias. Indeed, we show that THOC5/FMIP tyrosine phosphorylation is seen in the cytosol in the human CML blast crisis K562 cell line as well as in primary human CML CD34+ cells, but this occurs to a lesser extent in non-CML CD34+ cells. The primitive CML CD34+ CD38- and CD34+ CD38- CD90+ leukaemia stem cells are able to initiate long-term proliferation and treatment resistance (Corbin, *et al* 2011, Costello, *et al* 2000, Florian, *et al* 2006), while our data suggest that increased THOC5/FMIP tyrosine phosphorylation is occurring in these leukaemic stem cells compared to normal stem cells. However, these results on primary material were obtained with few replicates and thus they should only be

considered as preliminary observations. Preliminary data also suggest that THOC5/FMIP tyrosine phosphorylation could be decreased with imatinib, dasatinib and nilotinib in CML CD34⁺ CD38⁻ cells to the same level as seen in the more mature CML CD34⁺ CD38⁺ cells. As dasatinib and nilotinib are able to target BCR/ABL PTK and Src family kinase members, a difference in efficacy between these drugs and imatinib in decreasing THOC5/FMIP tyrosine phosphorylation might have been expected. Preliminary data suggest that it might be the case for the most primitive CML CD34⁺ CD38⁻ CD90⁺ cell population, for which imatinib might be less effective in reducing THOC5/FMIP tyrosine phosphorylation compared to dasatinib and nilotinib. Thus, our preliminary data did suggest that high THOC5/FMIP tyrosine phosphorylation found in CML CD34⁺, CD34⁺ CD38⁻, CD34⁺ CD38⁺ and CD34⁺ CD38⁻ CD90⁺ cells compared to control cells was indicative of BCR/ABL PTK downstream signalling. It is noteworthy that BCR/ABL and other leukaemogenic PTKs enhance production of reactive oxygen species and this effect can be reverted by tyrosine kinase inhibitors (Cramer, *et al* 2008, Koptyra, *et al* 2006).

As well as being mediated by genotoxic stress, Src activation has been shown to be regulated by CD45 phosphatase, a key transmembrane glycoprotein involved in haemopoiesis by regulating signalling cascades as well as the structure of the stem cell niche. CD45 deficiency may result in abnormal TCR threshold activation, modified response to cytokines, altered lymphocyte survival as well as impaired stem cell motility and bone remodelling (Shivtiel, *et al* 2008, Tchilian and Beverley 2006). CD45 has been shown to be inactivated with H₂O₂ by modification of a cysteine in its active site (Lee and Esselman 2002, Rider, *et al* 2003). However, CD45 may also have a specific role in promoting oxidative signalling (Qin and Chock 2002). CD45 is able to dephosphorylate Src on either inhibitory tyrosine 527 or on the activating tyrosine 416, thus potentially having antagonistic action on different Src family kinase members and at different lineage development stages (Hermiston, *et al* 2009). Using CD45 null/WT mast and Lin⁻ cells, we have shown that CD45 phosphatase is required for Src activation, as determined by its autophosphorylation on tyrosine 416, and downstream Thoc5/Fmip phosphorylation on tyrosine 225. However, it would be interesting to confirm upregulation of Src inhibiting

phosphorylation on tyrosine 527 in the absence of CD45. Furthermore, our data indicate that an active CD45-Src axis is required for Thoc5/Fmip tyrosine phosphorylation following genotoxic stress. This observation would suggest that CD45 may be involved in the regulation of the response to oxidative stress by potentiating Src activation and Thoc5/Fmip tyrosine phosphorylation. Also, it would be interesting to test whether Thoc5/Fmip functions in regulating apoptosis in primitive cells are linked to CD45 (Dupere-Minier, *et al* 2010, Mancini, *et al* 2010). As CD45 also regulates motility, a process impaired in leukaemia, we further investigated the connection between Thoc5/Fmip and CD45 with stimulation of CD45 by SDF-1/CXCR4. Stromal-derived factor 1 (SDF-1/CXCL-12) is a chemokine expressed by the bone marrow stromal cells which plays a key role in the migration of haemopoietic stem/progenitor cells to bone marrow during fetal development and then their retention during adult life (Kucia, *et al* 2004, Kucia, *et al* 2005, Whetton and Graham 1999). Our data showed that Thoc5/Fmip tyrosine phosphorylation may be also mediated by the SDF-1/CXCR4 pathway. However, preliminary data using Thoc5/Fmip WT and Thoc5/Fmip Y225F expression in Ba/F3 cells would suggest that Thoc5/Fmip phosphotyrosine 225 is not required for motility regulation in response to SDF-1 (data not shown). To summarise our findings, Thoc5/Fmip phosphorylation on tyrosine 225 is mediated by Src activation following oxidative stress, and by several proteins controlling Src activation, such as CD45 and SDF-1/CXCR4.

As the modulation of Thoc5/Fmip tyrosine phosphorylation in response to genotoxic stress may be related to its role in apoptosis regulation, we next tested whether Thoc5/Fmip phosphotyrosine 225 mediates an adverse response to cellular stress. Here, we have shown that the expression of Thoc5/Fmip Y225F phosphomutant could reduce significantly the level of apoptosis induced by short exposure (20 min) to oxidative stress compared to control cells. Given the linkage of THO complex to Hsp70 expression, we determined if Hsp70 expression was altered in these experiments. Hsp70 is a chaperone protein involved in haemopoiesis which has been linked to imatinib and etoposide resistance in CML cells (Evdonin, *et al* 2006, Pocaly, *et al* 2007). Hsp70 mRNA export is inhibited in co-depletion of Thoc1 and Thoc2 and in the absence of Thoc5/Fmip (Katahira, *et al* 2009, Rehwinkel, *et al*

2004). However, neither the amount of Hsp70 nor the level of Hsp40, another THO complex target responding to oxidative stress, changed reproducibly following oxidative stress or between the overexpression of Thoc5/Fmip and its mutated form (Jacobs and Marnett 2007, Kim, *et al* 2008).

In contrast to Src inhibition, MEK1/2 and ATM inhibition resulted in a steady phosphorylation increase on Thoc5/Fmip tyrosine 225. This suggested that ATM and MEK1/2 downstream signalling could regulate and reduce the amount of Thoc5/Fmip phosphorylation after genotoxic stress. Interestingly, ATM failure is known to increase oxidative stress (Ito, *et al* 2004), which could be the source of more Thoc5/Fmip tyrosine phosphorylation. ERK is a kinase downstream of MEK1/2, ATM and EGFR signalling and is required for cell cycle arrest and apoptosis after genotoxic stress (Tang, *et al* 2002). Interestingly, ERK is predicted to bind Thoc5/Fmip on leucine 229, close to tyrosine 225, according to Scansite Motif Scanner (http://scansite.mit.edu/motifscan_seq.phtml). This region would correspond to the motif [K/R]₂₋₃-X₁₋₆-[L/I]-X-[L/I] (Grewal, *et al* 2006), called ERK Docking (D)-domain. This result would suggest that ERK might bind to the predicted ERK D-domain of Thoc5/Fmip depending on whether tyrosine 225 is phosphorylated. Indeed, the binding of ERK to Thoc5/Fmip could reduce phosphorylation on tyrosine 225 while inactivated ERK release would free up space for tyrosine kinases such as Src to increase phosphorylation. As Thoc5/Fmip tyrosine phosphoresidue was found in the cytosol, it was tested whether its localization was due to nuclear export, but instead of blocking phosphorylated tyrosine 225 in the nucleus, more phosphorylation could be observed in the cytosol after leptomycin B treatment. This suggested that either leptomycin B activated a stress response in the cytosol or Thoc5/Fmip is exported through a second nuclear export system. Alternatively, this response to leptomycin B could be due to MEK1 translocation to the nucleus and its resulting inactivation giving similar result as the inhibition of MEK1/2 with U0126.

Interestingly, it has been shown that ATM/MEK/ERK pathway and Src can lead to NF- κ B activation and promote cell survival following oxidative stress (Ahmed, *et al* 2009, Lluís, *et*

al 2007, Magne, *et al* 2006, Panta, *et al* 2004). Preliminary experiments suggested that Thoc5/Fmip Y225F would activate more NF- κ B than Thoc5/Fmip WT by increasing the degradation of I κ B following etoposide and H₂O₂ exposure (data not shown). This would support the apoptosis assay results showing an anti-apoptotic effect of Y225F mutant overexpression following exposure to etoposide and H₂O₂.

Thoc5/Fmip is required for primitive cell survival (Mancini, *et al* 2010) and has been shown to modulate the specific nuclear export of mRNAs involved in cell development and haemopoiesis (Guria, *et al* 2011). Haemopoiesis is primed by ROS, while the loss of ATM function increases ROS production and precipitates the loss of self-renewal (Ito, *et al* 2004, Owusu-Ansah and Banerjee 2009). ATM, p53 and FoxO3 compose a network responsible to fine tune the level of cellular ROS (Ghaffari 2008) during cell development. The regulation of Thoc5/Fmip tyrosine 225 by oxidative stress may be linked with its functional role in haemopoiesis in coordination with other second messengers. Indeed, Thoc5/Fmip is expressed and phosphorylated on tyrosine 225 following M-CSF stimulation while Thoc5/Fmip ectopic expression increases the level of PIP3, a second messenger also enhanced by M-CSF signalling (Carney, *et al* 2009). Here, we report that ATM inhibition increases the level of Thoc5/Fmip tyrosine phosphorylation at a low level while several studies have shown that Thoc5/Fmip is phosphorylated by ATM on serine 307 following ionizing radiation and etoposide (Matsuoka, *et al* 2007, Ramachandran, *et al* 2011). Also ATM and p53 are required to block Thoc5/Fmip function in the export of mRNA involved in cell differentiation following etoposide exposure, although this action is not dependent on phosphorylation of serine 307 (Matsuoka, *et al* 2007, Ramachandran, *et al* 2011). Interestingly, Thoc5/Fmip phosphorylation on serine 307 is reduced upon expression of some leukaemogenic PTKs in Ba/F3 cells, such as BCR/ABL, NPM/ALK and TEL/PDGFR β (data not shown). Thus, the regulation of Thoc5/Fmip phosphoresidues and its mRNA binding properties by ATM might be part of an intricate network involved in the regulation of mRNA export by the THO/TREX complex in response to oxidative stress during haemopoietic development.

In conclusion, we propose that the action of leukaemogenic PTKs such as BCR/ABL, NPM/ALK and TEL/PDGFR β on Thoc5/Fmip tyrosine 225 could affect Thoc5/Fmip function in haemopoiesis regarding its response to oxidative stress, cytokines, and chemokines (Figure 4.21). High Thoc5/Fmip tyrosine phosphorylation could be promoted by leukaemogenic PTKs *via* ROS production and Src tyrosine kinase activation thereby continuously priming a stress response potentially impairing mRNA export and normal cell differentiation as well as apoptosis signalling during disease progression (Baud and Karin 2009, Guria, *et al* 2011, Johnson 2008, Ramachandran, *et al* 2011).

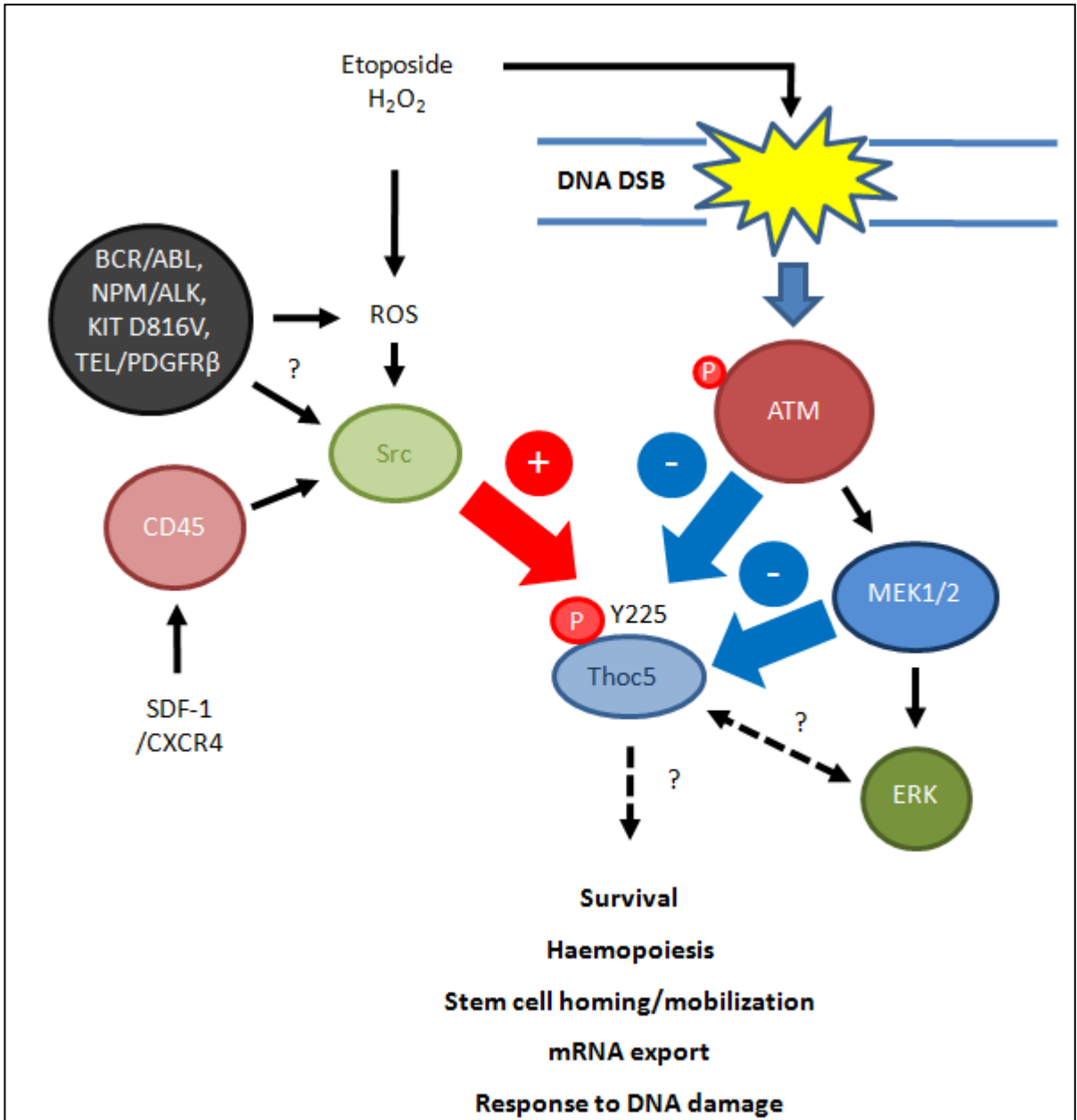


Figure 4.21: Thoc5/Fmip phosphorylation on tyrosine 225 and its potential biological functions. Leukaemogenic PTKs such as BCR/ABL, NPM/ALK, KIT D816V and TEL/PDGFR β stimulate the production of ROS by the deregulation of NADPH oxidase and mitochondrial electron transport chain which results in Src activation and Thoc5/Fmip phosphorylation on tyrosine 225. This event is also promoted by the addition of etoposide and H₂O₂. The chemokine SDF-1, *via* its receptor CXCR4 activation, may also lead to Thoc5/Fmip tyrosine phosphorylation following phosphatase CD45 and Src activation. Conversely, ATM and MEK1/2 inhibit Thoc5/Fmip tyrosine phosphorylation, while ATM has been shown to reduce oxidative stress in haemopoietic stem cells. It is also possible that ATM activation following DNA double strand breaks induced by etoposide or H₂O₂ may control the transient Thoc5/Fmip phosphorylation downstream of Src by the activation of ERK, which is predicted to bind to Thoc5/Fmip leucine 229. Thoc5/Fmip tyrosine phosphorylation may prime an oxidative stress response resulting in regulation of mRNA export; cell differentiation, stem cell chemotaxis, response to DNA damage or survival/apoptosis decisions.

Chapter 5.

General discussion, future work and conclusion

5.1. General discussion

Chronic myeloid leukaemia (CML) progression is thought to be promoted by the genomic instability resulting from BCR/ABL PTK signalling (Skorski 2002). Protein tyrosine kinase inhibitors exist to treat patients with CML but resistance may occur, especially in advanced stages of the disease (Tefferi and Gilliland 2007). BCR/ABL PTK and other leukaemogenic PTKs have been shown to affect the regulation of cellular oxidative stress by enabling the production of reactive oxygen species (ROS) through the modulation of NADPH oxidases (Naughton, *et al* 2009). The cellular toxicity of ROS, as well as other genotoxic stresses, is counterbalanced by anti-apoptotic signals such as Bcl-2 expression or the activation of NF- κ B transcription factor which mediates the expression of antioxidant enzymes (Droge 2002, Maehara, *et al* 2000, Zhang, *et al* 1997). These enzymes as well as ATM, p53 and FoxO3 tightly control the level of ROS during haemopoietic cell development, which are required to prime stem cell differentiation simultaneously with the loss of stem cell renewal capacity (Ghaffari 2008, Ito, *et al* 2004, Owusu-Ansah and Banerjee 2009). However the ability of leukaemogenic PTKs to promote cell survival after cellular and genotoxic stress leads to the accumulation of DNA damage resulting in an increased probability of DNA misrepair, mutations and chromosomal abnormalities, potentially coming from overchallenged and deregulated DNA double strand break repair mechanisms such as homologous recombination (HR), non-homologous end-joining (NHEJ) or single-strand annealing (SSA). Indeed, the expression level of a substantial number of proteins and enzymes involved in these DNA repair pathways have been shown to be altered in the presence of BCR/ABL and other leukaemogenic PTKs. It is the case for WRN, CtIP, DNA ligase III, DNA ligase IV, Rad51, Nbs1, BRCA1, DNA PKcs, Parp-1, BLM, Artemis among others (Cramer, *et al* 2008, Fernandes, *et al* 2009, Nowicki, *et al* 2004,

Poplawski and Blasiak 2010, Salles, *et al* 2011, Sallmyr, *et al* 2008b, Sallmyr, *et al* 2008c, Slupianek, *et al* 2002, Slupianek, *et al* 2006, Slupianek, *et al* 2011b, Slupianek, *et al* 2001). These regulations at the protein level have been shown to affect the fidelity of the DNA repair pathways in some instances and promote genomic instability (Salles, *et al* 2011, Slupianek, *et al* 2011b, Slupianek, *et al* 2001).

Nonetheless, the response to DNA damage is unequivocally mediated by protein post-translational modifications such as phosphorylation, methylation, ubiquitination or acetylation (Cohn and D'Andrea 2008, Lee, *et al* 2010b, Matsuoka, *et al* 2007, van Attikum and Gasser 2009). Such modifications and the subsequent effects on DNA repair proteins, like Rad51 modification on tyrosine 315 and Nbs1 on serine 343, can lead to imatinib resistance in the treatment of leukaemia (Rink, *et al* 2007, Slupianek, *et al* 2001). We therefore aimed at demonstrating that BCR/ABL PTK expression could alter in a global manner the response to genotoxic stress signalling at the protein phosphorylation level.

First, we were able to define the response of Ba/F3 cells to DNA damage induced with etoposide in the presence and absence of BCR/ABL PTK using γ H2AX and apoptosis assays. Then we used phosphopeptide-centric quantitative phosphoproteomics to identify 44 phosphoentities regulated by both the expression of BCR/ABL PTK and etoposide, corresponding to 33 phosphosites. We found that the crosstalk of BCR/ABL PTK on the genotoxic stress signalling may be multi-faceted as it could create, block, sustain and change the intensity of the response to etoposide. We described that the expression of the oncogene may affect protein phosphorylation regulated by etoposide stress on the histone H2AX DNA repair platform (serine 139 and tyrosine 142), Mediator of DNA damage checkpoint 1 (MDC1) (serine 595 and serine 1053), and the negative differentiation regulator Hemogen (NDR/Hemogen/EDAG) (serine 380), among 21 proteins in total. Intriguingly, several proteins potentially involved in mitotic spindle assembly and sister chromatid cohesion such as Zfp828 (serine 532), Incenp (serine 284) and Cbx3 (serine 93) were regulated by both BCR/ABL PTK and etoposide (Itoh, *et al* 2011, Lachner, *et al* 2001, Resnick, *et al* 2006, Tanaka, *et al* 2002). Interestingly, sister chromatid exchange is increased

by BCR/ABL PTK expression (Deutsch, *et al* 2003), while it has been described that unfaithful sister chromatid cohesion may lead to cancer and chromosomal instability (Draviam, *et al* 2004, Morrison, *et al* 2003).

We further validated Hemogen phosphorylation upon etoposide exposure only in the presence of BCR/ABL PTK using AQUA™ technology and SRM assay because of its strong link with acute myeloid leukaemia (AML) and haemopoiesis (An, *et al* 2005, Li, *et al* 2004, Liu, *et al* 2004, Marcucci, *et al* 2005, Yang, *et al* 2001, Yang, *et al* 2006). Hemogen expression has been shown to activate the anti-apoptotic NF- κ B transcription factor while it might be involved in heterochromatin DNA repair downstream of ATM and 53BP1 *via* its association with Heterochromatin protein 1 (HP1) and Trim28/TIF1-beta/KAP-1 (Ayoub, *et al* 2008, Ayoub, *et al* 2009, Ball and Yokomori 2009, Goodarzi, *et al* 2008, Goodarzi, *et al* 2009, Li, *et al* 2004, Loyola, *et al* 2009, Luijsterburg, *et al* 2009, Noon, *et al* 2010). Intriguingly, Hemogen might also work in spindle assembly along with HP1, Incenp, Cbx3 and Zfp828 (Ainsztein, *et al* 1998, Vermeulen, *et al* 2010).

Additionally, we also found phosphoentities only regulated by BCR/ABL PTK on proteins such as DNA ligase 1 (serine 199), DNA topoisomerase 2a (serine 1373), Kdm2a (serine 692) and Whsc1 (serine 437). Although these were not regulated by etoposide, the potential modulation of these proteins involved in the regulation of the histone methylation code as well as DNA repair, DNA topology or chromosome segregation might result in the differential recruitment of DNA repair proteins at the site of DNA damage as well as a potentially compromised DNA repair, causing genomic and chromosomal instability (Burden and Osheroff 1998, Montecucco and Biamonti 2007, Subramanian, *et al* 2005, van Attikum and Gasser 2009, Wang 2002).

Hyperrecombination and chromosomal instability can be generated by the stimulation of activation-induced cytidine deaminase (AID), an enzyme converting cytidine to uridine involved in somatic hypermutation, B cell class-switch hyperrecombination and able to promote CML lymphoid blast crisis (Gruber, *et al* 2010, Klemm, *et al* 2009). AID activity is

stimulated in THO complex mutants, characterized by transcription-associated mutation and recombination, resulting in genetic instability associated with the formation of RNA-DNA hybrids called R-loops (Gomez-Gonzalez and Aguilera 2007, Gomez-Gonzalez, *et al* 2009). Evidence suggests that THO complex is important in the regulation of DNA repair proteins involved in NHEJ (e.g. Ku80 and DNA ligase IV) and heat shock proteins (e.g. Hsp40 and Hsp70), while AID-mediated DNA double strand breaks may be resolved by NHEJ (Rehwinkel, *et al* 2004, Ruiz, *et al* 2011). In this study, we showed that Thoc5/Fmip cytoplasmic tyrosine phosphorylation is mediated by the proto-oncogene Src, whose kinase family is a source of imatinib resistance in advance stages of leukaemia. We also demonstrated that this event is induced by genotoxic stress and that Src family kinase is downstream of different leukaemogenic PTK signalling, CD45 phosphatase and the chemokine SDF-1. Moreover, increased THOC5/FMIP tyrosine phosphorylation was also found in CD34+ CD38- CD90+ cancer stem cells. This modulation may be relevant to treatment resistance and cell differentiation as Thoc5/Fmip has been shown to be required for monocytic development and haemopoietic stem cell survival *in vivo* while ATM and p53 regulate Thoc5/Fmip binding properties with mRNA involved in cell differentiation in response to etoposide (Carney, *et al* 2009, Mancini, *et al* 2010, Ramachandran, *et al* 2011). Thus the impact of genotoxic stress and leukaemogenic PTKs on Thoc5/Fmip phosphoresidues regulated by ATM (tyrosine 225 and serine 307, data not shown) suggests that the regulation of mRNA export by the THO/TREX complex during haemopoietic development may be impaired in response to oxidative stress and external signals (Guria, *et al* 2011, Ramachandran, *et al* 2011). BCR/ABL and other leukaemogenic PTKs might continuously activate a genotoxic stress response on Thoc5/Fmip altering mRNA export, cell differentiation and possibly apoptosis signalling (Mancini, *et al* 2010). This regulation might also stimulate transcription-associated mutation and recombination *via* the formation of R-loops and AID activation to generate genomic instability during disease progression (Gomez-Gonzalez, *et al* 2009, Klemm, *et al* 2009, Ruiz, *et al* 2011).

5.2. Future work

The identification of multiple protein phosphosites potentially modulated by both etoposide and BCR/ABL PTK requires validation with an alternative method for each site. This could be performed by mass spectrometry using SRM assay as shown above, or the design of phosphopeptide-specific antibodies. Priority might be given to proteins involved in sister chromatid cohesion or in the recruitment of DNA repair proteins such as Incenp and MDC1 respectively, due to their crucial role in the maintenance of genomic stability (Draviam, *et al* 2004, Jungmichel and Stucki 2010, Morrison, *et al* 2003, Wu, *et al* 2008, Xie, *et al* 2007). It would be particularly interesting to perform site-directed mutagenesis of MDC1 phosphorylation sites to understand the role of these sites in orchestrating the recruitment of DNA repair proteins, the loading of MDC1 onto H2AX signalling platform and cell fate decisions. As the synergistic action of both BCR/ABL PTK and etoposide action has been confirmed in this study for the murine Hemogen on serine 380, it would be particularly important to address this regulation on the human Hemogen sequence. It would be possible to do so by designing a new AQUA™ peptide or raising a phosphoantibody against the human sequence. As our data suggest that the phosphorylated Hemogen form found in the presence of BCR/ABL PTK and etoposide exposure is not abundant in Ba/F3 cells, i.e. estimated at approximately 20 fmol of phosphopeptide from 100 µg of nuclear proteins (equivalent to 2 million cells), these experiments are challenging. Thus, preliminary experiments may be performed using the K562 CML cell line before investigating the response of human CML primary samples with these drugs. To study the importance of Hemogen for BCR/ABL PTK-mediated cell survival and DNA repair, experiments using siRNA targeting Hemogen expression may be performed in combination with etoposide treatment, apoptosis and γ H2AX assays. Human and murine phosphomutant forms could be expressed separately in Ba/F3 cells to investigate the role of different phosphorylated Hemogen sequences in response to etoposide using the same assays. Hemogen interactome studies may be performed using immunoprecipitation of phosphorylated Hemogen to determine if its phosphorylation

recruits heterochromatin protein 1 (HP1) and Trim28/TIF-1beta/KAP-1 in the presence and absence of ATM inhibitor or 53BP1 siRNA. Kinase inhibition could also be carried out to further study the upstream pathways regulating Hemogen phosphorylation. Chromatin immunoprecipitation before and after DNA damage with Hemogen antibodies would also enable the identification of the pathway(s) controlled by this transcription factor.

It would be particularly interesting to delineate the role of Thoc5/Fmip tyrosine 225 phosphorylation regarding RNA processing and mRNA export in response to oxidative stress. This could be performed with Thoc5/Fmip null MEFs and the expression of several phosphomutants, as Thoc5/Fmip null haemopoietic cells do not survive. As the export of several mRNAs involved in cell differentiation has been found to be regulated by the exposure to etoposide, one could study the impact of Thoc5/Fmip Y225F expression on a subset of mRNA export targets under these conditions using cytosolic preparation and RT-PCR. Alternatively, a transcriptomic analysis could also be performed on cytosolic preparation under conditions affecting Thoc5/Fmip phosphorylation. Src as well as ATM and MEK/ERK activation after etoposide treatment can lead to NF- κ B activation and cell survival (Ahmed, *et al* 2009, Lluís, *et al* 2007, Panta, *et al* 2004). As the expression of Thoc5/Fmip Y225F may reduce apoptosis levels and increase the degradation of I κ B following etoposide and H₂O₂ treatment (data not shown), appropriate experiments should be performed to determine if NF- κ B is more activated in the presence of Thoc5/Fmip Y225F phosphomutant. Thus nuclear preparation, western blot, luciferase assay and electrophoretic mobility shift assay (EMSA) could be performed to determine the degree of activation of NF- κ B.

Further experiments on the effects of tyrosine 225 phosphorylation on Thoc5/Fmip action, interactome, mRNA association and cellular localization are also warranted.

5.3. Conclusion

We described the modulation of protein phosphorylation dynamics in response to genotoxic stress by the expression of leukaemogenic PTKs, a phenomenon which is believed to precipitate disease progression by blocking normal cell differentiation and promoting treatment resistance. Such modulation could be identified on several key proteins of the DNA damage response as well as haemopoietic development. Potentially deregulated, these proteins might promote unfaithful DNA repair, genomic instability, anti-apoptotic signalling and abnormal cell differentiation, resulting in leukaemia progression from a chronic phase disease to a more aggressive cancer.

Chapter 6.

References

Books, websites and electronic reports

- Cancer Research UK. (2011) CancerStats Incidence. Available:
http://info.cancerresearchuk.org/prod_consump/groups/cr_common/@nre/@sta/documents/generalcontent/cr_072111.pdf. Last accessed 15th Sep 2011.
- de Hoffmann, E. & Stroobant, V. (2007) Mass spectrometry : Principles and applications. *WILEY-VCH*, 3rd ed.
- Haematological Malignancy Research Network. (2011) Incidence statistics. Available:
<http://www.hmrn.org/Statistics/Incidence.aspx>. Last accessed 15th Sep 2011.

Publications

- Abe, T., Ishiai, M., Hosono, Y., Yoshimura, A., Tada, S., Adachi, N., Koyama, H., Takata, M., Takeda, S., Enomoto, T. & Seki, M. (2008) KU70/80, DNA-PKcs, and Artemis are essential for the rapid induction of apoptosis after massive DSB formation. *Cellular Signalling*, **20**, 1978-1985.
- Aebersold, R. & Mann, M. (2003) Mass spectrometry-based proteomics. *Nature*, **422**, 198-207.
- Affer, M., Dao, S., Liu, C., Olshen, A.B., Mo, Q., Viale, A., Lambek, C.L., Marr, T.G. & Clarkson, B.D. (2011) Gene expression differences between enriched normal and chronic myelogenous leukemia quiescent stem/progenitor cells and correlations with biological abnormalities. *Journal of oncology*, **2011**, 798592.
- Aguilera, A. (2005) Cotranscriptional mRNP assembly: from the DNA to the nuclear pore. *Current Opinion in Cell Biology*, **17**, 242-250.
- Ahmed, K.M., Nantajit, D., Fan, M., Murley, J.S., Grdina, D.J. & Li, J.J. (2009) Coactivation of ATM/ERK/NF-kappa B in the low-dose radiation-induced radioadaptive response in human skin keratinocytes. *Free Radical Biology and Medicine*, **46**, 1543-1550.
- Ainsztein, A.M., Kandels-Lewis, S.E., Mackay, A.M. & Earnshaw, W.C. (1998) INCENP centromere and spindle targeting: Identification of essential conserved motifs and involvement of heterochromatin protein HP1. *Journal of Cell Biology*, **143**, 1763-1774.
- Albajar, M., Teresa Gomez-Casares, M., Llorca, J., Mauleon, I., Vaque, J.P., Acosta, J.C., Bermudez, A., Donato, N., Delgado, M.D. & Leon, J. (2011) MYC in chronic myeloid leukemia: induction of aberrant DNA synthesis and association with poor response to imatinib. *Molecular Cancer Research*, **9**, 564-576.
- Amarante-Mendes, G.P., Kim, C.N., Liu, L., Huang, Y., Perkins, C.L., Green, D.R. & Bhalla, K. (1998) Bcr-Abl exerts its antiapoptotic effect against diverse apoptotic stimuli

- through blockage of mitochondrial release of cytochrome c and activation of caspase-3. *Blood*, **91**, 1700-1705.
- An, L.L., Li, G., Wu, K.F., Ma, X.T., Zheng, G.G., Qiu, L.G. & Song, Y.H. (2005) High expression of EDAG and its significance in AML. *Leukemia*, **19**, 1499-1502.
- Andersson, L. & Porath, J. (1986) Isolation of phosphoproteins by immobilized metal (Fe-3+) affinity-chromatography. *Analytical Biochemistry*, **154**, 250-254.
- Arlinghaus, R.B. (2002) Bcr: a negative regulator of the Bcr-Abl oncoprotein in leukemia. *Oncogene*, **21**, 8560-8567.
- Armirotti, A. & Damonte, G. (2010) Achievements and perspectives of top-down proteomics. *Proteomics*, **10**, 3566-3576.
- Ayoub, N., Jeyasekharan, A.D., Bernal, J.A. & Venkitaraman, A.R. (2008) HP1-beta mobilization promotes chromatin changes that initiate the DNA damage response. *Nature*, **453**, 682-U614.
- Ayoub, N., Jeyasekharan, A.D. & Venkitaraman, A.R. (2009) Mobilization and recruitment of HP1 - A bimodal response to DNA breakage. *Cell Cycle*, **8**, 2945-2950.
- Bai, R.Y., Dieter, P., Peschel, C., Morris, S.W. & Duyster, J. (1998) Nucleophosmin-anaplastic lymphoma kinase of large-cell anaplastic lymphoma is a constitutively active tyrosine kinase that utilizes phospholipase C-gamma to mediate its mitogenicity. *Molecular and Cellular Biology*, **18**, 6951-6961.
- Bakkenist, C.J. & Kastan, M.B. (2003) DNA damage activates ATM through intermolecular autophosphorylation and dimer dissociation. *Nature*, **421**, 499-506.
- Balasubramanian, K., Mirnikjoo, B. & Schroit, A.J. (2007) Regulated externalization of phosphatidylserine at the cell surface - Implications for apoptosis. *Journal of Biological Chemistry*, **282**, 18357-18364.
- Baldassarre, G., Battista, S., Belletti, B., Thakur, S., Pentimalli, F., Trapasso, F., Fedele, M., Pierantoni, G., Croce, C.M. & Fusco, A. (2003) Negative regulation of BRCA1 gene expression by HMGA1 proteins accounts for the reduced BRCA1 protein levels in sporadic breast carcinoma. *Molecular and Cellular Biology*, **23**, 2225-2238.
- Ball, A.R., Jr. & Yokomori, K. (2009) Revisiting the role of heterochromatin protein 1 in DNA repair. *Journal of Cell Biology*, **185**, 573-575.
- Bantscheff, M., Schirle, M., Sweetman, G., Rick, J. & Kuster, B. (2007) Quantitative mass spectrometry in proteomics: a critical review. *Analytical and Bioanalytical Chemistry*, **389**, 1017-1031.
- Barlow, C., Hirotsune, S., Paylor, R., Liyanage, M., Eckhaus, M., Collins, F., Shiloh, Y., Crawley, J.N., Ried, T., Tagle, D. & WynshawBoris, A. (1996) ATM-deficient mice: A paradigm of ataxia telangiectasia. *Cell*, **86**, 159-171.
- Barnett, C. & Krebs, J.E. (2011) WSTF does it all: a multifunctional protein in transcription, repair, and replication. *Biochemistry and Cell Biology-Biochimie Et Biologie Cellulaire*, **89**, 12-23.
- Basecke, J., Griesinger, F., Trumper, L. & Brittinger, G. (2002) Leukemia- and lymphoma-associated genetic aberrations in healthy individuals. *Annals of Hematology*, **81**, 64-75.
- Baud, V. & Karin, M. (2009) Is NF-kappa B a good target for cancer therapy? Hopes and pitfalls. *Nature Reviews Drug Discovery*, **8**, 33-40.

- Beausoleil, S.A., Jedrychowski, M., Schwartz, D., Elias, J.E., Villen, J., Li, J.X., Cohn, M.A., Cantley, L.C. & Gygi, S.P. (2004) Large-scale characterization of HeLa cell nuclear phosphoproteins. *Proceedings of the National Academy of Sciences of the United States of America*, **101**, 12130-12135.
- Beghini, A., Peterlongo, P., Ripamonti, C.B., Larizza, L., Cairoli, R., Morra, E. & Mecucci, C. (2000) C-kit mutations in core binding factor leukemias. *Blood*, **95**, 726-727.
- Benneriah, Y., Daley, G.Q., Mesmasson, A.M., Witte, O.N. & Baltimore, D. (1986) The chronic myelogenous leukemia specific p210-protein is the product of the BCR/ABL hybrid gene. *Science*, **233**, 212-214.
- Bennetzen, M.V., Larsen, D.H., Bunkenborg, J., Bartek, J., Lukas, J. & Andersen, J.S. (2010) Site-specific phosphorylation dynamics of the nuclear proteome during the DNA damage response. *Molecular & Cellular Proteomics*, **9**, 1314-1323.
- Bentley, D.J., Harrison, C., Ketchen, A.M., Redhead, N.J., Samuel, K., Waterfall, M., Ansell, J.D. & Melton, D.W. (2002) DNA ligase I null mouse cells show normal DNA repair activity but altered DNA replication and reduced genome stability. *Journal of Cell Science*, **115**, 1551-1561.
- Bergemann, A.D., Cole, F. & Hirschhorn, K. (2005) The etiology of Wolf-Hirschhorn syndrome. *Trends in Genetics*, **21**, 188-195.
- Bettinger, B.T., Gilbert, D.M. & Amberg, D.C. (2004) Actin up in the nucleus. *Nature Reviews Molecular Cell Biology*, **5**, 410-415.
- Bhatia, R., Holtz, M., Niu, N., Gray, R., Snyder, D.S., Sawyers, C.L., Arber, D.A., Slovak, M.L. & Forman, S.J. (2003) Persistence of malignant hematopoietic progenitors in chronic myelogenous leukemia patients in complete cytogenetic remission following imatinib mesylate treatment. *Blood*, **101**, 4701-4707.
- Bicho, C.C., Alves, F.d.L., Chen, Z.A., Rappsilber, J. & Sawin, K.E. (2010) A genetic engineering solution to the "arginine conversion problem" in stable isotope labeling by amino acids in cell culture (SILAC). *Molecular & Cellular Proteomics*, **9**, 1567-1577.
- Birkenkamp, K.U., Essafi, A., van der Vos, K.E., da Costa, M., Hui, R.C.Y., Holstege, F., Koenderman, L., Lam, E.W.F. & Coffey, P.J. (2007) FOXO3a induces differentiation of Bcr-Abl- transformed cells through transcriptional down-regulation of Id1. *Journal of Biological Chemistry*, **282**, 2211-2220.
- Blackledge, N.P., Zhou, J.C., Tolstorukov, M.Y., Farcas, A.M., Park, P.J. & Klose, R.J. (2010) CpG islands recruit a histone H3 lysine 36 demethylase. *Molecular Cell*, **38**, 179-190.
- Blake, S.J., Lyons, A.B. & Hughes, T.P. (2009) Nilotinib inhibits the Src-family kinase LCK and T-cell function in vitro. *Journal of cellular and molecular medicine*, **13**, 599-601.
- Bodenmiller, B., Mueller, L.N., Mueller, M., Domon, B. & Aebersold, R. (2007) Reproducible isolation of distinct, overlapping segments of the phosphoproteome. *Nature Methods*, **4**, 231-237.
- Boersema, P.J., Foong, L.Y., Ding, V.M.Y., Lemeer, S., van Breukelen, B., Philp, R., Boekhorst, J., Snel, B., den Hertog, J., Choo, A.B.H. & Heck, A.J.R. (2010) In-depth qualitative and quantitative profiling of tyrosine phosphorylation using a combination of phosphopeptide immunoaffinity purification and stable isotope dimethyl labeling. *Molecular & Cellular Proteomics*, **9**, 84-99.
- Boersema, P.J., Mohammed, S. & Heck, A.J.R. (2009) Phosphopeptide fragmentation and analysis by mass spectrometry. *Journal of Mass Spectrometry*, **44**, 861-878.

- Boissan, M., Feger, F., Guillosson, J.J. & Arock, M. (2000) c-Kit and c-kit mutations in mastocytosis and other hematological diseases. *Journal of Leukocyte Biology*, **67**, 135-148.
- Boisvert, F.-M., Lam, Y.W., Lamont, D. & Lamond, A.I. (2010) A quantitative proteomics analysis of subcellular proteome localization and changes induced by DNA damage. *Molecular & Cellular Proteomics*, **9**, 457-470.
- Bothmer, A., Robbiani, D.F., Feldhahn, N., Gazumyan, A., Nussenzweig, A. & Nussenzweig, M.C. (2010) 53BP1 regulates DNA resection and the choice between classical and alternative end joining during class switch recombination. *Journal of Experimental Medicine*, **207**, 855-865.
- Bouwman, P., Aly, A., Escandell, J.M., Pieterse, M., Bartkova, J., van der Gulden, H., Hiddingh, S., Thanasoula, M., Kulkarni, A., Yang, Q., Haffty, B.G., Tommiska, J., Blomqvist, C., Drapkin, R., Adams, D.J., Nevanlinna, H., Bartek, J., Tarsounas, M., Ganesan, S. & Jonkers, J. (2010) 53BP1 loss rescues BRCA1 deficiency and is associated with triple-negative and BRCA-mutated breast cancers. *Nature Structural & Molecular Biology*, **17**, 688-U656.
- Branford, S. & Hughes, T.P. (2011) Mutational analysis in chronic myeloid leukemia: when and what to do? *Current Opinion in Hematology*, **18**, 111-116.
- Bree, R.T., Neary, C., Samali, A. & Lowndes, N.F. (2004) The switch from survival responses to apoptosis after chromosomal breaks. *DNA Repair*, **3**, 989-995.
- Brehme, M., Hantschel, O., Colinge, J., Kaupe, I., Panyavsky, M., Koecher, T., Mechtler, K., Bennett, K.L. & Superti-Furga, G. (2009) Charting the molecular network of the drug target Bcr-Abl. *Proceedings of the National Academy of Sciences of the United States of America*, **106**, 7414-7419.
- Bulavin, D.V. & Fornace, A.J. (2004) p38 MAP kinase's emerging role as a tumor suppressor. *Advances in Cancer Research*, Vol 92, **92**, 95-118.
- Bulavin, D.V., Phillips, C., Nannenga, B., Timofeev, O., Donehower, L.A., Anderson, C.W., Appella, E. & Fornace, A.J. (2004) Inactivation of the Wip1 phosphatase inhibits mammary tumorigenesis through p38 MAPK-mediated activation of the p16(Ink4a)-p19(Arf) pathway. *Nature Genetics*, **36**, 343-350.
- Bunting, S.F., Callen, E., Wong, N., Chen, H.-T., Polato, F., Gunn, A., Bothmer, A., Feldhahn, N., Fernandez-Capetillo, O., Cao, L., Xu, X., Deng, C.-X., Finkel, T., Nussenzweig, M., Stark, J.M. & Nussenzweig, A. (2010) 53BP1 inhibits homologous recombination in Brca1-deficient cells by blocking resection of DNA breaks. *Cell*, **141**, 243-254.
- Burden, D.A. & Osheroff, N. (1998) Mechanism of action of eukaryotic topoisomerase II and drugs targeted to the enzyme. *Biochimica Et Biophysica Acta-Gene Structure and Expression*, **1400**, 139-154.
- Burke, B.A. & Carroll, M. (2010) BCR-ABL: a multi-faceted promoter of DNA mutation in chronic myelogenous leukemia. *Leukemia*, **24**, 1105-1112.
- Calabretta, B. & Perrotti, D. (2004) The biology of CML blast crisis. *Blood*, **103**, 4010-4022.
- Cammas, F., Herzog, M., Lerouge, T., Chambon, P. & Losson, R. (2004) Association of the transcriptional corepressor TIF1 beta with heterochromatin protein 1 (HP1): an essential role for progression through differentiation. *Genes & Development*, **18**, 2147-2160.

- Cann, K.L. & Hicks, G.G. (2007) Regulation of the cellular DNA double-strand break response. *Biochemistry and Cell Biology-Biochimie Et Biologie Cellulaire*, **85**, 663-674.
- Carney, L., Pierce, A., Rijnen, M., Sanchez, M.B.G., Hamzah, H.G., Zhang, L., Tamura, T. & Whetton, A.D. (2009) THOC5 couples M-CSF receptor signaling to transcription factor expression. *Cellular Signalling*, **21**, 309-316.
- Carroll, M., Tomasson, M.H., Barker, G.F., Golub, T.R. & Gilliland, D.G. (1996) The TEL platelet-derived growth factor beta receptor (PDGF beta R) fusion in chronic myelomonocytic leukemia is a transforming protein that self-associates and activates PDGF beta R kinase-dependent signaling pathways. *Proceedings of the National Academy of Sciences of the United States of America*, **93**, 14845-14850.
- Castor, A., Nilsson, L., Astrand-Grundstrom, I., Buitenhuis, M., Ramirez, C., Anderson, K., Strombeck, B., Garwicz, S., Bekassy, A.N., Schmiegelow, K., Lausen, B., Hokland, P., Lehmann, S., Juliusson, G., Johansson, B. & Jacobsen, S.E.W. (2005) Distinct patterns of hematopoietic stem cell involvement in acute lymphoblastic leukemia. *Nature Medicine*, **11**, 630-637.
- Chen, J., Schmitt, A., Chen, B., Rojewski, M., Ruesseler, V., Fei, F., Yu, Y., Yu, X., Ringhoffer, M., von Harsdorf, S., Greiner, J., Goetzz, M., Guillaume, P., Doehner, H., Bunjes, D. & Schmitt, M. (2008a) Nilotinib hampers the proliferation and function of CD8(+) T lymphocytes through inhibition of T cell receptor signalling. *Journal of Cellular and Molecular Medicine*, **12**, 2107-2118.
- Chen, L., Nievera, C.J., Lee, A.Y.-L. & Wu, X. (2008b) Cell cycle-dependent complex formation of BRCA1.CtIP.MRN is important for DNA double-strand break repair. *Journal of Biological Chemistry*, **283**, 7713-7720.
- Chen, Y., Takita, J., Choi, Y.L., Kato, M., Ohira, M., Sanada, M., Wang, L., Soda, M., Kikuchi, A., Igarashi, T., Nakagawara, A., Hayashi, Y., Mano, H. & Ogawa, S. (2008c) Oncogenic mutations of ALK kinase in neuroblastoma. *Nature*, **455**, 971-U956.
- Chesi, M., Nardini, E., Lim, R.S.C., Smith, K.D., Kuehl, W.M. & Bergsagel, P.L. (1998) The t(4;14) translocation in myeloma dysregulates both FGFR3 and a novel gene, MMSET, resulting in IgH/MMSET hybrid transcripts. *Blood*, **92**, 3025-3034.
- Chew, J., Biswas, S., Shreeram, S., Humaidi, M., Wong, E.T., Dhillon, M.K., Teo, H., Hazra, A., Fang, C.C., Lopez-Collazo, E., Bulavin, D.V. & Tergaonkar, V. (2009) WIP1 phosphatase is a negative regulator of NF-kappa B signalling. *Nature Cell Biology*, **11**, 659-U493.
- Choudhary, C., Olsen, J.V., Brandts, C., Cox, J., Reddy, P.N.G., Boehmer, F.D., Gerke, V., Schmidt-Arras, D.-E., Berdel, W.E., Mueller-Tidow, C., Mann, M. & Serve, H. (2009) Mislocalized activation of oncogenic RTKs switches downstream signaling outcomes. *Molecular Cell*, **36**, 326-339.
- Chow, K.U., Nowak, D., Trepohl, B., Hochmuth, S., Schneider, B., Hoelzer, D., Mitrou, P.S., Bergmann, L., Ottmann, O.G. & Boehrer, S. (2007) The tyrosine kinase inhibitor AMN107 (Nilotinib) exhibits off-target effects in lymphoblastic cell lines. *Leukemia & Lymphoma*, **48**, 1379-1388.
- Chowdhury, D., Keogh, M.C., Ishii, H., Peterson, C.L., Buratowski, S. & Lieberman, J. (2005) gamma-H2AX dephosphorylation by protein phosphatase 2A facilitates DNA double-strand break repair. *Molecular Cell*, **20**, 801-809.

- Cimprich, K.A. & Cortez, D. (2008) ATR: an essential regulator of genome integrity. *Nature Reviews Molecular Cell Biology*, **9**, 616-627.
- Cohn, M.A. & D'Andrea, A.D. (2008) Chromatin recruitment of DNA repair proteins: lessons from the Fanconi anemia and double-strand break repair pathways. *Molecular Cell*, **32**, 306-312.
- Cook, P.J., Ju, B.G., Telese, F., Wang, X., Glass, C.K. & Rosenfeld, M.G. (2009) Tyrosine dephosphorylation of H2AX modulates apoptosis and survival decisions. *Nature*, **458**, 591-U553.
- Cooke, M.S., Evans, M.D., Dizdaroglu, M. & Lunec, J. (2003) Oxidative DNA damage: mechanisms, mutation, and disease. *FASEB Journal*, **17**, 1195-1214.
- Copland, M., Hamilton, A., Eirick, L.J., Baird, J.W., Allan, E.K., Jordanides, N., Barow, M., Mountford, J.C. & Holyoake, T.L. (2006) Dasatinib (BMS-354825) targets an earlier progenitor population than imatinib in primary CML but does not eliminate the quiescent fraction. *Blood*, **107**, 4532-4539.
- Corbin, A.S., Agarwal, A., Loriaux, M., Cortes, J., Deininger, M.W. & Druker, B.J. (2011) Human chronic myeloid leukemia stem cells are insensitive to imatinib despite inhibition of BCR-ABL activity. *Journal of Clinical Investigation*, **121**, 396-409.
- Costello, R.T., Mallet, F., Gaugler, B., Sainty, D., Arnoulet, C., Gastaut, J.A. & Olive, D. (2000) Human acute myeloid leukemia CD34(+)/CD38(-) progenitor cells have decreased sensitivity to chemotherapy and fas-induced apoptosis, reduced immunogenicity, and impaired dendritic cell transformation capacities. *Cancer Research*, **60**, 4403-4411.
- Cramer, K., Nieborowska-Skorska, M., Koptyra, M., Slupianek, A., Penserga, E.T.P., Eaves, C.J., Aulitzky, W. & Skorski, T. (2008) BCR/ABL and other kinases from chronic myeloproliferative disorders stimulate single-strand annealing, an unfaithful DNA double-strand break repair. *Cancer Research*, **68**, 6884-6888.
- Cross, N.C.P., Daley, G.Q., Green, A.R., Hughes, T.P., Jamieson, C., Manley, P., Mughal, T., Perrotti, D., Radich, J., Skoda, R., Soverini, S., Vainchenker, W., Verstovsek, S., Villeval, J.L. & Goldman, J.M. (2008) BCR-ABL1-positive CML and BCR-ABL1-negative chronic myeloproliferative disorders: some common and contrasting features. *Leukemia*, **22**, 1975-1989.
- Cully, M., You, H., Levine, A.J. & Mak, T.W. (2006) Beyond PTEN mutations: the PI3K pathway as an integrator of multiple inputs during tumorigenesis. *Nature Reviews Cancer*, **6**, 184-192.
- Cumming, G., Fidler, F. & Vaux, D.L. (2007) Error bars in experimental biology. *Journal of Cell Biology*, **177**, 7-11.
- Daley, G.Q. & Baltimore, D. (1988) Transformation of an interleukin-3-dependent hematopoietic-cell line by the chronic myelogenous leukemia-specific P210bcr/Abl protein. *Proceedings of the National Academy of Sciences of the United States of America*, **85**, 9312-9316.
- Daley, G.Q., McLaughlin, J., Witte, O.N. & Baltimore, D. (1987) The CML-specific p210 BCR/ABL protein, unlike v-ABL, does not transform NIH/3T3 fibroblasts. *Science*, **237**, 532-535.

- Daley, G.Q., Vanetten, R.A. & Baltimore, D. (1990) Induction of chronic myelogenous leukemia in mice by the p210BCR/ABL gene of the Philadelphia-chromosome. *Science*, **247**, 824-830.
- de Hoon, M.J.L., Imoto, S., Nolan, J. & Miyano, S. (2004) Open source clustering software. *Bioinformatics*, **20**, 1453-1454.
- de Jonge, H.J.M., de Bont, E.S.J.M., Valk, P.J.M., Schuringa, J.J., Kies, M., Woolthuis, C.M., Delwel, R., Veeger, N.J.G.M., Vellenga, E., Lowenberg, B. & Huls, G. (2009) AML at older age: age-related gene expression profiles reveal a paradoxical down-regulation of p16(INK4A) mRNA with prognostic significance. *Blood*, **114**, 2869-2877.
- Deguchi, Y., Kimura, S., Ashihara, E., Niwa, T., Hodohara, K., Fujiyama, Y. & Maekawa, T. (2008) Comparison of imatinib, dasatinib, nilotinib and INNO-406 in imatinib-resistant cell lines. *Leukemia Research*, **32**, 980-983.
- Delhommeau, F., Pisani, D.F., James, C., Casadevall, N., Constantinescu, S. & Vainchenker, W. (2006) Oncogenic mechanisms in myeloproliferative disorders. *Cellular and Molecular Life Sciences*, **63**, 2939-2953.
- Deribe, Y.L., Pawson, T. & Dikic, I. (2010) Post-translational modifications in signal integration. *Nature Structural & Molecular Biology*, **17**, 666-672.
- Deutsch, E., Dugray, A., AbdulKarim, B., Marangoni, E., Maggiorella, L., Vaganay, S., M'Kacher, R., Rasy, S.D., Eschwege, F., Vainchenker, W., Turhan, A.G. & Bourhis, J. (2001) BCR-ABL down-regulates the DNA repair protein DNA-PKcs. *Blood*, **97**, 2084-2090.
- Deutsch, E., Jarrousse, S., Buet, D., Dugray, A., Bonnet, M.L., Vozenin-Brotons, M.C., Guilhot, F., Turhan, A.G., Feunteun, J. & Bourhis, J. (2003) Down-regulation of BRCA1 in BCR-ABL-expressing hematopoietic cells. *Blood*, **101**, 4583-4588.
- Deveraux, Q.L., Roy, N., Stennicke, H.R., Van Arsdale, T., Zhou, Q., Srinivasula, S.M., Alnemri, E.S., Salvesen, G.S. & Reed, J.C. (1998) IAPs block apoptotic events induced by caspase-8 and cytochrome c by direct inhibition of distinct caspases. *Embo Journal*, **17**, 2215-2223.
- Deveraux, Q.L., Takahashi, R., Salvesen, G.S. & Reed, J.C. (1997) X-linked IAP is a direct inhibitor of cell-death proteases. *Nature*, **388**, 300-304.
- Dierov, J., Dierova, R. & Carroll, M. (2004) BCR/ABL translocates to the nucleus and disrupts an ATR-dependent intra-S phase checkpoint. *Cancer Cell*, **5**, 275-285.
- Dierov, J., Sanchez, P.V., Burke, B.A., Padilla-Nash, H., Putt, M.E., Ried, T. & Carroll, M. (2009) BCR/ABL induces chromosomal instability after genotoxic stress and alters the cell death threshold. *Leukemia*, **23**, 279-286.
- Difilippantonio, S., Gapud, E., Wong, N., Huang, C.-Y., Mahowald, G., Chen, H.T., Kruhlak, M.J., Callen, E., Livak, F., Nussenzweig, M.C., Sleckman, B.P. & Nussenzweig, A. (2008) 53BP1 facilitates long-range DNA end-joining during V(D)J recombination. *Nature*, **456**, 529-U557.
- Dimitrova, N., Chen, Y.-C.M., Spector, D.L. & de Lange, T. (2008) 53BP1 promotes non-homologous end joining of telomeres by increasing chromatin mobility. *Nature*, **456**, 524-U551.

- Dittmann, K., Mayer, C., Kehlbach, R., Rothmund, M.-C. & Rodemann, H.P. (2009) Radiation-induced lipid peroxidation activates src kinase and triggers nuclear EGFR transport. *Radiotherapy and Oncology*, **92**, 379-382.
- Dodson, H. & Morrison, C.G. (2009) Increased sister chromatid cohesion and DNA damage response factor localization at an enzyme-induced DNA double-strand break in vertebrate cells. *Nucleic Acids Research*, **37**, 6054-6063.
- Dolado, I., Swat, A., Ajenjo, N., De Vita, G., Cuadrado, A. & Nebreda, A.R. (2007) p38 alpha MAP kinase as a sensor of reactive oxygen species in tumorigenesis. *Cancer Cell*, **11**, 191-205.
- Donato, N.J., Wu, J.Y., Stapley, J., Gallick, G., Lin, H., Arlinghaus, R. & Talpaz, M. (2003) BCR-ABL independence and LYN kinase overexpression in chronic myelogenous leukemia cells selected for resistance to STI571. *Blood*, **101**, 690-698.
- Dosil, M., Wang, S.L. & Lemischka, I.R. (1993) Mitogenic signaling and substrate-specificity of the FLK2/FLT3 receptor tyrosine kinase in fibroblasts and interleukin 3-dependent hematopoietic-cells. *Molecular and Cellular Biology*, **13**, 6572-6585.
- Downs, J.A. (2007) Chromatin structure and DNA double-strand break responses in cancer progression and therapy. *Oncogene*, **26**, 7765-7772.
- Draviam, V.M., Xie, S. & Sorger, P.K. (2004) Chromosome segregation and genomic stability. *Current Opinion in Genetics & Development*, **14**, 120-125.
- Droge, W. (2002) Free radicals in the physiological control of cell function. *Physiological Reviews*, **82**, 47-95.
- Druker, B.J., Sawyers, C.L., Kantarjian, H., Resta, D.J., Reese, S.F., Ford, J.M., Capdeville, R. & Talpaz, M. (2001) Activity of a specific inhibitor of the BCR-ABL tyrosine kinase in the blast crisis of chronic myeloid leukemia and acute lymphoblastic leukemia with the philadelphia chromosome. *New England Journal of Medicine*, **344**, 1038-1042.
- Dubrez, L., Eymin, B., Sordet, O., Droin, N., Turhan, A.G. & Solary, E. (1998) BCR-ABL delays apoptosis upstream of procaspase-3 activation. *Blood*, **91**, 2415-2422.
- Duncan, P.I., Stojdl, D.F., Marius, R.M., Scheit, K.H. & Bell, J.C. (1998) The Clk2 and Clk3 dual-specificity protein kinases regulate the intranuclear distribution of SR proteins and influence pre-mRNA splicing. *Experimental Cell Research*, **241**, 300-308.
- Dupere-Minier, G., Desharnais, P. & Bernier, J. (2010) Involvement of tyrosine phosphatase CD45 in apoptosis. *Apoptosis*, **15**, 1-13.
- El Bounkari, O., Guria, A., Klebba-Faerber, S., Claussen, M., Pieler, T., Griffiths, J.R., Whetton, A.D., Koch, A. & Tamura, T. (2009) Nuclear localization of the pre-mRNA associating protein THOC7 depends upon its direct interaction with Fms tyrosine kinase interacting protein (FMIP). *Febs Letters*, **583**, 13-18.
- Elliott, B., Richardson, C. & Jasin, M. (2005) Chromosomal translocation mechanisms at intronic Alu elements in mammalian cells. *Molecular Cell*, **17**, 885-894.
- Essers, M.A.G., de Vries-Smits, L.M.M., Barker, N., Polderman, P.E., Burgering, B.M.T. & Korswagen, H.C. (2005) Functional interaction between beta-catenin and FOXO in oxidative stress signaling. *Science*, **308**, 1181-1184.
- Evdonin, A.L., Guzhova, I.V., Margulis, B.A. & Medvedeva, N.D. (2006) Extracellular heat shock protein 70 mediates heat stress-induced epidermal growth factor receptor transactivation in A431 carcinoma cells. *Febs Letters*, **580**, 6674-6678.

- Feldhahn, N., Henke, N., Melchior, K., Duy, C., Soh, B.N., Klein, F., von Levetzow, G., Giebel, B., Li, A., Hofmann, W.-K., Jumaa, H. & Mueschen, M. (2007) Activation-induced cytidine deaminase acts as a mutator in BCR-ABL1-transformed acute lymphoblastic leukemia cells. *Journal of Experimental Medicine*, **204**, 1157-1166.
- Fenn, J.B., Mann, M., Meng, C.K., Wong, S.F. & Whitehouse, C.M. (1989) Electrospray ionization for mass-spectrometry of large biomolecules. *Science*, **246**, 64-71.
- Fernandes, M.S., Reddy, M.M., Gonneville, J.R., DeRoo, S.C., Podar, K., Griffin, J.D., Weinstock, D.M. & Sattler, M. (2009) BCR-ABL promotes the frequency of mutagenic single-strand annealing DNA repair. *Blood*, **114**, 1813-1819.
- Fialkow, P.J., Gartler, S.M. & Yoshida, A. (1967) Clonal origin of chronic myelocytic leukemia in man. *Proceedings of the National Academy of Sciences of the United States of America*, **58**, 1468-&.
- Fialkow, P.J., Jacobson, R.J. & Papayannopoulou, T. (1977) Chronic myelocytic-leukemia - Clonal origin in a stem-cell common to granulocyte, erythrocyte, platelet and monocyte-macrophage. *American Journal of Medicine*, **63**, 125-130.
- Florian, S., Sonneck, K., Hauswirth, A.W., Krauth, M.T., Schernthaner, G.H., Sperr, W.R. & Valent, P. (2006) Detection of molecular targets on the surface of CD34+/CD38-stem cells in various myeloid malignancies. *Leukemia & Lymphoma*, **47**, 207-222.
- Fnu, S., Williamson, E.A., De Haro, L.P., Brenneman, M., Wray, J., Shaheen, M., Radhakrishnan, K., Lee, S.-H., Nickoloff, J.A. & Hromas, R. (2011) Methylation of histone H3 lysine 36 enhances DNA repair by nonhomologous end-joining. *Proceedings of the National Academy of Sciences of the United States of America*, **108**, 540-545.
- Forman, H.J., Maiorino, M. & Ursini, F. (2010) Signaling functions of reactive oxygen species. *Biochemistry*, **49**, 835-842.
- Frescas, D., Guardavaccaro, D., Kuchay, S.M., Kato, H., Poleshko, A., Basrur, V., Elenitoba-Johnson, K.S., Katz, R.A. & Pagano, M. (2008) KDM2A represses transcription of centromeric satellite repeats and maintains the heterochromatic state. *Cell Cycle*, **7**, 3539-3547.
- Friedman, J.S., Rebel, V.I., Derby, R., Bell, K., Huang, T.T., Kuypers, F.A., Epstein, C.J. & Burakoff, S.J. (2001) Absence of mitochondrial superoxide dismutase results in a murine hemolytic anemia responsive to therapy with a catalytic antioxidant. *Journal of Experimental Medicine*, **193**, 925-934.
- Furitsu, T., Tsujimura, T., Tono, T., Ikeda, H., Kitayama, H., Koshimizu, U., Sugahara, H., Butterfield, J.H., Ashman, L.K., Kanayama, Y., Matsuzawa, Y., Kitamura, Y. & Kanakura, Y. (1993) Identification of mutations in the coding sequence of the protooncogene c-KIT in a human mast-cell leukemia-cell line causing ligand-independent activation of c-KIT product. *Journal of Clinical Investigation*, **92**, 1736-1744.
- Gabai, V.L., Sherman, M.Y. & Yaglom, J.A. (2010) HSP72 depletion suppresses gamma H2AX activation by genotoxic stresses via p53/p21 signaling. *Oncogene*, **29**, 1952-1962.
- Gallien, S., Duriez, E. & Domon, B. (2011) Selected reaction monitoring applied to proteomics. *Journal of Mass Spectrometry*, **46**, 298-312.

- Gao, Y., Katyal, S., Lee, Y., Zhao, J., Rehg, J.E., Russell, H.R. & McKinnon, P.J. (2011) DNA ligase III is critical for mtDNA integrity but not Xrcc1-mediated nuclear DNA repair. *Nature*, **471**, 240-U134.
- Garcia, B.A., Thomas, C.E., Kelleher, N.L. & Mizzen, C.A. (2008) Tissue-specific expression and post-translational modification of histone H3 variants. *Journal of Proteome Research*, **7**, 4225-4236.
- Geiger, T., Cox, J., Ostasiewicz, P., Wisniewski, J.R. & Mann, M. (2010) Super-SILAC mix for quantitative proteomics of human tumor tissue. *Nature Methods*, **7**, 383-U364.
- Geiger, T., Wisniewski, J.R., Cox, J., Zanivan, S., Kruger, M., Ishihama, Y. & Mann, M. (2011) Use of stable isotope labeling by amino acids in cell culture as a spike-in standard in quantitative proteomics. *Nature Protocols*, **6**, 147-157.
- George, R.E., Sanda, T., Hanna, M., Frohling, S., Luther, W., II, Zhang, J., Ahn, Y., Zhou, W., London, W.B., McGrady, P., Xue, L., Zozulya, S., Gregor, V.E., Webb, T.R., Gray, N.S., Gilliland, D.G., Diller, L., Greulich, H., Morris, S.W., Meyerson, M. & Look, A.T. (2008) Activating mutations in ALK provide a therapeutic target in neuroblastoma. *Nature*, **455**, 975-978.
- Gerber, S.A., Rush, J., Stemman, O., Kirschner, M.W. & Gygi, S.P. (2003) Absolute quantification of proteins and phosphoproteins from cell lysates by tandem MS. *Proceedings of the National Academy of Sciences of the United States of America*, **100**, 6940-6945.
- Gesbert, F. & Griffin, J.D. (2000) Bcr/Abl activates transcription of the Bcl-X gene through STAT5. *Blood*, **96**, 2269-2276.
- Ghaffari, S. (2008) Oxidative stress in the regulation of normal and neoplastic hematopoiesis. *Antioxidants & Redox Signaling*, **10**, 1923-1940.
- Ghaffari, S., Jagani, Z., Kitidis, C., Lodish, H.F. & Khosravi-Far, R. (2003) Cytokines and BCR-ABL mediate suppression of TRAIL-induced apoptosis through inhibition of forkhead FOXO3a transcription factor. *Proceedings of the National Academy of Sciences of the United States of America*, **100**, 6523-6528.
- Gilliland, D.G. & Griffin, J.D. (2002) The roles of FLT3 in hematopoiesis and leukemia. *Blood*, **100**, 1532-1542.
- Gioia, R., Leroy, C., Drullion, C., Lagarde, V., Etienne, G., Dulucq, S., Lippert, E., Roche, S., Mahon, F.-X. & Pasquet, J.-M. (2011) Quantitative phosphoproteomics revealed interplay between Syk and Lyn in the resistance to nilotinib in chronic myeloid leukemia cells. *Blood*, **118**, 2211-2221.
- Goldman, J.M. & Melo, J.V. (2008) BCR-ABL in chronic myelogenous leukemia - How does it work? *Acta Haematologica*, **119**, 212-217.
- Golub, T.R., Barker, G.F., Lovett, M. & Gilliland, D.G. (1994) Fusion of PDGF receptor-beta to a novel ETS-like gene, TEL, in chronic myelomonocytic leukemia with T(512) chromosomal translocation. *Cell*, **77**, 307-316.
- Gomez-Gonzalez, B. & Aguilera, A. (2007) Activation-induced cytidine deaminase action is strongly stimulated by mutations of the THO complex. *Proceedings of the National Academy of Sciences of the United States of America*, **104**, 8409-8414.
- Gomez-Gonzalez, B., Felipe-Abrio, I. & Aguilera, A. (2009) The S-phase checkpoint is required to respond to R-loops accumulated in THO mutants. *Molecular and Cellular Biology*, **29**, 5203-5213.

- Gong, Z.H., Brackertz, M. & Renkawitz, R. (2006) SUMO modification enhances p66-mediated transcriptional repression of the Mi-2/NuRD complex. *Molecular and Cellular Biology*, **26**, 4519-4528.
- Gonzalez-Barrera, S., Prado, F., Verhage, R., Brouwer, J. & Aguilera, A. (2002) Defective nucleotide excision repair in yeast hpr1 and tho2 mutants. *Nucleic Acids Research*, **30**, 2193-2201.
- Goodarzi, A.A., Noon, A.T., Deckbar, D., Ziv, Y., Shiloh, Y., Loebrich, M. & Jeggo, P.A. (2008) ATM signaling facilitates repair of DNA double-strand breaks associated with heterochromatin. *Molecular Cell*, **31**, 167-177.
- Goodarzi, A.A., Noon, A.T. & Jeggo, P.A. (2009) The impact of heterochromatin on DSB repair. *Biochemical Society Transactions*, **37**, 569-576.
- Gotlib, J., Cools, J., Malone, J.M., Schrier, S.L., Gilliland, D.G. & Coutre, S.E. (2004) The HP1L1-PDGF α fusion tyrosine kinase in hypereosinophilic syndrome and chronic eosinophilic leukemia: implications for diagnosis, classification, and management. *Blood*, **103**, 2879-2891.
- Graham, S.M., Jorgensen, H.G., Allan, E., Pearson, C., Alcorn, M.J., Richmond, L. & Holyoake, T.L. (2002) Primitive, quiescent, Philadelphia-positive stem cells from patients with chronic myeloid leukemia are insensitive to STI571 in vitro. *Blood*, **99**, 319-325.
- Grewal, S., Molina, D.M. & Bardwell, L. (2006) Mitogen-activated protein kinase (MAPK)-docking sites in MAPK kinases function as tethers that are crucial for MAPK regulation in vivo. *Cellular Signalling*, **18**, 123-134.
- Groban, E.S., Narayanan, A. & Jacobson, M.P. (2006) Conformational changes in protein loops and helices induced by post-translational phosphorylation. *Plos Computational Biology*, **2**, 238-250.
- Gronborg, M., Kristiansen, T.Z., Stensballe, A., Andersen, J.S., Ohara, O., Mann, M., Jensen, O.N. & Pandey, A. (2002) A mass spectrometry-based proteomic approach for identification of serine/threonine-phosphorylated proteins by enrichment with phospho-specific antibodies - Identification of a novel protein, Frigg, as a protein kinase A substrate. *Molecular & Cellular Proteomics*, **1**, 517-527.
- Gruber, F.X., Hjorth-Hansen, H., Mikkola, I., Stenke, L. & Johansen, T. (2006) A novel Bcr-Abl splice isoform is associated with the L248V mutation in CML patients with acquired resistance to imatinib. *Leukemia*, **20**, 2057-2060.
- Gruber, T.A., Chang, M.S., Sposto, R. & Mueschen, M. (2010) Activation-induced cytidine deaminase accelerates clonal evolution in BCR-ABL1-driven B-cell lineage acute lymphoblastic leukemia. *Cancer Research*, **70**, 7411-7420.
- Gu, T.L., Tothova, Z., Scheijen, B., Griffin, J.D., Gilliland, D.G. & Sternberg, D.W. (2004) NPM-ALK fusion kinase of anaplastic large-cell lymphoma regulates survival and proliferative signaling through modulation of FOXO3a. *Blood*, **103**, 4622-4629.
- Gu, Z.M., Flemington, C., Chittenden, T. & Zambetti, G.P. (2000) Ei24, a p53 response gene involved in growth suppression and apoptosis. *Molecular and Cellular Biology*, **20**, 233-241.
- Guo, F., Rocha, K., Bali, P., Pranpat, M., Fiskus, W., Boyapalle, S., Kumaraswamy, S., Balasis, M., Greedy, B., Armitage, E.S.M., Lawrence, N. & Bhalla, K. (2005a) Abrogation of heat shock protein 70 induction as a strategy, to increase

- antileukemia activity of heat shock protein 90 inhibitor 17-allylamino-demethoxy geldanamycin. *Cancer Research*, **65**, 10536-10544.
- Guo, F., Sigua, C., Bali, P., George, P., Fiskus, W., Scuto, A., Annavarapu, S., Mouttaki, A., Sondarva, G., Wei, S., Wu, J., Djeu, J. & Bhalla, K. (2005b) Mechanistic role of heat shock protein 70 in Bcr-Abl-mediated resistance to apoptosis in human acute leukemia cells. *Blood*, **105**, 1246-1255.
- Guria, A., Tran, D.D.H., Ramachandran, S., Koch, A., El Bounkari, O., Dutta, P., Hauser, H. & Tamura, T. (2011) Identification of mRNAs that are spliced but not exported to the cytoplasm in the absence of THOC5 in mouse embryo fibroblasts. *Rna-a Publication of the Rna Society*, **17**, 1048-1056.
- Gygi, S.P., Rist, B., Gerber, S.A., Turecek, F., Gelb, M.H. & Aebersold, R. (1999a) Quantitative analysis of complex protein mixtures using isotope-coded affinity tags. *Nature Biotechnology*, **17**, 994-999.
- Gygi, S.P., Rochon, Y., Franza, B.R. & Aebersold, R. (1999b) Correlation between protein and mRNA abundance in yeast. *Molecular and Cellular Biology*, **19**, 1720-1730.
- Habraken, Y. & Piette, J. (2006) NF-kappa B activation by double-strand breaks. *Biochemical Pharmacology*, **72**, 1132-1141.
- Hager, J.W. (2002) A new linear ion trap mass spectrometer. *Rapid Communications in Mass Spectrometry*, **16**, 512-526.
- Haim, N., Roman, J., Nemeč, J. & Sinha, B.K. (1986) Peroxidative free-radical formation and O-demethylation of etoposide(VP-16) and teniposide(VM-26). *Biochemical and Biophysical Research Communications*, **135**, 215-220.
- Hamdane, M., DavidCordonnier, M.H. & Dhalluin, J.C. (1997) Activation of p65 NF-kappa B protein by p210BCR-ABL in myeloid cell line (p210BCR-ABL activates p65 NF-kappa B). *Oncogene*, **15**, 2267-2275.
- Han, C.X., Zhang, X.R., Xu, W.R., Wang, W.B., Qian, H. & Chen, Y.C. (2005) Cloning of the nucleostemin gene and its function in transforming human embryonic bone marrow mesenchymal stem cells into F6 tumor cells. *International Journal of Molecular Medicine*, **16**, 205-213.
- Heinrich, R., Neel, B.G. & Rapoport, T.A. (2002) Mathematical models of protein kinase signal transduction. *Molecular Cell*, **9**, 957-970.
- Helleday, T., Petermann, E., Lundin, C., Hodgson, B. & Sharma, R.A. (2008) DNA repair pathways as targets for cancer therapy. *Nature Reviews Cancer*, **8**, 193-204.
- Hermiston, M.L., Zikherman, J. & Zhu, J.W. (2009) CD45, CD148, and Lyp/Pep: critical phosphatases regulating Src family kinase signaling networks in immune cells. *Immunological Reviews*, **228**, 288-311.
- Hess, J.F., Bourret, R.B. & Simon, M.I. (1988) Histidine phosphorylation and phosphoryl group transfer in bacterial chemotaxis. *Nature*, **336**, 139-143.
- Hirschginsberg, C., Lemaistre, A.C., Kantarjian, H., Talpaz, M., Cork, A., Freireich, E.J., Trujillo, J.M., Lee, M.S. & Stass, S.A. (1990) Ras mutations are rare events in Philadelphia chromosome-negative/BCR gene rearrangement-negative chronic myelogenous leukemia, but are prevalent in chronic myelomonocytic leukemia. *Blood*, **76**, 1214-1219.
- Hole, P.S., Darley, R.L. & Tonks, A. (2011) Do reactive oxygen species play a role in myeloid leukemias? *Blood*, **117**, 5816-5826.

- Hole, P.S., Pearn, L., Tonks, A.J., James, P.E., Burnett, A.K., Darley, R.L. & Tonks, A. (2010) Ras-induced reactive oxygen species promote growth factor-independent proliferation in human CD34(+) hematopoietic progenitor cells. *Blood*, **115**, 1238-1246.
- Hopfgartner, G., Varesio, E., Tschappat, V., Grivet, C., Bourgoigne, E. & Leuthold, L.A. (2004) Triple quadrupole linear ion trap mass spectrometer for the analysis of small molecules and macromolecules. *Journal of Mass Spectrometry*, **39**, 845-855.
- Horejsi, Z., Falck, J., Bakkenist, C.J., Kastan, M.B., Lukas, J. & Bartek, J. (2004) Distinct functional domains of Nbs1 modulate the timing and magnitude of ATM activation after low doses of ionizing radiation. *Oncogene*, **23**, 3122-3127.
- Hu, Q.Z., Noll, R.J., Li, H.Y., Makarov, A., Hardman, M. & Cooks, R.G. (2005) The Orbitrap: a new mass spectrometer. *Journal of Mass Spectrometry*, **40**, 430-443.
- Hu, Y.G., Liu, Y.H., Pelletier, S., Buchdunger, E., Warmuth, M., Fabbro, D., Hallek, M., Van Etten, R.A. & Li, S.G. (2004) Requirement of Src kinases Lyn, Hck and Fgr for BCR-ABL1-induced B-lymphoblastic leukemia but not chronic myeloid leukemia. *Nature Genetics*, **36**, 453-461.
- Huang, M., Whang, P., Chodaparambil, J.V., Pollyea, D.A., Kusler, B., Xu, L., Felsner, D.W. & Mitchell, B.S. (2011) Reactive oxygen species regulate nucleostemin oligomerization and protein degradation. *Journal of Biological Chemistry*, **286**, 11035-11046.
- Iiyama, M., Kakihana, K., Kurosu, T., Miura, O. (2006) Reactive oxygen species generated by hematopoietic cytokines play roles in activation of receptor-mediated signaling and in cell cycle progression. *Cellular Signalling*, **18**, 174-182.
- Ito, K., Hirao, A., Arai, F., Matsuoka, S., Takubo, K., Hamaguchi, I., Nomiyama, K., Hosokawa, K., Sakurada, K., Nakagata, N., Ikeda, Y., Mak, T.W. & Suda, T. (2004) Regulation of oxidative stress by ATM is required for self-renewal of haematopoietic stem cells. *Nature*, **431**, 997-1002.
- Ito, K., Hirao, A., Arai, F., Takubo, K., Matsuoka, S., Miyamoto, K., Ohmura, M., Naka, K., Hosokawa, K., Ikeda, Y. & Suda, T. (2006) Reactive oxygen species act through p38 MAPK to limit the lifespan of hematopoietic stem cells. *Nature Medicine*, **12**, 446-451.
- Itoh, G., Kanno, S.-i., Uchida, K.S.K., Chiba, S., Sugino, S., Watanabe, K., Mizuno, K., Yasui, A., Hirota, T. & Tanaka, K. (2011) CAMP (C13orf8, ZNF828) is a novel regulator of kinetochore-microtubule attachment. *Embo Journal*, **30**, 130-144.
- Jacobs, A.T. & Marnett, L.J. (2007) Heat shock factor 1 attenuates 4-hydroxynonenal-mediated apoptosis - Critical role for heat shock protein 70 induction and stabilization of Bcl-X-L. *Journal of Biological Chemistry*, **282**, 33412-33420.
- Jadayel, D.M., Osborne, L.R., Coignet, L.J.A., Zani, V.J., Tsui, L.C., Scherer, S.W. & Dyer, M.J.S. (1998) The BCL7 gene family: deletion of BCL7B in Williams syndrome. *Gene*, **224**, 35-44.
- Jagani, Z., Singh, A. & Khosravi-Far, R. (2008) FoxO tumor suppressors and BCR-ABL-induced leukemia: A matter of evasion of apoptosis. *Biochimica Et Biophysica Acta-Reviews on Cancer*, **1785**, 63-84.
- James, C., Ugo, V., Le Couedic, J.P., Staerk, J., Delhommeau, F., Lacout, C., Garcon, L., Raslova, H., Berger, R., Bennaceur-Griscelli, A., Villeval, J.L., Constantinescu, S.N.,

- Casadevall, N. & Vainchenker, W. (2005) A unique clonal JAK2 mutation leading to constitutive signalling causes polycythaemia vera. *Nature*, **434**, 1144-1148.
- Jamieson, C.H.M., Ailles, L.E., Dylla, S.J., Muijtjens, M., Jones, C., Zehnder, J.L., Gotlib, J., Li, K., Manz, M.G., Keating, A., Sawyers, C.L. & Weissman, I.L. (2004) Granulocyte-macrophage progenitors as candidate leukemic stem cells in blast-crisis CML. *New England Journal of Medicine*, **351**, 657-667.
- Janoueix-Lerosey, I., Lequin, D., Brugieres, L., Ribeiro, A., de Pontual, L., Combaret, V., Raynal, V., Puisieux, A., Schleiermacher, G., Pierron, G., Valteau-Couanet, D., Frebourg, T., Michon, J., Lyonnet, S., Amiel, J. & Delattre, O. (2008) Somatic and germline activating mutations of the ALK kinase receptor in neuroblastoma. *Nature*, **455**, 967-U951.
- Jensen, S.S. & Larsen, M.R. (2007) Evaluation of the impact of some experimental procedures on different phosphopeptide enrichment techniques. *Rapid Communications in Mass Spectrometry*, **21**, 3635-3645.
- Jiang, J., Yu, H., Shou, Y., Neale, G., Zhou, S., Lu, T. & Sorrentino, B.P. (2010) Hemgn is a direct transcriptional target of HOXB4 and induces expansion of murine myeloid progenitor cells. *Blood*, **116**, 711-719.
- Jimeno, S., Rondon, A.G., Luna, R. & Aguilera, A. (2002) The yeast THO complex and mRNA export factors link RNA metabolism with transcription and genome instability. *Embo Journal*, **21**, 3526-3535.
- Johnson, D.E. (2008) Src family kinases and the MEK/ERK pathway in the regulation of myeloid differentiation and myeloid leukemogenesis. *Advances in Enzyme Regulation, Vol 48*, **48**, 98-112.
- Jorgensen, H.G., Allan, E.K., Jordanides, N.E., Mountford, J.C. & Holyoake, T.L. (2007) Nilotinib exerts equipotent antiproliferative effects to imatinib and does not induce apoptosis in CD34(+) CML cells. *Blood*, **109**, 4016-4019.
- Jousset, C., Carron, C., Boureux, A., Quang, C.T., Oury, C., DusanterFourt, I., Charon, M., Levin, J., Bernard, O. & Ghysdael, J. (1997) A domain of TEL conserved in a subset of ETS proteins defines a specific oligomerization interface essential to the mitogenic properties of the TEL-PDGFR beta oncoprotein. *Embo Journal*, **16**, 69-82.
- Jungmichel, S. & Stucki, M. (2010) MDC1: The art of keeping things in focus. *Chromosoma*, **119**, 337-349.
- Juntilla, M.M., Patil, V.D., Calamito, M., Joshi, R.P., Birnbaum, M.J. & Koretzky, G.A. (2010) AKT1 and AKT2 maintain hematopoietic stem cell function by regulating reactive oxygen species. *Blood*, **115**, 4030-4038.
- Kagan, V.E., Kuzmenko, A.I., Tyurina, Y.Y., Shvedova, A.A., Matura, T. & Yalowich, J.C. (2001) Pro-oxidant and antioxidant mechanisms of etoposide in HL-60 cells: Role of myeloperoxidase. *Cancer Research*, **61**, 7777-7784.
- Kahn, P. (1995) From genome to proteome: Looking at a cell's proteins. *Science*, **270**, 369-370.
- Kamata, H., Honda, S., Maeda, S., Chang, L.F., Hirata, H. & Karin, M. (2005) Reactive oxygen species promote TNF alpha-induced death and sustained JNK activation by inhibiting MAP kinase phosphatases. *Cell*, **120**, 649-661.

- Kanakura, Y., Ikeda, H., Kitayama, H., Sugahara, H. & Furitsu, T. (1993) Expression, function and activation of the proto-oncogene c-Kit product in human leukemia cells. *Leukemia & Lymphoma*, **10**, 35-41.
- Kang, S.W., Chae, H.Z., Seo, M.S., Kim, K.H., Baines, I.C. & Rhee, S.G. (1998) Mammalian peroxiredoxin isoforms can reduce hydrogen peroxide generated in response to growth factors and tumor necrosis factor-alpha. *Journal of Biological Chemistry*, **273**, 6297-6302.
- Karanjawala, Z.E., Murphy, N., Hinton, D.R., Hsieh, C.L. & Lieber, M.R. (2002) Oxygen metabolism causes chromosome breaks and is associated with the neuronal apoptosis observed in DNA double-strand break repair mutants. *Current Biology*, **12**, 397-402.
- Karas, M., Bahr, U., Ingendoh, A., Nordhoff, E., Stahl, B., Strupat, K. & Hillenkamp, F. (1990) Principles and applications of matrix-assisted UV laser desorption ionization mass spectrometry. *Analytica Chimica Acta*, **241**, 175-185.
- Karas, M. & Hillenkamp, F. (1988) Laser desorption ionization of proteins with molecular masses exceeding 10000 Daltons. *Analytical Chemistry*, **60**, 2299-2301.
- Karas, M., Ingendoh, A., Bahr, U. & Hillenkamp, F. (1989) Ultraviolet-laser desorption ionization mass spectrometry of femtomolar amounts of large proteins. *Biomedical and Environmental Mass Spectrometry*, **18**, 841-843.
- Kass, E.M., Moynahan, M.E. & Jasin, M. (2010) Loss of 53BP1 is a gain for BRCA1 mutant cells. *Cancer Cell*, **17**, 423-425.
- Katahira, J., Inoue, H., Hurt, E. & Yoneda, Y. (2009) Adaptor Aly and co-adaptor Thoc5 function in the Tap-p15-mediated nuclear export of HSP70 mRNA. *Embo Journal*, **28**, 556-567.
- Kebarle, P. & Peschke, M. (2000) On the mechanisms by which the charged droplets produced by electrospray lead to gas phase ions. *Analytica Chimica Acta*, **406**, 11-35.
- Keene, P., Mendelow, B., Pinto, M.R., Bezwoda, W., Macdougall, L., Falkson, G., Ruff, P. & Bernstein, R. (1987) Abnormalities of chromosome 12P13 and malignant proliferation of eosinophils - A nonrandom association. *British Journal of Haematology*, **67**, 25-31.
- Kharas, M.G., Okabe, R., Ganis, J.J., Gozo, M., Khandan, T., Paktinat, M., Gilliland, D.G. & Gritsman, K. (2010) Constitutively active AKT depletes hematopoietic stem cells and induces leukemia in mice. *Blood*, **115**, 1406-1415.
- Khokhlatchev, A.V., Canagarajah, B., Wilsbacher, J., Robinson, M., Atkinson, M., Goldsmith, E. & Cobb, M.H. (1998) Phosphorylation of the MAP kinase ERK2 promotes its homodimerization and nuclear translocation. *Cell*, **93**, 605-615.
- Kim, J.H., Chu, S.C., Gramlich, J.L., Pride, Y.B., Babendreier, E., Chauhan, D., Salgia, R., Podar, K., Griffin, J.D. & Sattler, M. (2005) Activation of the PI3K/mTOR pathway by BCR-ABL contributes to increased production of reactive oxygen species. *Blood*, **105**, 1717-1723.
- Kim, S.-A., Chang, S., Yoon, J.-H. & Ahn, S.-G. (2008) TAT-Hsp40 inhibits oxidative stress-mediated cytotoxicity via the inhibition of Hsp70 ubiquitination. *Febs Letters*, **582**, 734-740.

- Kirkpatrick, D.S., Gerber, S.A. & Gygi, S.P. (2005) The absolute quantification strategy: a general procedure for the quantification of proteins and post-translational modifications. *Methods*, **35**, 265-273.
- Kitayama, H., Kanakura, Y., Furitsu, T., Tsujimura, T., Oritani, K., Ikeda, H., Sugahara, H., Mitsui, H., Kanayama, Y., Kitamura, Y. & Matsuzawa, Y. (1995) Constitutively activating mutations of c-KIT receptor tyrosine kinase confer factor-independent growth and tumorigenicity of factor-dependent hematopoietic cell lines. *Blood*, **85**, 790-798.
- Klco, J.M., Kreisel, F.H., Zehnbaauer, B.A., Kulkarni, S., Hassan, A. & Frater, J.L. (2008) The spectrum of adult B-lymphoid leukemias with BCR-ABL: Molecular diagnostic, cytogenetic, and clinical laboratory perspectives. *American Journal of Hematology*, **83**, 901-907.
- Klejman, A., Schreiner, S.J., Nieborowska-Skorska, M., Slupianek, A., Wilson, M., Smithgall, T.E. & Skorski, T. (2002) The Src family kinase Hck couples BCR/ABL to STAT5 activation in myeloid leukemia cells. *Embo Journal*, **21**, 5766-5774.
- Klemm, L., Duy, C., Iacobucci, I., Kuchen, S., von Levetzow, G., Feldhahn, N., Henke, N., Li, Z., Hoffmann, T.K., Kim, Y.-m., Hofmann, W.-K., Jumaa, H., Groffen, J., Heisterkamp, N., Martinelli, G., Lieber, M.R., Casellas, R. & Mueschen, M. (2009) The B cell mutator AID promotes B lymphoid blast crisis and drug resistance in chronic myeloid leukemia. *Cancer Cell*, **16**, 232-245.
- Konishi, A., Shimizu, S., Hirota, J., Takao, T., Fan, Y.H., Matsuoka, Y., Zhang, L.L., Yoneda, Y., Fujii, Y., Skouitchi, A.I. & Tsujimoto, Y. (2003) Involvement of histone H1.2 in apoptosis induced by DNA double-strand breaks. *Cell*, **114**, 673-688.
- Koptyra, M., Falinski, R., Nowicki, M.O., Stoklosa, T., Majsterek, I., Nieborowska-Skorska, M., Blasiak, J. & Skorski, T. (2006) BCR/ABL kinase induces self-mutagenesis via reactive oxygen species to encode imatinib resistance. *Blood*, **108**, 319-327.
- Koptyra, M., Stoklosa, T., Hoser, G., Glodkowska-Mrowka, E., Seferynska, I., Klejman, A., Blasiak, J. & Skorski, T. (2011) Monoubiquitinated Fanconi anemia D2 (FANCD2-Ub) is required for BCR-ABL1 kinase-induced leukemogenesis. *Leukemia : official journal of the Leukemia Society of America, Leukemia Research Fund, U.K.*, **25**, 1259-1267.
- Krishnan, N., Jeong, D.G., Jung, S.-K., Ryu, S.E., Xiao, A., Allis, C.D., Kim, S.J. & Tonks, N.K. (2009) Dephosphorylation of the C-terminal tyrosyl residue of the DNA damage-related histone H2A.X is mediated by the protein phosphatase Eyes absent. *Journal of Biological Chemistry*, **284**, 16066-16070.
- Kucia, M., Jankowski, K., Reza, R., Wysoczynski, M., Bandura, L., Allendorf, D.J., Zhang, J., Ratajczak, J. & Ratajczak, M.Z. (2004) CXCR4-SDF-1 signalling, locomotion, chemotaxis and adhesion. *Journal of Molecular Histology*, **35**, 233-245.
- Kucia, M., Reza, R., Miekus, K., Wanzeck, J., Wojakowski, W., Janowska-Wieczorek, A., Ratajczak, J. & Ratajczak, M.Z. (2005) Trafficking of normal stem cells and metastasis of cancer stem cells involve similar mechanisms: Pivotal role of the SDF-1-CXCR4 axis. *Stem Cells*, **23**, 879-894.
- Kuramochi, S., Moriguchi, T., Kuida, K., Endo, J., Semba, K., Nishida, E. & Karasuyama, H. (1997) LOK is a novel mouse STE20-like protein kinase that is expressed predominantly in lymphocytes. *Journal of Biological Chemistry*, **272**, 22679-22684.

- la Cour, T., Kiemer, L., Molgaard, A., Gupta, R., Skriver, K. & Brunak, S. (2004) Analysis and prediction of leucine-rich nuclear export signals. *Protein Engineering Design & Selection*, **17**, 527-536.
- Lachner, M., O'Carroll, N., Rea, S., Mechtler, K. & Jenuwein, T. (2001) Methylation of histone H3 lysine 9 creates a binding site for HP1 proteins. *Nature*, **410**, 116-120.
- Ladner, C., Ehninger, G., Gey, K.F. & Clemens, M.R. (1989) Effect of etoposide (VP16-213) on lipid-peroxidation and antioxidant status in a high-dose radiochemotherapy regimen. *Cancer Chemotherapy and Pharmacology*, **25**, 210-212.
- Lamarche, B.J., Orazio, N.I. & Weitzman, M.D. (2010) The MRN complex in double-strand break repair and telomere maintenance. *Febs Letters*, **584**, 3682-3695.
- Lancrin, C., Sroczynska, P., Stephenson, C., Allen, T., Kouskoff, V. & Lacaud, G. (2009) The haemangioblast generates haematopoietic cells through a haemogenic endothelium stage. *Nature*, **457**, 892-895.
- Larsen, M.R., Thingholm, T.E., Jensen, O.N., Roepstorff, P. & Jorgensen, T.J.D. (2005) Highly selective enrichment of phosphorylated peptides from peptide mixtures using titanium dioxide microcolumns. *Molecular & Cellular Proteomics*, **4**, 873-886.
- Lauring, J., Abukhdeir, A.M., Konishi, H., Garay, J.P., Gustin, J.P., Wang, Q., Arceci, R.J., Matsui, W. & Park, B.H. (2008) The multiple myeloma-associated MMSET gene contributes to cellular adhesion, clonogenic growth, and tumorigenicity. *Blood*, **111**, 856-864.
- Lee, C.F., Griffiths, S., Rodriguez-Suarez, E., Pierce, A., Unwin, R.D., Jaworska, E., Evans, C.A., Gaskell, S.J. & Whetton, A.D. (2010a) Assessment of downstream effectors of BCR/ABL protein tyrosine kinase using combined proteomic approaches. *Proteomics*, **10**, 3321-3342.
- Lee, H.-S., Park, J.-H., Kim, S.-J., Kwon, S.-J. & Kwon, J. (2010b) A cooperative activation loop among SWI/SNF, gamma-H2AX and H3 acetylation for DNA double-strand break repair. *Embo Journal*, **29**, 1434-1445.
- Lee, K. & Esselman, W.J. (2002) Inhibition of PTPS by H₂O₂ regulates the activation of distinct MAPK pathways. *Free Radical Biology and Medicine*, **33**, 1121-1132.
- Lee, T.H., Kim, S.U., Yu, S.L., Kim, S.H., Park, D.S., Moon, H.B., Dho, S.H., Kwon, K.S., Kwon, H.J., Han, Y.H., Jeong, S., Kang, S.W., Shin, H.S., Lee, K.K., Rhee, S.G. & Yu, D.Y. (2003) Peroxiredoxin II is essential for sustaining life span of erythrocytes in mice. *Blood*, **101**, 5033-5038.
- Lehar, S.M., Naeh, M., Jacks, T., Vater, C.A., Chittenden, T. & Guild, B.C. (1996) Identification and cloning of EI24, a gene induced by p53 in etoposide-treated cells. *Oncogene*, **12**, 1181-1187.
- Lerza, R., Castello, G., Sessarego, M., Cavallini, D. & Pannacciulli, I. (1992) Myelodysplastic syndrome associated with increased bone marrow fibrosis and translocation (5;12)(q33; p12.3). *British Journal of Haematology*, **82**, 476-477.
- Levine, R.L., Wadleigh, M., Cools, J., Ebert, B.L., Wernig, G., Huntly, B.J.P., Boggon, T.J., Wlodarska, L., Clark, J.J., Moore, S., Adelsperger, J., Koo, S., Lee, J.C., Gabriel, S., Mercher, T., D'Andrea, A., Frohling, S., Dohner, K., Marynen, P., Vandenberghe, P., Mesa, R.A., Tefferi, A., Griffin, J.D., Eck, M.J., Sellers, W.R., Meyerson, M., Golub, T.R., Lee, S.J. & Gilliland, D.G. (2005) Activating mutation in the tyrosine kinase

- JAK2 in polycythemia vera, essential thrombocythemia, and myeloid metaplasia with myelofibrosis. *Cancer Cell*, **7**, 387-397.
- Li, C.Y., Zhan, Y.Q., Li, W., Xu, C.W., Xu, W.X., Yu, D.H., Peng, R.Y., Cui, Y.F., Yang, X., Hou, N., Li, Y.H., Dong, B., Sun, H.B. & Yang, X.M. (2007a) Overexpression of a hematopoietic transcriptional regulator EDAG induces myelopoiesis and suppresses lymphopoiesis in transgenic mice. *Leukemia*, **21**, 2277-2286.
- Li, C.Y., Zhan, Y.Q., Xu, C.W., Xu, W.X., Wang, S.Y., Lv, J., Zhou, Y., Yue, P.B., Chen, B. & Yang, X.M. (2004) EDAG regulates the proliferation and differentiation of hematopoietic cells and resists cell apoptosis through the activation of nuclear factor-kappa B. *Cell Death and Differentiation*, **11**, 1299-1308.
- Li, S.G., Ilaria, R.L., Million, R.P., Daley, G.Q. & Van Etten, R.A. (1999) The P190, P210, and P230 forms of the BCR/ABL oncogene induce a similar chronic myeloid leukemia-like syndrome in mice but have different lymphoid leukemogenic activity. *Journal of Experimental Medicine*, **189**, 1399-1412.
- Li, Y., Lin, A.W., Zhang, X., Wang, Y., Wang, X. & Goodrich, D.W. (2007b) Cancer cells and normal cells differ in their requirements for Thoc1. *Cancer Research*, **67**, 6657-6664.
- Limbo, O., Chahwan, C., Yamada, Y., de Bruin, R.A.M., Wittenberg, C. & Russell, P. (2007) Ctp1 is a cell-cycle-regulated protein that functions with Mre11 complex to control double-strand break repair by homologous recombination. *Molecular Cell*, **28**, 134-146.
- Liu, C.C., Chou, Y.L. & Ch'ang, L.Y. (2004) Down-regulation of human NDR gene in megakaryocytic differentiation of erythroleukemia K562 cells. *Journal of Biomedical Science*, **11**, 104-116.
- Liu, C.M., Li, Y.M., Semenov, M., Han, C., Baeg, G.H., Tan, Y., Zhang, Z.H., Lin, X.H. & He, X. (2002) Control of beta-catenin phosphorylation/degradation by a dual-kinase mechanism. *Cell*, **108**, 837-847.
- Lluis, J.M., Buricchi, F., Chiarugi, P., Morales, A. & Fernandez-Checa, J.C. (2007) Dual role of mitochondrial reactive oxygen species in hypoxia signaling: Activation of nuclear factor-kappa B via c-SRC- and oxidant-dependent cell death. *Cancer Research*, **67**, 7368-7377.
- Longley, B.J., Metcalfe, D.D., Tharp, M., Wang, X.M., Tyrrell, L., Lu, S.Z., Heitjan, D. & Ma, Y.S. (1999) Activating and dominant inactivating c-KIT catalytic domain mutations in distinct clinical forms of human mastocytosis. *Proceedings of the National Academy of Sciences of the United States of America*, **96**, 1609-1614.
- Lowndes, N.F. (2010) The interplay between BRCA1 and 53BP1 influences death, aging, senescence and cancer. *DNA Repair*, **9**, 1112-1116.
- Loyola, A., Tagami, H., Bonaldi, T., Roche, D., Quivy, J.P., Imhof, A., Nakatani, Y., Dent, S.Y.R. & Almouzni, G. (2009) The HP1 alpha-CAF1-SetDB1-containing complex provides H3K9me1 for Suv39-mediated K9me3 in pericentric heterochromatin. *Embo Reports*, **10**, 769-775.
- Lu, C., Zhu, F., Cho, Y.-Y., Tang, F., Zykova, T., Ma, W.-y., Bode, A.M. & Dong, Z. (2006) Cell apoptosis: Requirement of H2AX in DNA ladder formation, but not for the activation of caspase-3. *Molecular Cell*, **23**, 121-132.

- Luijsterburg, M.S., Dinant, C., Lans, H., Stap, J., Wiernasz, E., Lagerwerf, S., Warmerdam, D.O., Lindh, M., Brink, M.C., Dobrucki, J.W., Aten, J.A., Fousteri, M.I., Jansen, G., Dantuma, N.P., Vermeulen, W., Mullenders, L.H.F., Houtsmuller, A.B., Verschure, P.J. & van Driel, R. (2009) Heterochromatin protein 1 is recruited to various types of DNA damage. *Journal of Cell Biology*, **185**, 577-586.
- Luna, R., Jimeno, S., Marin, M., Huertas, P., Garcia-Rubio, M. & Aguilera, A. (2005) Interdependence between transcription and mRNP processing and export, and its impact on genetic stability. *Molecular Cell*, **18**, 711-722.
- Macurek, L., Lindqvist, A., Voets, O., Kool, J., Vos, H.R. & Medema, R.H. (2010) Wip1 phosphatase is associated with chromatin and dephosphorylates gamma H2AX to promote checkpoint inhibition. *Oncogene*, **29**, 2281-2291.
- Maehara, K., Hasegawa, T. & Isobe, K. (2000) A NF-kappa B p65 subunit is indispensable for activating manganese superoxide: Dismutase gene transcription mediated by tumor necrosis factor-alpha. *Journal of Cellular Biochemistry*, **77**, 474-486.
- Magne, N., Toillon, R.A., Bottero, V., Didelot, C., Van Houtte, P., Gerard, J.P. & Peyron, J.F. (2006) NF-kappa B modulation and ionizing radiation: mechanisms and future directions for cancer treatment. *Cancer Letters*, **231**, 158-168.
- Majeti, R., Park, C.Y. & Weissman, I.L. (2007) Identification of a hierarchy of multipotent hematopoietic progenitors in human cord blood. *Cell Stem Cell*, **1**, 635-645.
- Makarov, A. (2000) Electrostatic axially harmonic orbital trapping: A high-performance technique of mass analysis. *Analytical Chemistry*, **72**, 1156-1162.
- Malgeri, U., Baldini, L., Perfetti, V., Fabris, S., Vignarelli, M.C., Colombo, G., Lotti, V., Compasso, S., Bogni, S., Lombardi, L., Maiolo, A.T. & Neri, A. (2000) Detection of t(4;14)(p16.3;q32) chromosomal translocation in multiple myeloma by reverse transcription-polymerase chain reaction analysis of IGH-MMSET fusion transcripts. *Cancer Research*, **60**, 4058-4061.
- Mancini, A., El Bounkari, O., Norrenbrock, A.F., Scherr, M., Schaefer, D., Eder, M., Banham, A.H., Pulford, K., Lyne, L., Whetton, A.D. & Tamura, T. (2007) FMIP controls the adipocyte lineage commitment of C2C12 cells by downmodulation of C/EBPalpha. *Oncogene*, **26**, 1020-1027.
- Mancini, A., Koch, A., Whetton, A.D. & Tamura, T. (2004) The M-CSF receptor substrate and interacting protein FMIP is governed in its subcellular localization by protein kinase C-mediated phosphorylation, and thereby potentiates M-CSF-mediated differentiation. *Oncogene*, **23**, 6581-6589.
- Mancini, A., Niemann-Seyde, S.C., Pankow, R., El Bounkari, O., Klebba-Farber, S., Koch, A., Jaworska, E., Spooncer, E., Gruber, A.D., Whetton, A.D. & Tamura, T. (2010) THOC5/FMIP, an mRNA export TREX complex protein, is essential for hematopoietic primitive cell survival in vivo. *Bmc Biology*, **8**, 17.
- Mann, M. & Wilm, M. (1994) Error tolerant identification of peptides in sequence databases by peptide sequence tags. *Analytical Chemistry*, **66**, 4390-4399.
- Marango, J., Shimoyama, M., Nishio, H., Meyer, J.A., Min, D.-J., Sirulnik, A., Martinez-Martinez, Y., Chesi, M., Bergsagel, P.L., Zhou, M.-M., Waxman, S., Leibovitch, B.A., Walsh, M.J. & Licht, J.D. (2008) The MMSET protein is a histone methyltransferase with characteristics of a transcriptional corepressor. *Blood*, **111**, 3145-3154.

- Marcucci, G., Baldus, C.D., Ruppert, A.S., Radmacher, M.D., Mrozek, K., Whitman, S.P., Kolitz, J.E., Edwards, C.G., Vardiman, J.W., Powell, B.L., Baer, M.R., Moore, J.O., Perrotti, D., Caligiuri, M.A., Carroll, A.J., Larson, R.A., de la Chapelle, A. & Bloomfield, C.D. (2005) Overexpression of the ETS-related gene, ERG, predicts a worse outcome in acute myeloid leukemia with normal karyotype: A cancer and leukemia group B study. *Journal of Clinical Oncology*, **23**, 9234-9242.
- Marinkovic, D., Zhang, X., Yalcin, S., Luciano, J.P., Brugnara, C., Huber, T. & Ghaffari, S. (2007) Foxo3 is required for the regulation of oxidative stress in erythropoiesis. *Journal of Clinical Investigation*, **117**, 2133-2144.
- Markowitz, D., Goff, S. & Bank, A. (1988) Construction and use of a safe and efficient amphotropic packaging cell line. *Virology*, **167**, 400-406.
- Maru, Y. & Witte, O.N. (1991) The Bcr gene encodes a novel serine threonine kinase activity within a single exon. *Cell*, **67**, 459-468.
- Matsuoka, S., Ballif, B.A., Smogorzewska, A., McDonald, E.R., Hurov, K.E., Luo, J., Bakalarski, C.E., Zhao, Z.M., Solimini, N., Lerenthal, Y., Shiloh, Y., Gygi, S.P. & Elledge, S.J. (2007) ATM and ATR substrate analysis reveals extensive protein networks responsive to DNA damage. *Science*, **316**, 1160-1166.
- McCarthy, B.A., Mansour, A., Lin, Y.-C., Kotenko, S. & Raveche, E. (2004) RNA interference of IL-10 in leukemic B-1 cells. *Cancer immunity : a journal of the Academy of Cancer Immunology*, **4**, 6.
- McGahan, A., Bissonnette, R., Schmitt, M., Cotter, K.M., Green, D.R. & Cotter, T.G. (1994) Bcr-Abl maintains resistance of chronic myelogenous leukemia cells to apoptotic cell death. *Blood*, **83**, 1179-1187.
- Meininger, C.J., Yano, H., Rottapel, R., Bernstein, A., Zsebo, K.M. & Zetter, B.R. (1992) The c-KIT receptor ligand functions as a mast cell chemoattractant. *Blood*, **79**, 958-963.
- Melo, J.V. & Barnes, D.J. (2007) Chronic myeloid leukaemia as a model of disease evolution in human cancer. *Nature Reviews Cancer*, **7**, 441-453.
- Meyn, M.A., III, Wilson, M.B., Abdi, F.A., Fahey, N., Schiavone, A.P., Wu, J., Hochrein, J.M., Engen, J.R. & Smithgall, T.E. (2006) Src family kinases phosphorylate the Bcr-Abl SH3-SH2 region and modulate Bcr-Abl transforming activity. *Journal of Biological Chemistry*, **281**, 30907-30916.
- Mezard, C. & Nicolas, A. (1994) Homologous, homeologous, and illegitimate repair of double-strand breaks during transformation of a wild-type strain and a Rad52 mutant strain of *Saccharomyces cerevisiae*. *Molecular and Cellular Biology*, **14**, 1278-1292.
- Migliaccio, E., Giorgio, M., Mele, S., Pelicci, G., Reboldi, P., Pandolfi, P.P., Lanfrancone, L. & Pelicci, P.G. (1999) The p66(shc) adaptor protein controls oxidative stress response and life span in mammals. *Nature*, **402**, 309-313.
- Miller, K.M., Tjeertes, J.V., Coates, J., Legube, G., Polo, S.E., Britton, S. & Jackson, S.P. (2010) Human HDAC1 and HDAC2 function in the DNA-damage response to promote DNA nonhomologous end-joining. *Nature Structural & Molecular Biology*, **17**, 1144-U1115.
- Mohammed, S. & Heck, A.J.R. (2011) Strong cation exchange (SCX) based analytical methods for the targeted analysis of protein post-translational modifications. *Current Opinion in Biotechnology*, **22**, 9-16.

- Molina, H., Yang, Y., Ruch, T., Kim, J.W., Mortensen, P., Otto, T., Nalli, A., Tang, Q.Q., Lane, M.D., Chaerkady, R. & Pandey, A. (2009) Temporal profiling of the adipocyte proteome during differentiation using a five-plex SILAC based strategy. *Journal of Proteome Research*, **8**, 48-58.
- Molina, T.J., Kishihara, K., Siderovski, D.P., Vanewijk, W., Narendran, A., Timms, E., Wakeham, A., Paige, C.J., Hartmann, K.U., Veillette, A., Davidson, D. & Mak, T.W. (1992) Profound block in thymocyte development in mice lacking p56(LCK). *Nature*, **357**, 161-164.
- Montecucco, A. & Biamonti, G. (2007) Cellular response to etoposide treatment. *Cancer Letters*, **252**, 9-18.
- Montoya, A., Beltran, L., Casado, P., Rodriguez-Prados, J.-C. & Cutillas, P.R. (2011) Characterization of a TiO(2) enrichment method for label-free quantitative phosphoproteomics. *Methods*, **54**, 370-378.
- Morris, S.W., Kirstein, M.N., Valentine, M.B., Dittmer, K.G., Shapiro, D.N., Saltman, D.L. & Look, A.T. (1994) Fusion of a kinase gene, ALK, to a nucleolar protein gene, NPM, in non-Hodgkin's lymphoma. *Science*, **263**, 1281-1284.
- Morrison, C., Vagnarelli, P., Sonoda, E., Takeda, S. & Earnshaw, W.C. (2003) Sister chromatid cohesion and genome stability in vertebrate cells. *Biochemical Society Transactions*, **31**, 263-265.
- Mosse, Y.P., Laudenslager, M., Longo, L., Cole, K.A., Wood, A., Attiyeh, E.F., Laquaglia, M.J., Sennett, R., Lynch, J.E., Perri, P., Laureys, G., Speleman, F., Kim, C., Hou, C., Hakonarson, H., Torkamani, A., Schork, N.J., Brodeur, G.M., Tonini, G.P., Rappaport, E., Devoto, M. & Maris, J.M. (2008) Identification of ALK as a major familial neuroblastoma predisposition gene. *Nature*, **455**, 930-U922.
- Mosser, D.D., Caron, A.W., Bourget, L., Meriin, A.B., Sherman, M.Y., Morimoto, R.I. & Massie, B. (2000) The chaperone function of hsp70 is required for protection against stress-induced apoptosis. *Molecular and Cellular Biology*, **20**, 7146-7159.
- Motoyama, A., Xu, T., Ruse, C.I., Wohlschlegel, J.A. & Yates, J.R., III (2007) Anion and cation mixed-bed ion exchange for enhanced multidimensional separations of peptides and phosphopeptides. *Analytical Chemistry*, **79**, 3623-3634.
- Moynahan, M.E., Chiu, J.W., Koller, B.H. & Jasin, M. (1999) Brca1 controls homology-directed DNA repair. *Molecular Cell*, **4**, 511-518.
- Moynahan, M.E. & Jasin, M. (1997) Loss of heterozygosity induced by a chromosomal double-strand break. *Proceedings of the National Academy of Sciences of the United States of America*, **94**, 8988-8993.
- Nagamachi, A., Yamasaki, N., Miyazaki, K., Oda, H., Miyazaki, M., Honda, Z.-i., Kominami, R., Inaba, T. & Honda, H. (2009) Haploinsufficiency and acquired loss of Bcl11b and H2AX induces blast crisis of chronic myelogenous leukemia in a transgenic mouse model. *Cancer Science*, **100**, 1219-1226.
- Nagata, H., Worobec, A.S., Oh, C.K., Chowdhury, B.A., Tannenbaum, S., Suzuki, Y. & Metcalfe, D.D. (1995) Identification of a point mutation in the catalytic domain of the protooncogene c-KIT in peripheral blood mononuclear cells of patients who have mastocytosis with an associated hematologic disorder. *Proceedings of the National Academy of Sciences of the United States of America*, **92**, 10560-10564.

- Naka, K., Hoshii, T., Muraguchi, T., Tadokoro, Y., Ooshio, T., Kondo, Y., Nakao, S., Motoyama, N. & Hirao, A. (2010) TGF-beta-FOXO signalling maintains leukaemia-initiating cells in chronic myeloid leukaemia. *Nature*, **463**, 676-U111.
- Nakada, S., Chen, G.I., Gingras, A.C. & Durocher, D. (2008) PP4 is a gamma H2AX phosphatase required for recovery from the DNA damage checkpoint. *Embo Reports*, **9**, 1019-1026.
- Nakamura, K., Sakai, W., Kawamoto, T., Bree, R.T., Lowndes, N.F., Takeda, S. & Taniguchi, Y. (2006) Genetic dissection of vertebrate 53BP1: A major role in non-homologous end joining of DNA double strand breaks. *DNA Repair*, **5**, 741-749.
- Nakata, Y., Kimura, A., Katoh, O., Kawaishi, K., Hyodo, H., Abe, K., Kuramoto, A. & Satow, Y. (1995) C-Kit point mutation of extracellular domain in patients with myeloproliferative disorders. *British Journal of Haematology*, **91**, 661-663.
- Nardi, V., Azam, M. & Daley, G.Q. (2004) Mechanisms and implications of imatinib resistance mutations in BCR-ABL. *Current Opinion in Hematology*, **11**, 35-43.
- Naughton, R., Quiney, C., Turner, S.D. & Cotter, T.G. (2009) Bcr-Abl-mediated redox regulation of the PI3K/AKT pathway. *Leukemia*.
- Neumann, C.A., Krause, D.S., Carman, C.V., Das, S., Dubey, D.P., Abraham, J.L., Bronson, R.T., Fujiwara, Y., Orkin, S.H. & Van Etten, R.A. (2003) Essential role for the peroxiredoxin Prdx1 in erythrocyte antioxidant defence and tumour suppression. *Nature*, **424**, 561-565.
- Nickoloff, J.A., De Haro, L.P., Wray, J. & Hromas, R. (2008) Mechanisms of leukemia translocations. *Current Opinion in Hematology*, **15**, 338-345.
- Nieborowska-Skorska, M., Stoklosa, T., Datta, M., Czechowska, A., Rink, L., Slupianek, A., Koptyra, M., Seferynska, I., Krszyna, K., Blasiak, J. & Skorski, T. (2006) ATR-Chk1 axis protects BCR/ABL leukemia cells from the lethal effect of DNA double-strand breaks. *Cell Cycle*, **5**, 994-1000.
- Nita-Lazar, A., Saito-Benz, H. & White, F.M. (2008) Quantitative phosphoproteomics by mass spectrometry: past, present, and future. *Proteomics*, **8**, 4433-4443.
- Noon, A.T., Shibata, A., Rief, N., Loebrich, M., Stewart, G.S., Jeggo, P.A. & Goodarzi, A.A. (2010) 53BP1-dependent robust localized KAP-1 phosphorylation is essential for heterochromatic DNA double-strand break repair. *Nature Cell Biology*, **12**, 177-U191.
- Nowell, P.C. & Hungerford, D.A. (1960) Minute chromosome in human chronic granulocytic leukemia. *Science*, **132**, 1497-1497.
- Nowicki, M.O., Falinski, R., Koptyra, M., Slupianek, A., Stoklosa, T., Gloc, E., Nieborowska-Skorska, M., Blasiak, J. & Skorski, T. (2004) BCR/ABL oncogenic kinase promotes unfaithful repair of the reactive oxygen species-dependent DNA double-strand breaks. *Blood*, **104**, 3746-3753.
- Obenauer, J.C., Cantley, L.C. & Yaffe, M.B. (2003) Scansite 2.0: proteome-wide prediction of cell signaling interactions using short sequence motifs. *Nucleic Acids Research*, **31**, 3635-3641.
- Oegema, K., Savoian, M.S., Mitchison, T.J. & Field, C.M. (2000) Functional analysis of a human homologue of the Drosophila actin binding protein anillin suggests a role in cytokinesis. *Journal of Cell Biology*, **150**, 539-551.
- Ong, S.E., Blagoev, B., Kratchmarova, I., Kristensen, D.B., Steen, H., Pandey, A. & Mann, M. (2002) Stable isotope labeling by amino acids in cell culture, SILAC, as a simple

- and accurate approach to expression proteomics. *Molecular & Cellular Proteomics*, **1**, 376-386.
- Owen, H.R., Elser, M., Cheung, E., Gersbach, M., Kraus, W.L. & Hottiger, M.O. (2007) MYBBP1a is a novel repressor of NF-kappa B. *Journal of Molecular Biology*, **366**, 725-736.
- Owusu-Ansah, E. & Banerjee, U. (2009) Reactive oxygen species prime Drosophila haematopoietic progenitors for differentiation. *Nature*, **461**, 537-U109.
- Oya, H., Yokoyama, A., Yamaoka, I., Fujiki, R., Yonezawa, M., Youn, M.-Y., Takada, I., Kato, S. & Kitagawa, H. (2009) Phosphorylation of Williams syndrome transcription factor by MAPK induces a switching between two distinct chromatin remodeling complexes. *Journal of Biological Chemistry*, **284**, 32472-32482.
- Palacios, R. & Steinmetz, M. (1985) Il3-dependent mouse clones that express B-220 surface-antigen, contain Ig genes in germ-line configuration, and generate B lymphocytes *in vivo*. *Cell*, **41**, 727-734.
- Palmer, R.H., Vernersson, E., Grabbe, C. & Hallberg, B. (2009) Anaplastic lymphoma kinase: signalling in development and disease. *Biochemical Journal*, **420**, 345-361.
- Palmisano, G. & Thingholm, T.E. (2010) Strategies for quantitation of phosphoproteomic data. *Expert Review of Proteomics*, **7**, 439-456.
- Pan, C., Olsen, J.V., Daub, H. & Mann, M. (2009) Global effects of kinase inhibitors on signaling networks revealed by quantitative phosphoproteomics. *Molecular & Cellular Proteomics*, **8**, 2796-2808.
- Panta, G.R., Kaur, S., Cavin, L.G., Cortes, M.L., Mercurio, F., Lothstein, L., Sweatman, T.W., Israel, M. & Arsur, M. (2004) ATM and the catalytic subunit of DNA-dependent protein kinase activate NF-kappa B through a common MEK extracellular signal-regulated kinase/p90(rsk) signaling pathway in response to distinct forms of DNA damage. *Molecular and Cellular Biology*, **24**, 1823-1835.
- Park, J.-H., Park, E.-J., Hur, S.-K., Kim, S. & Kwon, J. (2009) Mammalian SWI/SNF chromatin remodeling complexes are required to prevent apoptosis after DNA damage. *DNA Repair*, **8**, 29-39.
- Park, J.-H., Park, E.-J., Lee, H.-S., Kim, S.J., Hur, S.-K., Imbalzano, A.N. & Kwon, J. (2006) Mammalian SWI/SNF complexes facilitate DNA double-strand break repair by promoting gamma-H2AX induction. *Embo Journal*, **25**, 3986-3997.
- Pastink, A., Eeken, J.C.J. & Lohman, P.H.M. (2001) Genomic integrity and the repair of double-strand DNA breaks. *Mutation Research-Fundamental and Molecular Mechanisms of Mutagenesis*, **480**, 37-50.
- Pene-Dumitrescu, T. & Smithgall, T.E. (2010) Expression of a Src family kinase in chronic myelogenous leukemia cells induces resistance to imatinib in a kinase-dependent manner. *Journal of Biological Chemistry*, **285**, 21446-21457.
- Peoples, R.J., Cisco, M.J., Kaplan, P. & Francke, U. (1998) Identification of the WBSCR9 gene, encoding a novel transcriptional regulator, in the Williams-Beuren syndrome deletion at 7q11.23. *Cytogenetics and Cell Genetics*, **82**, 238-246.
- Perrera, C., Colombo, R., Valsasina, B., Carpinelli, P., Troiani, S., Modugno, M., Gianellini, L., Cappella, P., Isacchi, A., Moll, J. & Rusconi, L. (2010) Identification of Myb-binding protein 1A (MYBBP1A) as a novel substrate for Aurora B kinase. *Journal of Biological Chemistry*, **285**, 11775-11785.

- Perrotti, D., Cesi, V., Trotta, R., Guerzoni, C., Santilli, G., Campbell, K., Iervolino, A., Condorelli, F., Gambacorti-Passerini, C., Caligiuri, M.A. & Calabretta, B. (2002) BCR-ABL suppresses C/EBP alpha expression through inhibitory action of hnRNP E2. *Nature Genetics*, **30**, 48-58.
- Pierce, A., Carney, L., Hamza, H.G., Griffiths, J.R., Zhang, L.Q., Whetton, B.A., Sanchez, M.B.G., Tamura, T., Sternberg, D. & Whetton, A.D. (2008a) THOC5 spliceosome protein: a target for leukaemogenic tyrosine kinases that affects inositol lipid turnover. *British Journal of Haematology*, **141**, 641-650.
- Pierce, A., Unwin, R.D., Evans, C.A., Griffiths, S., Carney, L., Zhang, L., Jaworska, E., Lee, C.F., Blinco, D., Okoniewski, M.J., Miller, C.J., Bitton, D.A., Spooncer, E. & Whetton, A.D. (2008b) Eight-channel iTRAQ enables comparison of the activity of six leukemogenic tyrosine kinases. *Molecular & Cellular Proteomics*, **7**, 853-863.
- Pikman, Y., Lee, B.H., Mercher, T., McDowell, E., Ebert, B.L., Gozo, M., Cuker, A., Wernig, G., Moore, S., Galinsky, I., DeAngelo, D.J., Clark, J.J., Lee, S.J., Golub, T.R., Wadleigh, M., Gilliland, D.G. & Levine, R.L. (2006) MPLW515L is a novel somatic activating mutation in myelofibrosis with myeloid metaplasia. *Plos Medicine*, **3**, 1140-1151.
- Pinton, P., Rimessi, A., Marchi, S., Orsini, F., Migliaccio, E., Giorgio, M., Contursi, C., Minucci, S., Mantovani, F., Wieckowski, M.R., Del Sal, G., Pelicci, P.G. & Rizzuto, R. (2007) Protein kinase C beta and prolyl isomerase 1 regulate mitochondrial effects of the life-span determinant p66(Shc). *Science*, **315**, 659-663.
- Plazas-Mayorca, M.D., Bloom, J.S., Zeissler, U., Leroy, G., Young, N.L., DiMaggio, P.A., Krugylak, L., Schneider, R. & Garcia, B.A. (2010) Quantitative proteomics reveals direct and indirect alterations in the histone code following methyltransferase knockdown. *Molecular Biosystems*, **6**, 1719-1729.
- Pocaly, M., Lagarde, V., Etienne, G., Ribeil, J.A., Claverol, S., Bonneu, M., Moreau-Gaudry, F., Guyonnet-Duperat, V., Hermine, O., Melo, J.V., Dupouy, M., Turcq, B., Mahon, F.X. & Pasquet, J.M. (2007) Overexpression of the heat-shock protein 70 is associated to imatinib resistance in chronic myeloid leukemia. *Leukemia*, **21**, 93-101.
- Poot, R.A., Bozhenok, L., van den Berg, D.L.C., Hawkes, N. & Varga-Weisz, P.D. (2005) Chromatin remodeling by WSTF-ISWI at the replication site - Opening a window of opportunity for epigenetic inheritance? *Cell Cycle*, **4**, 543-546.
- Poplawski, T. & Blasiak, J. (2010) BCR/ABL downregulates DNA-PK(CS)-dependent and upregulates backup non-homologous end joining in leukemic cells. *Molecular Biology Reports*, **37**, 2309-2315.
- Puttick, J., Baker, E.N. & Delbaere, L.T.J. (2008) Histidine phosphorylation in biological systems. *Biochimica Et Biophysica Acta-Proteins and Proteomics*, **1784**, 100-105.
- Qin, S.F. & Chock, P.B. (2002) Tyrosine phosphatase CD45 regulates hydrogen peroxide-induced calcium mobilization in B cells. *Antioxidants & Redox Signaling*, **4**, 481-490.
- Quennet, V., Beucher, A., Barton, O., Takeda, S. & Loebrich, M. (2011) CtIP and MRN promote non-homologous end-joining of etoposide-induced DNA double-strand breaks in G1. *Nucleic Acids Research*, **39**, 2144-2152.
- Rainey, M.D., Charlton, M.E., Stanton, R.V. & Kastan, M.B. (2008) Transient inhibition of ATM kinase is sufficient to enhance cellular sensitivity to ionizing radiation. *Cancer Research*, **68**, 7466-7474.

- Ramachandran, S., Tran, D.D., Klebba-Faerber, S., Kardinal, C., Whetton, A.D. & Tamura, T. (2011) An ataxia-telangiectasia-mutated (ATM) kinase mediated response to DNA damage down-regulates the mRNA-binding potential of THOC5. In: *RNA*.
- Rappsilber, J., Mann, M. & Ishihama, Y. (2007) Protocol for micro-purification, enrichment, pre-fractionation and storage of peptides for proteomics using StageTips. *Nature Protocols*, **2**, 1896-1906.
- Ratain, M.J. & Rowley, J.D. (1992) Therapy-related acute myeloid leukemia secondary to inhibitors of Topoisomerase II - From the bedside to the target genes. *Annals of Oncology*, **3**, 107-111.
- Reddy, M.M., Fernandes, M.S., Salgia, R., Levine, R.L., Griffin, J.D. & Sattler, M. (2011) NADPH oxidases regulate cell growth and migration in myeloid cells transformed by oncogenic tyrosine kinases. *Leukemia*, **25**, 281-289.
- Rehwinkel, J., Herold, A., Gari, K., Kocher, T., Rode, M., Ciccarelli, F.L., Wilm, M. & Izaurralde, E. (2004) Genome-wide analysis of mRNAs regulated by the THO complex in *Drosophila melanogaster*. *Nature Structural & Molecular Biology*, **11**, 558-566.
- Renner, A.G., Dos Santos, C., Recher, C., Bailly, C., Creancier, L., Kruczynski, A., Payraastre, B. & Manenti, S. (2009) Polo-like kinase 1 is overexpressed in acute myeloid leukemia and its inhibition preferentially targets the proliferation of leukemic cells. *Blood*, **114**, 659-662.
- Resnick, T.D., Satinover, D.L., MacIsaac, F., Stukenberg, P.T., Earnshaw, W.C., Orr-Weaver, T.L. & Carmena, M. (2006) INCENP and Aurora B promote meiotic sister chromatid cohesion through localization of the Shugoshin MEI-S332 in *Drosophila*. *Developmental Cell*, **11**, 57-68.
- Reuther, J.Y., Reuther, G.W., Cortez, D., Pendergast, A.M. & Baldwin, A.S. (1998) A requirement for NF-kappa B activation in Bcr-Abl-mediated transformation. *Genes & Development*, **12**, 968-981.
- Rhee, S.G., Chae, H.Z. & Kim, K. (2005) Peroxiredoxins: A historical overview and speculative preview of novel mechanisms and emerging concepts in cell signaling. *Free Radical Biology and Medicine*, **38**, 1543-1552.
- Ribeil, J.-A., Zermati, Y., Vandekerckhove, J., Cathelin, S., Kersual, J., Dussiot, M., Coulon, S., Moura, I.C., Zeuner, A., Kirkegaard-Sorensen, T., Varet, B., Solary, E., Garrido, C. & Hermine, O. (2007) Hsp70 regulates erythropoiesis by preventing caspase-3-mediated cleavage of GATA-1. *Nature*, **445**, 102-105.
- Richardson, C., Stark, J.M., Ommundsen, M. & Jasin, M. (2004) Rad51 overexpression promotes alternative double-strand break repair pathways and genome instability. *Oncogene*, **23**, 546-553.
- Riches, L.C., Lynch, A.M. & Gooderham, N.J. (2008) Early events in the mammalian response to DNA double-strand breaks. *Mutagenesis*, **23**, 331-339.
- Rider, D.A., Sinclair, A.J. & Young, S.P. (2003) Oxidative inactivation of CD45 protein tyrosine phosphatase may contribute to T lymphocyte dysfunction in the elderly. *Mechanisms of Ageing and Development*, **124**, 191-198.
- Rink, L., Slupianek, A., Stoklosa, T., Nieborowska-Skorska, M., Urbanska, K., Seferynska, I., Reiss, K. & Skorski, T. (2007) Enhanced phosphorylation of Nbs1, a member of DNA repair/checkpoint complex Mre11-RAD50-Nbs1, can be targeted to increase

- the efficacy of imatinib mesylate against BCR/ABL-positive leukemia cells. *Blood*, **110**, 651-660.
- Ritov, V.B., Goldman, R., Stoyanovsky, D.A., Menshikova, E.V. & Kagan, V.E. (1995) Antioxidant paradoxes of phenolic compounds: Peroxyl radical scavenger and lipid antioxidant, etoposide (VP-16), inhibits sarcoplasmic reticulum CA(2+)-ATPase via thiol oxidation by its phenoxyl radical. *Archives of Biochemistry and Biophysics*, **321**, 140-152.
- Robertson, E.F., Hoyt, J.C. & Reeves, H.C. (1988) Evidence of histidine phosphorylation in isocitrate lyase from *Escherichia coli*. *Journal of Biological Chemistry*, **263**, 2477-2482.
- Roepstorff, P. & Fohlman, J. (1984) Proposal for a common nomenclature for sequence ions in mass spectra of peptides. *Biomedical Mass Spectrometry*, **11**, 601-601.
- Rogakou, E.P., Pilch, D.R., Orr, A.H., Ivanova, V.S. & Bonner, W.M. (1998) DNA double-stranded breaks induce histone H2AX phosphorylation on serine 139. *Journal of Biological Chemistry*, **273**, 5858-5868.
- Rosado, J.A., Redondo, P.C., Salido, G.M., Gomez-Arteta, E., Sage, S.O. & Pariente, J.A. (2004) Hydrogen peroxide generation induces pp60(src) activation in human platelets - Evidence for the involvement of this pathway in store-mediated calcium entry. *Journal of Biological Chemistry*, **279**, 1665-1675.
- Roskoski, R. (2005) Src kinase regulation by phosphorylation and dephosphorylation. *Biochemical and Biophysical Research Communications*, **331**, 1-14.
- Rowley, J.D. (1973) New consistent chromosomal abnormality in chronic myelogenous leukemia identified by quinacrine fluorescence and giemsa staining. *Nature*, **243**, 290-293.
- Rubbi, L., Titz, B., Brown, L., Galvan, E., Komisopoulou, E., Chen, S.S., Low, T., Tahmasian, M., Skaggs, B., Mueschen, M., Pellegrini, M. & Graeber, T.G. (2011) Global phosphoproteomics reveals crosstalk between Bcr-Abl and negative feedback mechanisms controlling Src signaling. *Science Signaling*, **4**.
- Ruiz, J.F., Gomez-Gonzalez, B. & Aguilera, A. (2011) AID induces double-strand breaks at Immunoglobulin switch regions and c-MYC causing chromosomal translocations in yeast THO mutants. *Plos Genetics*, **7**.
- Saldanha, A.J. (2004) Java Treeview-extensible visualization of microarray data. *Bioinformatics*, **20**, 3246-3248.
- Salles, D., Mencialha, A.L., Ireno, I.C., Wiesmueller, L. & Abdelhay, E. (2011) BCR-ABL stimulates mutagenic homologous DNA double-strand break repair via the DNA-end-processing factor CtIP. *Carcinogenesis*, **32**, 27-34.
- Sallmyr, A., Fan, J., Datta, K., Kim, K.T., Grosu, D., Shapiro, P., Small, D. & Rassool, F. (2008a) Internal tandem duplication of FLT3 (FLT3/ITD) induces increased ROS production, DNA damage, and misrepair: implications for poor prognosis in AML. *Blood*, **111**, 3173-3182.
- Sallmyr, A., Fan, J. & Rassool, F.V. (2008b) Genomic instability in myeloid malignancies: Increased reactive oxygen species (ROS), DNA double strand breaks (DSBs) and error-prone repair. *Cancer Letters*, **270**, 1-9.
- Sallmyr, A., Tomkinson, A.E. & Rassool, F.V. (2008c) Up-regulation of WRN and DNA ligase III alpha in chronic myeloid leukemia: consequences for the repair of DNA double-strand breaks. *Blood*, **112**, 1413-1423.

- Samanta, A., Perazzona, B., Chakraborty, S., Sun, X., Modi, H., Bhatia, R., Priebe, W. & Arlinghaus, R. (2011) Janus kinase 2 regulates Bcr-Abl signaling in chronic myeloid leukemia. *Leukemia*, **25**, 463-472.
- Santra, M., Zhan, F.H., Tian, E.M., Barlogie, B. & Shaughnessy, J. (2003) A subset of multiple myeloma harboring the t(4;14)(p16;q32) translocation lacks FGFR3 expression but maintains an IGH/MMSET fusion transcript. *Blood*, **101**, 2374-2376.
- Sattler, M., Verma, S., Shrikhande, G., Byrne, C.H., Pride, Y.B., Winkler, T., Greenfield, E.A., Salgia, R. & Griffin, J.D. (2000) The BCR/ABL tyrosine kinase induces production of reactive oxygen species in hematopoietic cells. *Journal of Biological Chemistry*, **275**, 24273-24278.
- Savitsky, K., Barshira, A., Gilad, S., Rotman, G., Ziv, Y., Vanagaite, L., Tagle, D.A., Smith, S., Uziel, T., Sfez, S., Ashkenazi, M., Pecker, I., Frydman, M., Harnik, R., Patanjali, S.R., Simmons, A., Clines, G.A., Sartiel, A., Gatti, R.A., Chessa, L., Sanal, O., Lavin, M.F., Jaspers, N.G.J., Malcolm, A., Taylor, R., Arlett, C.F., Miki, T., Weissman, S.M., Lovett, M., Collins, F.S. & Shiloh, Y. (1995) A single ataxia-telangiectasia gene with a product similar to PI-3 kinase. *Science*, **268**, 1749-1753.
- Sawyers, C.L. (1999) Chronic myeloid leukemia. *New England Journal of Medicine*, **340**, 1330-1340.
- Scheijen, B., Ngo, H.T., Kang, H. & Griffin, J.D. (2004) FLT3 receptors with internal tandem duplications promote cell viability and proliferation by signaling through Foxo proteins. *Oncogene*, **23**, 3338-3349.
- Schirmer, E.C., Yates, J.R., 3rd & Gerace, L. (2003) MudPIT: A powerful proteomics tool for discovery. *Discovery medicine*, **3**, 38-39.
- Schwaller, J., Frantsve, J., Aster, J., Williams, I.R., Tomasson, M.H., Ross, T.S., Peeters, P., Van Rompaey, L., Van Etten, R.A., Ilaria, R., Marynen, P. & Gilliland, D.G. (1998) Transformation of hematopoietic cell lines to growth-factor independence and induction of a fatal myelo- and lymphoproliferative disease in mice by retrovirally transduced TEL/JAK2 fusion genes. *Embo Journal*, **17**, 5321-5333.
- Scott, L.M., Tong, W., Levine, R.L., Scott, M.A., Beer, P.A., Stratton, M.R., Futreal, P.A., Erber, W.N., McMullin, M.F., Harrison, C.N., Warren, A.J., Gilliland, D.G., Lodish, H.F. & Green, A.R. (2007) JAK2 exon 12 mutations in polycythemia vera and idiopathic erythrocytosis. *New England Journal of Medicine*, **356**, 459-468.
- Sherman, J., McKay, M.J., Ashman, K. & Molloy, M.P. (2009) How specific is my SRM?: The issue of precursor and product ion redundancy. *Proteomics*, **9**, 1120-1123.
- Shiloh, Y. & Rotman, G. (1996) Ataxia-telangiectasia and the ATM gene: Linking neurodegeneration, immunodeficiency, and cancer to cell cycle checkpoints. *Journal of Clinical Immunology*, **16**, 254-260.
- Shilov, I.V., Seymour, S.L., Patel, A.A., Loboda, A., Tang, W.H., Keating, S.P., Hunter, C.L., Nuwaysir, L.M. & Schaeffer, D.A. (2007) The paragon algorithm, a next generation search engine that uses sequence temperature values and feature probabilities to identify peptides from tandem mass spectra. *Molecular & Cellular Proteomics*, **6**, 1638-1655.
- Shiotani, B. & Zou, L. (2009) Single-stranded DNA orchestrates an ATM-to-ATR switch at DNA breaks. *Molecular Cell*, **33**, 547-558.

- Shivtiel, S., Kollet, O., Lapid, K., Schajnovitz, A., Goichberg, P., Kalinkovich, A., Shezen, E., Tesio, M., Netzer, N., Petit, I., Sharir, A. & Lapidot, T. (2008) CD45 regulates retention, motility, and numbers of hematopoietic progenitors, and affects osteoclast remodeling of metaphyseal trabecules. *Journal of Experimental Medicine*, **205**, 2381-2395.
- Siitonen, T., Alaruikka, P., Mantymaa, P., Savolainen, E.R., Kavanagh, T.J., Krejsa, C.M., Franklin, C.C., Kinnula, V. & Koistinen, P. (1999) Protection of acute myeloblastic leukemia cells against apoptotic cell death by high glutathione and gamma-glutamylcysteine synthetase levels during etoposide-induced oxidative stress. *Annals of Oncology*, **10**, 1361-1367.
- Sillaber, C., Gesbert, F., Frank, D.A., Sattler, M. & Griffin, J.D. (2000) STAT5 activation contributes to growth and viability in Bcr/Abl-transformed cells. *Blood*, **95**, 2118-2125.
- Simsek, D., Brunet, E., Wong, S.Y.-W., Katyal, S., Gao, Y., McKinnon, P.J., Lou, J., Zhang, L., Li, J., Rebar, E.J., Gregory, P.D., Holmes, M.C. & Jasin, M. (2011) DNA ligase III promotes alternative nonhomologous end-joining during chromosomal translocation formation. *PLoS genetics*, **7**, e1002080.
- Simsek, T., Kocabas, F., Zheng, J., DeBerardinis, R.J., Mahmoud, A.I., Olson, E.N., Schneider, J.W., Zhang, C.C. & Sadek, H.A. (2010) The distinct metabolic profile of hematopoietic stem cells reflects their location in a hypoxic niche. *Cell Stem Cell*, **7**, 380-390.
- Sinha, B.K., Trush, M.A., Balaraman & Kalyanaraman (1985) Microsomal interactions and inhibition of lipid peroxidation by etoposide (VP-16, 213) - Implications for mode of action. *Biochemical Pharmacology*, **34**, 2036-2040.
- Sinha, B.K., Trush, M.A. & Kalyanaraman, B. (1983) Free-radical metabolism of VP-16 and inhibition of anthracycline-induced lipid peroxidation. *Biochemical Pharmacology*, **32**, 3495-3498.
- Skorski, T. (2002) BCR/ABL regulates response to DNA damage: the role in resistance to genotoxic treatment and in genomic instability. *Oncogene*, **21**, 8591-8604.
- Slupianek, A., Dasgupta, Y., Ren, S.-Y., Gurdek, E., Donlin, M., Nieborowska-Skorska, M., Fleury, F. & Skorski, T. (2011a) Targeting RAD51 phosphotyrosine-315 to prevent unfaithful recombination repair in BCR-ABL1 leukemia. *Blood*, **118**, 1062-1068.
- Slupianek, A., Gurdek, E., Koptyra, M., Nowicki, M.O., Siddiqui, K.M., Groden, J. & Skorski, T. (2005) BLM helicase is activated in BCR/ABL leukemia cells to modulate responses to cisplatin. *Oncogene*, **24**, 3914-3922.
- Slupianek, A., Hoser, G., Majsterek, I., Bronisz, A., Malecki, M., Blasiak, J., Fishel, R. & Skorski, T. (2002) Fusion tyrosine kinases induce drug resistance by stimulation of homology-dependent recombination repair, prolongation of G(2)/M phase, and protection from apoptosis. *Molecular and Cellular Biology*, **22**, 4189-4201.
- Slupianek, A., Jozwiakowski, S.K., Gurdek, E. & Skorski, T. (2009) BCR/ABL kinase interacts with and phosphorylates the RAD51 paralog, RAD51B. *Leukemia*, **23**, 2308-2310.
- Slupianek, A., Nowicki, M.O., Koptyra, M. & Skorski, T. (2006) BCR/ABL modifies the kinetics and fidelity of DNA double-strand breaks repair in hematopoietic cells. *DNA Repair*, **5**, 243-250.

- Slupianek, A., Poplawski, T., Jozwiakowski, S.K., Cramer, K., Pytel, D., Stoczynska, E., Nowicki, M.O., Blasiak, J. & Skorski, T. (2011b) BCR/ABL stimulates WRN to promote survival and genomic instability. *Cancer Research*, **71**, 842-851.
- Slupianek, A., Schmutte, C., Tomblin, G., Nieborowska-Skorska, M., Hoser, G., Nowicki, M.O., Pierce, A.J., Fishel, R. & Skorski, T. (2001) BCR/ABL regulates mammalian RecA homologs, resulting in drug resistance. *Molecular Cell*, **8**, 795-806.
- Smart, D.J., Halicka, H.D., Schmuck, G., Traganos, F., Darzynkiewicz, Z. & Williams, G.M. (2008) Assessment of DNA double-strand breaks and gamma H2AX induced by the topoisomerase II poisons etoposide and mitoxantrone. *Mutation Research-Fundamental and Molecular Mechanisms of Mutagenesis*, **641**, 43-47.
- Smith, D.L., Burthem, J. & Whetton, A.D. (2003) Molecular pathogenesis of chronic myeloid leukaemia. *Expert Rev Mol Med*, **5**, 1-27.
- Solier, S. & Pommier, Y. (2009) The apoptotic ring A novel entity with phosphorylated histones H2AX and H2B and activated DNA damage response kinases. *Cell Cycle*, **8**, 1853-1859.
- Solier, S. & Pommier, Y. (2011) MDC1 cleavage by caspase-3: A novel mechanism for inactivating the DNA damage response during apoptosis. *Cancer Research*, **71**, 906-913.
- Somervaille, T.C.P. & Cleary, M.L. (2009) Mutant CEBPA: Priming stem cells for myeloid leukemogenesis. *Cell Stem Cell*, **5**, 453-454.
- Spooner, E., Brouard, N., Nilsson, S.K., Williams, B., Liu, M.C., Unwin, R.D., Blinco, D., Jaworska, E., Simmons, P.J. & Whetton, A.D. (2008) Developmental fate determination and marker discovery in hematopoietic stem cell biology using proteomic fingerprinting. *Molecular & Cellular Proteomics*, **7**, 573-581.
- Stark, J.M., Pierce, A.J., Oh, J., Pastink, A. & Jasin, M. (2004) Genetic steps of mammalian homologous repair with distinct mutagenic consequences. *Molecular and Cellular Biology*, **24**, 9305-9316.
- Stec, I., Wright, T.J., van Ommen, G.J.B., de Boer, P.A.J., van Haeringen, A., Moorman, A.F.M., Altherr, M.R. & den Dunnen, J.T. (1998) WHSC1, a 90 kb SET domain-containing gene, expressed in early development and homologous to a Drosophila dysmorphia gene maps in the Wolf-Hirschhorn syndrome critical region and is fused to IgH in t(4;14) multiple myeloma. *Human Molecular Genetics*, **7**, 1071-1082.
- Steen, H. & Mann, M. (2004) The ABC's (and XYZ's) of peptide sequencing. *Nature Reviews Molecular Cell Biology*, **5**, 699-711.
- Stein, S.J. & Baldwin, A.S. (2011) NF-kappaB suppresses ROS levels in BCR-ABL(+) cells to prevent activation of JNK and cell death. In: *Oncogene*.
- Stephan, A.K., Kliszczak, M., Dodson, H., Cooley, C. & Morrison, C.G. (2011) Roles of vertebrate Smc5 in sister chromatid cohesion and homologous recombinational repair. *Molecular and Cellular Biology*, **31**, 1369-1381.
- Stoklosa, T., Poplawski, T., Koptyra, M., Nieborowska-Skorska, M., Basak, G., Slupianek, A., Rayevskaya, M., Seferynska, I., Herrera, L., Blasiak, J. & Skorski, T. (2008) BCR/ABL inhibits mismatch repair to protect from apoptosis and induce point mutations. *Cancer Research*, **68**, 2576-2580.
- Stucki, M. (2009) Histone H2A.X Tyr142 phosphorylation: A novel sWitCH for apoptosis? *DNA Repair*, **8**, 873-876.

- Su, C.Y., Chong, K.Y., Edelstein, K., Lille, S., Khardori, R. & Lai, C.C. (1999) Constitutive hsp70 attenuates hydrogen peroxide-induced membrane lipid peroxidation. *Biochemical and Biophysical Research Communications*, **265**, 279-284.
- Su, C.Y., Chong, K.Y., Owen, O.E., Dillmann, W.H., Chang, C.S. & Lai, C.C. (1998) Constitutive and inducible hsp70s are involved in oxidative resistance evoked by heat shock or ethanol. *Journal of Molecular and Cellular Cardiology*, **30**, 587-598.
- Subramanian, J., Vijayakumar, S., Tomkinson, A.E. & Arnheim, N. (2005) Genetic instability induced by overexpression of DNA ligase I in budding yeast. *Genetics*, **171**, 427-441.
- Sugiyama, N., Masuda, T., Shinoda, K., Nakamura, A., Tomita, M. & Ishihama, Y. (2007) Phosphopeptide enrichment by aliphatic hydroxy acid-modified metal oxide chromatography for nano-LC-MS/MS in proteomics applications. *Molecular & Cellular Proteomics*, **6**, 1103-1109.
- Sumara, I., Gimenez-Abian, J.F., Gerlich, D., Hirota, T., Kraft, C., de la Torre, C., Ellenberg, J. & Peters, J.M. (2004) Roles of polo-like kinase 1 in the assembly of functional mitotic spindles. *Current Biology*, **14**, 1712-1722.
- Sung, P.A., Libura, J. & Richardson, C. (2006) Etoposide and illegitimate DNA double-strand break repair in the generation of MLL translocations: New insights and new questions. *DNA Repair*, **5**, 1109-1118.
- Taflin, D.C., Ward, T.L. & Davis, E.J. (1989) Electrified droplet fission and the Rayleigh limit. *Langmuir*, **5**, 376-384.
- Takada, Y., Mukhopadhyay, A., Kundu, G.C., Mahabeleshwar, G.H., Singh, S. & Aggarwal, B.B. (2003) Hydrogen peroxide activates NF-kappa B through tyrosine phosphorylation of I kappa B alpha and serine phosphorylation of p65 - Evidence for the involvement of I kappa B alpha kinase and Syk protein-tyrosine kinase. *Journal of Biological Chemistry*, **278**, 24233-24241.
- Takeda, S., Nakamura, K., Taniguchi, Y. & Paull, T.T. (2007) Ctp1/CtIP and the MRN complex collaborate in the initial steps of homologous recombination. *Molecular Cell*, **28**, 351-352.
- Talpaz, M., Shah, N.P., Kantarjian, H., Donato, N., Nicoll, J., Paquette, R., Cortes, J., O'Brien, S., Nicaise, C., Bleickardt, E., Blackwood-Chirchir, M.A., Iyer, V., Chen, T.-T., Huang, F., Decillis, A.P. & Sawyers, C.L. (2006) Dasatinib in imatinib-resistant Philadelphia chromosome-positive leukemias. *New England Journal of Medicine*, **354**, 2531-2541.
- Tamura, T., Mancini, A., Joos, H., Koch, A., Hakim, C., Dumanski, J., Weidner, K.M. & Niemann, H. (1999) FMIP, a novel Fms-interacting protein, affects granulocyte/macrophage differentiation. *Oncogene*, **18**, 6488-6495.
- Tanaka, T.U., Rachidi, N., Janke, C., Pereira, G., Galova, M., Schiebel, E., Stark, M.J.R. & Nasmyth, K. (2002) Evidence that the Ipl1-Sli15 (Aurora kinase-INCENP) complex by altering promotes chromosome bi-orientation kinetochore-spindle pole connections. *Cell*, **108**, 317-329.
- Tang, D.M., Wu, D.H., Hirao, A.H., Lahti, J.M., Liu, L.Q., Mazza, B., Kidd, V.J., Mak, T.W. & Ingram, A.J. (2002) ERK activation mediates cell cycle arrest and apoptosis after DNA damage independently of p53. *Journal of Biological Chemistry*, **277**, 12710-12717.

- Tang, K.Q. & Smith, R.D. (2001) Physical/chemical separations in the break-up of highly charged droplets from electrosprays. *Journal of the American Society for Mass Spectrometry*, **12**, 343-347.
- Tavner, F.J., Simpson, R., Tashiro, S., Favier, D., Jenkins, N.A., Gilbert, D.J., Copeland, N.G., Macmillan, E.M., Lutwyche, J., Keough, R.A., Ishii, S. & Gonda, T.J. (1998) Molecular cloning reveals that the p160 myb-binding protein is a novel, predominantly nucleolar protein which may play a role in transactivation by Myb. *Molecular and Cellular Biology*, **18**, 989-1002.
- Tchilian, E.Z. & Beverley, P.C.L. (2006) Altered CD45 expression and disease. *Trends in Immunology*, **27**, 146-153.
- Tefferi, A. & Gilliland, D.G. (2007) Oncogenes in myeloproliferative disorders. *Cell Cycle*, **6**, 550-566.
- Thingholm, T.E., Jensen, O.N. & Larsen, M.R. (2009) Analytical strategies for phosphoproteomics. *Proteomics*, **9**, 1451-1468.
- Thingholm, T.E., Jensen, O.N., Robinson, P.J. & Larsen, M.R. (2008) SIMAC (sequential elution from IMAC), a phosphoproteomics strategy for the rapid separation of monophosphorylated from multiply phosphorylated peptides. *Molecular & Cellular Proteomics*, **7**, 661-671.
- Thorner, K., Colomba, A., Ceccato, L., Delsol, G., Payrastra, B. & Gaits-Iacovoni, F. (2009) Reactive oxygen species and lipoxygenases regulate the oncogenicity of NPM-ALK-positive anaplastic large cell lymphomas. *Oncogene*, **28**, 2690-2696.
- Till, J.E. & McCulloch, E.A. (1961) Direct measurement of radiation sensitivity of normal mouse bone marrow cells. *Radiation Research*, **14**, 213-&.
- Tothova, Z., Kollipara, R., Huntly, B.J., Lee, B.H., Castrillon, D.H., Cullen, D.E., McDowell, E.P., Lazo-Kallanian, S., Williams, I.R., Sears, C., Armstrong, S.A., Passegue, E., DePinho, R.A. & Gilliland, D.G. (2007) FoxOs are critical mediators of hematopoietic stem cell resistance to physiologic oxidative stress. *Cell*, **128**, 325-339.
- Trinei, M., Giorgio, M., Cicalese, A., Barozzi, S., Ventura, A., Migliaccio, E., Milia, E., Padura, I.M., Raker, V.A., Maccarana, M., Petronilli, V., Minucci, S., Bernardi, P., Lanfrancone, L. & Pelicci, P.G. (2002) A p53-p66Shc signalling pathway controls intracellular redox status, levels of oxidation-damaged DNA and oxidative stress-induced apoptosis. *Oncogene*, **21**, 3872-3878.
- Tsai, R.Y.L. & McKay, R.D.G. (2002) A nucleolar mechanism controlling cell proliferation in stem cells and cancer cells. *Genes & Development*, **16**, 2991-3003.
- Tsai, W.-B., Chung, Y.M., Takahashi, Y., Xu, Z. & Hu, M.C.T. (2008) Functional interaction between FOXO3a and ATM regulates DNA damage response. *Nature Cell Biology*, **10**, 460-U215.
- Turner, S.D. & Alexander, D.R. (2006) Fusion tyrosine kinase mediated signalling pathways in the transformation of haematopoietic cells. *Leukemia*, **20**, 572-582.
- Tyers, M. & Mann, M. (2003) From genomics to proteomics. *Nature*, **422**, 193-197.
- Unwin, R.D., Evans, C.A. & Whetton, A.D. (2006a) Relative quantification in proteomics: new approaches for biochemistry. *Trends in Biochemical Sciences*, **31**, 473-484.
- Unwin, R.D., Griffiths, J.R., Leverentz, M.K., Grallert, A., Hagan, I.M. & Whetton, A.D. (2005a) Multiple reaction monitoring to identify sites of protein phosphorylation with high sensitivity. *Molecular & Cellular Proteomics*, **4**, 1134-1144.

- Unwin, R.D., Griffiths, J.R. & Whetton, A.D. (2009) A sensitive mass spectrometric method for hypothesis-driven detection of peptide post-translational modifications: multiple reaction monitoring-initiated detection and sequencing (MIDAS). *Nature Protocols*, **4**, 870-877.
- Unwin, R.D., Pierce, A., Watson, R.B., Sternberg, D.W. & Whetton, A.D. (2005b) Quantitative proteomic analysis using isobaric protein tags enables rapid comparison of changes in transcript and protein levels in transformed cells. *Molecular & Cellular Proteomics*, **4**, 924-935.
- Unwin, R.D., Smith, D.L., Blinco, D., Wilson, C.L., Miller, C.J., Evans, C.A., Jaworska, E., Baldwin, S.A., Barnes, K., Pierce, A., Spooncer, E. & Whetton, A.D. (2006b) Quantitative proteomics reveals posttranslational control as a regulatory factor in primary hematopoietic stem cells. *Blood*, **107**, 4687-4694.
- Unwin, R.D. & Whetton, A.D. (2006) Systematic proteome and transcriptome analysis of stem cell populations. *Cell Cycle*, **5**, 1587-1591.
- Unwin, R.D. & Whetton, A.D. (2007) How will haematologists use proteomics? *Blood Reviews*, **21**, 315-326.
- Valeri, A., Eugenia Alonso-Ferrero, M., Rio, P., Roser Pujol, M., Casado, J.A., Perez, L., Jacome, A., Agirre, X., Jose Calasanz, M., Hanenberg, H., Surralles, J., Prosper, F., Albella, B. & Bueren, J.A. (2010) Bcr/Abl interferes with the Fanconi anemia/BRCA pathway: Implications in the chromosomal instability of chronic myeloid leukemia cells. *Plos One*, **5**.
- Valerie, K. & Povirk, L.F. (2003) Regulation and mechanisms of mammalian double-strand break repair. *Oncogene*, **22**, 5792-5812.
- van Attikum, H. & Gasser, S.M. (2009) Crosstalk between histone modifications during the DNA damage response. *Trends in Cell Biology*, **19**, 207-217.
- van der Horst, A. & Burgering, B.M.T. (2007) Stressing the role of FoxO proteins in lifespan and disease. *Nature Reviews Molecular Cell Biology*, **8**, 440-450.
- Vermeulen, M., Eberl, H.C., Matarese, F., Marks, H., Denissov, S., Butter, F., Lee, K.K., Olsen, J.V., Hyman, A.A., Stunnenberg, H.G. & Mann, M. (2010) Quantitative interaction proteomics and genome-wide profiling of epigenetic histone marks and their readers. *Cell*, **142**, 967-980.
- Walter, S.A., Cutler, R.E., Martinez, R., Gishizky, M. & Hill, R.J. (2003) Stk10, a new member of the polo-like kinase family highly expressed in hematopoietic tissue. *Journal of Biological Chemistry*, **278**, 18221-18228.
- Walz, C., Crowley, B.J., Hudon, H.E., Gramlich, J.L., Neuberg, D.S., Podar, K., Griffin, J.D. & Sattler, M. (2006) Activated Jak2 with the V617F point mutation promotes G(1)/S phase transition. *Journal of Biological Chemistry*, **281**, 18177-18183.
- Wang, J.C. (2002) Cellular roles of DNA topoisomerases: A molecular perspective. *Nature Reviews Molecular Cell Biology*, **3**, 430-440.
- Warmuth, M., Danhauser-Riedl, S. & Hallek, M. (1999) Molecular pathogenesis of chronic myeloid leukemia: implications for new therapeutic strategies. *Annals of Hematology*, **78**, 49-64.
- Wasinger, V.C., Cordwell, S.J., Cerpapojak, A., Yan, J.X., Gooley, A.A., Wilkins, M.R., Duncan, M.W., Harris, R., Williams, K.L. & Humpherysmith, I. (1995) Progress

- with gene-product mapping of the Mollicutes: *Mycoplasma genitalium*. *Electrophoresis*, **16**, 1090-1094.
- Waterworth, W.M., Kozak, J., Provost, C.M., Bray, C.M., Angelis, K.J. & West, C.E. (2009) DNA ligase 1 deficient plants display severe growth defects and delayed repair of both DNA single and double strand breaks. *Bmc Plant Biology*, **9**.
- Weissman, I.L. (2000) Stem cells: Units of development, units of regeneration, and units in evolution. *Cell*, **100**, 157-168.
- Wernig, G., Gonneville, J.R.R., Crowley, B.J., Rodrigues, M.S., Reddy, M.M., Hudon, H.E., Walz, C., Reiter, A., Podar, K., Royer, Y., Constantinescu, S.N., Tomasson, M.H., Griffin, J.D., Gilliland, D.G. & Sattler, M. (2008) The Jak2V617F oncogene associated with myeloproliferative diseases requires a functional FERM domain for transformation and for expression of the Myc and Pim proto-oncogenes. *Blood*, **111**, 3751-3759.
- Whetton, A.D. & Graham, G.J. (1999) Homing and mobilization in the stem cell niche. *Trends in Cell Biology*, **9**, 233-238.
- Whitehouse, C.M., Dreyer, R.N., Yamashita, M. & Fenn, J.B. (1985) Electrospray interface for liquid chromatographs and mass spectrometers. *Analytical Chemistry*, **57**, 675-679.
- Williams, R.S., Williams, J.S. & Tainer, J.A. (2007) Mre11-Rad50-Nbs1 is a keystone complex connecting DNA repair machinery, double-strand break signaling, and the chromatin template. *Biochemistry and Cell Biology-Biochimie Et Biologie Cellulaire*, **85**, 509-520.
- Winter, D., Seidler, J., Ziv, Y., Shiloh, Y. & Lehmann, W.D. (2009) Citrate Boosts the Performance of Phosphopeptide Analysis by UPLC-ESI-MS/MS. *Journal of Proteome Research*, **8**, 418-424.
- Wiseman, H. & Halliwell, B. (1996) Damage to DNA by reactive oxygen and nitrogen species: Role in inflammatory disease and progression to cancer. *Biochemical Journal*, **313**, 17-29.
- Witze, E.S., Old, W.M., Resing, K.A. & Ahn, N.G. (2007) Mapping protein post-translational modifications with mass spectrometry. *Nature Methods*, **4**, 798-806.
- Wolf-Yadlin, A., Hautaniemi, S., Lauffenburger, D.A. & White, F.M. (2007) Multiple reaction monitoring for robust quantitative proteomic analysis of cellular signaling networks. *Proceedings of the National Academy of Sciences of the United States of America*, **104**, 5860-5865.
- Woodcock, S.A., Rooney, C., Lontos, M., Connolly, Y., Zoumpourlis, V., Whetton, A.D., Gorgoulis, V.G. & Malliri, A. (2009) Src-induced disassembly of adherens junctions requires localized phosphorylation and degradation of the Rac activator Tiam1. *Molecular Cell*, **33**, 639-653.
- Wu, G., Chai, J.J., Suber, T.L., Wu, J.W., Du, C.Y., Wang, X.D. & Shi, Y.G. (2000) Structural basis of IAP recognition by Smac/DIABLO. *Nature*, **408**, 1008-1012.
- Wu, L.M., Luo, K.T., Lou, Z.K. & Chen, J.J. (2008) MDC1 regulates intra-S-phase checkpoint by targeting NBS1 to DNA double-strand breaks. *Proceedings of the National Academy of Sciences of the United States of America*, **105**, 11200-11205.
- Xiao, A., Li, H., Shechter, D., Ahn, S.H., Fabrizio, L.A., Erdjument-Bromage, H., Ishibe-Murakami, S., Wang, B., Tempst, P., Hofmann, K., Patel, D.J., Elledge, S.J. & Allis,

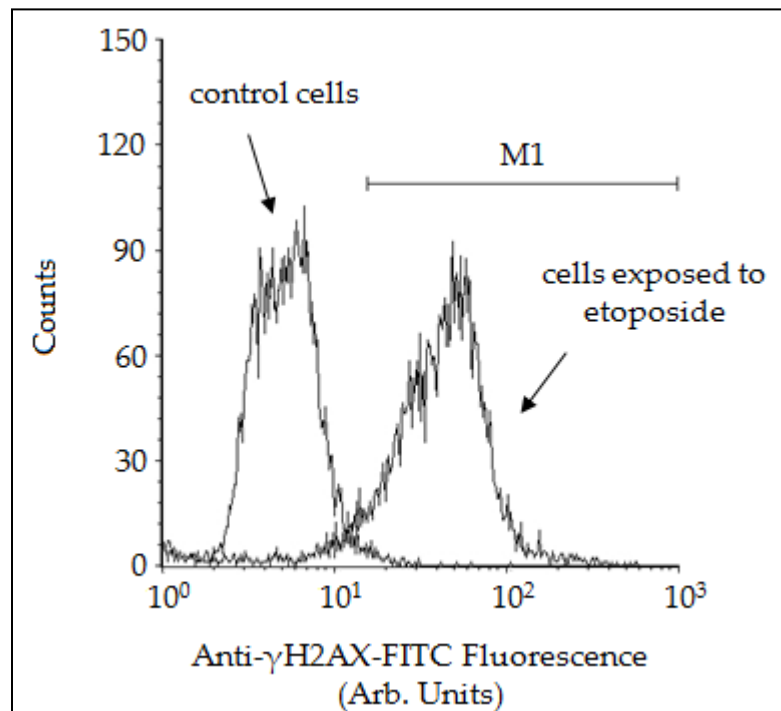
- C.D. (2009) WSTF regulates the H2A.X DNA damage response via a novel tyrosine kinase activity. *Nature*, **457**, 57-U57.
- Xie, A., Hartlerode, A., Stucki, M., Odate, S., Puget, N., Kwok, A., Nagaraju, G., Yan, C., Alt, F.W., Chen, J., Jackson, S.P. & Scully, R. (2007) Distinct roles of chromatin-associated proteins MDC1 and 53BP1 in mammalian double-strand break repair. *Molecular Cell*, **28**, 1045-1057.
- Yalcin, S., Marinkovic, D., Mungamuri, S.K., Zhang, X., Tong, W., Sellers, R. & Ghaffari, S. (2010) ROS-mediated amplification of AKT/mTOR signalling pathway leads to myeloproliferative syndrome in Foxo3(-/-) mice. *Embo Journal*, **29**, 4118-4131.
- Yalcin, S., Zhang, X., Luciano, J.P., Mungamuri, S.K., Marinkovic, D., Vercherat, C., Sarkar, A., Grisotto, M., Taneja, R. & Ghaffari, S. (2008) Foxo3 is essential for the regulation of ataxia telangiectasia mutated and oxidative stress-mediated homeostasis of hematopoietic stem cells. *Journal of Biological Chemistry*, **283**, 25692-25705.
- Yang, L.V., Nicholson, R.H., Kaplan, J., Galy, A. & Li, L. (2001) Hemogen is a novel nuclear factor specifically expressed in mouse hematopoietic development and its human homologue EDAG maps to chromosome 9q22, a region containing breakpoints of hematological neoplasms. *Mechanisms of Development*, **104**, 105-111.
- Yang, L.V., Wan, J., Ge, Y., Fu, Z., Kim, S.Y., Fujiwara, Y., Taub, J.W., Matherly, L.H., Eliason, J. & Li, L. (2006) The GATA site-dependent hemogen promoter is transcriptionally regulated by GATA1 in hematopoietic and leukemia cells. *Leukemia*, **20**, 417-425.
- Yao, Z., Flash, I., Raviv, Z., Yung, Y., Asscher, Y.D., Pleban, S. & Seger, R. (2001) Non-regulated and stimulated mechanisms cooperate in the nuclear accumulation of MEK1. *Oncogene*, **20**, 7588-7596.
- Yeh, C.H., Tseng, R., Zhang, Z., Cortes, J., O'Brien, S., Giles, F., Hannah, A., Estrov, Z., Keating, M., Kantarjian, H. & Albitar, M. (2009) Circulating heat shock protein 70 and progression in patients with chronic myeloid leukemia. *Leukemia Research*, **33**, 212-217.
- Yi, E.C., Li, X.J., Cooke, K., Lee, H., Raught, B., Page, A., Aneliunas, V., Hieter, P., Goodlett, D.R. & Aebersold, R. (2005) Increased quantitative proteome coverage with C-13/C-12-based, acid-cleavable isotope-coded affinity tag reagent and modified data acquisition scheme. *Proteomics*, **5**, 380-387.
- Yoshimura, K., Kitagawa, H., Fujiki, R., Tanabe, M., Takezawa, S., Takada, I., Yamaoka, I., Yonezawa, M., Kondo, T., Furutani, Y., Yagi, H., Yoshinaga, S., Masuda, T., Fukuda, T., Yamamoto, Y., Ebihara, K., Li, D.Y., Matsuoka, R., Takeuchi, J.K., Matsumoto, T. & Kato, S. (2009) Distinct function of 2 chromatin remodeling complexes that share a common subunit, Williams syndrome transcription factor (WSTF). *Proceedings of the National Academy of Sciences of the United States of America*, **106**, 9280-9285.
- Young, N.L., DiMaggio, P.A. & Garcia, B.A. (2010) The significance, development and progress of high-throughput combinatorial histone code analysis. *Cellular and Molecular Life Sciences*, **67**, 3983-4000.
- Yun, M.H. & Hiom, K. (2009) CtIP-BRCA1 modulates the choice of DNA double-strand-break repair pathway throughout the cell cycle. *Nature*, **459**, 460-U184.

- Zhang, P., Liu, B., Kang, S.W., Seo, M.S., Rhee, S.G. & Obeid, L.M. (1997) Thioredoxin peroxidase is a novel inhibitor of apoptosis with a mechanism distinct from that of Bcl-2. *Journal of Biological Chemistry*, **272**, 30615-30618.
- Zhang, Y. & Rowley, J.D. (2006) Chromatin structural elements and chromosomal translocations in leukemia. *DNA Repair*, **5**, 1282-1297.
- Zhang, Y., Wolf-Yadlin, A., Ross, P.L., Pappin, D.J., Rush, J., Lauffenburger, D.A. & White, F.M. (2005) Time-resolved mass spectrometry of tyrosine phosphorylation sites in the epidermal growth factor receptor signaling network reveals dynamic modules. *Molecular & Cellular Proteomics*, **4**, 1240-1250.

Chapter 7.

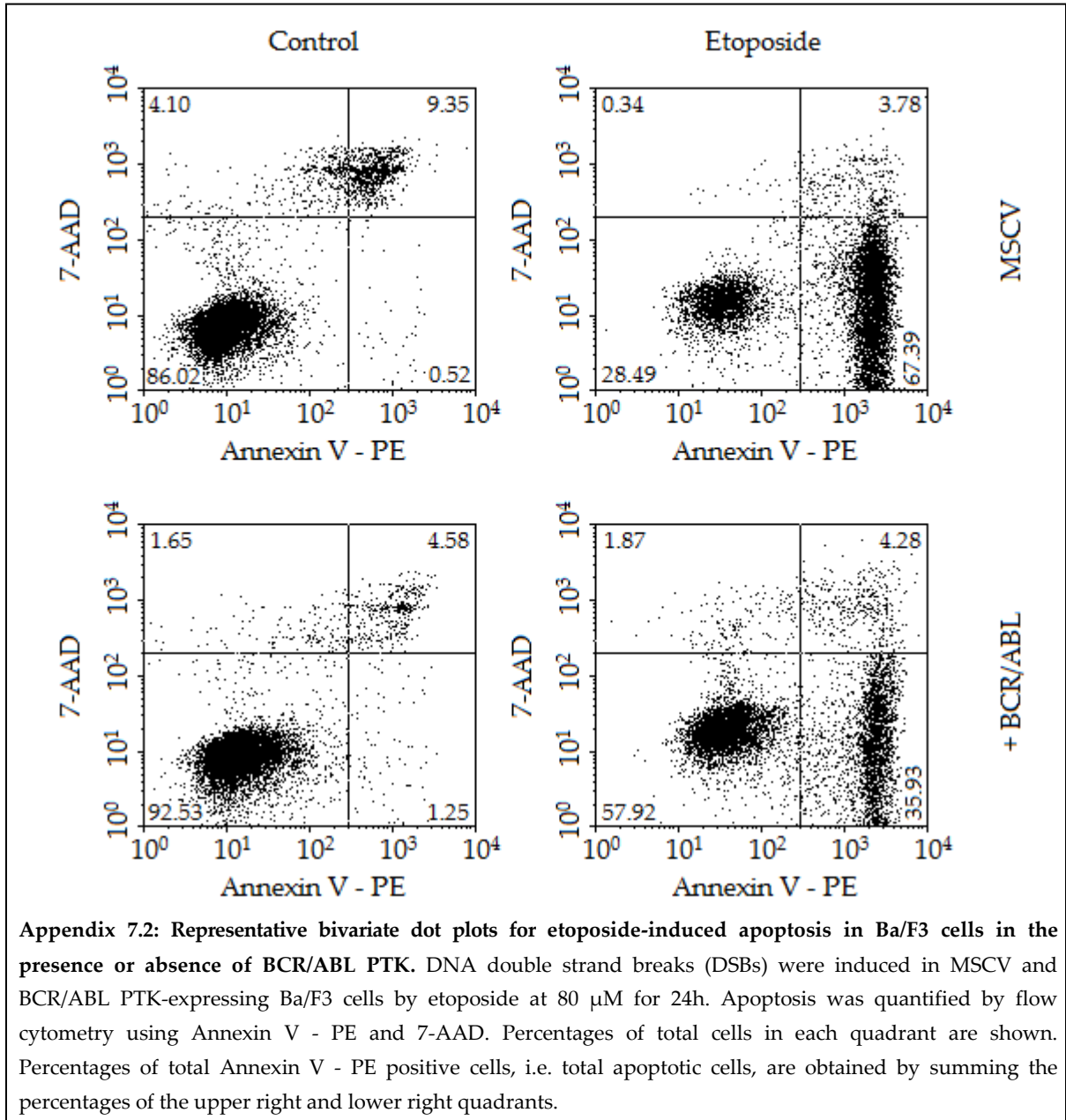
Appendices

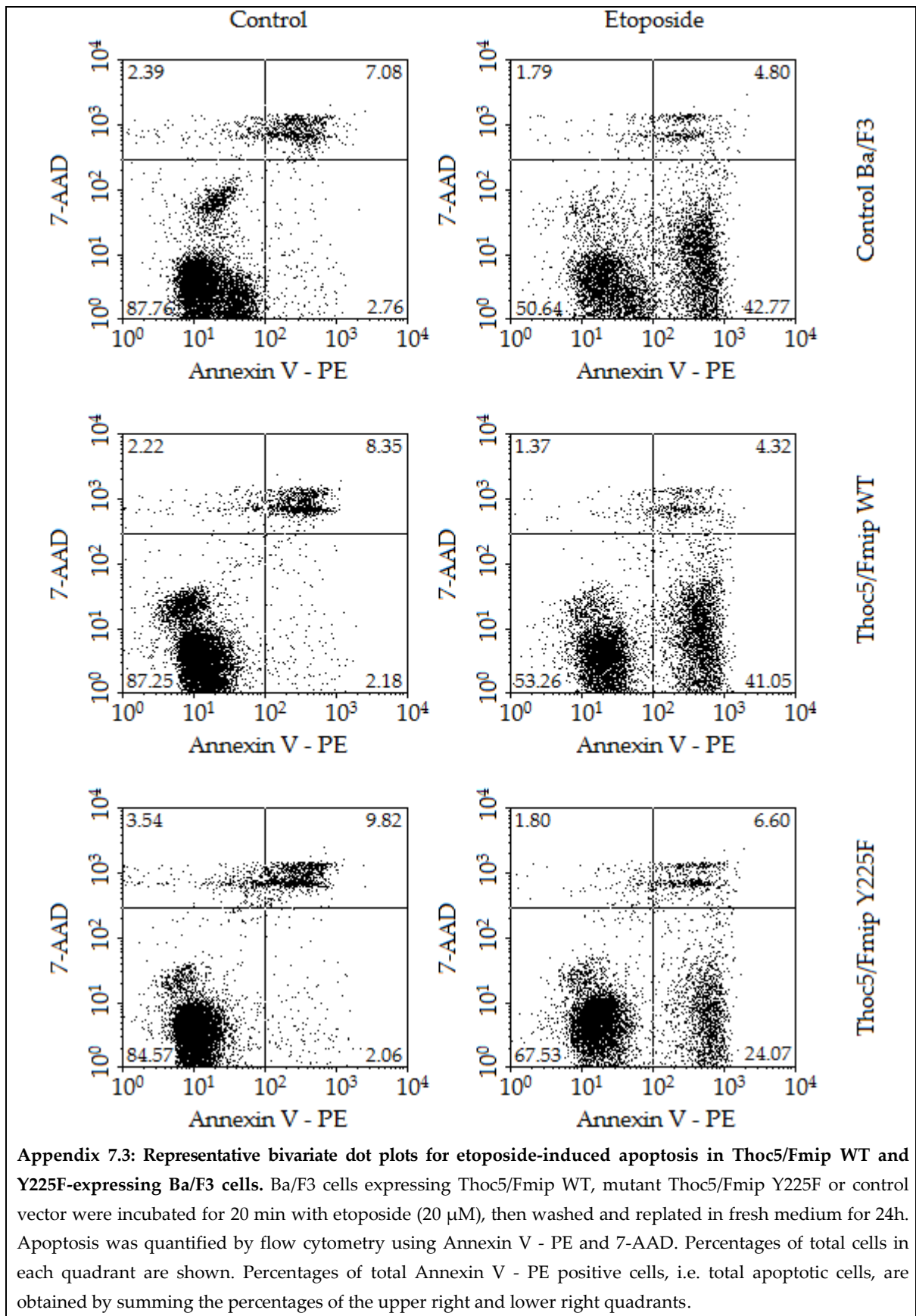
7.1. γ H2AX assay with flow cytometry



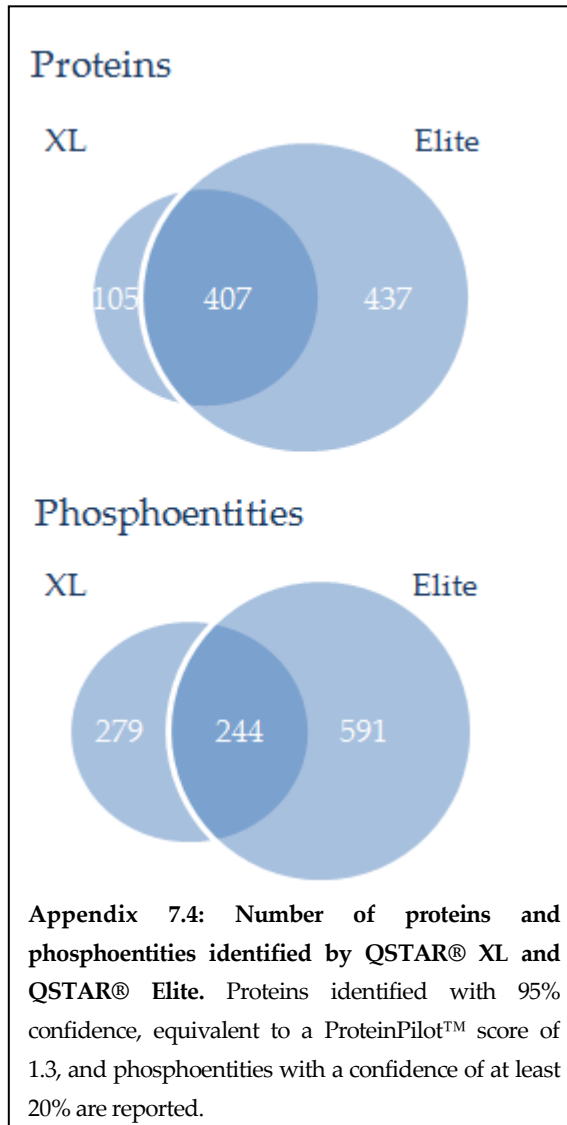
Appendix 7.1: Representative histogram overlay of anti- γ H2AX-FITC fluorescence for control cells and cells exposed to etoposide. DNA double strand breaks (DSBs) were induced in Ba/F3 cells with etoposide at 80 μ M for 20 min. Control and treated cells were fixed, permeabilised and incubated with anti- γ H2AX-FITC antibody and fluorescence was analysed by flow cytometry. DNA DSBs were quantified using the median fluorescence of anti- γ H2AX-FITC for each population. Alternatively, the percentage of anti- γ H2AX-FITC positive cells was determined above the fluorescence of the control population (gate M1).

7.2. Apoptosis assay with flow cytometry













7.3. Comparison between QSTAR® XL and QSTAR® Elite




7.4. Phosphoentities potentially regulated by etoposide and/or BCR/ABL PTK

Appendix 7.5: Phosphosite-specific action of BCR/ABL PTK only (1/2)

Name	Phosphosite	Phosphoentity	Average Log ₂ (ratios)				Student's t-test p-value			
										
Abi1	T215*	K..TLEPVKPPTVPNDYMT[Pho]SPAR..L	1.491	1.483	0.060	0.041	0.000	0.000	0.771	0.835
Abi1	Y213	K..TLEPVKPPTVPNDY[Pho]MTSPAR..L	1.351	1.361	0.017	0.016	0.000	0.000	0.922	0.926
Abl1	T394*	R..LMTGDTYT[Pho]AHAGAK..F	1.627	1.813	-0.076	0.099	0.000	0.000	0.749	0.641
Bcr	Y643	K..NSLETLLY[Pho]KPVDR..V	3.412	4.064	-0.399	0.242	0.000	0.000	0.076	0.267
Cast	T479	K..SNDTSQT[Pho]PPGETVPR..A	-0.484	-0.510	-0.095	-0.133	0.031	0.023	0.684	0.565
Dkc1	S481	K..TVLES[Pho]GGETGDGDN[Dea]DTTKK..K	-0.852	-0.703	0.153	0.291	0.000	0.002	0.476	0.183
Dok1	T447*	K..GFSSDT[Pho]ALYSQVQK..S	0.604	0.556	0.100	0.041	0.006	0.012	0.637	0.837
Eif5b	S215	K..SVPTVDS[Pho]GNEDDDSSFK..I	0.726	0.825	-0.140	0.033	0.001	0.000	0.543	0.863
Eif5b	S114	K..TSFDENDS[Pho]EELEDKDSK..S	0.628	0.498	0.224	0.083	0.004	0.024	0.302	0.694
Enah	S740	R..TNTMN[Dea]GSKS[Pho]PVISRPK..S	0.454	0.478	-0.077	-0.064	0.039	0.030	0.746	0.789
Hist1h1b	S18	M..S[Ace]E[Deh]TAPAETAAPAPVEKS[Pho]PAK..K	0.486	0.440	0.102	0.211	0.027	0.045	0.631	0.330
Hnrnpc	S229*	K..QADLS[Pho]FSSPVEMKNEK..S	-0.455	-0.549	0.071	-0.034	0.043	0.014	0.734	0.894
Inpp5d	S935	K..STLS[Pho]PDQQLTAWSYDQLPK..D	-1.617	-1.703	-0.018	-0.019	0.000	0.000	0.953	0.949
Jun	S73	K..LAS[Pho]PELER..L	-0.877	-0.915	0.389	0.340	0.000	0.000	0.076	0.121

 BCR/ABL:MSCV

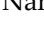

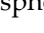
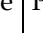
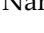

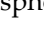
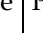
 MSCV+etoposide:MSCV

 BCR/ABL+etoposide:MSCV+etoposide

 BCR/ABL+etoposide :BCR/ABL


[Ace]: acetylation, [Dea]: deamidation, [Deh]: dehydration, [Pho]: phosphorylation. * manual validation did not enable phosphosite assignment with confidence.

Appendix 7.6: Phosphosite-specific action of BCR/ABL PTK only (2/2)

Name	Phosphosite	Phosphoentity	Average Log ₂ (ratios)				Student's t-test p-value			
										
Kdm2a	S692	R..KIEES[Pho]DEEAVQAK..V	-0.554	-0.605	0.014	-0.047	0.013	0.007	0.931	0.848
Lig1	S199	K..EGDQLIVP[Oxi]S[Pho]EPT[Deh]KSPESVTLTK..T	0.756	0.561	-0.159	-0.366	0.001	0.011	0.486	0.104
Mybbp1a	T1277*	K..LSQVN[Dea]GAT[Pho]PVSPIEP..E	-0.609	-0.568	0.128	0.158	0.007	0.011	0.550	0.465
Myc	T58/S62	K..KFELLPT[Pho]PPLS[Pho]PSR..R	-0.618	-0.440	0.240	0.406	0.006	0.050	0.271	0.064
Myc	S164*	R..KDSTLS[Pho]PAR..G	-0.537	-0.666	-0.202	-0.342	0.016	0.003	0.375	0.128
Ncf2	S332	R..LQLS[Pho]PGHK..Q	-0.624	-0.692	-0.034	-0.113	0.005	0.002	0.896	0.626
Nop56	S554	R..KFS[Pho]EEPEVAANFTK..S	-0.747	-1.185	0.238	-0.212	0.001	0.000	0.274	0.351
Nup35	S258	R..GVLSS[Pho]PSLAFTTPIR..T	-0.641	-0.616	0.193	0.209	0.004	0.006	0.372	0.337
Pabpn1	S146	K..QMNMS[Pho]PPPGN[Amm]AGPVIM[Oxi]SLEEK..M	-0.532	-0.457	-0.154	-0.090	0.018	0.042	0.501	0.703
Ranbp2	S954	R..FESPATGILS[Pho]PR..G	0.528	0.596	0.184	0.241	0.017	0.007	0.394	0.268
Snap23	S110	K..ATWGDGGDNS[Pho]PSNVVSK..Q	0.532	0.787	-0.049	0.195	0.016	0.000	0.842	0.369
Top2a	S1373	K..TQGSSMS[Pho]VVDLESVKDSVPASPGVPAADFP AETE QSKPSK..K	-0.484	-0.617	0.133	-0.011	0.031	0.006	0.534	0.978
Whsc1	S437	R..GVGS[Pho]PAGR..K	0.584	0.503	-0.253	-0.345	0.008	0.022	0.263	0.125

 BCR/ABL:MSCV

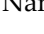

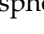
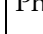
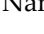

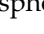
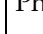
 MSCV+etoposide:MSCV

 BCR/ABL+etoposide:MSCV+etoposide

 BCR/ABL+etoposide :BCR/ABL


[Amm]: loss of ammonia, [Dea]: deamidation, [Deh]: dehydration, [Oxi]: oxidation, [Pho]: phosphorylation. * manual validation did not enable phosphosite assignment with confidence.

Appendix 7.7: Phosphosite-specific crosstalk between BCR/ABL PTK and etoposide action (1/3)

Name	Phosphosite	Phosphoentity	Average Log ₂ (ratios)				Student's t-test p-value			
										
Anln	S293	K..ASS[Pho]PVTAATFITENR..E	-0.178	-0.614	0.007	-0.441	0.436	0.006	0.958	0.050
Anln	S318	K..TAS[Pho]PLKTEAR..K	-0.737	-0.386	-0.631	-0.291	0.001	0.086	0.005	0.197
Bcl7c	S126	K..GAEPSPGGTPQPSRPGS[Pho]PTGPPEVITEDTQPPQLGQER..D	0.433	-0.135	-0.306	-0.792	0.049	0.558	0.174	0.000
Cbx3	S93	K..RKS[Pho]LSDSEDDSK..S	-0.308	-0.525	-0.869	-1.098	0.172	0.019	0.000	0.000
Clk3	S157	R..YRS[Pho]PEPDPYLSYR..W	0.135	-0.611	0.512	-0.248	0.528	0.006	0.020	0.274
Gatad2a	S181	K..EATAQKPTASSGS[Pho]TVTTTPPLVR..G	-0.292	-0.531	-0.496	-0.747	0.196	0.018	0.027	0.001
Gnl3	S95	R..KLEVS[Pho]PGDEQSNVETR..E	0.095	0.461	-0.609	-0.254	0.653	0.036	0.006	0.261
Hemgn	S380	K..EFTVPIVSS[Pho]QK..T	0.545	2.693	0.280	2.416	0.013	0.000	0.200	0.000
Hist1h1a	S183	K..KVAKS[Pho]PAK..A	0.375	0.570	-1.396	-1.212	0.087	0.010	0.000	0.000
Hist1h1a	T4	S..E[Lys]T[Pho]APVAQAASTATEKPAAAK..K	0.535	0.653	0.577	0.684	0.015	0.003	0.009	0.002
Hist1h1b	T135	K..KPAGAT[Pho]PK..K	0.475	-0.059	-1.343	-1.889	0.031	0.806	0.000	0.000
Hist1h1b	S186	K..AAKS[Pho]PAKPK..A	0.554	0.327	-1.364	-1.602	0.012	0.135	0.000	0.000
Hist1h1b	S18	M..S[Ace]ET[Deh]APAETAAPAPVEKS[Pho]PAK..K	0.454	0.019	-0.411	-0.858	0.039	0.916	0.067	0.000
Hist1h1b	S18	E..TAPAETAAPAPVEKS[Pho]PAK..K	0.490	0.512	-0.595	-0.584	0.026	0.020	0.008	0.009
Hist1h1b	S18	M..SETAPAETAAPAPVEKS[Pho]PAK..K	0.677	0.655	-0.436	-0.472	0.002	0.003	0.052	0.035
Hist1h1d	T18	M..S[Ace]ETAPAAPAAPAPVEKT[Pho]PVKK..K	0.568	-0.061	-2.229	-2.869	0.010	0.801	0.000	0.000

 BCR/ABL:MSCV









 MSCV+etoposide:MSCV

 BCR/ABL+etoposide:MSCV+etoposide

 BCR/ABL+etoposide :BCR/ABL


[Ace]: acetylation, [Deh]: dehydration, [Lys]: Lysine-addition, [Pho]: phosphorylation.

Appendix 7.8: Phosphosite-specific crosstalk between BCR/ABL PTK and etoposide action (2/3)

Name	Phosphosite	Phosphoentity	Average Log ₂ (ratios)				Student's t-test p-value			
										
Hist1h1d	T18	A..PAAPAAPAPVEKT[Pho]PVKK..K	0.437	0.109	-2.459	-2.798	0.047	0.608	0.000	0.000
Hist1h1d	T18	M..S[Ace]ETAPAAPAAPAPVEKT[Pho]PVK..K	0.459	-0.243	-1.722	-2.197	0.037	0.283	0.000	0.000
Hist1h1d	T4	M..S[Ace]ET[Pho]APAAPAAPAPVE[Cat]K..T	0.746	0.734	1.359	1.336	0.001	0.001	0.000	0.000
Hist1h1d	T18	A..PAAPAAPAPVEKT[Pho]PVK..K	0.511	0.056	-0.804	-1.270	0.020	0.783	0.000	0.000
Hist1h1d	T4	M..S[Ace]ET[Pho]APAAPAAPAPVEK..T	0.423	0.613	0.680	0.709	0.054	0.005	0.002	0.001
Hist1h1e	T18	A..PAAPAAPAPAEKT[Pho]PVKK..K	0.685	0.604	-2.696	-2.788	0.002	0.006	0.000	0.000
Hist1h1e	T18	A..PAAPAPAEKT[Pho]PVKK..K	0.546	0.712	-2.583	-2.427	0.013	0.001	0.000	0.000
Hist1h1e	T18	M..S[Ace]ETAPAAPAAPAPAEKT[Pho]PVKK..K	0.597	0.416	-2.217	-2.416	0.007	0.058	0.000	0.000
Hist1h1e	T18	M..S[Ace]ETAPAAPAAPAPAEKT[Pho]PVK..K	0.861	0.526	-1.615	-1.962	0.000	0.017	0.000	0.000
Hist1h1e	T18	A..PAAPAAPAPAEKT[Pho]PVK..K	0.563	0.349	-1.341	-1.566	0.011	0.112	0.000	0.000
Hist1h1e	S187	K..KAPKS[Pho]PAK..A	0.398	0.576	-1.021	-0.855	0.070	0.009	0.000	0.000
Hist1h1e	T4*	M..S[Ace]ET[Pho]APAAPAAPAPAEK..T	0.462	0.386	0.690	0.569	0.035	0.078	0.002	0.010

 BCR/ABL:MSCV

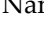
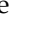

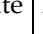
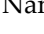
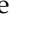

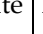
 MSCV+etoposide:MSCV

 BCR/ABL+etoposide:MSCV+etoposide

 BCR/ABL+etoposide :BCR/ABL


[Ace]: acetylation, [Cat]: sodium adduct, [Pho]: phosphorylation. * manual validation did not enable phosphosite assignment with confidence.

Appendix 7.9: Phosphosite-specific crosstalk between BCR/ABL PTK and etoposide action (3/3)

Name	Phosphosite	Phosphoentity	Average Log ₂ (ratios)				Student's t-test p-value			
										
Hmga1	S36	R..KQPPVS[Pho]PGTALVGSQK..E	0.450	-0.080	-1.152	-1.693	0.041	0.734	0.000	0.000
Hmga1	S99*/S103	K..KLEKEEEEGIS[Pho]QESS[Pho]EEEEQ..	0.568	-0.103	0.238	-0.448	0.010	0.659	0.274	0.046
Hnrnpc	S229	K..QADLS[Pho]FSSPVEMK..N	-0.270	-0.500	-0.794	-1.030	0.231	0.026	0.000	0.000
Incenp	S284	R..S[Pho]LISQDSQVPLASK..Y	-0.446	0.125	-0.711	-0.152	0.047	0.558	0.001	0.508
Lig1	S67	R..N[Dea]QVVPESDS[Pho]PVKR..T	0.489	0.295	-0.420	-0.625	0.026	0.177	0.062	0.005
Mdc1	S1053*	R..SS[Pho]TRTPELIVPVDPELQPSTSTEQVIPK..L	0.235	0.704	0.132	0.725	0.281	0.001	0.538	0.001
Mdc1	S595	R..SQSGS[Pho]PAAPVEQVVIHTDTSGDPTLPQR..E	0.481	0.492	-0.455	-0.456	0.029	0.025	0.042	0.042
Mybbp1a	T1277*	K..LSQVN[Dea]GAT[Pho]PVSPIEPESK..K	0.394	-0.700	0.332	-0.773	0.073	0.002	0.129	0.001
Mybbp1a	T1162	K..DIPSDT[Pho]QSPVSTK..R	0.436	-0.043	-0.220	-0.710	0.047	0.864	0.332	0.002
Mybbp1a	T1277	K..LSQVN[Dea]GAT[Pho]PVS[Deh]PIEPESK..K	-0.470	-0.195	-0.531	-0.266	0.036	0.392	0.018	0.239
Mybbp1a	S1280	K..LSQVN[Dea]GAT[Deh]PVS[Pho]PIEPESK..K	-0.537	-0.289	-0.482	-0.246	0.017	0.201	0.032	0.278
Mybbp1a	S1280	K..LSQVN[Dea]GAT[Deh]PVS[Pho]PIE..P	-0.549	0.038	-0.538	0.039	0.014	0.847	0.016	0.846
Safb2	T344*	R..KHQAQAEALGT[Pho]GGGAGM[Oxi]N[Hex]C[Met]EPVGLEEPVEQSSTAAQLPEATSQELVR..A	-0.160	-0.441	-0.786	-1.079	0.486	0.049	0.000	0.000
Spnb2	S2340	R..AQ[Dea]T[Did]LPTSVVTITSESS[Pho]PGKR..E	0.438	0.494	-0.511	-0.466	0.046	0.025	0.023	0.038
Stk10	T950	K..LSEEAEPRTT[Pho]PSK..A	-0.983	-0.169	-0.587	0.214	0.000	0.460	0.009	0.324
Zfp828	S532	K..AVLPAS[Pho]PEPR..K	-0.200	-0.475	-0.385	-0.672	0.380	0.034	0.086	0.003

 BCR/ABL:MSCV

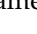
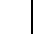
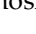
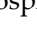




 MSCV+etoposide:MSCV

 BCR/ABL+etoposide:MSCV+etoposide

 BCR/ABL+etoposide :BCR/ABL


[Dea]: deamidation, [Deh]: dehydration, [Did]: loss of 2 atoms of Hydrogen, [Hex]: glycosylation (hexose), [Met]: β-methylthiolation, [Oxi]: oxidation, [Pho]: phosphorylation. * manual validation did not enable phosphosite assignment with confidence.

Appendix 7.10: Phosphosite-specific action of etoposide only (1/3)

Name	Phosphosite	Phosphoentity	Average Log ₂ (ratios)				Student's t-test p-value			
										
Acly	S455	R..TAS[Pho]FSESR..A	0.263	0.217	0.490	0.433	0.228	0.318	0.026	0.049
Bclaf1	S177	K..KAEGEPQEES[Pho]PLK..S	0.284	0.170	-0.775	-0.900	0.194	0.432	0.001	0.000
Btbd12	S926/S940	R..GILISPAKS[Pho]PPIDLTQSVPEPLS[Pho]PR..A	0.312	-0.069	0.878	0.485	0.153	0.774	0.000	0.027
Ddx21	S144 (S181)	K..GKEAN[Dea]GDAGEKS[Pho]PK..L	0.080	0.156	-0.722	-0.657	0.704	0.470	0.001	0.003
Eif4g1	S1211	R..KAAS[Pho]LTEDR..G	0.010	0.054	0.878	0.911	0.947	0.793	0.000	0.000
H2ax	S139	K..KASQAS[Pho]QEY..	0.170	0.146	1.443	1.408	0.430	0.496	0.000	0.000
Hist1h1a	T4*	M..S[Ace]ET[Pho]APVAQAASTATEKPAAAK..K	0.329	0.389	0.702	0.736	0.133	0.076	0.001	0.001
Hist1h1b	S18	A..APAPVEKS[Pho]PAK..K	0.419	0.273	-0.539	-0.696	0.056	0.212	0.016	0.002
Hist1h1b	S18	A..APAPVEKS[Pho]PAKK..K	0.123	0.079	-0.551	-0.606	0.566	0.707	0.014	0.007
Hist1h1b	S18	A..PAPVEKS[Pho]PAK..K	0.410	0.353	-0.455	-0.524	0.062	0.107	0.043	0.019
Hist1h1b	S18	M..S[Ace]ETAPAETAAPAPVEKS[Pho]PAK..K	0.285	0.276	-0.503	-0.523	0.192	0.206	0.025	0.020
Hist1h1b	S18	A..PAPVEKS[Pho]PAKK..K	0.229	0.391	-0.631	-0.481	0.293	0.075	0.005	0.032
Hist1h1b	S18	A..PAETAAPAPVEKS[Pho]PAKK..K	0.268	0.324	-0.687	-0.457	0.218	0.139	0.002	0.042
Hist1h1c/d	T146 (147)	K..KATGAAT[Pho]PK..K	0.312	-0.195	-1.713	-2.232	0.154	0.392	0.000	0.000

 BCR/ABL:MSCV

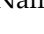
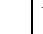
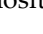
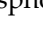
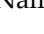
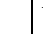
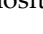
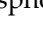
 MSCV+etoposide:MSCV

 BCR/ABL+etoposide:MSCV+etoposide

 BCR/ABL+etoposide :BCR/ABL


[Ace] : acetylation, [Dea]: deamidation, [Pho]: phosphorylation. * manual validation did not enable phosphosite assignment with confidence.

Appendix 7.11: Phosphosite-specific action of etoposide only (2/3)

Name	Phosphosite	Phosphoentity	Average Log ₂ (ratios)				Student's t-test p-value			
										
Mcm6	S704	R..FN[Dea]GSSEDAS[Pho]QETVSKPSLR..L	-0.052	0.377	0.981	1.388	0.833	0.086	0.000	0.000
Mdc1	S929	K..DLEGLASAPIITGSQADGGKGDPLS[Pho]PGR..Q	0.157	-0.133	-0.441	-0.742	0.467	0.563	0.050	0.001
Mdc1	S929	K..GDPLS[Pho]PGR..Q	0.171	0.296	-0.667	-0.554	0.429	0.176	0.003	0.013
Mdc1	S929	K..DLEGLASAPIITGS[Ser]Q[Dea]ADGGKGDPLS[Pho]PGR..Q	0.038	0.019	-0.455	-0.486	0.846	0.915	0.042	0.030
Mki67	S2333	R..EGHS[Pho]PLSK..S	0.062	0.125	-0.485	-0.447	0.762	0.560	0.031	0.046
Mta1	S576	K..SAPVIN[Dea]N[Dea]GS[Pho]PTILGK..R	0.346	-0.109	-0.582	-1.049	0.114	0.637	0.009	0.000
Mta1	S576	K..SAPVINNGS[Pho]PTILGK..R	0.099	-0.054	-0.703	-0.867	0.641	0.824	0.002	0.000
Mta1	S576	K..SAPVINN[Dea]GS[Pho]PTILGK..R	0.038	-0.094	-0.710	-0.860	0.847	0.689	0.001	0.000
Mybbp1a	S6	M..A[Ace]EMKS[Pho]PTKAEPATPAEAAQSDR..H	0.022	-0.134	-1.625	-1.736	0.903	0.559	0.000	0.000
Mybbp1a	S6	M..A[Ace]EM[Oxi]KS[Pho]PTKAEPATPAEAAQSDR..H	-0.076	-0.301	-1.483	-1.623	0.747	0.182	0.000	0.000
Nfil3	S301	K..GPIHS[Pho]PVELQR..V	0.110	-0.419	-0.702	-1.243	0.605	0.062	0.002	0.000
Nol7	S129	R..KLLPDAVLEQ[Dea]LTTAS[Ser]EADIKKS[Pho]PENVK..V	-0.109	-0.020	-0.596	-0.518	0.638	0.945	0.008	0.021
Nsmce4a	S375	K..TFEISEPVIPLSQS[Pho]QQR..L	0.142	0.084	0.664	0.596	0.509	0.689	0.003	0.007
Orc11	S332	K..LGVDNTLS[Pho]PIRN[Dea]GLR..S	0.233	0.095	-1.187	-1.337	0.285	0.652	0.000	0.000

 BCR/ABL:MSCV

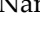


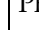
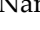


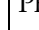
 MSCV+etoposide:MSCV

 BCR/ABL+etoposide:MSCV+etoposide

 BCR/ABL+etoposide :BCR/ABL


[Ace] : acetylation, [Dea]: deamidation, [Oxi]: oxidation, [Pho]: phosphorylation, [Ser]: serine to oxoalanine.

Appendix 7.12: Phosphosite-specific action of etoposide only (3/3)

Name	Phosphosite	Phosphoentity	Average Log ₂ (ratios)				Student's t-test p-value			
										
Pdcd11	S1438*	K..NLIELSLPSTGRPDVFS[Pho]PAPEPK..Q	-0.171	-0.176	-0.661	-0.677	0.453	0.442	0.003	0.002
Pds5a	S1300	R..AAGS[Pho]QESLEAGNAK..A	-0.263	-0.196	1.268	1.323	0.244	0.388	0.000	0.000
Rpl4	S295	R..ILKS[Pho]PEIQR..A	0.201	0.409	-0.784	-0.588	0.355	0.062	0.000	0.009
Safb2	S365*	R..KHQAQAEALGTGGGAGM[Oxi]N[Hex]C[Met]EPVGLLEE PVEQSS[Pho]TAAQLPEATSQELVR..A	-0.343	-0.247	-1.162	-1.077	0.127	0.275	0.000	0.000
Smc3	S1083	R..GSGS[Pho]QSSVPSVDQFTGVGIR..V	-0.101	-0.292	0.928	0.725	0.664	0.196	0.000	0.001
Taok1	S421	R..ASDPQS[Pho]PPQVSR..H	0.074	-0.362	-0.502	-0.949	0.722	0.108	0.025	0.000
Trim28	S473	R..SRS[Pho]GEGEVSGLLR..K	0.076	0.211	0.692	0.816	0.717	0.331	0.002	0.000
Tp53bp1	T906	K..EGDIIPPLTGAT[Pho]PPLIGHLK..L	0.227	0.307	1.317	1.248	0.297	0.161	0.000	0.000
Tp53bp1	S549*	R..TEEDRENTQIDDTEPLSPVS[Pho]NSK..L	-0.081	0.207	-0.940	-0.661	0.731	0.339	0.000	0.003
Tp53bp1	S546*	R..TEEDRENTQIDDTEPLS[Pho]PVSNSK..L	-0.056	-0.045	-0.562	-0.564	0.818	0.856	0.012	0.012
Zfp592	S39	K..EAIQAPSEENES[Pho]PLK..S	0.034	-0.121	-0.576	-0.530	0.863	0.601	0.010	0.018
Zfp828	S394	R..KTALPLS[Pho]PEHWK..A	-0.081	-0.272	-0.687	-0.889	0.730	0.229	0.002	0.000
Zfp828	S394	K..TALPLS[Pho]PEHWK..A	-0.071	-0.097	-0.503	-0.540	0.766	0.678	0.025	0.016

 BCR/ABL:MSCV

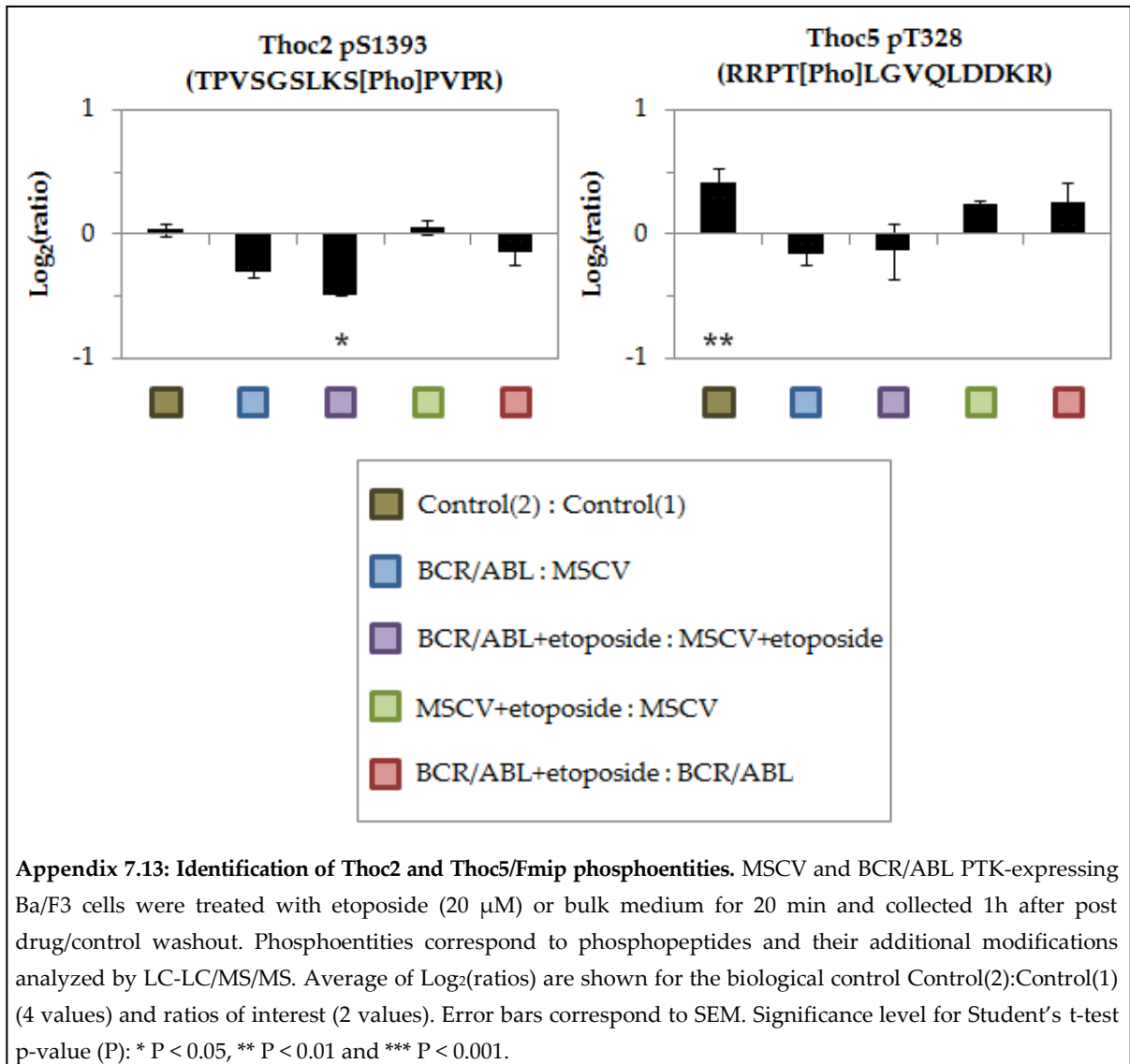
 MSCV+etoposide:MSCV

 BCR/ABL+etoposide:MSCV+etoposide

 BCR/ABL+etoposide :BCR/ABL

[Hex]: glycosylation (hexose), [Met]: β-methylthiolation, [Oxi]: oxidation, [Pho]: phosphorylation. * manual validation did not enable phosphosite assignment with confidence.

7.5. Phosphoentities of THO complex members in the presence of BCR/ABL PTK and etoposide



7.6. Controls for absolute quantification (AQUA™) of Hemogen phosphorylation on serine 380

